STUDIES ON PHYSIOLOGICAL IMPORTANCE OF HFQ AND SRNA TARGETS IN *ACINETOBACTER BAUMANNII*

Ph.D. THESIS

by

ATIN SHARMA

DEPARTMENT OF BIOTECHNOLOGY
INDIAN INSTITUTE OF TECHNOLOGY ROORKEE
ROORKEE - 247667, INDIA
JUNE, 2018

STUDIES ON PHYSIOLOGICAL IMPORTANCE OF HFQ AND SRNA TARGETS IN *ACINETOBACTER BAUMANNII*

A THESIS

Submitted in partial fulfilment of the requirements for the award of the degree of

DOCTOR OF PHILOSOPHY

in

BIOTECHNOLOGY

by

ATIN SHARMA

DEPARTMENT OF BIOTECHNOLOGY
INDIAN INSTITUTE OF TECHNOLOGY ROORKEE
ROORKEE – 247 667 (INDIA)
JUNE, 2018

©INDIAN INSTITUTE OF TECHNOLOGY ROORKEE, ROORKEE- 2018
ALL RIGHTS RESERVED

INDIAN INSTITUTE OF TECHNOLOGY ROORKEE

ROORKEE

CANDIDATE'S DECLARATION

I hereby certify that the work which is being presented in the thesis entitled **"STUDIES ON PHYSIOLOGICAL IMPORTANCE OF HFQ AND SRNA TARGETS IN *ACINETOBACTER BAUMANNII*"** in partial fulfilment of the requirements for the award of the Degree of Doctor of Philosophy and submitted in the Department of Biotechnology of the Indian Institute of Technology Roorkee is an authentic record of my own work carried out during a period from July, 2012 to June, 2018 under the supervision of **Dr. Ranjana Pathania**, Associate Professor, Department of Biotechnology, Indian Institute of Technology Roorkee.

The matter presented in this thesis has not been submitted by me for the award of any other degree of this or any other Institute.

(ATIN SHARMA)

This is to certify that the above statement made by the candidate is correct to the best of our knowledge.

(Ranjana Pathania)
Supervisor

Date: _____

The Ph. D. Viva-Voce Examination of **Mr. ATIN SHARMA**, Research Scholar, has been held on……

Chairman, SRC

Signature of External Examiner

This to certify that the student has made all the corrections in the thesis.

Signature of Supervisors

Head of the Department

In memory of the moments that were lost in pursuit of this prestigious degree...

Abstract

Acinetobacter baumannii is one of the major causes of hospital acquired infections all over the world and one the most frequently isolated nosocomial pathogen in India. This Gram-negative coccobacillus causes a myriad of diseases like hospital acquired pneumonia, meningitis, bacteraemia, urinary tract infections, wound infections and other soft tissue infections. However, the bacterium has gained worldwide notoriety for rapidly developing resistance to most of the antimicrobials and global dissemination of pan-drug resistant strains. Much of the information on determinants of antimicrobial resistance, virulence factors and survival strategies of this bacterium has poured in recently which includes our foray into identification of small RNA in this highly successful nosocomial pathogen.

Small RNAs are short non-coding regulatory RNA molecules that interact with their target mRNAs in antisense manner, thereby affecting their translation, and adding an extra post-transcriptional layer to the overall gene regulation scheme in bacteria. This sRNA-mRNA interaction is often assisted by chaperone proteins, of which Hfq is a major player throughout the Gram-negative genera. We identified 31 putative sRNA in *A. baumannii* and characterized a novel sRNA, AbsR25, in our previous study. This subsequently led to the identification of Hfq protein in *A. baumannii*. The *A. baumannii* Hfq is unusually long due to an unstructured C-terminal extension. Our experiments prove that this seemingly unimportant part is required for efficient sRNA interaction and plays a significant role in maintaining the phenotype that is dependent on the presence of functional Hfq.

In an earlier endeavor of our research group, AbsR25 was identified as a novel sRNA that regulates the expression of efflux pump genes including A1S_1331. Such efflux pumps are determinants of antibiotic resistance and A1S_1331, rechristened as AbaF, was indeed found in this study to be responsible for intrinsic fosfomycin resistance in *A. baumannii*. Apart from antibiotic efflux, AbaF was also determined to be involved in extruding biofilm material and important for virulence of *A. baumannii*.

From the aforementioned 31 candidate sRNA, AbsR1, a novel small RNA was validated by Northern blotting in the present work. This 89 nt long sRNA is present in the intergenic region between 50S ribosome subunit coding genes and conserved throughout the *A. baumannii* strains. The over expression of AbsR1 at acidic challenge and decreased viability of *A. baumannii ΔAbsR1* cells in acidic conditions indicates that AbsR1 might be involved in regulation of cellular response to acidic stress.

From the same list of candidate sRNAs, AbsR10 coding region was identified to be exclusive to *A. baumannii*. PCR primers designed to amplify this unique target region could identify all the clinical strains present in the lab with 100% accuracy. Moreover, the detection was specific as no amplification was achieved when the template DNA from other Gram negative and Gram-positive pathogens was used. The PCR based detection system was shown to rapidly detect *A. baumannii* from simulated clinical surfaces without any enrichment. Quantitative detection of *A. baumannii* could also be made using qPCR, which also led to enhancement in the sensitivity of the detection system.

Acknowledgement

They say it's the journey that teaches you a lot about your destination. The pursuit of PhD has been a journey traversing through the vast lands of grueling labor, rocky terrains of failed experiments, joyous highways of accepted publications, gushing waves of long discussions and quiet mountainous trails of self-motivation. As this long journey approaches its destination, I wish to acknowledge everyone who inspired me to embark on this ride, motivated me throughout my expedition, became a part of this excursion and wished me *bon voyage*. So, before I acknowledge the most important associate in this journey, the sailor of the ship, my supervisor, I wish to remember the people who the encouragement for me to set forth on this path.

It all begins in the family. I am grateful to my family for never questioning my career choices and always inspiring me to achieve the best. Even when at times I felt bogged down by problems, they were right behind me to pamper, push and support. I might not have made frequent visits home during the tenure of my PhD but I always felt their presence. I have not only been lucky to have a motivating family but also encouraging teachers throughout my academic life. Mr. Joydeep Bandopadhyay, Mrs. Kamini Sharma, Mrs. Krishna Srivastava, Mrs. Tania Bagchi, Mrs. Manjula Rawal, Mrs. Rita Bansal, Mrs. Lata Menon and Mr. Sukhwinder Singh are some of my school teachers who have had a great impact in shaping my personality in my formative years and creating my interest in quest for knowledge and science. I was blessed with professors like Dr. Swati Sinha, Dr. Navneet Batra, Dr. Varinder Kumar, Dr. Akhlash Pratap, Ms. Tamanna Aggarwal and Dr. Jagtar Singh, who watered the seedling of science at the college and university level that was planted by my school teachers. I still remember Dr. Sinha being the only staff member at the college who supported me in my extra-curricular activities stressing on the fact that no scientist ought to be a socially awkward moron.

However, the real test of patience began with the journey itself. I am extremely indebted to my supervisor Dr. Ranjana Pathania for taking me under her tutelage and giving wings to my long-cherished dream of pursuing the highest embodiment of academia, a PhD. She has always been a very concerned mentor, be it professionally or personally. She took the pains of running from pillar to post when I was declined a transfer of fellowship and my hopes of continuing my dream run were bleak. If it were my family and teachers who helped laying the foundation of a castle, it was my supervisor who ensured it was built strong and sturdy. She always had immense faith in my abilities and trusted me with the matters pertaining to the lab. I have been fortunate enough to be able to bring my ideas to her without any hesitation and to be supported to put them to action without any second thoughts. I will always remember those long discussions not just about

my own project but about all the projects in the lab, about newer avenues, about improving the quality of research, about upgrading the standards of the lab and about the wonder called science. She trusted me with a lot of lab responsibilities and I hope I did a good, if not an excellent, job. I have definitely not been a very easy student with my raw enthusiasm and energy, but she always had a piece of advice to channelize it in the right direction. I am grateful to her for keeping up with my shenanigans. Though I had been reluctant initially, but her insistence on making me write more, sit through with her through the grants' applications and other official communication really helped me hone my scientific writing. It was only when I had to write my own manuscripts that I realized the benefit of all that exercise. It also appeared to me at times that I had been burdened with responsibilities while being made to assist her in multiple activities, but ultimately it helped me develop my overall temperament as a scientist in making. From my early days in the lab, she realized my interests and hobbies and never discouraged me from pursuing them. Instead, she pushed me to participate in various departmental activities. She has always lent an ear to my problems and counselled me using her own life experiences.

I cannot help but take Dr. Naveen Kumar Navani's name in the same breath as my supervisor's as I have always considered him as my co-supervisor. Though he isn't one on paper, he has been closely associated with all my projects and has been the one ready with suggestions at any stage of experimentation. He has a knack for picking up non-conventional and exciting projects which I have had the pleasure of being a part of. He is constantly looking for the next big thing in science which often led to very interesting discussions that acted as brain teasers for me. Though my supervisor has always been opposed to the ideas of using short cuts, Dr. Navani always shared the bits and tricks he had learnt from his experience to make a researcher's life easier. He is one of the smartest guys I have come across and I often try to emulate his confidence at scientific presentations, ability to deal with vendors and his managerial prowess. If it was my supervisor who was steering my ship throughout this journey, he was an ideal first mate to the captain who took on all the responsibilities in her absence.

Though all credits are due to my supervisor for her guidance, it was my senior Dr. Rajnikant Sharma, who mentored me and taught me the trick of the trade. He spent genuine effort at training me in the lab and had immense patience to deal with all my queries and doubts. I was in awe of the hard work he used to put in the lab even in the last few months of his PhD where most of the students feel saturated. He had gathered a great deal of experience over time and shared tips that no protocols ever mentioned. He has also been a great friend as I could talk to him just about anything. He is still fondly remembered as the star of the dinner table conversations despite having left the hostel years ago.

As a young and timid new addition to the group, I was taken under the wing by doting and caring seniors in the lab. I cherish the fond memories of evening tea with the whole entourage which included Dr. Santosh Srivastava, Dr. Supriya Patil, Dr. Parmesh Lambadi, Dr. Piyush Kalra, Dr. Jitendra Sahoo, Dr. Tapas Bhattacharyya, Dr. Rekha Sharma, Dr. Manasi Gupta and Mr. Abhijeet. Dr. Santosh was a rare talent who would always take out a page from the wealth of knowledge he had gained by reading and share his ideas. Dr. Paramesh will always be remembered for his sincere dedication to his work and his jovial nature. I still despise him for his Mohammad Aziz like voice and the torture we all had to bear while he sang his lungs out, but I accepted it as a punishment for injuring his nose in a cricket match really early in my days as a PhD student. A special mention must go to Dr. Manasi who always provided the comfort of a family. Be it the endless *chai pe charcha* at her home or the car driving lessons she gave me or just being the selflessly helping person she has always been. She has been like an elder sister and I will always hold her in high regards for that.

Apart from the lab, there were other seniors in the department who were equally affable and treated me like their younger sibling. Dr. Pradeep Palakshan, Dr. Bibekanand Kar, Dr. Purushotham Selvakumar, Dr. Prabhat Tomar, Dr. Madan Mohan Rout and Dr. Umesh made me a part of their troupe very quickly and I never felt lonely at a new place. I will remember the fiercely contested cricket matches we had which ended up in heated debates and chicken biryani. Playing cricket was really a pleasure with you and it suddenly ended as you people graduated.

Besides such caring seniors, I got a very intelligent and entertaining company from my peers and juniors in the lab. I am thankful to Timsy, Pradeep, Rajat, Jawed, Vineet, Shahnawaz, Vandana, Anupama, Mehak, Somok, Kuldip, Shubham, Dillip, Namrata, Akshay, Mohan and Ravi, for their kind help and for never declining my requests for carrying out odd jobs on my behalf. I am really obliged. A special thanks to Vineet for the *hfq* deletion mutant which had been a lingering issue for a very long time. This thesis would not have been complete without that big assist. I also wish to acknowledge him for those bike-riding lessons and infusing a new confidence and attitude in me.

Due to my obligations as a teaching assistant, I was able to come in contact with some brilliant young minds who hold the future of science. Though I won't be able to name all of them, I am thankful to all the M.Sc. students that I have had the chance of instructing as a TA. It was extremely challenging to teach bright pupils and I was always fearful of tough-to-crack problems emanating from the inquisitive brains. My experience with them helped me grow and learn a different aspect of being a researcher. With them it was a two-way learning process. While I tried to teach them some new concepts in research, they actually showed me alternative viewpoints to look at the same concepts. The fact that I see some of those students taking up research as a career

makes me feel really proud. I got to interact even more closely with some of those students who actually worked with me and assisted me in my projects. Abin, Amit, Biswajeet, Poushali, Shalini, Jyoti, Swapnil, Kasturika and Aditi are all close to my heart for making me experience the joy of being a pedagogue and a supervisor to them. I will remember Amit, who later transitioned into a permanent lab member, as the brightest of the pack, who I had no qualms in asking conceptual problems that even I could not comprehend. Then there were other lab members Samarth, Chirag, Shubham Rathore, Priyanka Sinha, Anshika, Arshad, Anupam, Priyanka Gandhi, Anupama Mandal, Shubham Pallod, Himanshu, Ananth and Soumyadeep who walked the walk for some time with me and their paths intersected with those of mine. It was indeed a pleasure to come in contact with these wonderful people. Arshad, the bard, and Samarth, the philosopher, were two special people and it feels great to see both of them excelling at science.

I was also benefitted by the presence of postdocs in the lab, who guided me and helped me with my academic problems. Dr. Vivek Gupta, Dr. Vikrant Rajput, Dr. Siva Ramakrishna Uppalapati, Dr. Rashmi, Dr. Shadab Parwez, Dr. Arun Beniwal and Dr. Ruchi Mutreja have been kind and generous senior associates with new perspectives to offer from their prior scientific endeavours. They have been a template postdoc I wish to transition into soon.

During the course of time, I also had some friendly associations with other people in the department. I wish to remember Dr. Meenu Gupta, Dr. Shilpi Aggarwal, Dr. Anamika Singh, Dr. Nikhil Kumar, Dr. Shruti Saran, Vijay, Harvijay, Neha, Aanchal, Pranav, Debpali, Nidhi, Krishnakant, Zia, Kartik, Shahank and Amol for those occasional banter, assistance and pleasant social exchanges. This list of friends would not be complete without mentioning Gagandeep, Karunava, Renu, Pragati, Vidhi, Anand, Dr. Sourabh, Dr. Manjot, Anand and Kriti. I am obliged to Karunava and Kriti for letting me accompany them in showing off their musical talents thereby letting me develop my own. Dr. Manjot has been a great friend and it was such a pleasure to reunite with him in IIT Roorkee after about ten long years.

Although I am mentioning them this late, they have been the life support system for me in IIT Roorkee. They are my special gang, Dr. Naren, Dr. Sidhharth, Dr. Alok, Shailendra, Rajat, Tamoghna, Madhusudhana, Snehasish and Rajesh. I could not imagine my life in this institute sans their company. If life could be compared to colours, I think we have used everything on the palette. I have shared just about every emotion with them and enjoyed each moment of togetherness. From discussions on science, society, politics, binge watching movies, outdoor adventures and misadventures, bitter quarrels and sobbing moments, every time we shared the time and space, we created memories to cherish forever. Such bonds are the ones to be kept

forever and I am truly blessed with the kind of brotherhood I received from you guys. Long live the acronym YKBCH, which is forever etched in my heart.

Though I have enjoyed the company of a lot of good friends, I have some really special people in my life who, despite all the distance, have infused me with mental strength, encouragement, vivaciousness and zeal through their ever-lasting presence in the back of my mind. Words can simply not describe the contribution that my dearest friends Sanyam, Tarun, Disha, Namrah and Prerna have made to my life. The level of confidence they had in me often beat my own faith in my abilities. I wish my words could express my heartfelt gratitude to these people.

I also wish to thank my SRC members Prof. A.K. Sharma, Prof. R. Prasad and Dr. P. Biswas for being very generous and making the formalities of the PhD a smooth ride. A very special thanks to Dr. Susan Gottesman, NIH, USA; Prof. Raghavan Varadarajan, IISc Bangalore, Prof. Udo Bläsi, University of Vienna, Austria; Dr. Brian Davies, Univeristy of Texas at Austin, USA; Prof. Partha Roy, IIT Roorkee; Dr. Kiran Ambatipudi, IIT Roorkee; Dr. Rahul Das, IISER Kolkata, Dr. Varsha Gupta, GMCH Chandigarh; and Dr. Ashima Bhardwaj, IIAR Gandhinagar; for lending scientific support by sharing biological materials and scientific advice.

Last but not the least, I wish to thank Him, for He is the one who pulls all the strings. I am thankful to Him for the bittersweet journey that this PhD has been. I have cursed bad times and I have been lucky to bask in sunshine as well, and for all of that I express my gratitude to Him.

A moment of silence for all the mice who lost their lives in experiments that made this thesis a successful compilation.

Atin Sharma

Contents

List of figures

List of tables

Abbreviations and symbols

ABC	ATP-Binding Cassette
AbsR	*Acinetobacter baumannii* small RNA
ANOVA	One-way analysis of variance
ATCC	American Type Culture Collection
ATP	Adenosine Triphosphate
BLAST	Basic Local Alignment Search Tool
bp	Base pair
BSA	Bovine serum albumin
CCCP	Cyanide 3-chlorophenylhydrazone
CD	Circular Dichroism
CDD	Conserved Domain Database
cDNA	Complementary Deoxyribose Nucleic Acid
CFU	Colony Forming Units
CLSI	Clinical and Laboratory Standards Institute
CRAB	Carbapenem Resistant *Acinetobacter baumannii*
CSP	Cold Shock Proteins
CTR	C-terminal region
CV	Crystal Violet
DIP	2,2-Dipyridyl
DMEM	Dulbecco's Modified Eagle's Medium
EMSA	Electrophoretic Mobility Shift Assay
ESBL	Extended-Spectrum β-Lactamases
ESKAPE	*Enterococcus faecium*, *Staphylococcus aureus*, *Klebsiella pneumoniae*, *Acinetobacter baumannii*, *Pseudomonas aeruginosa*, and *Enterobacter* species
EtBr	Ethidium bromide
EUCAST	European Committee on Antimicrobial Susceptibility Testing
FITC	Fluorescein isothiocyanate
GFP	Green Fluorescent Protein
GMQE	Global Model Quality Estimation
GRP	Glycine Rich Protein
Hfq	Host factor required for Qβ phage replication

IAEC	Institute Animal Ethics Committee
ICL	International Clonal Lineages
ICU	Intensive Care Unit
IDSA	Infectious Diseases Society of America
IPTG	Isopropyl β-D-1-thiogalactopyranoside
LB	Luria Broth
MALDI-TOF MS	Matrix-assisted laser desorption/ionization time-of-flight mass spectrometry
MATE	Multidrug And Toxic compound Extrusion
MDR	Multi-drug resistant
MFS	Major Facilitator Superfamily
MH	Mueller Hinton
MIC	Minimum Inhibitory Concentration
mRNA	Messenger RNA
MSA	Multiple sequence alignment
NB	Nutrient Broth
NCBI	National Center for Biotechnology Information
NFW	Nuclease-Free Water
NHSN	National Health Safety Network
Ni-NTA	Nickel-nitrilotriacetic acid
nt	Nucleotide
OD	Optical Density
ONPG	ortho-Nitrophenyl-β-galactoside
PAGE	Polyacrylamide Gel Electrophoresis
PBS	Phosphate Buffered Saline
PCR	Polymerase Chain Reaction
PDB	Protein Data Bank
PDR	Pan-drug resistant
PMF	Peptide Mass Fingerprint
qPCR	Quantitative Polymerase Chain Reaction
RACE	Rapid Amplification of cDNA Ends
RND	Resistance-Nodulation Division
RT-PCR	Reverse Transcriptase Polymerase Chain Reaction
SD	Shine Dalgarno

SDS	Sodium Dodecyl Sulphate
SMR	small multidrug resistance
sRNA	Small Ribonucleic Acid
TCA	Tricholoroacetic acid
TFA	Trifluoroacetic acid
TOF	time-of-flight
UTI	Urinary Tract Infections
UTR	Untranslated Region
WT	Wild type
XDR	Extremely-drug resistant

1 Introduction

Acinetobacter baumannii has emerged as an extremely troublesome Gram-negative nosocomial pathogen. It is a non-motile, strictly aerobic coccobacilli that has gained notoriety for causing nosocomial infections in critically ill patients all over the world [1]. Perhaps the most striking feature of *A. baumannii* is not its virulence but its drug resistance [2]. In the 1970s, *A. baumannii* infections were easily treated using the prevalent antibiotics, however, now more than 63% of *A. baumannii* infections are caused by multi-drug resistant *A. baumannii* [3]. The Infectious Diseases Society of America (IDSA) has recommended *A. baumannii* as one of the most drug resistant bacterial pathogens collectively known as ESKAPE pathogens (*Enterococcus faecium*, *Staphylococcus aureus*, *Klebsiella pneumoniae*, *Acinetobacter baumannii*, *Pseudomonas aeruginosa*, and *Enterobacter* species) [4]. Drug resistance in *A. baumannii* is a result of alteration in membrane permeability, modification in antibiotic targets, expression of antibiotic modifying enzymes and active efflux of antibiotics. The expression of various determinants of antibiotic resistance is regulated by mobile genetic elements and *A. baumannii* strains are reportedly naturally competent, which aids in rapid acquisition of antibiotic resistance. There are numerous reports on isolation of multi-, extremely- and pan-drug resistant strains of *A. baumannii* from various geographical locations [5]. Initially considered a harmless commensal, *A. baumannii* accounts for 20% of the infectious outbreaks in ICUs worldwide [6]. It is responsible for about 80% of all the infections caused by *Acinetobacter* species [7]. Although it can colonize healthy individuals, it causes severe soft tissue infections in immunocompromised individuals especially children and the elderly. The bacterium has a formidable ability to maintain viability even under harsh environmental conditions [1]. It forms sturdy biofilms and resists the action of many detergents and cleaning agents which aid its persistence in hospital environments. Equipment like the catheters are one of the most frequent modes of dissemination of *A. baumannii* infections which range from hospital-acquired pneumonia, burn infections, wound infections to severe bacteremia and meningitis. The clinical importance of *A. baumannii* garnered mainstream attention when it was isolated from wounded American soldiers returning from Iraq, leading to the bacterium being labelled as 'Iraqibacter' [8]. Since then, a lot of progress has been made in studying this interesting bacterium in terms of its physiology. Numerous virulence factors including capsular polysaccharides, porins, lipopolysaccharides, outer membrane proteins, proteases, phospholipases, secretion systems, and metal-chelating systems have been identified and characterized [9].

Our group has a long-standing interest in understanding the molecular basis of regulation of drug resistance and virulence in *A. baumannii*. We focused our research efforts in small RNA (sRNA) which are known to play important regulatory roles in pathogenic bacteria. Small RNA are versatile post-transcriptional regulators of gene expression in bacteria. They are 50-500 nucleotide long non-coding RNA molecules that are generally present in the intergenic regions and carry rho-independent terminators [10]. Much like their eukaryotic counterparts, miRNA, they base-pair with their mRNA targets in an antisense manner and result in either stabilization of the mRNA or its degradation, depending on the type of interaction. Based on their genomic locus, sRNA could be *cis*-acting, that are transcribed from the strand opposite to their target mRNA, or *trans*-acting, which are transcribed from a location away from their target mRNA. Unlike the *cis*-acting sRNA, *trans*-acting sRNA have a limited complementarity to their targets for antisense based interaction. This interaction is often assisted by an RNA chaperone protein, creating a complex circuit involving sRNA-mRNA-chaperone protein. In an attempt to unravel this circuitry in *A. baumannii*, our group reported computational prediction of 31 candidate small RNA [11]. Further studies were conducted on one of these candidates, AbsR25. This small RNA was found to be overexpressed in presence of increasing amounts of NaCl and repressed in presence of efflux substrate EtBr. Of the other sRNA, two, AbsR11 and AbsR28 were also validated but no further studies were carried out to assess the characteristics and physiological roles of other putative sRNA. Prediction of AbsR25 targets revealed a lot of transporter proteins which are generally involved in solute transport including drugs. Such transporters or efflux pumps have been widely reported to extrude out antibiotics which leads to ineffective build-up of antibiotic inside the cell and protects the cellular targets. These proteins work up against the concentration gradient by actively deriving energy from ATP hydrolysis or proton/ion gradients, depending upon the family to which they belong [12]. Efflux pumps could be specific for a particular substrate or might be able to efflux put a range of unrelated substrates with different specificities. This correlates with their ability to confer antibiotic resistance as efflux pumps could be multi-drug or specific for a single drug. Most of the predicted targets of AbsR25 belonged to the Major Facilitator Superfamily (MFS) of transporters. Of these targets, A1S_1331, was negatively regulated by AbsR25 as there was a several fold decrease in the expression of A1S_1331 when AbsR25 was overexpressed in *A. baumannii*. Although MFS transporters have been implicated in antibiotic resistance, the importance of A1S_1331 in maintaining this phenotype was not known.

Since *trans*-acting small RNA require an RNA chaperone protein for assistance in interaction with their cognate mRNA targets and there were no such proteins reported in *A. baumannii*, it

was pertinent to identify and characterize the RNA chaperone in *A. baumannii*. Bacteria express many RNA binding proteins of which only a few fulfil the chaperoning functions. Even among the common chaperone proteins like cold shock proteins (Csp), ribosomal proteins, StpA, Ro proteins, Hfq is the major player in sRNA based regulation [13]. Lately, chaperones like ProQ, RocC and FinO have been identified, but these chaperones are restricted, as yet, to only a certain sRNA in select bacterial species and have been speculated to be important in bacteria lacking a functional Hfq homolog [14]. Hfq was first identified as the host factor required for Qβ phage replication. It is a distant homolog of eukaryotic Sm like proteins that interact with RNA molecules. It forms a donut shaped hexamer which presents two different faces, distal and proximal, for RNA interaction and a central pore [15]. The rim of the donut forms an additional surface of sRNA-mRNA interaction. Hfq assists the sRNA-mRNA interaction as well as sRNA-mRNA-protein interactions by increasing the local concentration of the interacting partners [16]. The gene coding for Hfq protein is an important factor for maintaining normal growth and stress response in many Gram-negative bacteria. Its deletion abolishes the sRNA based regulation, leading to impaired ability of the bacterial cells to adapt to the environmental conditions [17]. The Hfq protein in a closely related bacterium *A. baylyi* was observed to carry a long C-terminal extension that is unique to the Moraxellaceae family [18]. This C-terminus shows a compositional bias towards the flexible amino acid glycine, which means that this C-terminus adopts a flexible coil like secondary structure instead of adopting a regular secondary structure like α-helix of β-sheet. Recent studies on functional importance of Hfq in *A. baumannii* have alluded that this extension might not serve any importance [19]. However, its presence in all of the members of Moraxellaceae family seems to be more than just a random mutation event carried down the line as proteins carrying amino acid repeats are known to play specific roles in bacterial physiology [20]. Therefore, further studies were required to determine the physiological importance of Hfq and its enigmatic extended C-terminus in *A. baumannii*.

In addition to providing information on a novel sRNA and its targets, our group's previous computational analysis led us to an interesting and unique candidate sRNA, AbsR10 [11]. Careful analysis of AbsR10 sequence revealed a particular region that was exclusively present in all of the sequenced *A. baumannii* genomes. Such unique signatures could be employed for PCR based detection of pathogens [21]. *A. baumannii* is a widespread clinical pathogen and conventional detection techniques often take long time and skilled personnel for precise identification. Since *A. baumannii* forms resistant biofilms on clinical surfaces, PCR based methods can be directly applied using the biofilm material to detect the bacterium. These methods are often amenable to

quantitative detection of bacteria using qPCR. However, the specificity of such a method could only be claimed after experimental validation.

Thus, our group's prior findings opened a lot of new avenues in understanding the physiology of *A. baumannii*. This thesis is an attempt to follow them in detail. The major objectives were to identify and characterize the small RNA chaperone Hfq in *A. baumannii*; characterize the MFS transporter A1S_1331, the primary target of AbsR25; validate a novel sRNA in *A. baumannii*; and develop a PCR based assay to identify *A. baumannii* using the candidate sRNA. The thesis has been split into multiple chapters according to these objectives. Chapter 2 provides a detailed review of already known information about *A. baumannii*, its biology, role of efflux pumps in drug resistance, sRNA, and the RNA chaperone Hfq. Chapter 5 is an attempt to address the enigmatic presence of an extra-long glycine rich C-terminus in Hfq protein of *A. baumannii*. It deals with determining what roles Hfq plays in physiology of *A. baumannii* and if the presence of this flexible tail is really important for this bacterium. Experiments were carried out to study the phenotype of *hfq* deletion mutant of *A. baumannii* and its subsequent complementation by truncated versions of Hfq carrying varying length of C-terminus. Chapter 6 seeks to functionally characterize the transport proteins that were found to be regulated by AbsR25. Studies were carried out to determine whether the primary target of AbsR25, A1S_1331 is involved in antibiotic efflux or not. A1S_1331 was cloned and expressed in an efflux deficient strain, *E. coli* KAM32, and its antibiotic susceptibility was determined. The gene coding for A1S_1331 was inactivated in *A. baumannii* and its effect on the phenotype was studied. Chapter 7 deals with the characterization of another candidate sRNA from the list of 31 sRNA determined previously. The sRNA, AbsR1, was characterized in terms of its expression, transcription start and stop sites, and its putative targets. The effect of deletion of AbsR1 on the physiology of *A. baumannii* was studied using some basic experiments which forms the foundation of the chapter. Finally, Chapter 8 presents an application-based aspect of a unique candidate sRNA, AbsR10. A PCR based assay was designed and optimized for detection of *A. baumannii* from clinical samples and hospital surfaces.

2 Review of literature

2.1 *Acinetobacter baumannii*

Acinetobacter baumannii is a well-known nosocomial pathogen associated with multi-drug resistant infections in patients receiving medical attention in the Intensive Care Units (ICUs) [22]. The genus *Acinetobacter* have been known for long, probably been isolated first in 1914, and have been known by different names before forming a separate genus [23,24]. The name '*Acinetobacter'* (from Greek 'akinetos', meaning non-motile) was suggested by Brisou and Pevot in 1954 but it didn't come to use till 1968 when Baumann et al. published a detailed study of the genus [25,26]. *Acinetobacter* genus contains about 50 species and most of them are harmless environmental microorganisms [27]. However, there is an increasing incidence of infections of *A. baumannii* ever since it was designated as a separate species in 1986 [28]. Other *Acinetobacter* species that cause clinical infections are: *A. calcoaceticus*, *A. lwoffii*, *A. seifertii*, *A. haemolyticus*, *A. junii*, *A. johnsonii*, *A. nosocomialis*, *A. pitti*, *A. schindleri* and *A. ursingii* [29–39]. However, *A. baumannii* is considered the most virulent of all the *Acinetobacter* species [40]. It is an oxidase negative, catalase positive, nonfermenting Gram negative bacterium that forms smooth and mucoid colonies on laboratory media. The *A. baumannii* cells are coccobacilli and appear as short rods when viewed microscopically (Figure 2.1). *Acinetobacter* spp are generally ubiquitous in nature found in moist environments, soil, wastewater, farms, wetlands, etc. [27]. However, the same cannot be said for *A. baumannii* as they are almost exclusive to the hospital environment with ICUs in particular. Although other infectious *Acinetobacter* spp like *A. calcoaceticus*, *A. lwoffii*, *A. nosocomialis* and *A. pitti* have been found on edible items like vegetables and meat and even on human skin, such incidence of *A. baumannii* is few and far between [41]. There are scattered as well as inconclusive reports of *A. baumannii* isolation from soil, vegetables, park benches and gaming consoles [42–44]. Although *A. baumannii* has been infrequently isolated from non-human animals, it is not clear if they are a primary reservoir or the isolation is just a result of contamination [45]. Healthy humans don't seem to harbor *A. baumannii*, therefore its unusual colonization of wounded American soldiers returning from Iraq earned it the moniker, 'Iraqibacter' [46]. Ironically, the frequency and severity of once considered a commensal opportunist, *A. baumannii*, has increased proportionately with improvement in medical equipment and sophistication. The *A. baumannii* outbreaks worldwide have been recognized to be caused by three major clonal lineages and most recently six such international clonal lineages (ICL) have been identified [47]. According to the US National Health Safety Network (NHSN) 2009-2010 report, *A. baumannii* was responsible for 1.8% of all hospital acquired infections [48].

The frequency was quite similar across Europe and some countries in South America [49–53]. However, in some South American countries, China, Thailand, Vietnam and India, the incidence is much higher and *A. baumannii* is the predominant nosocomial pathogen [54–64]. According to an estimate, there are about 45,000 cases of *A. baumannii* infections per year in US and a mean one million infections worldwide, every year [65].

Figure 2.1. Scanning electron micrograph of *Acinetobacter baumannii* ATCC 17978.

2.1.1 Clinical manifestations

Acinetobacter baumannii causes a range of nosocomial infections including wound infections, skin and soft tissue infections, urinary tract infections and secondary meningitis [66]. Although the predominant sites of nosocomial infections change with time, the most important infections by *A. baumannii* with the resulting in highest mortality are ventilator-associated pneumonia (nosocomial pneumonia) and bloodstream infections (bacteremia) [67,68]. Respiratory infections are more common in patients already suffering from underlying ailments or who have undergone surgical operations. *A. baumannii* finds its way into the body through their open wounds, intravascular catheters and mechanical ventilators. The bacterial cells adhere to the plastic tubes and form resistant biofilms that assist their dissemination [69]. Aspiration of droplets contaminated with *A. baumannii* cells allows a direct passage unhindered by the host defense mechanisms. *A. baumannii* pneumonia is similar to most Gram negative pneumonias [70] with symptoms like fever, sputum production, neutrophilia, etc. In some reports, pneumonia has been the predominant, being responsible for 26.7% [71], 33% [72] and even 47.9% [73] of all *A. baumannii* nosocomial infections. Crude mortality rates range from 30% to as high as 75% [70,73]. *A. baumannii* infections are more frequently associated with male gender and older age as well [22]. *A. baumannii* can also cause community-acquired infections, majorly pneumonia (accounting for 85% of all community-acquired *A. baumannii* infections) [30,74]. Such

infections are common in warm and humid environments found in countries like Australia, China, India, Taiwan and Thailand [74–76]. Again, these infections seem to be common among males and associated with old age, alcoholism, diabetes, smoking and pulmonary diseases. Community-acquired pneumonia is more dangerous as mortality rates could be as high as 60% [77]. Bacteremia is often the outcome of excessive pneumonia, trauma, surgical operations, catheters and intravenous devices and burns [70,78,79].

2.1.2 Antibiotic resistance

Unlike other serious pathogens, *A. baumannii* is not highly virulent and does not produce any major toxins or cytolysins [80]. However, what makes this bacterium stand out is its ability to resist the action of antibiotics. *A. baumannii* has become resistant to most of the antibiotics in used including β-lactams, aminoglycosides, quinolones leading to frequent isolation of multi-drug and pan-drug resistant strains [81–83] (Table 2.1). The Infectious Diseases Society of America (IDSA) has listed *A. baumannii* as one of the most drug resistant ESKAPE (*Enterococcus faecium*, *Staphylococcus aureus*, *Klebsiella pneumoniae*, *Acinetobacter baumannii*, *Pseudomonas aeruginosa* and *Enterobacter* spp.) organisms [4]. Drug resistance in *A. baumannii* results from one or more of the following mechanisms: alteration in membrane permeability to avoid the entry of drugs, enzymatic modification of the drugs which makes them ineffective, mutations in the drug targets that allow them to escape the drugs and active efflux of drugs that doesn't allow an effective build-up of drug in the cellular milieu (Figure 2.2). Not surprisingly, *A. baumannii* strains are multi-drug resistant (MDR, resistant to more than one antibiotic of at least three classes), extremely-drug resistant (XDR, resistant to more than one antibiotic of all but two classes), and pan-drug resistant (PDR, resistant to all antibiotics) [84]. A serious problem is the widespread dissemination of carbapenem resistant *A. baumannii* (Figure 2.3). Such bacteria are often resistant to most of the antibiotics and their treatment requires the use of antibiotics of last resort like colistin and tigecycline [2]. Unfortunately, these drugs have a dubious safety profile and *A. baumannii* has evolved resistance against them as well [2].

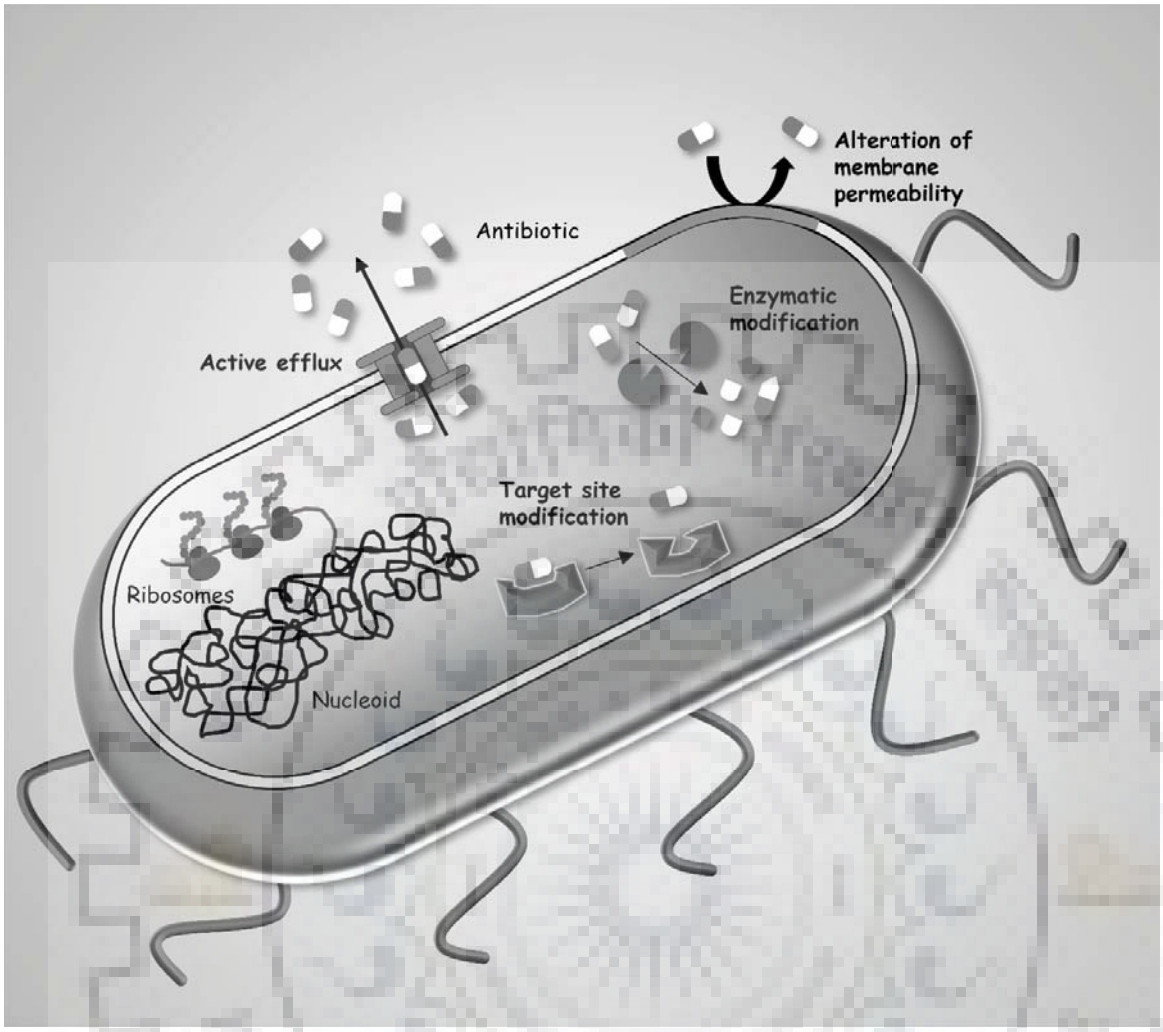

Figure 2.2. The four major mechanisms of antibiotic resistance in bacteria: (i) Alteration of membrane permeability, (ii) Enzymatic modification of antibiotics, (iii) Mutation of target sites, and (iv) active efflux of antibiotics.

Table 2.1. A summary of antibiotic resistance mechanisms in *Acinetobacter baumannii*.

Antimicrobial	Resistance mechanism	Class/ family	Protein	Reference
β-Lactams	Chromosomal cephalosporinase	Class C	AmpC	[85]
	Carbapenem-hydrolyzing class D β-lactamases	Class D	OXA-51-like	[86]
			OXA-23-like	[87]

		OXA-24/40-like	[88]
		OXA-58-like	[89]
		OXA-143-like	[90]
Metallo-β-lactamases	Class B	IMP	[91]
		VIM	[91]
		SIM-1	[91]
		NDM	[92]
Other β-lactamases	Class A	TEM	[93]
		SHV	[94]
		SCO-1	[95]
		CARB	[96]
		PER	[97]
		VEB	[98]
		CTX-M	[99]
		GES	[100]
		KPC	[101]
	Class D	OXA-2, 10, 20, 37	[93,102,103]
Decreased permeability		CarO	[104]
		47 kDa OMP	[105]
		44 kDa OMP	[105]
		37 kDa OMP	[105]

			33-36 kDa OMP	[106]
			22-33 kDa OMP	[107]
			HMP-AB	[108]
			43 kDa OMP	[109]
	Efflux pump	RND	AdeABC	[110]
			AdeIJK	[111]
	Modified penicillin-binding proteins		PBP	[112]
Aminoglycosides	Aminoglycoside-modifying enzymes		Acetyltransferases	[113]
			Nucleotidyltransferases	[113]
			Phosphotransferases	[113]
	Target binding site modification	ArmA	16S rRNA methylases	[114]
	Efflux	RND	AdeABC	[110]
		MATE	AbeM	[115]
Quinolones	Target site mutations		GyrA/ParC	[116]
	Efflux pump	RND	AdeABC	[110]
			AdeIJK	[111]
			AdeFGH	[117]
		MATE	AbeM	[115]
		SMR	AbeS	[118]
Chloramphenicol	Efflux pump	RND	AdeABC	[110]

			AdeIJK	[111]
			AdeFGH	[117]
		MFS	CmlA	[119]
			CraA	[120]
		MATE	AbeM	[115]
		SMR	AbeS	[118]
Tetracyclines	Efflux pump	MFS	TetA	[121]
			TetB	[119]
	Ribosomal protection		TetM	[122]
Tigecycline	Efflux pump	RND	AdeABC	[110]
			AdeIJK	[111]
Fosfomycin	Efflux pump	MFS	AbaF	[123]
Polymyxins	Lipid A modification		PmrCAB	[124]
	Loss of lipopolysaccharide		LpxABC	[125]
	Porin loss			[126]

Figure 2.3. Global incidence of carbapenem resistant *Acinetobacter baumannii* (CRAB) [127].

The rapid evolution of drug resistance in *A. baumannii* could be attributed to acquisition of novel genetic elements through lateral gene transfer and modification of intrinsic determinants of resistance. Insertion sequences, integrons, transposons and plasmids are responsible for providing novel genetic information to the bacterium whereas modification of intrinsic determinants occurs via mutations or insertion/deletion of mobile genetic elements that lead to altered expression of intrinsic mechanisms of resistance or alter the membrane permeability. Moreover, the dynamic proteomic changes also allow the bacterium to switch from drug-sensitive to drug resistant phenotype [128].

2.1.2.1 Cephalosporins

Cephalosporins are one of the classes of β-lactams that were initially less prone to inhibition by β-lactamases. Most of the *A. baumannii* strains are resistant to cephalosporins, including third- and fourth-generation agents, due to the production of AmpC β-lactamase [85]. Although it is expressed at basal levels, presence of upstream insertion sequences and presence of a strong promoter enhance its expression, leading to clinically relevant resistance [129]. Additionally, *A. baumannii* also produces extended-spectrum β-lactamases (ESBL) which lead to clinically relevant cephalosporin resistance [130,131].

2.1.2.2 Carbapenems

The expression of carbapenem degrading carbapenemases is the primary reason for carbapenem resistance in *A. baumannii*. Similar to the aforementioned AmpC β-lactamase, the bacterium naturally expresses a chromosomally encoded OXA-51-group carbapenemase. However, its expression, again analogous to AmpC, increases due to insertion of strong promoter upstream

the gene leading to elevated carbapenem resistance [86,132]. Carbapenemases are often acquired through mobile plasmids. Major groups of acquired carbapenemases in *A. baumannii* include, OXA-23, -43, -48, -58 and -143 [133]. Non-OXA group of carbapenemases include the dreadful metallo-β-lactamase, NDM-1 which has been reported in multiple isolates of *A. baumannii* [134,135].

2.1.2.3 Aminoglycosides

A. baumannii produces various aminoglycoside modifying enzymes as acquired determinants of resistance [136]. Apart from this, the bacterium has a new mechanism to resist the aminoglycosides, 16S ribosomal RNA methyltransferase like ArmA. ArmA methylases a guanine residue in the A site of 16s rRNA and prevents aminoglycoside binding [137]. ArmA producing *A. baumannii* are highly resistant to gentamycin, tobramycin and amikacin.

2.1.2.4 Fluoroquinolones

Fluoroquinolones are the most widely used first line antibiotics for regular treatment of respiratory and urinary tract infections caused by bacterial pathogens including *A. baumannii*. These antibiotics inhibit DNA synthesis by binding to DNA gyrase and topoisomerase IV, leading to cell death. The primary mechanism of fluoroquinolone resistance is mutations in the target genes [138]. However, many efflux pumps are over expressed in *A. baumannii* leading to effective fluoroquinolone resistance [117]. There is a speculation that yet unknown mechanisms also result in fluoroquinolone resistance as a study isolated fluoroquinolone resistant *A. baumannii* without any detectable changes in the genotype of the cells [139].

2.1.2.5 Colistin

Colistin is a cyclic cationic peptide that exerts its bactericidal action via binding to the lipid A. Being one of the very few drugs that are active against carbapenem resistant *A. baumannii* (CARB), colistin is often considered as the antibiotic of last resort [2]. Therefore, emergence of resistance against colistin is of grave concern. Modification of the target is the major mode of colistin resistance. *A. baumannii* often adds phosphoethanolamine to the lipid A as a modification mechanism [140]. Another proposed mechanism is the complete loss of polysaccharide, which is more common in laboratory isolates than the clinical strains [141].

2.1.2.6 Tetracyclines

Tetracyclines are also inhibitors of protein synthesis due to their affinity towards 30S ribosomal subunit. *A. baumannii* has achieved tetracycline resistance by expressing multiple Tet efflux

pumps. Apart from this, certain Tet proteins, especially the homologs of the *S. aureus* TetM protein, bind to the 70S ribosome and protect the ribosome from tetracycline binding [142].

2.1.3 Efflux pumps

As noted above, there are four broad mechanisms of antibiotic resistance, (i) alteration in membrane permeability to avoid antibiotic entry, (ii) mutations in the antibiotic targets, (iii) enzymatic modifications in antibiotic to inactivate it, and (iv) expression of efflux pumps that actively pump out antibiotic from the cellular milieu [143]. These efflux pumps prevent the antibiotic from reaching its target by expelling them against the concentration gradient representing a major mechanism of resistance [144]. These pumps are energized either by ATP lysis (primary efflux pumps) or by ion/proton gradients (secondary efflux pumps). These membrane-bound proteins can be classified according to their structural similarity, energy usage (electrochemical gradient or ATP hydrolysis) and substrate specificity. Five recognized families of bacterial efflux pumps are: (i) the ATP-binding cassette (ABC) superfamily, (ii) the resistance-nodulation division (RND) superfamily; (iii) the major facilitator superfamily (MFS), (iv) the multidrug and toxic compound extrusion (MATE) family, and (v) the small multidrug resistance (SMR) family (Figure 2.4) [12]. Efflux pumps belonging to all but ABC superfamily have been identified and characterized in *A. baumannii* (Table 2.2) [145].

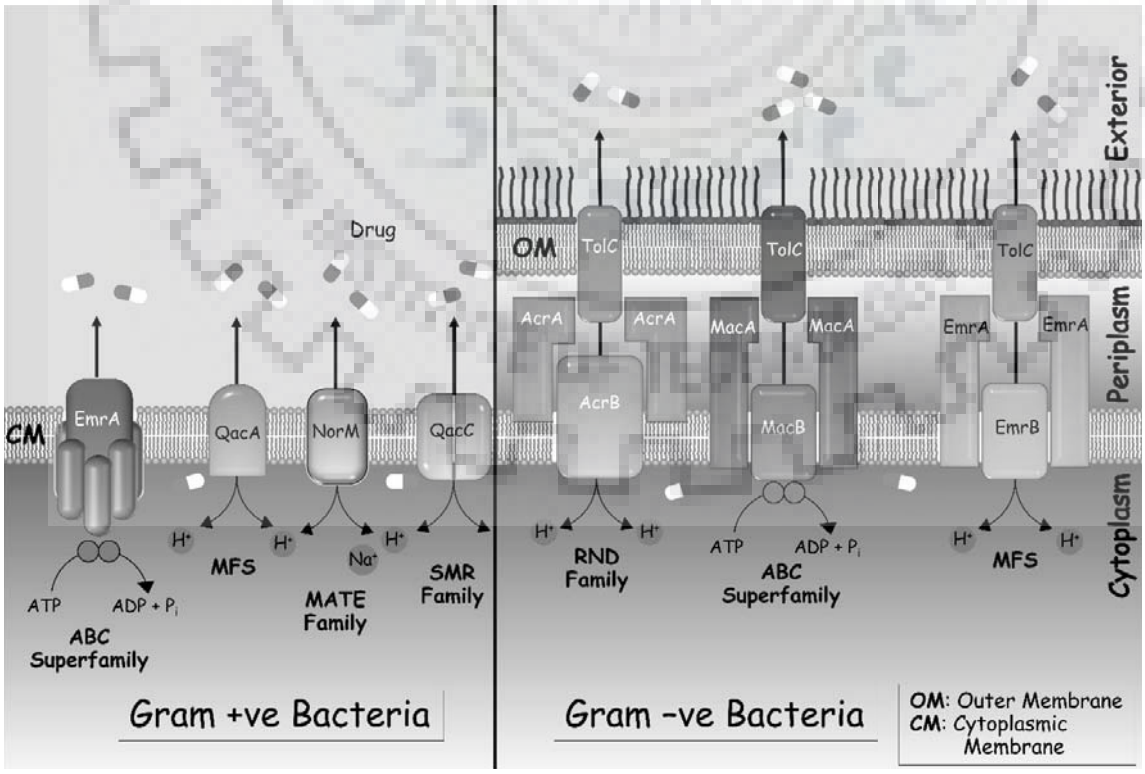

Figure 2.4. The five families of bacterial efflux pumps.

Table 2.2 A summary of efflux pumps characterized in *A. baumannii* and their substrates.

Efflux pump	Substrate antibiotics	Reference
RND superfamily		
AdeABC	Aminoglycosides, fluoroquinolones, trimethoprim, tetracyclines, macrolides, chloramphenicol, β-lactams	[146]
AdeIJK	β-lactams, quinolones, chloramphenicol, trimethoprim, fusidic acid, lincosamides, tetracyclines, sulfadoxine, macrolides	[146]
AdeFGH	Quinolones, chloramphenicol	[146]
EmrA	Aminoglycosides, imipenem, colistin	[147]
AbeD	Ceftriaxone, gentamycin, tobramycin, rifampin, erythromycin, ertapenem, amikacin	
MFS		
Tet(A) and Tet(B)	Tetracyclines, minocycline	[148]
AmvA	Amikacin, fluoroquinolones, erythromycin, novobiocin, tetracycline	[149]
AbaF	Fosfomycin	[123]
CraA	Chloramphenicol	[120]
MATE family		
AbeM	Aminoglycosides, Quinolones, β-lactams, imipenem, erythromycin, chloramphenicol	[115]
SMR family		
AbeS	Erythromycin, novobiocin, chloramphenicol, Chlorhexidine, fluoroquinolones,	[118]

2.1.4 Virulence factors

Acinetobacter baumannii is the most virulent species in the genus *Acinetobacter*, superseding *A. calcoaceticus*, *A. lwoffii*, *A. junii*, *A. baylyi* and *A. haemolyticus* [150]. However, studying *A. baumannii* virulence has been difficult due to unavailability of suitable infection models. Healthy

mice are generally resistant to infection by *A. baumannii* unless used at very high inoculum (>10^9 CFU), which is not very relevant physiologically [151,152]. Thus, artificial models for *A. baumannii* infections have been made in mice by using intraperitoneal route of infection or by using porcine mucin as an adjuvant [66]. Apart from this, induced neutropenia has also been used to simulate immunocompromised state [153]. Some studies have found that rats are susceptible to lethal *Acinetobacter* pneumonia without being immunocompromised [154]. Skin and wound infection models in rats have also been utilized to study the difference in virulence pattern of different strains [154].

The larva of wax moth *Galleria* has also found application as model for *Acinetobacter* infection. Studies have revealed that seemingly considered avirulent strains of *A. baumannii* (like ATCC 17978) caused lethal infections in *Galleria*. A very interesting observation made using this infection model is that the sessile bacteria obtained after disrupting the biofilms are more virulent than the planktonic forms [155]. *Caenorhabditis elegans* has also been used as an infection model is some studies [156]. Recently, *A. baumannii* virulence was studied in zebrafish larvae [157]. However, *A. baumannii* ATCC 17978 that is avirulent in mice and humans was found to be highly virulent in zebrafish, which casts a doubt over the suitability of this model. Unfortunately, *in vitro* assays for virulence factors correlate very poorly with clinical outcomes [155,158]. Therefore, more effort and sincere consideration is required while defining virulence factors in *A. baumannii*. With the availability of a suitable infection model, new and interesting information could be obtained on virulence of *A. baumannii* as the pathogen-host crosstalk remains largely unexplored in the bacterium [159].

Despite such setbacks, technological advances in genetics and molecular biology have helped immensely in studying *A. baumannii* virulence factors. Transposon libraries and whole genome sequencing is a great resource to identify potential virulence factors. Much of the new information on virulence factors of *A. baumannii* has emerged as a result (Table 1.3).

Motility is one of the virulence factors for this otherwise non motile bacterium [66]. *A. baumannii* is resistant to the action of disinfectants and is desiccation resistant. Under desiccation stress, the bacterium develops thick cell walls and stays viable on the surfaces for years [160]. Ethanol exposure has been reported to increase *A. baumannii* virulence in *Galleria* [161]. The bacterial capsule also serves as a primary virulence factor being responsible for bacterial defense against opsonization and complement mediated destruction [162,163]. The LPS has also been shown to have a major impact on virulence of *A. baumannii* [164,165]. However, its exact role is not so clear. Iron acquisition, biofilm formation, adherence, phospholipases, outer membrane vesicles

and altered penicillin-binding proteins (PBPs) are some other notable virulence factors in *A. baumannii*. The outer membrane protein A (OmpA/Omp38) has received considerable attention as a virulence factor as it is involved in adhesion to host epithelium, biofilm formation, and induction of host apoptosis and complement resistance.

Table 2.3. A summary of virulence factors described for *A. baumannii*. Taken with permission from [166].

Virulence factor(s)	Model	Outcome(s)	Reference
***In vitro* only**			
OmpA	Cell cytotoxicity	OmpA was administered to eukaryotic cells and induced cell death (note that endotoxin levels on the protein not reported)	[167]
OmpA	Complement lysis of OmpA mutant of *A. baumannii* 19606 vs. wild type	OmpA mutant resisted alternative pathway complement lysis in vitro	[168]
CpaA	Blood coagulation	Purified CpaA protease reduced coagulation of human plasma	[169]
BfmS	Various assays comparing BfmS mutant on ATCC 17978 background to the wild type	BfmS mutant had diminished biofilm formation, reduced adherence to cells, and sensitization to serum killing	[170]

Porins (CarO and OprD-like)	Growth rate, cytotoxicity of a clinical isolate vs ATCC 19606 strain (non-isogenic pair)	A clinical pan-drug-resistant isolate with reduced CarO and OprD-like expression grew more slowly and was less cytotoxic in a cellular assay	[109]
CFTR inhibitory factor (CiF)	Gene expression and function	Gene homologous to CiF from *Pseudomonas aeruginosa* is found in *A. nosocomialis* and *A. baumannii*	[171]
Biofilm gene (*LH92_11085*)	Characterization of gene expression and biofilm formation in *A. baumannii* MAR002	MAR002 overexpresses biofilm and has 25-fold increased expression of *LH92_11085*	[172]
Oxidative resistance (KatG and KatE)	Mutants of *A. baumannii* and *A. nosocomialis* tested *in vitro*	Mutants had increased susceptibility to oxidative killing and neutrophil killing	[173]
Adherence, invasion, and cytotoxicity	5 clinical isolates of *A. baumannii* and 6 clinical isolates of *A. pittii* tested in adherence, invasion, and cytotoxicity of lung epithelial cells	Adherence, invasion, and cytotoxicity not detected despite testing strains that	[174]

		had caused clinical disease	
***In vivo*–invertebrate models**			
NfuA (iron acquisition scaffold protein)	NfuA knockout in ATCC 19606 strain vs wild-type strain	Knockout strain more sensitive to oxidative stress and modestly less lethal in *Galleria*	[175]
EntA (enterobactin precursor synthetic gene)	EntA knockout in ATCC 19606 vs wild-type strain	Knockout strain modestly less lethal in *Galleria*	[176]
Superoxide dismutase (SOD)	SOD knockout in ATCC 17978 vs wild-type strain	Knockout strain more sensitive to oxidative stress and less lethal in *Galleria*	[177]
TonB (energetics of nutrient uptake)	TonB mutant of ATCC 19606 vs wild-type strain	Variable impact on lethality in *Galleria* but impacted adherence to epithelial cells	[178]
OXA-40 gene (carbapenemase)	Clinical isolates with or without the OXA-40 gene	OXA-40-containing isolates appeared to kill *Galleria* more slowly	[179]
AbuO (outer membrane protein)	AbuO knockout of *A. baumannii* AYE (origin unclear) with infection in *C. elegans*	Knockout displayed increased susceptibility to antibiotics and disinfectant and modestly reduced	[180]

		lethality in *C. elegans*	
SecA (iron acquisition)	Transposon mutant disruption of SecA in *A. baumannii* 19606	Mutant displayed modest reduction in lethality in *Galleria*	[181]
pmrB (colistin resistance due to altered LPS charge)	Clinical isolate with spontaneous *pmrB* mutation	Mutant displayed no reduction in strain fitness, growth, or lethality in *Galleria*	[182]
lpxACD, *pmrB* (colistin resistance due to loss of LPS synthesis genes [*lpx*] or altered LPS charge [*pmr*])	Clinical strains serially passaged on colistin	*lpxACD* mutants had growth defects and loss of virulence, whereas *pmrB* mutants had no change in growth or virulence in *Galleria*	[165]
Phospholipase D	Disruption of 3 phospholipase D genes in ATCC 19606	Reduced virulence in *Galleria*	[183]
Type VI secretion system (T6SS)	T6SS was compared in ATCC 17978, a nonclinical isolate (DSM30011), and 3 clinical isolates	Only the nonclinical isolate expressed a highly functional T6SS, which played a role in colonization in *Galleria*	[184]
SurA1 (surface antigen protein)	Knockout of SurA1 from *A. baumannii* CCGGD201101 (an isolate from diseased chicks)	Knockout had decreased growth rate, increased killing in serum, and decreased virulence in *Galleria*	[185]

AdeRS (Acinetobacter drug efflux pump regulator)	Deletion of AdeRS from *A. baumannii* AYE or S1	Knockouts had decreased biofilm formation; S1 but not AYE knockout had decreased virulence in *Galleria*	[186]
gacA and *gacS* (regulator genes), *abaI* (quorum sensing), *paaA* (phenylalanine catabolism)	ATCC 17978 and knockouts infected via blood in zebrafish embryos	Knockout strains had attenuated virulence in the zebrafish model, and the *paaA* knockout produced more phenylalanine, which triggered more neutrophil attraction to the site of infection	[157]
Multiple genes regarding stress response, osmotic stress, capsule, and LPS genes	Comparison of *Acinetobacter* strains in *Galleria*, including transposon disruptants	*Galleria* distinguished known avirulent (ATCC 17978) and virulent (5075) strains of *A. baumannii*, with the former causing some lethality and the latter 100% fatal. *A. baylyi* ADP1 was less virulent than *A. baumannii* ATCC 17978. A variety of genes disrupted by transposon insertion in *A. baumannii* 5075	[187]

		modulated mortality in *Galleria*.	
***In vivo*–nonlethal vertebrate models**			
Serum/complement resistance	Clinical isolates in Long-Evans rat soft tissue infection (subcutaneous)	Sensitivity to complement correlated with rapidity of soft tissue clearance in vivo	[154]
Phospholipase D	C57BL/6 intranasal lung infection (>3 × 108 inoculum) with transposon mutant clinical CSF isolate 98-37-09 vs wild type	Disruption resulted in serum sensitivity and no difference in lung bacterial density, but the mutant strain had lower bacterial blood density following pneumonia	[152]
Heme consumption	Nonlethal intranasal infection with *A. baumannii* LAC-4 clinical isolate, treatment with an inhibitor of heme acquisition vs placebo	Mice infected with LAC-4 and treated with heme acquisition inhibitor had modestly reduced lung bacterial density and bacteremia	[188]
PTK and EpsA (capsular polysaccharide regulators)	Long-Evans rat soft tissue infection with knockouts on *A. baumannii* 307-0294 clinical isolate background vs wild type	Disruption resulted in diminished growth in human ascitic fluid, human serum, and rat soft tissue	[162]

OmpA, LpsB, GacA	Transposon mutant library of *A. baumannii* ATCC 17978 infected intranasally into C57BL/6 mice	CFU differences at 24 h detected for strains with mutations of various genes, including *lpsB* (LPS biosynthesis), *ompA*, and *gacA*	[189]
LipA (lipase)	Tail vein infection of DBA mice made neutropenic with cyclophosphamide and infected with LipA knockout in *A. baumannii* ATCC 17978 vs wild type	LipA knockout demonstrated reduced competition fitness during nonlethal infection in mice	[153]
AdeABC and AdeIJK (efflux pump regulators)	intranasal and intraperitoneal infection of C57BL/6 mice with clinical isolate *A. baumannii* BM4587 or its isogenic Ade mutants	Increase in bacterial burden during intraperitoneal infection with the *adeABC* mutant, decreased with *adeIJK* mutant, no change after lung infection (intranasal)	[190]
Zur (zinc uptake regulator)	Intranasal infection of C57BL/6 mice with *A. baumannii* ATCC 17978 or a Zur knockout strain	No difference in lung bacterial burden, but liver burden lower for the Zur knockout strain	[191]
ZigA (zinc chaperone)	Intranasal infection of C57BL/6 mice with *A. baumannii* ATCC 17978 or a ZigA knockout strain	No difference in lung bacterial burden, but liver burden lower	[192]

		for the ZigA knockout strain	
FeoB (ferrous iron transport), DDC (cell wall cross-linking), PntB (pyridine metabolism), FepA (enterobactin receptor)	Intravenous infection in CBA/J mice with a transposon mutant library of *A. baumannii* ATCC 17978 treated with cyclophosphamide to make them neutropenic, using competitive growth by spleen bacterial density, or in human serum, as read-outs	Defects in these genes altered competitive growth/relative bacterial density in the spleens or serum	[193]
***In vivo*–lethal vertebrate models**			
Inoculum mixed with porcine mucin			
pmrB	Intraperitoneal infection in C57BL/6 mice with ≥108 organisms of *pmrB* mutant in *A. baumannii* ATCC 19606 vs wild type	*pmrB* mutant had lower bacterial density and less mortality	[194]
pmrB	Intraperitoneal infection in C57BL/6 mice with ≥107.9 organisms of a clinical spontaneous *pmrB* mutant of *A. baumannii* CR17 (cerebrospinal fluid strain) vs its pretreatment parent strain	*pmrB* mutant had reduced *in vivo* fitness in competition with wild type and lower mortality at low, but not high (i.e., >105) inocula	[195]
pmrA (altered LPS charge)	Intratracheal lung infection in Sprague-Dawley rats with a spontaneous mutant of *A. baumannii* respiratory clinical	*pmrA* mutant had reduced lethality	[196]

	isolate vs its pretreatment isogenic strain		
Ciprofloxacin resistance (mutation not described)	Intraperitoneal infection in C57BL/6 mice with 106, 107, or 108 *A. baumannii* clinical strain serially passaged in subtherapeutic ciprofloxacin vs its parent	Ciprofloxacin-resistant strain induced lower mortality	[197]
Acinetobactin (iron siderophore)	*Galleria* as well as intraperitoneal infection in C57BL/6 mice with 106 or 105 *A. baumannii* acinetobactin knockouts in ATCC 19606 vs wild type	Knockout strain induced lower mortality in *Galleria* and in mice	[198]
pglC (capsule)	Intraperitoneal infection in BALB/c mice infected with *pglC* knockout in ATCC 17978 vs wild type	Capsule-deficient mutant strain was avirulent compared to wild type	[199]
Omp33	Intraperitoneal infection in C57BL/6 mice with 106, 107, or 108 Omp33 knockout in *A. baumannii* 17978 vs wild type	Knockout strain displayed growth defect *in vitro*, and reduced lethality in mice	[200]
MapA (Omp33-36)	Intraperitoneal infection in C57BL/6 mice with Omp33-36 knockout in *A. baumannii* 17978 vs wild type	Knockout displayed a 12-h delay in death (but all mice died)	[201]
gacS (sensor kinase) and *paaE* (phenylacetic acid [PAA] catabolic pathway)	Intraperitoneal infection in BALB/c mice infected with knockouts in ATCC 17978 vs wild type	*gacS* and *paaE* mutant strains had attenuated mortality in mice	[202]

Infections in wild-type mice without porcine mucin

RecA (DNA damage repair)	Intraperitoneal infection in CD1 mice with 2 × 108 RecA knockout of *A. baumannii* ATCC 17978 vs wild type	RecA mutant was more sensitive to oxidative damage, macrophage killing, and heat exposure in vitro and caused mildly reduced lethality compared to wild-type strain (7% vs 20%)	[203]
pmrB, *lpxA*, *lpxA*, *lpxC*, *lpxD* (LPS genes)	Intraperitoneal infection in BALB/c mice with knockouts in *A. baumannii* 19606 vs wild type	*lpx* mutants had reduced in vitro growth while *pmrB* mutant did not; *lpx* mutants had attenuated virulence in both *C. elegans* and in mice, but *pmrB* mutant had attenuated virulence only in *C. elegans* and not in mice	[164]
OmpA	*In vitro* studies followed by tracheal aspiration pneumonia using Ab5075 strain in wild-type C57BL/6 mice	Transposon-disrupted OmpA strain was nonlethal in 5 mice, whereas 3 of 4 mice infected with wild-type died (note the small numbers of mice)	[204]

Capsule	Intraperitoneal infection of C57BL/6 mice with *A. baumannii* ATCC 17978 strains which were induced to overproduce capsule or strains with mutations in capsule production	Strains expressing enhanced capsule were resistant to serum/complement, and more lethal in mice	[163]
UspA (universal stress protein A)	Intranasal and intraperitoneal infection of C57BL/6 mice with UspA knockout in *A. baumannii* ATCC 17978 vs wild type	Modest difference in lung CFU during nonlethal infection and no significant difference in survival during intraperitoneal lethal infection	[205]

2.2 Small RNA

Bacteria regulate many physiological processes using non coding small RNA (sRNA) [206]. These post-transcriptional regulators of gene expression are 50-500 nt long and assist bacteria to adapt, survive and cope up with various environmental conditions (Table 2.4) [207]. Similar to their eukaryotic counterparts, miRNA, sRNA modulate the expression of their target mRNA by base pairing [208]. Based on their origin, sRNA could be *cis*- or *trans*-acting relative to their target mRNA. Most of the *cis*-encoded sRNA are present in vicinity of their target mRNAs, whereas the *trans*-encoded sRNA are generally present at sites away from the target mRNAs [206]. Unlike the *cis*-encoded sRNA, the *trans*-encoded sRNA display limited complementarity to their targets and often require a chaperone Hfq for stable interaction with their targets. This immensely expands their repertoire of targets and imparts them ability to be global regulators of physiological response [15].

Since the discovery of the first sRNA, MicF, hundreds of small RNA have been reported across the bacterial species. Initial attempts at identification of sRNA in bacteria were made using computational algorithms, exploiting the characteristics of these regulators [209]. With advancements in technology, microarray and deep sequencing have enabled identification of hundreds of sRNA in a relatively short period of time and with exemplary accuracy [210,211].

Table 2.4 Summary of functional roles of small RNA with a prototype example.

Prototype sRNA	Physiological role	Reference
Iron homeostasis		
RyhB	Expressed under iron limiting conditions, inhibits non-essential iron utilizing proteins, and activates ShiA for siderophore synthesis.	[212]
Membrane and surface remodeling		
MicF	Represses the expression of OmpF to regulate cellular response to change in osmolarity	[213]
MicA	Represses OmpA translation and curtails the *de novo* synthesis, represses PhoPQ two-component system	[214]
Motility and biofilm		
OmrAB, RydC, McaS	Prevent curli synthesis and stabilize biofilms	[215]
Regulation of transporters		
GcvB	Downregulates peptide transporters and other amino acid transporters, also targets a global transcription factor to adapt to nutrient availability	[216]
Sugar metabolism		
Spot42	Expressed in presence of glucose and repressed in presence of other carbon sources. Participates in catabolite repression.	[217]
SgrS	Targets uptake of phospho-sugars to prevent accumulation of nonmetabolizable sugars. Also codes for a protein SgrT which blocks glucose import.	[218]

Regulation of transcription factors		
DsrA, RprA, ArcZ	Activate the translation of rpoS mRNA (σ^S expression).	[219]
VqmR	Regulates VpdT, a transcription factor that controls biofilm formation.	[220]
Controlling virulence gene expression		
TarB	Indirectly regulates (through a cascade of effectors) chemotaxis and intestinal colonization by *V. cholerae*.	[221]
IsrJ and IsrM	Affect effector protein translocation into the host cells and pathogenesis.	[222,223]
InvR	Represses OmpD expression and affects virulence	[224]
Toxin-antitoxin systems		
IstR1	Represses a membrane inserting toxin TisB	[225]

The general mode of sRNA action is achieved by antisense base pairing to their target mRNA [226]. This interaction either leads to inhibition or activation of expression of the target gene. The effective base pairing is determined by the sequence complementarity but also depends on other factors like a stable stem-loop structure, a U-rich tract and a seed region of initiation of interaction [227]. For the trans-encoded sRNA, Hfq assisted base pairing is a common phenomenon. A U-rich sequence provides for Hfq interaction and/or stability of sRNA [228]. This interaction stabilizes the sRNA and promotes base-pairing with the targets. Although most of the sRNA exert a negative regulation, there are certain sRNA that activate the expression of target genes.

2.2.1 Repression of gene expression by *trans*-encoded sRNA

Most of the reported sRNA negatively regulate the expression of their targets. For efficient translation, the Shine Dalgarno (SD) sequence on the mRNA is recognized by the anti-SD sequence on the 16S rRNA. This base-pairing forms the basis of translation initiation, a rate limiting step in bacterial gene expression [229]. Any hindrance to the SD: anti-SD base pairing inhibits translation of mRNA [230]. Under stress, bacteria downregulate the expression of

metabolic genes to favour survival and sRNA assist in inhibition of translation by disturbing the SD: anti-SD base pairing and a few other mechanisms.

2.2.1.1 Base-pairing with RBS of mRNA

Complementary base-pairing between sRNA and the boundary of RBS prevents 30S ribosome interaction and initiation of translation. A majority of regulatory sRNA exert their negative regulation through this mechanism. This base-pairing often occludes the SD sequence and/or the AUG start codon. In a few cases, this pairing extends to nucleotides downstream the first codon as well [231]. RyhB is a 90 nt long sRNA in *E. coli* that follows this mechanism of regulatory action [232]. This small RNA is negatively regulated by the ferric uptake regulator (Fur). Under iron abundance, Fur represses the expression of RyhB, however, when iron is limiting, the RyhB levels increase (Figure 2.5). RyhB negatively regulates the expression of numerous iron-metabolizing non-essential genes. With assistance from Hfq, RyhB downregulates the expression of methionine sulfoxide reductase (MsrB), by interacting with two different sites in the *msrB* mRNA [233]. Base-pairing on the first site inhibits the entry of 30S ribosome, whereas interaction with a second site, that includes the SD sequence, signals RNase E mediated degradation of RyhB-*msrB* duplex.

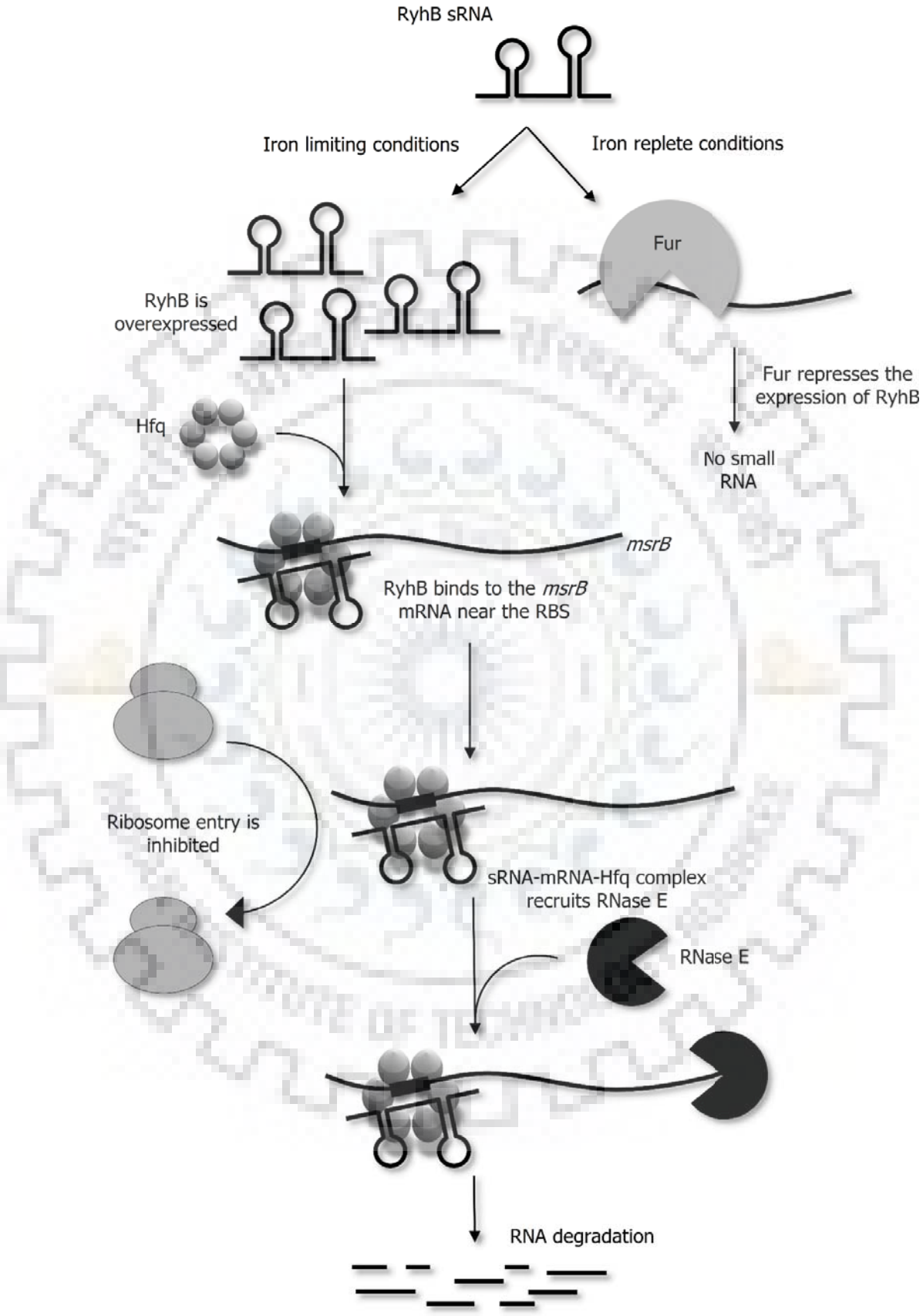

Figure 2.5. sRNA mediated repression of gene expression by masking RBS and recruitment of RNase E.

2.2.1.2 RNase recruitment and degradation of target RNA

Inhibition of translation by sRNA often leads to degradation of the sRNA-mRNA duplex by ribonucleases. In *E. coli*, RNase E is the major ribonuclease involved in sRNA-mRNA turnover [234]. The sRNA are generally protected from RNase E mediated degradation by Hfq. However, Hfq dependent sRNA-mRNA duplex formation helps in recruitment of RNase E and subsequent duplex degradation. Hfq interacts with the unstructured C-terminus of RNase E, leading to the formation of a complex including the sRNA-mRNA duplex [235]. This increases the local concentration of RNase E, facilitating its attack on the double stranded RNA. This scheme is common for many sRNA like RyhB, SgrS, OmrA and MicA. Apart from RNAse E, other ribonucleases like RNase Z and RNase III are also involved in RNA turnover [236,237].

2.2.1.3 Interference by Hfq

Another mechanism of translational repression is the recruitment of accessory proteins like Hfq in the vicinity of sRNA-mRNA binding [238]. This leads to interference in ribosome recruitment and inhibition of translation. The Spot42 small RNA in *E. coli* regulates the expression of *sdhC* mRNA in a similar manner [217]. The sRNA binds about 48 nt upstream the start codon with no direct interaction with the RBS. However, its interaction with mRNA recruits Hfq which binds to the mRNA at the site where S1 ribosomal protein interacts. This leads to inhibition of translation initiation and repression of *sdhC* (Figure 2.6).

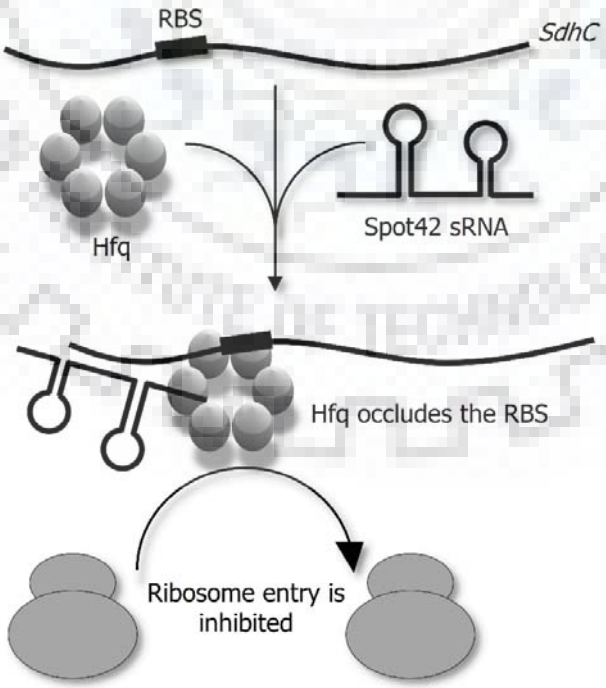

Figure 2.6. sRNA mediated repression of gene expression by recruitment of Hfq for occlusion of RBS.

2.2.2 Activation of gene expression by *trans*-encoded sRNA

Contrary to a majority of sRNA that negatively regulate the expression of their targets, some sRNA positively regulate the expression of their targets leading to increased expression of the mRNA.

2.2.2.1 Stabilization of target mRNA

mRNA is unstable and absence of a sRNA regulator might make it further unstable by exposing the mRNA to the ribonuclease attacks. Pairing between sRNA and mRNA can prevent degradation by ribonucleases. Such a scheme is observed in case of SgrS sRNA in *E. coli* and *Salmonella* sp. [239]. This small RNA is responsible for regulation of glucose phosphate induced stress. A phosphatase responsible for removal of phosphate from sugars is coded by *yigL* gene. SgrS base pairs with the *yigL* mRNA. This interaction masks an RNase E sensitive site on the mRNA which prevents the progression of RNase E. The SgrS pairing also exposes RBS by disrupting an intrinsic inhibitory structure, thereby facilitating *yigL* expression [240] (Figure 2.7).

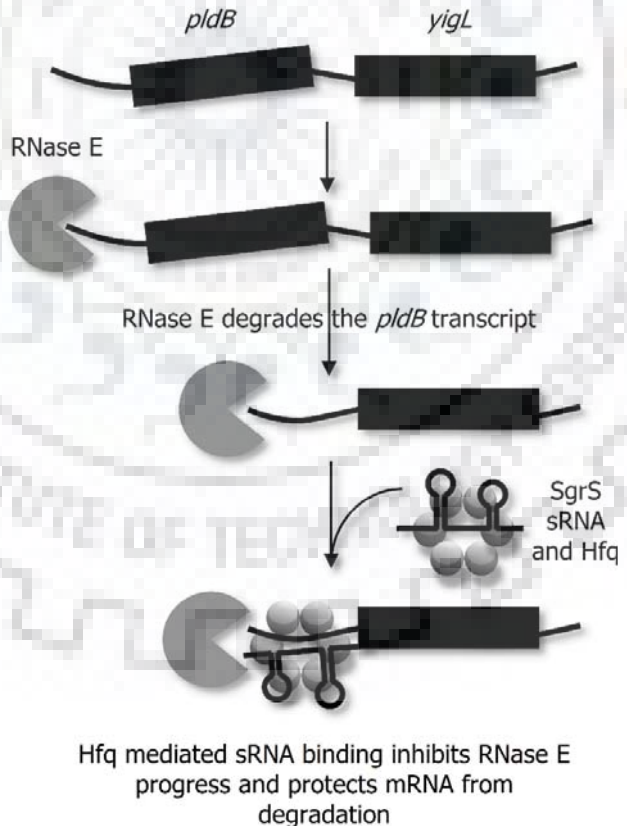

Figure 2.7. sRNA mediated activation of expression by protection of mRNA transcript from RNase E.

2.2.2.2 Initiation of translation

The 5' UTR of an mRNA may contain a sequence complementary to the mRNA resulting in a secondary structure that sequesters the RBS. sRNA can bind to this leader sequence, releasing the RBS and leading to subsequent translation [241]. The expression of σ^S, a stationary phase sigma factor in *E. coli* is dependent on this mechanism [242]. The 5' UTR of *rpoS*, the gene coding for σ^S, folds into a complex hairpin structure, sequestering the RBS. This secondary structure is recognized by the RNase III as a substrate. However, the RNase mediated degradation is prevented by at least three different sRNA, DsrA, RprA and AcrZ [219]. These sRNA bind to specific sites on the rpoS mRNA, preventing the folding of 5' UTR into the inhibitory secondary structure and exposing the RBS (Figure 2.8).

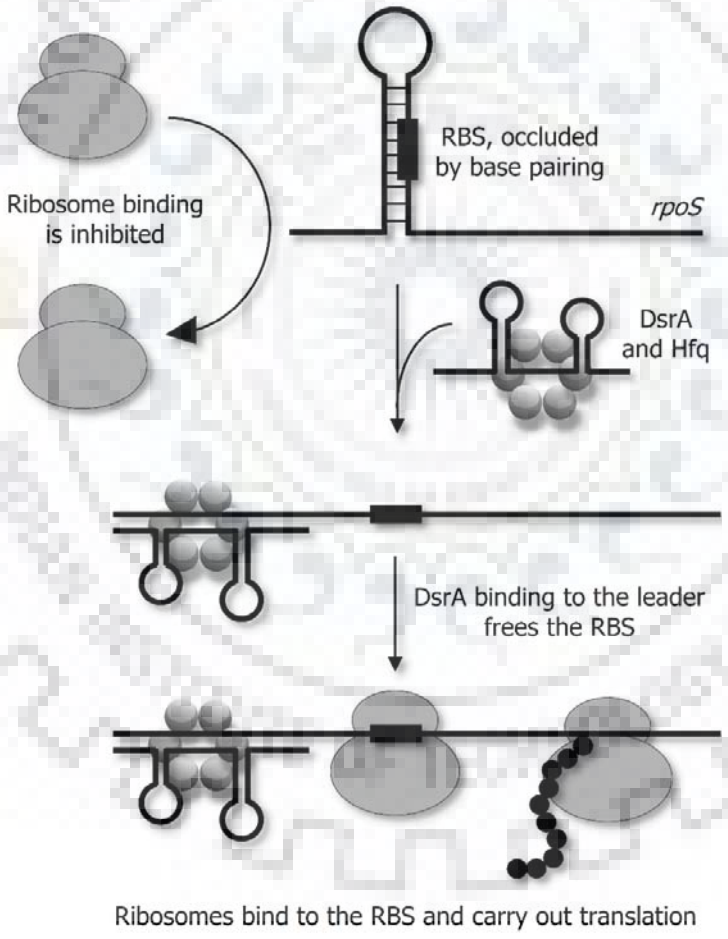

Figure 2.8. sRNA mediated activation of gene expression by melting the inhibitory secondary structure to allow ribosome binding.

2.2.2.3 Transcription antitermination

Although *rpoS* activation is achieved by the so-called anti-antisense mechanism, a new mode of sRNA dependent *rpoS* activation has recently been reported. This antitermination system

operates to inhibit Rho-dependent termination of transcription in the 5' UTR of *rpoS* [243]. Rho can potentially bind to a Rho loading site in the 5' UTR of *rpoS*, leading to premature transcription termination and repression of expression. However, the three sRNA that bind to the *rpoS* leader, DsrA, ArcZ and RprA, bind in proximity to this Rho loading site. This prevents the Rho dependent transcription termination and activates the expression of *rpoS*.

2.3 Hfq

Hfq was first identified as the host factor required for Qβ phage replication in *E. coli* [244]. It is a hexameric protein that serves as a central sRNA chaperone in many Gram negative bacteria [245]. Hfq is related to the eukaryotic Sm or the archaeal Lsm proteins which carry a Sm domain that is involved in RNA binding [246]. Hfq assists small RNA with limited complementarity to bind to its cognate target mRNA, making it an important factor in sRNA mediated regulatory circuitry [247]. In fact, deletion or inactivation of *hfq* results in pleotropic affects reflecting its importance in sRNA mediated regulation [17]. In addition to sRNA, Hfq interacts with many protein partners helping in their recruitment.

2.3.1 Hfq interacts with sRNA and proteins *in vivo*

Various immunoprecipitation experiments have revealed that Hfq binds to a host of sRNA and proteins *in vivo* [248]. *In vitro* studies have confirmed that it binds to sRNA rather strongly. Typically, hundreds of sRNA are available for binding at a particular moment and Hfq protein pool is saturated. Hfq, therefore, serves as a platform on which the interacting RNA partners meet. A molar excess of Hfq would be problematic, since it is rarely possible for two RNAs to be present simultaneously on an Hfq hexamer [249]. Several proteins also co-purify with Hfq, suggesting protein-protein interactions [250]. Ribosomal proteins, helicases, RNases, H-NS, poly-A-polymerase are some of the proteins that have been found associated with Hfq [251–255]

2.3.2 Binding surfaces on Hfq structure

The structurally important part of the Hfq sequence is conserved and a consensus structure has been determined by crystallographic studies [256]. The N-terminus of Hfq carries the Sm domain that allows it to form hexamers with a doughnut like structure that presents two distinct faces for RNA binding (Figure 2.9). The distal face preferentially binds to the polyA-tract in RNAs (AAYAAYAA or ARNx), with up to 18 nt accommodated on the hexamer [257]. These motifs are generally found in the 5' end of the target mRNAs. The proximal face of Hfq binds shorter A/U-rich sequences and its affinity is increased by the 3'-OH [258].

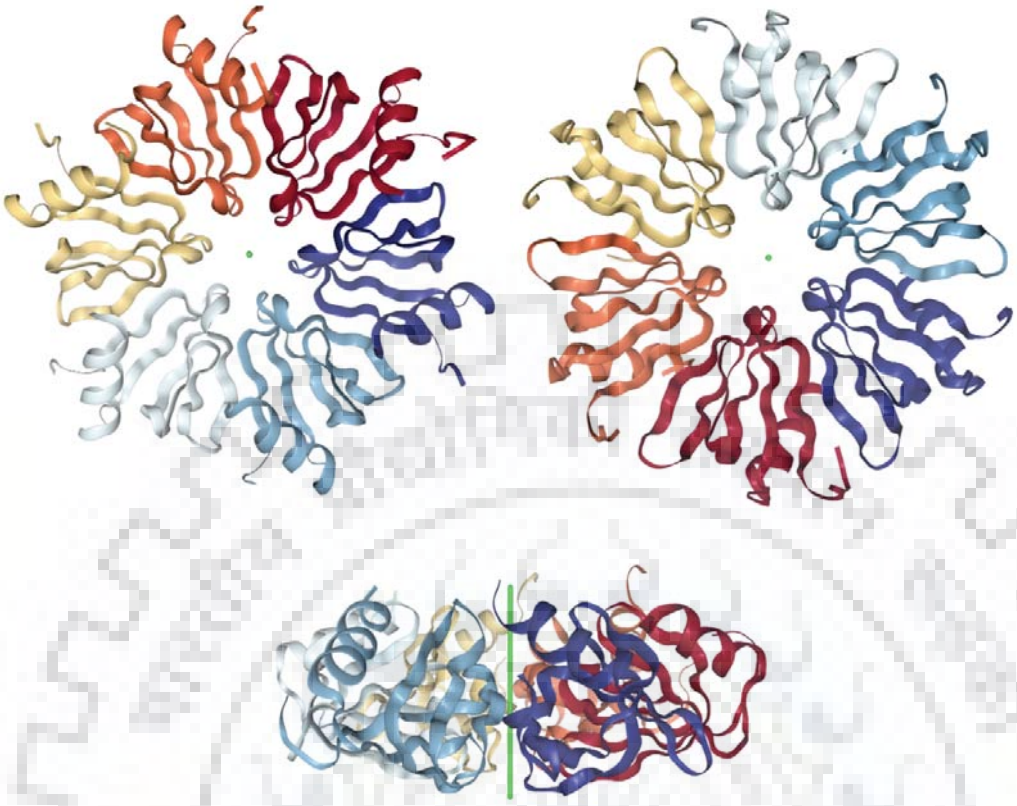

Figure 2.9. *E. coli* Hfq and its different faces for RNA interaction (clockwise from the top left) proximal face, distal face and the rim [259].

This also suggests how sRNA bind with U-rich internal sequences anchored by a terminator and also explain the protection from 3' exonucleolytic degradation [260]. The lateral rim of Hfq also presents another surface for RNA binding. The region consists of arginine residues which assist in RNA binding [16]. The residues important for RNA binding have been determined by mutational analysis. Beyond the core Sm motif (after 66 amino acid residues), the length and composition of C-terminus of Hfq is highly variable. The residues in the C-terminus do not conform to any secondary structure and are thought to impart flexibility to Hfq to interact with the protein and RNA partners. Studies with C-terminal truncated Hfq proteins have yielded controversial results, however, the importance of C-terminus in cycling of sRNA is now universally accepted [261–264].

2.3.3 RNA binding and sRNA-mRNA pairing

Typically, sRNA are preferentially bound to the proximal face with the mRNAs preferentially taking up the binding site on the distal face [265]. However, there is no rule of thumb. A model for sRNA binding to the Hfq has been designed. mRNA binds to the Hfq distal face through its A-rich sequences and the sRNA binding begins at the proximal face and the lateral rim. For Hfq

mediated assistance in base pairing, the target sequence in mRNA and the seed sequence in the sRNA should not be bound to Hfq but present as free sequences to interact. This is assisted by folding changes induced by Hfq and the arginine patches on the rim could promote the alignment of the seed and the target single strands [266]. This model is in line with the information obtained from a recent co-crystal structure of RydC-Hfq (Figure 2.10) [267]. In case of *rpoS*/DsrA interaction, based in SHAPE and SAXS analysis, a specific model of Hfq action has

Figure 2.10. *E. coli* Hfq with RydC sRNA [267].

been proposed [268]. After base-pairing. sRNA-mRNA complex dissociates from the Hfq by RNA-driven cycling [265]. The progression of the duplex itself may also disrupt the RNA-Hfq contacts [16].

There are two different models for describing how Hfq promotes this RNA pairing. The first takes in to account the binding rates of sRNA-mRNA pairs, which are low but increase dramatically in presence of Hfq [265,269,270]. The other model suggests that Hfq causes a decreased K_d values of sRNA-target RNA pairs [271]. It is still debatable as to which model is better.

2.3.4 Cycling of RNA on Hfq

For Hfq to assist base pairing of multiple sRNA and mRNA pairs, a rapid exchange of RNAs is required. There are hundreds of RNA with nanomolar K_d values and considering limited cellular pool of Hfq molecules, rapid and efficient cycling of RNA is very important [272]. The *in vivo* time for sRNA to exert its effects on targets is typically 1-2 minutes which cannot be explained with *in vitro* identified tight sRNA-Hfq binding and slow dissociation [265]. It is unlikely that a passive cycling, where a particular RNA must dissociate before binding of an incoming RNA, would be able to account for the fast regulation seen *in vivo* as it is limited by slow first-order dissociation. However, an active cycling model, where the incoming RNA competitively binds to an RNA-Hfq complex and replaces the resident RNA (following second order kinetics), can match with the time frame of *in vivo* regulation. The active cycling model fits the properties of a homohexamer too. RNA contacts a particular monomer at a time and at the same time another monomer is available for the competitive incoming RNA to bind. *In vivo* studies support that active cycling works best when Hfq is limiting [249,273]. The importance of cycling was addressed in a theoretical study aimed to address the complexity induced by numerous sRNA and target mRNAs vying for Hfq chaperoning [274].

2.3.5 The C-terminus of Hfq

The C-terminus of Hfq doesn't conform to a fixed secondary structure. Moreover, a great deal of variation in the size of the C-terminus is observed. Early attempts to determine its significance resulted in studies reporting its importance in hexamer stabilization and nucleic acid binding [275]. There are conflicting reports on the utility of this C-terminal region in sRNA-Hfq based regulation. Hfq truncations lacking the C-terminus were found to be deficient in autoregulation and unable to promote RyhB dependent repression of *sodB* in *E. coli*. The shorter versions were also unable to activate *in vivo* expression of *rpoS*, which was achieved by the longer versions [261]. However, reports also suggest that the C-terminus plays only a minor role, if any, in sRNA based riboregulation. There was no significant difference in binding of sRNA to *rpoS* leader in presence of truncated Hfq *in vitro* [262]. In a more classical approach, based on genetic

complementation, the *E. coli hfq* null mutant was successfully complemented by Hfq with varying length of C-terminus [276]. Such studies suggest that the C-terminus of Hfq could be dispensable in terms of phenotypic effects. Recent studies have, however, revealed, that the flexible nature of C-terminus allows for the cycling of sRNA on the Hfq core. The acidic tip of the C-terminus competes for binding to the basic residues on the rim and helps the duplex RNA to detach from the chaperone surface [263,264].

2.3.6 Hfq and pathogenic bacteria

Much information on functional importance of Hfq has been derived from studying the phenotype of *hfq* deletion mutants. The impact of loss of *hfq* has been studied in various pathogenic bacteria in terms of growth, biofilm formation, motility, stress adaptation and virulence [17]. The deletion of *hfq* results in reduced growth in most of the cases (Table 2.5). The cells are often susceptible to stress conditions when *hfq* is deleted. This extends to virulence potential of the pathogens as most of them display reduced virulence in infection models and mammalian cell lines. Even antibiotic resistance profile of some pathogens is affected. These observations stem from the importance of sRNA-based regulation that is active in these pathogens. The impact of Hfq on virulence of pathogenic bacteria warrants the case for designating Hfq itself as an important virulence factor [277].

Table 2.5. Characteristics of *hfq* deletion mutants in various bacterial pathogens.

Bacterium	Growth defect	Impaired motility	Increased sensitivity to									Impaired biofilm formation	Reduced virulence	Ref
			Starvation	Ethanol	Oxidative stress	Acid stress	High Osmolarity	Detergent	Antimicrobial	Iron limitation	Heat stress			
B. abortus	+		+		+	+							+	[278]
B. cepacia	-	+	+		+		+				+		+	[279]
EHEC	+	+				+								[280,281]
UPEC	-	+			+	+			+			+	+	[282]
F. tularensis	+						+	+			+		+	[283,284]
L. pneumophila	+									+			-	[285]
M. catarrhalis	+				+		+							[286]
N. meningitidis	+		+		+		+	+	+				+	[287,288]
N. gonorrhoeae	+	-											-	[289]
P. aeruginosa	+	+	+		+								+	[290]
S. flexneri													+	[291]
S. sonnei													+	[292]
S. typhimurium	+	+											+	[293–295]
S. enteritidis	+	-				+			+		+		+	[296]
V. cholerae	+												+	[297]
V. parahaemolyticus	+													[298]
Y. pestis	+		+		+		-		+		+		+	[299]
L. monocytogenes	-		+	+	-	-	+	+	-		-		+	[300]
S. aureus	-				-		-				-			[301]
V. pseudotuberculosis	-	-			+								+	[302,303]
S. maltophilia	+	+		-	-		-		+			+	+	[304]
C. difficile	+				+					+		+		[305]
H. ducreyi													+	[306]
C. sakazakii	+	increase			+								+	[307]
K. pneumoniae					+						+		+	[308]
F. novicida	+				+	+	+				+	+		[309]
B. pertussis	+												+	[310]
H. influenzae	-												+	[311]
B. subtilis	+													[312]

3 Objectives

Acinetobacter baumannii has established itself as a highly successful nosocomial pathogen owing to its formidable ability to rapidly develop drug resistance and survive on inanimate surfaces for long durations. Although the bacterium had been known for decades, it came to the fore after multiple outbreaks of drug resistant infections and isolation of pan-drug resistant strains worldwide. For better understanding and tackling infections caused by *A. baumannii* it is important to study the mechanisms of resistance, virulence factors and regulation of their expression. Small RNAs are regulators of gene expression at the post-transcriptional level and have been deemed important in bacterial physiology. With the aim explore sRNA landscape in *A. baumannii*, our research group's previous endeavor resulted in identification of 31 candidate small RNAs in this bacterium. Out of these 31, three were validated by Northern blotting and one of those three, AbsR25 was studied in detail. The novel sRNA, AbsR25, was determined to be involved in regulation of efflux pump genes. However, the physiological roles of these putative efflux pump genes in *A. baumannii* was not known. Moreover, an important mediator of sRNA-mRNA interaction, the RNA chaperone protein Hfq, was not characterized in *A. baumannii*, whose presence was indicated by prediction of trans-acting sRNA.

Apart from AbsR25, 11 and 28, our group's previous report on small RNA in *A. baumannii* predicted 28 more candidate sRNA. Since sRNA are important regulators of stress response in Gram negative bacteria and one of the sRNA validated in the lab was implicated in regulation of efflux pumps, the characterization of the rest of the candidate sRNA was warranted. Interestingly, the sequences of a few predicted sRNA were specific for *A. baumannii* which could be exploited as markers of this bacterium. PCR based methods have been designed for rapid detection of pathogens with high accuracy using such marker sequences as conventional methods of pathogen detection are often time consuming and inaccurate. However, a non-coding region-based detection method had not been designed for identification of *A. baumannii*.

Thus, based on the avenues opened up by the previous studies carried out in the lab, four major objectives were decided to be achieved in this work:

1. To characterize the RNA chaperone protein, Hfq, in *A. baumannii.*

2. To characterize A1S_1331, the primary target of AbsR25 sRNA.

3. To validate and characterize a novel sRNA AbsR1 in *A. baumannii.*

4. To develop a PCR based assay for detection of *A. baumannii* on clinical surfaces.

4 Experimental procedures

4.1 Bioinformatic prediction of Hfq homolog in *Acinetobacter baumannii*

Bioinformatic prediction of Hfq homolog in *Acinetobacter baumannii* was made using sequence similarity search tools like BLAST and ClustalW. The sequence information of the complete proteome and genome of *Acinetobacter baumannii* ATCC 17978 is available over the NCBI server. The sequence of Hfq proteins from different representative Gram-negative bacteria, including closely related *Acinetobacter baylyi*, *Pseudomonas aeruginosa* and *Moraxella catarrhalis* was analyzed by performing multiple sequence alignment using the EBI ClustalW tool (http://www.ebi.ac.uk/Tools/msa/clustalw2). The alignment was visualized using the ESPript server (http://espript.ibcp.fr/ESPript/ESPript/).

4.2 Homology modelling of *A. baumannii* Hfq

The sequence of *A. baumannii* Hfq, A1S_3785, was retrieved from the NCBI protein database. The sequence was used as a query to perform a BLAST search against the PDB database. The nearest homolog, the *P. aeruginosa* Hfq was selected as a template and the information was submitted to SWISS-MODEL for modelling (https://swissmodel.expasy.org/). The PDB file generated from SWISS-MODEL was downloaded and viewed using PyMOL (https://www.pymol.org/).

4.3 Cloning of Hfq and the truncated versions

The protein annotated as A1S_3785 was designated as Hfq in *A. baumannii* as it was evident from the sequence alignment that it was the Hfq homolog in *A. baumannii*. The gene coding for this protein, *hfq*, was amplified using the primers OligoRPT22 and OligoRPT23. The primers introduced restriction sites for PscI and XhoI restriction enzymes. PscI is an isocaudomer of NcoI and was used instead in the forward primer to avoid a frameshift mutation in the cloned sequence. The plasmid pET-28a plasmid (Novagen, Merck, USA) was selected for recombinant Hfq expression due to presence of C-terminus hexa-histidine tag for ease of purification. The *hfq* PCR product was digested with PscI and XhoI (Table 4.1). However, the plasmid pET 28 was digested with NcoI and XhoI restriction enzymes (Table 4.2).

Table 4.1 Restriction digestion of *hfq* PCR product.

Component	Amount
10X Tango buffer	2.0 µl
PCR product	500 ng
PscI	0.5 µl
XhoI	1.0 µl
Nuclease free water	To make up 20 µl

Table 4.2 Restriction digestion of pET 28 plasmid.

Component	Amount
10X Tango buffer	4.0 µl
pET 28	500 ng
NcoI	0.5 µl
XhoI	0.5 µl
Nuclease free water	To make up 20 µl

The digestion was carried out for 2 hours at 37°C. 0.5 µl of FastAP® alkaline phosphatase was added to the plasmid digestion mixture and incubated at 37°C for 15 more minutes. The enzymes were inactivated by incubation at 75°C for 5 minutes. The digested products were gel purified using MinElute kit (Qiagen). A typical ligation mixture was prepared as follows (Table 4.3):

Table 4.3 Ligation of *hfq* PCR product and pET 28 plasmid.

Component	Amount
10X T4 ligase buffer	1.5 µl
Digested PCR product	A 1:3 molar ratio (plasmid: insert) with at
Digested pET 28	least 50 ng DNA
10 mM rATP	1.5 µl
T4 DNA ligase	1.0 µl
Nuclease free water	To make up 15 µl

Ligation was carried out at 22°C for 2 hours. The ligation mixture was transformed into electrocompetent *E. coli* DH5α and the colonies were selected on kanamycin (50µg/ml) containing medium. Plasmids were isolated from the colonies obtained and were digested by XbaI (NcoI site was destroyed due to use of PscI in cloning) and XhoI enzymes. The recombinant plasmid and the strain thus obtained was designated pRPT2 and RPT 150, respectively. The plasmid was transformed into *E. coli* BL21 DE3 for protein expression and the strain was

designated as RPT 125. In a similar manner Hfq_{66}, Hfq_{72} and Hfq_{92} were also cloned in pET-28 plasmid. The forward primer for all the constructs was the same however reverse primers (carrying XhoI site) were OligoRPT24, OligoRPT25 and OligoRPT26, respectively. The plasmids coding for Hfq_{66}, Hfq_{72} and Hfq_{92} were named as pRPT3, pRPT4 and pRPT5, respectively and the *E. coli* DH5α strains carrying these plasmids were designated as RPT 180, 115, 181, respectively.

4.4 Heterologous expression of recombinant Hfq and its variants

The full length and truncated Hfq proteins were expressed as hexa-histidine derivatives in *E. coli* BL21 DE3. A single colony was picked from LB agar plate supplemented with 50μg/ml kanamycin and inoculated into LB broth containing similar amount of antibiotic. The cells were allowed to grow overnight at 37°C with 250 rpm agitation. The overnight culture was diluted to 1% in fresh medium containing kanamycin and incubated at 37°C with 250 rpm agitation till OD_{600} of the suspension reached 0.8. The culture was induced with the addition of 0.2 mM isopropyl β-D-thiogalactopyranoside (IPTG) and further incubated for 4 more hours at similar conditions. After four hours of incubation, the cells were harvested by centrifugation and the expression of protein was checked by boil prep SDS-PAGE. The samples were resolved on a Tricine-SDS-PAGE, which offers better resolution than conventional SDS-PAGE that involves glycine instead of tricine. The composition of Tricine-SDS-PAGE buffers and gel can be found in Appendix I.

The cells were subsequently resuspended in lysis buffer (Appendix I) and lysed in a high-pressure cell disruptor (Constant systems) using manufacturer recommended settings. The cell lysate was centrifuged at 15000 g for 30 minutes to remove cellular debris. The clear supernatant was collected for purification of the recombinant protein.

A chromatography column was prepared using a 20 ml syringe and Ni-NTA matrix (Qiagen). The column was washed with MilliQ water before being equilibrated with equilibration buffer (Appendix I). The cell lysate was added to the column and incubated overnight at 4°C on a rotatory gyromixer (Tarsons, India). After incubation the flow through from the column was collected and stored at 4°C. The column was washed with 10-bed volumes of wash buffer I followed by wash buffer II (Appendix I). The wash fractions were also saved and stored at 4°C. After washing the column, the pure protein was eluted in elution buffer (Appendix I) in 1 ml fractions. The flow of the column was throughout maintained using a flow controller. The fractions were analyzed on 10% Tricine-SDS-PAGE and the fractions containing the His-tagged

protein were pooled. The pooled fractions were dialyzed against a dialysis buffer (Appendix I) to remove imidazole. After overnight dialysis at 4°C, the protein sample was concentrated by passing it through a 3 kDa (Millipore) cut-off filter. The purified and concentrated protein was stored at -20°C until further use.

4.5 Gel retardation assay

Hfq is an RNA chaperone and therefore displays an *in vitro* RNA binding activity. To assess this RNA binding ability, gel-retardation assays are generally performed. The electrophoretic mobility shift assay (EMSA) is a gel retardation assay where protein-RNA complexes are resolved on a low percentage native gel, the mobility of the components being assisted by electric charge. At a set end point the movement of RNA alone is compared with the movement of protein-RNA complex to determine the binding of protein to the RNA molecules. A retarded movement of RNA in a complex with protein signifies an affinity between the protein and the RNA molecule. The whole EMSA procedure can be divided into different stages.

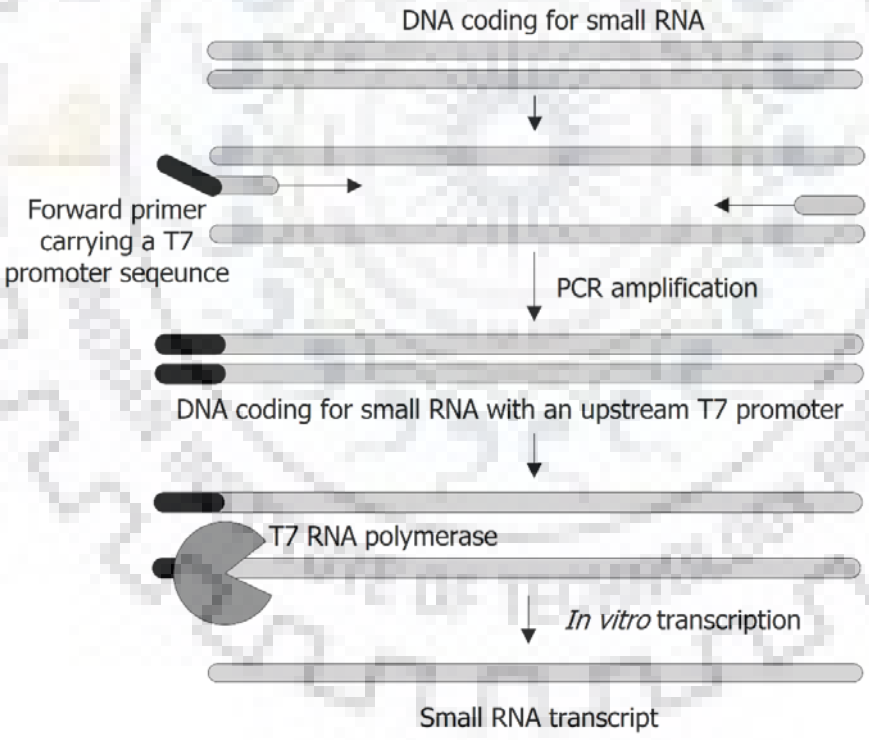

Figure 4.1 Preparation of small RNA transcript for gel retardation assay.

4.5.1 Preparation of DNA template

The sRNA-protein interaction study requires purified sRNA in copious amounts. A PCR based strategy was designed to prepare target sRNA in large amounts. The forward primer carries the T7 promoter sequence which is added just before the sRNA coding gene. This allows for production of RNA using T7 RNA polymerase in an *in vitro* transcription reaction (Figure 4.1).

Using this strategy, DNA templates for small RNAs AbsR1, AbsR25, MicA and DsrA were prepared using the primers listed in Appendix V. The PCR reaction was carried out as follows (Table 4.4):

Table 4.4 Reaction mixture for amplification of DNA coding for small RNA.

Component	Amount
10X Ex Taq buffer	5.0 µl
2 mM dNTPs	5.0 µl
10 µM forward primer	1.0 µl
10 µM reverse primer	1.0 µl
Template DNA (gDNA)	Upto 10 ng
Ex Taq DNA polymerase	1.0 unit
Nuclease free water	To make up 50.0 µl

The PCR product was gel purified using QiaMinelute kit (Qiagen, USA) and was used for transcription.

4.5.2 *In vitro* transcription of DNA template

Once a purified DNA template was obtained, *in vitro* transcription was carried out. The T7 RNA polymerase transcribes linear DNA template carrying T7 promoter region to produce multiple copies of small RNA. A typical reaction mixture for *in vitro* transcription is as follows (Table 4.5):

Table 4.5 *In vitro* transcription using T7 RNA polymerase.

Component	Amount
5X Transcription buffer	10 µl
10 mM rNTPs solution	10 µl
Template DNA	1 µg
T7 RNA polymerase	30 units
RNase inhibitor	50 units
DEPC treated water	To make up 50 µl

After incubation at 37°C for 2 hours, 2 µl of DNase I (1 U/µl) was added and the mixture was further incubated at 37°C to eliminate the DNA template. The DNase I reaction was stopped by adding EDTA at a final concentration of 2.5 mM and inactivating the enzyme by 10 minutes incubation at 70°C.

4.5.3 Purification of small RNAs

The small RNAs thus obtained were purified using QIAquick nucleotide removal kit that is specially used for purification of small length nucleotides and gives higher yield. The purification was carried out according to the manufacturer's instructions and the purified small RNAs were run on 2% agarose gel to check. The sRNAs were quantified using a Nanodrop spectrophotometer.

4.5.4 Binding and resolving the RNA-protein complex

To assess the sRNA-Hfq interactions by EMSA, a specialized EMSA kit from Life Technologies, USA was utilized. The kit contains a binding buffer, a SYBR Green based staining solution for nucleic acids and a SYPRO Ruby based staining solution for proteins. A typical binding reaction was arranged as follows (Table 4.6):

Table 4.6 Reaction mixture for gel retardation assay (EMSA).

Component	Amount
5X binding buffer	2 µl
RNA sample	2 pmol
Hfq protein/BSA	Variable
RNase-free water	To make up 10 µl

BSA was added to one of the reactions to check for any non-specific sRNA-protein interactions. 8% native gel was prepared for resolving the sRNA-Hfq complexes (Appendix I). The gel was pre-run in 0.5X TBE at 100V till the current reached 10 mA. The samples were mixed with 6x gel loading dye provided with the kit and was loaded onto the gel after the wells were thoroughly rinsed using a syringe. Empty wells were loaded with 50% glycerol or 1x loading dye in volume equivalent to the samples. The samples were run for approximately 2 hours till the xylene cyanol traversed 3/4th of the gel.

4.5.5 Visualization of the RNA-protein complexes

The gel was carefully taken out of the plates and washed in the running buffer (0.5X TBE). A 30 ml solution of SYBR Green (provided within the kit) was prepared by diluting the parent stock 10,000 times in 0.5X TBE. The gel was stained in a plastic container protected from light and kept on a gel rocker for about 20 minutes. After staining the extra stain was removed by washing the gel twice in copious amounts of distilled water for about 10 seconds. The gel was then wrapped up in a cling film and taken to the typhoon scanner for visualization. The typhoon

scanner was set for SYBR Green fluorescence and the gel was kept on the fluor stage. The image recorded from the typhoon scanner was subsequently exported in '.tiff' format.

4.6 Isothermal calorimetry

Isothermal Calorimetry was performed using MicroCal iTC200 (Malvern Instruments Ltd., UK). The truncated Hfq protein samples were diluted in a dilution buffer (20 mM Tris-Cl pH 8.0, 150 mM NaCl, 5% glycerol). The AbsR25 sRNA was transcribed *in-vitro* using T7 RNA polymerase (ThermoScientific, USA) as described in the section 3.5.2. To concentrate the sRNA, the sRNA in solution was precipitated in presence of 2.5 M ammonium chloride and 0.6 volumes of isopropanol. The mixture was allowed to stand at room temperature for about an hour. The pellet was collected by centrifugation at 12,000 g for 10 minutes. The resulting pellet was washed in 70% ethanol and finally resuspended in the dilution buffer. The sRNA concentration was determined using Nanodrop spectrophotometer. About 50 µl of 20 µM sRNA and 400 µl of 1 µM protein samples were degassed at room temperature. The degassed RNA was titrated into 200 µl of purified protein over 25 injections of µl each with constant stirring of 800 rpm, 2-minute injection spacing and 25°C thermo-statting. Data were analyzed using Origin (version).

4.7 Generation of an *hfq* deletion mutant *A. baumannii*

An *A. baumannii hfq* deletion mutant was generated following the homologous recombination-based approach as described earlier (Figure 4.2). Briefly, A 500 bp upstream (US) and 500 bp downstream (DS) region was cloned with kanamycin cassette (KanFRT) between them, in pUC18 plasmid leading to the plasmid, pRPT25. The plasmid pRPT25 was maintained in *E. coli* DH5α resulting in strain, RPT 186. Using the PCR primers, OligoRPT39 and OligoRPT40, a 1.75 kb region was amplified from the pRPT25 carrying KanFRT flanked by 125 bp US and DS region of *hfq*. This recombineering PCR product was transformed into *A. baumannii* cells expressing RecT homolog. The *A. baumannii* cells selected after transformation and screened positive for allele replacement were designated as RPT 233.

hfq deletion strain of *A. baumannii* was generated following PCR based homologous recombination. *A. baumannii* cells were made recombination-competent by expressing an *A. baumannii recT* homolog from a plasmid, pAT02. A recombineering construct carrying a 500 bp region upstream and 500 bp region downstream of *hfq* coding region and carrying a kanamycin cassette flanked by FRT sites (KanFRT) was generated by cloning different parts together. Finally, a recombineering PCR product was amplified from this construct carrying the kanamycin

cassette flanked by 125 bp of upstream and downstream regions. This recombineering PCR product was transformed into *A. baumannii* cells expressing RecT. Recombinant cells were selected on kanamycin containing medium and were confirmed for allele replacement by PCR. Another plasmid pAT03, expressing FLP recombinase enzyme was transformed in recombinant cells carrying kanamycin at the genomic locus of *hfq*. FLP recombinase enzyme excised the region between the FRT sites leaving just a small scar sequence, resulting in a markerless *hfq* deletion mutant.

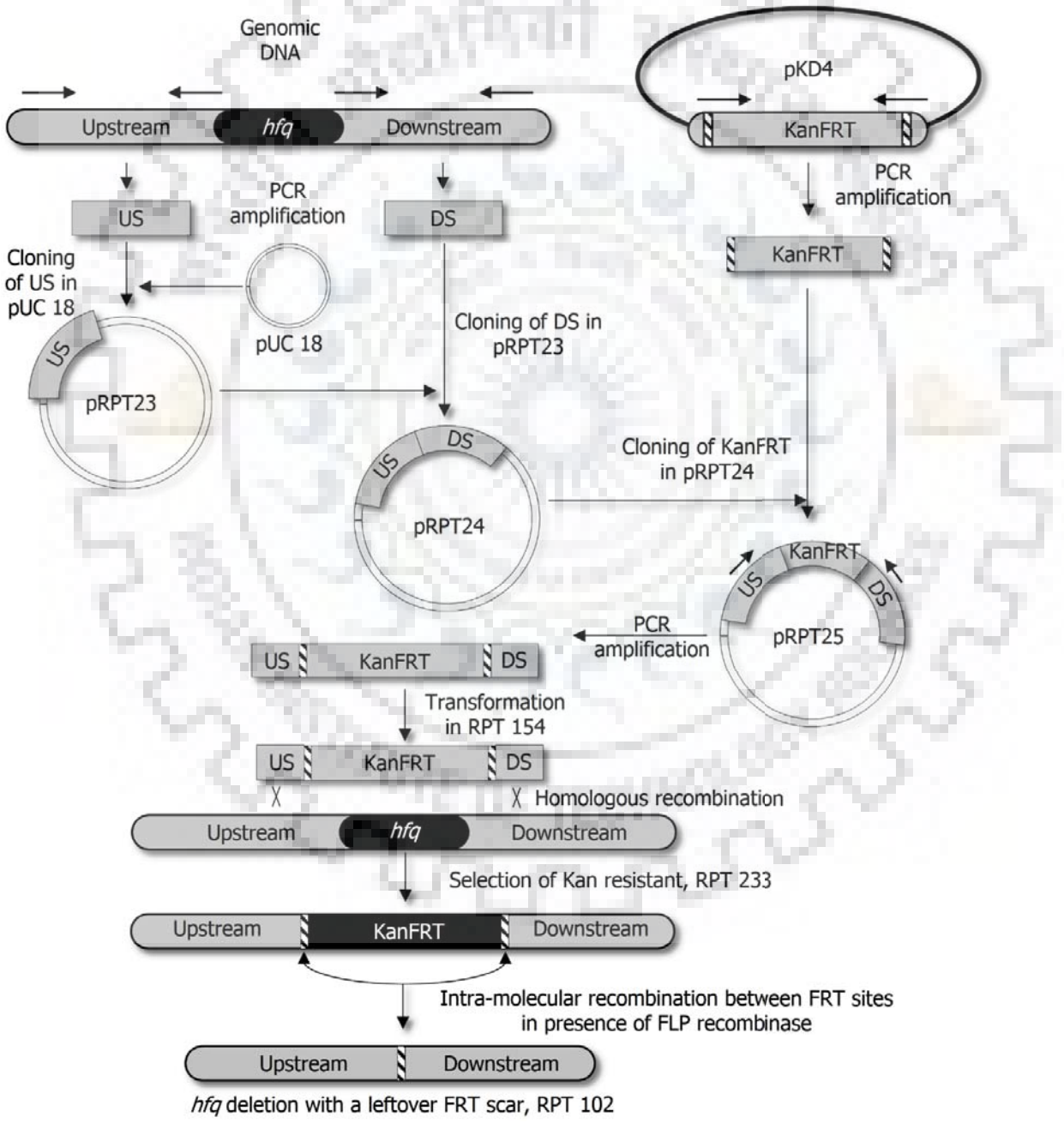

Figure 4.2 Generation of *hfq* deletion mutant *A. baumannii*.

4.7.1 Generation of *A. baumannii* strain expressing *A. baumannii* RecT

The *A. baumannii* ATCC 17978 cells were made electrocompetent by repeatedly washing with ice-cold 10% glycerol. A single colony *A. baumannii* ATCC 17978 was inoculated in 5 ml of LB and incubated at 37°C overnight. The culture was diluted 100 times in fresh 500 ml LB and the cells were grown to early log phase culture (OD_{600} = 0.6). The cells were centrifuged at 2500 g for 20 minutes at 4°C. The supernatant was discarded and the cells were kept on ice all the times. The cell pellet was dissolved in equal amount of 10% glycerol and the suspension was again centrifuged. The cell pellet obtained was resuspended in 100 ml of 10% glycerol and centrifuged again. The final pellet obtained was resuspended in 500 µl of 10% glycerol and 50 µl aliquots of the cells were prepared. The aliquots were stored at -80°C till further use.

A 50 µl aliquot of electrocompetent cells was thawed completely, taken in a 2 mm electroporation cuvette and the plasmid pAT02 was added. Electroporation was carried out at 2300 kV and the cells were immediately resuspended in 1000 µl of pre-warmed SOC medium. The cells were incubated at 37°C for an hour before spreading on LB plates supplemented with 100 µg/ml ampicillin. The plates were incubated for 12 hours and the resulting colonies were selected which were designated as RPT 154.

A single colony of RPT 154 was picked, inoculated into LB broth supplemented with 100 µg/ml ampicillin and incubated overnight at 37°C overnight with agitation. The overnight culture was diluted 100 times in fresh LB-ampicillin broth supplemented with 2 mM IPTG (for expression of recombinase) and grown till early log phase (OD_{600} = 0.6). The cells were subsequently harvested by centrifugation and made electrocompetent by washing with ice-cold 10% glycerol (as described earlier). The electrocompetent cells of RPT 154 were stored at -80°C till further use.

4.7.2 Generation of recombineering construct and recombineering PCR product

Primers OligoRPT33 and OligoRPT34 were designed for amplification of a 500 bp upstream region of *hfq* (US) carrying an EcoRI and a BamHI restriction site on the ends. Similarly, primers OligoRPT35 and OligoRPT36 were designed to amplify a 500 bp region downstream of *hfq* (DS) and carrying the restriction sites for BamHI and HindIII. Another set of primers OligoRPT37 and OligoRPT38, carrying BamHI restriction site on either end was designed for amplification of kanamycin resistance cassette (KanFRT). The genomic DNA of *A. baumannii* served as a template for amplification of US and DS while KanFRT was amplified using a plasmid pKD4 as template. Typical PCR reaction for amplification of these products is given below (Table 4.7).

Table 4.7 General PCR mixture for amplification of US, DS and KanFRT.

Component	Amount
10X Ex Taq buffer	5.0 µl
2 mM dNTPs	5.0 µl
10 µM forward primer	1.0 µl
10 µM reverse primer	1.0 µl
Template DNA (gDNA/plasmid)	Upto 10 ng
Ex Taq DNA polymerase	1.0 unit
Nuclease free water	To make up 50.0 µl

Upon amplification, all the three PCR products were gel purified and quantitated. The US PCR product and the plasmid pUC18 were digested with EcoRI and BamHI (Table 4.8).

Table 4.8 Restriction digestion of US PCR product and pUC18 plasmid.

Component	Amount
10X Tango buffer	4.0 µl
US PCR product/pUC 18 plasmid	500 ng
BamHI	1.0 µl
EcoRI	0.5 µl
Nuclease free water	To make up 20 µl

The digestion was carried out at 37°C for 2 hours. 0.5 µl of FastAP® alkaline phosphatase was added to the plasmid digestion mixture and incubated at 37°C for 10 more minutes. The enzymes were inactivated by incubation at 75°C for 5 minutes. The digested products were gel purified using MinElute kit (Qiagen). A typical ligation mixture was prepared as follows (Table 4.9):

Table 4.9 Ligation of US PCR product and pUC 18 plasmid.

Component	Amount
10X T4 ligase buffer	1.5 µl
Digested PCR product	A 1:3 molar ratio (plasmid: insert) with at least 50
Digested plasmid	ng DNA
10 mM rATP	1.5 µl
T4 DNA ligase	1.0 µl
Nuclease free water	To make up 15 µl

Ligation was carried out at 22°C for 2 hours. The ligation mixture was transformed into electrocompetent *E. coli* DH5α and the transformants were selected on LB agar plate supplemented with 100 µg/ml ampicillin. The recombinant plasmid was designated as pRPT23. The DS PCR product was subsequently cloned in the BamHI and HindIII sites of pRPT23 (Table 4.10).

Table 4.10 Digestion of DS PCR product and pRPT23 plasmid.

Component	Amount
10X Tango buffer	4.0 µl
DS PCR product/pRPT23 plasmid	500 ng
BamHI	1.0 µl
HindIII	1.0 µl
Nuclease free water	To make up 20 µl

The digestion was carried out at 37°C for 2 hours. 0.5 µl of FastAP® alkaline phosphatase was added to the plasmid digestion mixture and incubated at 37°C for 10 more minutes. The enzymes were inactivated by incubation at 75°C for 5 minutes. The digested products were gel purified using MinElute kit (Qiagen) and ligated as follows (Table 4.11):

Table 4.11 Ligation of digested pRPT23 and DS PCR product.

Component	Amount
10X T4 ligase buffer	1.5 µl
Digested PCR product	A 1:3 molar ratio (plasmid: insert) with at least 50
Digested plasmid	ng DNA
10 mM rATP	1.5 µl
T4 DNA ligase	1.0 µl
Nuclease free water	To make up 15 µl

Ligation was carried out at 22°C for 2 hours. The ligation mixture was transformed into electrocompetent *E. coli* DH5α and the transformants were selected on LB agar plate supplemented with 100 µg/ml ampicillin. The recombinant plasmid was designated as pRPT24. The plasmid pRPT24 and KanFRT PCR products were digested with BamHI (Table 4.12).

Table 4.12 Digestion of KanFRT PCR product and pRPT24 plasmid.

Component	Amount
10X Buffer BamHI	1.0 µl

KanFRT PCR product/pRPT24 plasmid	500 ng
BamHI	1.0 µl
Nuclease free water	To make up 10 µl

The digestion was carried out at 37°C for 2 hours. 0.5 µl of FastAP® alkaline phosphatase was added to the plasmid digestion mixture and incubated at 37°C for 10 more minutes. The enzymes were inactivated by incubation at 75°C for 5 minutes. The digested products were gel purified using MinElute kit (Qiagen) and ligated as follows (Table 4.13):

Table 4.13 Ligation of KanFRT PCR product and pRPT24 plasmid.

Component	Amount
10X T4 ligase buffer	1.5 µl
Digested PCR product	A 1:3 molar ratio (plasmid: insert) with at least 50
Digested plasmid	ng DNA
10 mM rATP	1.5 µl
T4 DNA ligase	1.0 µl
Nuclease free water	To make up 15 µl

Ligation was carried out at 22°C for 2 hours. The ligation mixture was transformed into electrocompetent *E. coli* DH5α and the transformants were selected on LB agar plate supplemented with 50 µg/ml kanamycin. The recombinant plasmid was designated as pRPT25. The plasmid pRPT25 was used as a template in a PCR reaction with primers OligoRPT39 and OligoRPT40, to amplify a recombineering PCR product that carries a 125 bp region upstream and downstream of *hfq* flanking the KanFRT (Table 4.14).

Table 4.14 PCR mixture for amplification of recombineering PCR product.

Component	Amount
10X Ex Taq buffer	10.0 µl
2 mM dNTPs	10.0 µl
10 µM OligoRPT39	1.25 µl
10 µM OligoRPT40	1.25 µl
pRPT25	Upto 20 ng
Ex Taq DNA polymerase	2.0 units
Nuclease free water	To make up 100.0 µl

The 1.75 (0.125 + 0.125 + 1.5) kb PCR product was excised form the gel. This PCR product was the required recombineering amplicon.

4.7.3 Screening of recombinant *A. baumannii* with replaced *hfq* allele

The recombineering PCR product was concentrated and 5 µg of this PCR product was used to transform electrocompetent cells of RPT 154, using an electroporator. The PCR product was added to a 50 µl aliquot of competent cells, with ~10^{10} cells, and electroporated at 1.8 kV in a 2 mm electroporation cuvette. The cells were incubated in 1 ml SOC medium, supplemented with 2 mM IPTG, for two hours and then spread on LB agar plates supplemented with kanamycin (15 µg/ml). After overnight incubation the colonies that appeared were picked up for a colony PCR using the primers OligoRPT4 and OligoRPT7 that would yield an amplicon of 2.4 kb in case of successful allele exchange by homologous recombination. The colony yielding a 2.4 kb PCR product was selected and streaked on LB agar plates supplemented with 15 µg/ml of kanamycin. The colony was purified was subsequent streaking on increasing amounts of kanamycin up to 50 µg/ml. The genomic DNA from this colony was isolated and a PCR reaction was carried out using the primers pair OligoRPT33 and OligoRPT36. A PCR product of kb confirmed allele replacement. The newly generated strain was designated as RPT 233.

4.7.4 Removal of KanFRT cassette to generate markerless deletion

A single colony RPT 233 was inoculated in 5 ml of LB and incubated at 37°C overnight. The culture was diluted 100 times in fresh 500 ml LB and the cells were grown to early log phase culture (OD_{600} = 0.6). The cells were centrifuged at 2500 g for 20 minutes at 4°C. The supernatant was discarded and the cells were kept on ice all the times. The cell pellet was dissolved in equal amount of 10% glycerol and the suspension was again centrifuged. The cell pellet obtained was resuspended in 100 ml of 10% glycerol and centrifuged again. The final pellet obtained was resuspended in 500 µl of 10% glycerol and 50 µl aliquots of the cells were prepared. Plasmid pAT03 was transformed into these electrocompetent cells of RPT 233. The transformants were selected on LB agar plates supplemented with 200 µg/ml ampicillin. The transformants were grown in LB broth in presence of 2 mM IPTG to induce the expression of FLP recombinase. After overnight growth at 37°C, the cells were selected for kanamycin sensitivity by replica plating on LB agar and LB agar plates supplemented with 15 µg/ml kanamycin. A PCR reaction using the primers OligoRPT33 and OligoRPT36 was carried out to confirm the excision of kanamycin resistance cassette. The *A. baumannii Δhfq* strain thus created was designated as RPT 102.

4.8 Mass spectrometric analysis by MALDI MS/MS

Wild type *A. baumannii* and *A. baumannii Δhfq* cells were grown overnight from a single colony in LB medium at 37°C with agitation. The cells were harvested from 2 ml of culture by centrifugation, washed in PBS and resuspended in 100 µl BugBuster master mix (Novagen, USA). The samples were incubated at room temperature for 20 minutes with gentle shaking. After incubation, the samples were centrifuged at 12000g for 20 minutes and the supernatant containing all the solubilized proteins was collected. An equal volume of 10% (w/v) Trichloroacetic acid (TCA) was added to the supernatant and incubated on ice for 30 minutes. The samples were centrifuged at 15000g for 15 minutes at 4°C and the protein pellet was washed thrice in ice cold absolute ethanol. The pellet was air dried to remove traces of ethanol and resuspended in 20 µl of 1X SDS-PAGE gel loading buffer (Appendix I). The samples were boiled at 95°C for 5 minutes, flash chilled on ice and resolved on 15% Tricine-SDS-PAGE (Appendix I). The purified recombinant hexa-histidine derivative of *A. baumannii* Hfq (expressed in *E. coli* BL21) was also included in the gel. A band observed at approximately 17 kDa, not detected in case of *A. baumannii Δhfq*, was excised from the gel (along with the corresponding zone from the *A. baumannii Δhfq* proteins), washed thrice in a solution of 50% v/v acetonitrile and 25 mM NH_4HCO_3, pH 7.8 at 37°C for 10 min and dried at room temperature in a CentriVap Concentrator (Labconco, USA). The dried products were covered with 8 µl (15ng/µl) of sequencing grade trypsin solution (Sigma Aldrich, USA) and digested overnight at 37°C. Products were recovered from the gel by sequential extractions with 10 µl of 0.1% (v/v) trifluoroacetic acid (TFA) and subsequently dried using CentriVap Concentrator (Labconco). Two µl of extract was deposited onto the MTP 384 ground steel MALDI target plate using 5 mg/ml α-cyano-4-hydroxy cinnamic acid (BrukerDaltonics, Germany) in 50% acetonitrile and 0.1% v/v TFA. Peptide mass fingerprint (PMF) and time-of-flight (TOF) -MS analyses were performed using a BrukerUltraflex III TOF/TOF mass spectrometer (BrukerDaltonics, Bremen, Germany). Spectral acquisition and analysis was performed using FlexControl Version 3.3 and FlexAnalysis 3.4 software (BrukerDaltonics, Germany).

Protein identification was carried out by correlation of mass spectra to entries in the NCBInr database (July 2015) using Mascot (2.4.1. Matrix Science, UK). Mascot MS/MS ion search criteria were as follows: taxonomy- Other Proteobacteria, trypsin digestion allowing up to one mis-cleavage, variable modification—oxidation of methionine, cysteine as carboxyamidomethylation or propionamide, peptide tolerance of 110 ppm and MS/MS tolerance of 0.2 Da. The ‘‘ion score cut-off’’ was manually set to 20, thereby eliminating the lowest quality

matches. A probability-based Mowse score using -10 log (P) >19 indicated identity ($p< 0.05$). To eliminate false positives, 1% FDR was applied at both protein and peptide level.

4.9 Complementation of *hfq* deletion using various constructs

4.9.1 Generation of complementing fragments by overlap extension PCR

For complementation of *hfq* deletion using different truncations, it was necessary to ensure that all the truncations carried the native *hfq* promoter and terminator. Therefore, to ensure this, complementing constructs were generated by overlap extension PCR (Figure 4.3). In case of Hfq_{66}, Hfq_{72} and Hfq_{92}, one set of primers (OligoRPT41 with OligoRPT52, 53 and 54) was used to amplify the truncated Hfq coding fragment along with the 5'UTR. Another set of primers (OligoRPT42 with OligoRPT47, 48 and 49) was designed to amplify the 3' UTR and carry a sequence complementary to the 3' end of the truncation in question, at the 5' end. Both the PCR products were purified, mixed in equimolar amounts to make up for a PCR reaction as follows (Table 4.15):

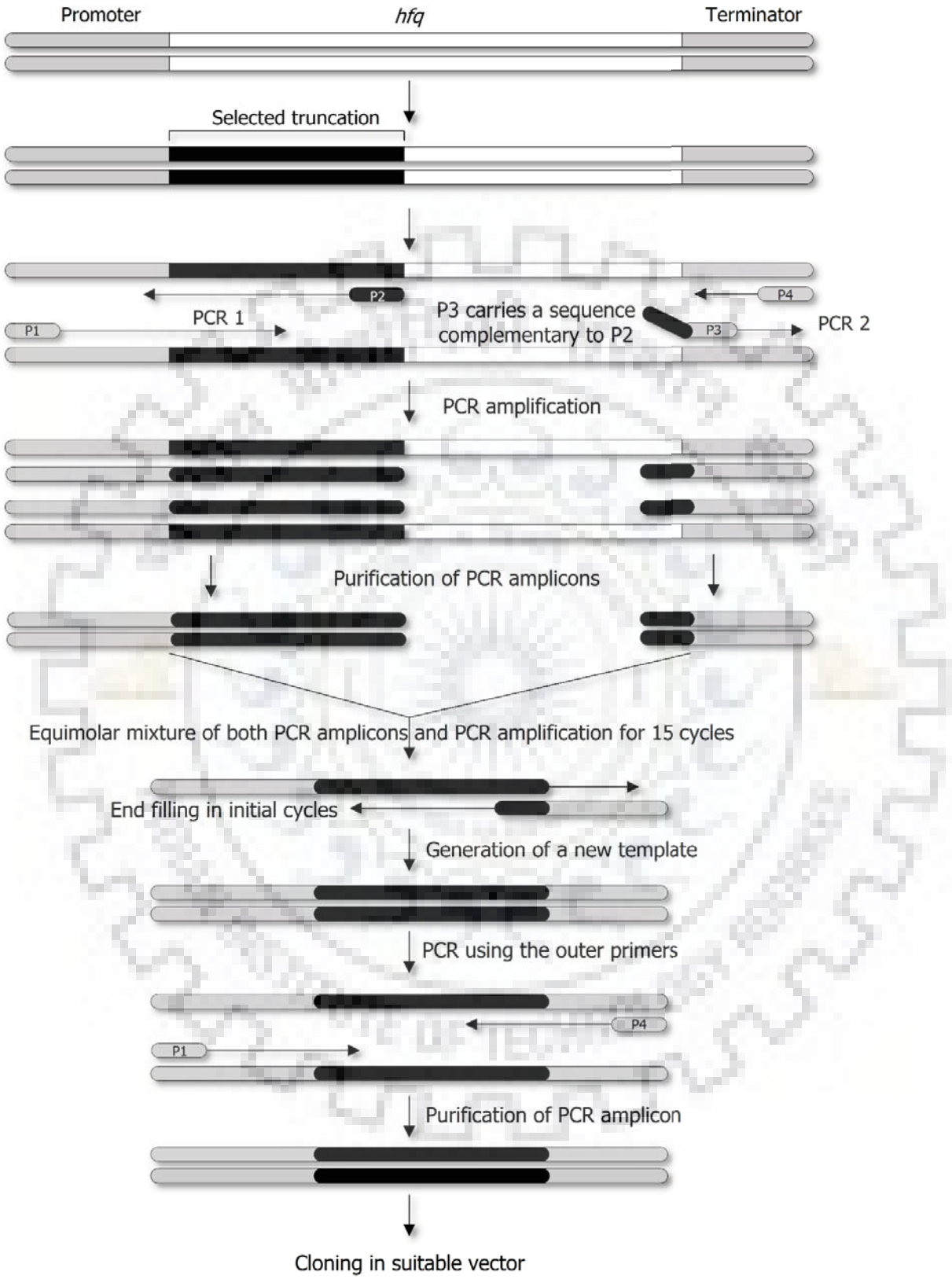

Figure 4.3. Generation of complementing constructs by overlap extension PCR.

Table 4.15 Overlap extension PCR for generation of complementing constructs.

Component	Amount
10X Ex Taq buffer	5 µl
2 mM dNTPs	5 µl
Equimolar mixture of PCR Products	30 µl
Ex Taq DNA polymerase	1 unit
Nuclease free water	To make up 50 µl

The reaction was carried out using the following protocol (Table 4.16):

Table 4.16 Cycling conditions for overlap extension PCR.

Event	Temperature	Time (mm:ss)
Initial denaturation	94°C	02:00
Cycle denaturation	94°C	00:30
Cycle annealing	54°C	00:25
Cycle extension	72°C	00:30

The reaction was allowed to run for 15 cycles, after which 1 µl of the primers OligoRPT41 and OligoRPT42 were added. The reaction was resumed for another 15 cycles at the same conditions with a final extension step lasting 10 minutes at 72°C. The final PCR product was assessed on gel and was of cumulative size of the two PCR fragments adjusted for the overlap.

In case of Hfq_{Ct} (the truncation carrying only the G-rich repeats), one set of primers was used to amplify the C-terminal domain along with the 3'UTR (OligoRPT51 and OligoRPT42). Another set of primers was designed to amplify the 5'UTR, carrying a sequence complementary to the 5' end of the aforementioned PCR product at its 3' end (OligoRPT41 and OligoRPT50). The amplification to ensure a fusion product was carried as described above.

4.9.2 Cloning the complementing fragments

The complementing fragments were amplified using the primers OligoRPT41 and OligoRPT42 that carry a BamHI restriction site at their 5' ends. The fragments were digested and cloned in the plasmid, pWHN678 as follows (Table 4.17):

Table 4.17 Restriction digestion of pWHN678 plasmid and overlap extension PCR products.

Component	Amount
10X FastDigest® Green buffer	1 µl

PCR product/pWHN678	500 ng
FastDigest® BamHI	0.5 µl
Nuclease free water	To make up 10 µl

The digestion was carried out at 37°C for 30 minutes. 0.5 µl of FastAP® alkaline phosphatase was added to the plasmid digestion mixture and incubated at 37°C for 10 more minutes. The enzymes were inactivated by incubation at 75°C for 5 minutes. The digested products were gel purified using MinElute kit (Qiagen). A typical ligation mixture was prepared as follows (Table 4.18):

Table 4.18 Ligation of pWHN678 plasmid and overlap extension PCR products.

Component	Amount
10X T4 ligase buffer	1.5 µl
Digested PCR product	A 1:3 molar ratio (plasmid: insert) with at
Digested pWHN678	least 50 ng DNA
10 mM rATP	1.5 µl
T4 DNA ligase	1.0 µl
Nuclease free water	To make up 15 µl

Ligation was carried out at 22°C for 2 hours. The ligation mixture was transformed into electrocompetent *E. coli* DH5α and the transformants were selected on LB agar plate supplemented with 30 µg/ml chloramphenicol. The recombinant plasmids were named as pRPT14, 15, 16, 17, 18 and 19. (Appendix IV). The recombinant plasmids were transformed into *A. baumannii Δhfq* and *E. coli Δhfq* leading to the strains mentioned in Appendix III. The plasmid pWHN678 was transformed into *A. baumannii Δhfq* and *E. coli Δhfq* as well as wild type *A. baumannii* and *E. coli* leading to the strains RPT 98 and RPT 258, respectively.

4.10 Western blotting to determine expression of truncated versions of Hfq

4.10.1 Preparation of cell lysate

Western blotting was carried out to determine the levels of expression of truncated versions of Hfq. A single colony of *A. baumannii* cells expressing the truncated as well as the wild type Hfq was inoculated in LB broth supplemented with 30 µg/ml chloramphenicol and incubated overnight at 37°C. The overnight culture was diluted 100 times in fresh LB supplemented with 30 µg/ml chloramphenicol and the cells were grown at 37°C till $OD_{600} \approx 1.2$. The cells were harvested and lysed in a lysis buffer (Appendix I) using a cell disruptor (Constant Systems, UK).

Total protein in cell lysate was determined by using Bradford's reagent (Appendix II). 25 µg of total protein was resolved on 12% Tricine-SDS-PAGE and the proteins were transferred to a nitrocellulose membrane.

4.10.2 Electrotransfer of proteins to nitrocellulose membrane

As soon as the proteins were resolved on the gel, the gel was removed from the plates and dipped in electrotransfer buffer (Appendix I). A nitrocellose membrane similar in size to the gel was cut and placed over the gel. Both the gel and the membrane were sandwiched between filter paper (BioRad, USA) and were assembled in the electrotransfer cassette (BioRad, USA). The cassette was put in the Mini-PROTEAN tetra cell, with the gel facing the –ve electrode and the membrane facing the +ve electrode. The electrotransfer was carried out for an hour at a constant voltage of 50V. An ice pack was kept in the tetra cell to prevent heating due to the current.

4.10.3 Preparation of membrane

After electrotransfer, the membrane was removed from the apparatus and put in a clean plastic container for further processing that includes washing and incubation with the antibodies.

4.10.3.1 Blocking

The membrane was incubated in 25 ml of blocking buffer (Appendix I) for one hour at room temperature. This ensures that the antibodies do not bind to non-specific targets. The container carrying the membrane was kept on a gel rocker all the times.

4.10.3.2 Incubation with primary antibody

After blocking, the buffer was drained and the membrane was incubated in 10 ml of primary antibody dilution made in blocking buffer. The anti-Hfq antibody (obtained from Dr. Susan Gottesman) was diluted 5000 times in blocking buffer prior to use. The membrane was incubated in the primary antibody for one hour at room temperature with gentle rocking.

4.10.3.3 Washing

After incubation with primary antibody, the membrane was washed in TBST buffer. Three washings, each for 10 minutes, were given to the membrane using 25 ml of TBST buffer.

4.10.3.4 Incubation with secondary antibody

The HRP-conjugated goat anti-rabbit antibody was diluted 50000 times in blocking buffer. The membrane was incubated with the diluted secondary antibody (25 ml) for 30 minutes at room temperature with gentle rocking.

4.10.3.5 Washing

After incubation with the secondary antibody, the membrane was again washed in TBST buffer. Three washings with 25 ml of TBST buffer were given for 15 minutes each. The last washing was given with TBS buffer to remove traces of Tween 20 which might interfere with the ECL substrate.

4.10.3.6 Development

After thorough washings, the membrane was prepared for visualization. ECL substrate (BioRad, USA) was used for development of a luminescent signal. In a dark room 1 ml of both the components of ECL kit was mixed and the membrane was dipped in the mixture for 5 minutes. The membrane was picked up and wrapped in a plastic sheet. A sheet of autoradiography film (Kodak, USA) was exposed to the membrane and incubated for 2 minutes. The film was developed in an alkaline developer solution and fixed in an acidic fixer solution. The film was washed in copious amounts of water. The film was scanned to digitalize the signal.

4.11 Complementation assays to determine importance of C-terminus

To determine the functional importance of the Hfq C-terminus, various assays were carried out to determine the complementation of *hfq* deletion mutant with various *hfq* truncations.

4.11.1 Growth kinetics

A single colony of the strains RPT 98, 234, 235, 236, 237, 238, 239 and 240 was inoculated in LB medium supplemented with 30 µg/ml chloramphenicol and incubated overnight at 37°C overnight with 220 rpm agitation. The overnight culture was diluted 100 times in fresh LB medium supplemented with 30 µg/ml chloramphenicol and incubated at 37°C with 220 rpm agitation. At regular intervals, the culture was withdrawn and OD_{600} was determined using BioSpectrometer basic (Eppendorf, Germany) spectrophotometer.

4.11.2 Utilization of carbon sources

The utilization of carbon sources was studied using Biolog bacterial identification system. This system identifies bacteria based on their growth in a Gen III 96-well microtiter plate containing different carbon sources. The tetrazolium dye present in every well assists in monitoring growth in a colorimetric assay. A single colony of *A. baumannii* was inoculated in an inoculation fluid provided by the manufacturer. The fluid was dispensed into the wells of Gen III plates (Biolog, USA). The plates were read in a Biolog plate reader after 12 hours of incubation at 37°C.

4.11.3 Stress tolerance

Stress tolerance was determined by carrying out assays that mimicked stress conditions that the bacterium is likely to face. These conditions were simulated and growth was assessed as follows.

4.11.3.1 Thermal stress

In case of *A. baumannii* cells, overnight culture was diluted 100 times in fresh LB supplemented with 30 µg/ml chloramphenicol and grown at 37°C till OD_{600} = 0.5. The cells were incubated at 65°C for 30 minutes and logarithmic dilutions of the culture were spread on LB agar plates. An aliquot of cells not exposed to high temperature was also spread as control. The plates were incubated overnight at 37°C and the resulting colonies were calculated. The percentage survival was determined by calculating the relative CFU count with respect to the control.

In case of *E. coli*, 10-fold dilutions of the overnight culture were made and 5 µl of each dilution was spotted on an LB agar plate (supplemented with 30 µg/ml chloramphenicol). The plate was incubated at 42°C. A control plate was kept at 37°C to assist in comparison.

4.11.3.2 Osmotic, nutritive and acid stress

For both *E. coli* and *A. baumannii*, 10-fold dilutions of the overnight culture were made in sterile PBS and 5 µl of each dilution was spotted on an LB agar plate (supplemented with 30 µg/ml chloramphenicol) containing 3% NaCl (w/v), 200 µM 2,2-Dipyridyl (an iron chelator) and agar plates made of LB at pH5. The plates were incubated overnight at 37°C. The dilutions were also spotted on a control plate, containing LB agar and chloramphenicol only, for comparison.

4.11.3.3 Oxidative stress

Overnight culture of *A. baumannii* cells was diluted 100 times in fresh LB supplemented with 30 µg/ml chloramphenicol and grown at 37°C till OD_{600} = 0.5. An aliquot of the cells was then subjected to treatment with 5 mM methyl viologen (an oxidizing agent). After 30 minutes of treatment, the cells were serially diluted in sterile PBS and the dilutions were spread on an LB agar plate. Another aliquot of the cells, not subjected to methyl viologen treatment, was also spread on LB agar and similarly incubated. The CFUs were determined and percentage survival of cells was determined by calculating the difference between the number of CFU in treated and untreated plates.

In case of *E. coli*, the oxidative stress was induced by addition of 100 µM H_2O_2 to the LB agar plate and assay was carried out similar to the osmotic and acid stress assay.

4.11.4 Autoregulation of *hfq*

Plasmid pR131hfq was a kind gift from Prof. Udo Bläsi, Max F. Perutz Laboratories, Vienna Biocenter, Austria. The plasmid was co-transformed into *E. coli Δhfq* along with the plasmids carrying the complementing constructs resulting in construction of new strains (Appendix III). The cells were grown overnight in LB supplemented with 100 µg/ml ampicillin (to maintain pR131hfq) and 30 µg/ml chloramphenicol. The cells were again diluted 100 times in fresh medium and grown till OD_{600} = 0.4 and were induced with 2 mM IPTG for 30 minutes. 1 ml of the culture was withdrawn and the cells were collected by centrifugation and washed in PBS. The washed cells were resuspended in 1 ml of Z-buffer. 100 µl of the cell suspension was taken in a clear flat bottom 96-well plate and the OD_{600} was measured. Cells in the rest of the suspension were permeabilized by addition of one drop of 0.1% SDS and two drops of chloroform were added and vortexed for 15-20 seconds. The mixture was incubated at room temperature for 15 minutes. 50 µl of the permeabilized cells were added to 50 µl of Z-buffer and 25 µl of ONPG (10 mg/ml) and incubated at 30°C till a yellow color developed. Stop solution (1 M Na_2CO_3) was added and OD_{450} of 100 µl solution was recorded in a clear flat bottom 96-well plate. The β-galactosidase activity was expressed as Miller units determined by the following equation:

$$Miller\ units = \frac{1000\ \times OD450}{Time\ (min) \times volume(ml) \times OD600}$$

4.11.5 Riboregulation of *sodB*

4.11.5.1 Removal of kanamycin resistance cassette (kan^r) from E. coli Δhfq

For co-expression studies, plasmids carrying kanamycin resistance cassette (kan^r) were used. However, all the Keio library strains carry a kanamycin resistance marker in their genome at the site of gene replacement. Therefore, it was necessary to remove this cassette for successful maintenance of plasmids. An FLP recombinase expressing plasmid, pCP20, was obtained from Prof. Raghavan Varadarajan, IISc Bangalore. The plasmid was transformed into *E. coli* Δ*hfq*. The transformants were grown in presence of 2 mM IPTG (to induce FLP recombinase expression) and assessed for kanamycin sensitivity (due to excision of kan^r cassette). The *E. coli* Δ*hfq* cells were cured of the pCP20 plasmid by repetitive growth in absence of selection pressure and designated as RPT 269.

4.11.5.2 Construction of sodB-gfp fusion

Using the primers oligoRPT43 and oligoRPT44, *gfp* was amplified from a GFP cassette containing vector, pPROBE-NT, using a high-fidelity DNA polymerase. The PCR product and the plasmid pRPT20 were digested according to the following reaction (Table 4.19).

Table 4.19 Restriction digestion of *gfp* PCR product and pRPT20 plasmid.

Component	Amount
10X BamHI buffer	2.0 µl
PCR product/pRPT20	500 ng
BamHI	0.5 µl
MluI	1.0 µl
Nuclease free water	To make up 20 µl

The digestion was carried out for 2 hours at 37°C. 0.5 µl of FastAP® alkaline phosphatase was added to the plasmid digestion mixture and incubated at 37°C for 10 more minutes. The enzymes were inactivated by incubation at 75°C for 5 minutes. The digested products were gel purified using MinElute kit (Qiagen). A typical ligation mixture was prepared as follows (Table 4.20):

Table 4.20 Ligation of *gfp* PCR product and pRPT20 plasmid.

Component	Amount
10X T4 ligase buffer	1.5 µl
Digested PCR product	A 1:3 molar ratio (plasmid: insert) with at
Digested pRPT20	least 50 ng DNA
10 mM rATP	1.5 µl
T4 DNA ligase	1.0 µl
Nuclease free water	To make up 15 µl

Ligation was carried out at 22°C for 2 hours. The ligation mixture was transformed into *E. coli* DH5α and the transformants were selected on LB agar plate supplemented with 50 µg/ml kanamycin. The recombinant plasmid thus generated was designated as pRPT21. The primers oligoRPT45 and oligoRPT46 were used to amplify *sodB* gene with its 5' UTR, using *A. baumannii* genomic DNA as a template. The PCR product and pRPT21 were digested according to the following reaction (Table 4.21).

Table 4.21 Restriction digestion of *sodB* PCR product and pRPT21 plasmid.

Component	Amount
10X BamHI buffer	2.0 µl
PCR product/pRPT21	500 ng
BamHI	0.5 µl
HindIII	1.0 µl
Nuclease free water	To make up 20 µl

The digestion was carried out for 2 hours at 37°C. 0.5 µl of FastAP® alkaline phosphatase was added to the plasmid digestion mixture and incubated at 37°C for 10 more minutes. The enzymes were inactivated by incubation at 75°C for 5 minutes. The digested products were gel purified using MinElute kit (Qiagen). A typical ligation mixture was prepared as follows (Table 4.22):

Table 4.22 Ligation of *sodB* PCR product and pRPT21 plasmid.

Component	Amount
10X T4 ligase buffer	1.5 µl
Digested PCR product	A 1:3 molar ratio (plasmid: insert) with at
Digested pRPT21	least 50 ng DNA
10 mM rATP	1.5 µl
T4 DNA ligase	1.0 µl
Nuclease free water	To make up 15 µl

Ligation was carried out at 22°C for 2 hours. The ligation mixture was transformed into *E. coli* DH5α and the transformants were selected on LB agar plate supplemented with 50 µg/ml kanamycin. The recombinant plasmid thus generated was designated as pRPT22. This plasmid pRPT22 has an in-frame *sodB-gfp* translational fusion under the control of *sodB* promoter.

4.11.5.3 Co-expression and ribo-regulation assay

The plasmid pRPT22 was transformed into *E. coli* Δ*hfq*. The complementing plasmids were co-transformed into these cells already carrying the plasmid pRPT22. The cells were grown overnight in LB containing kanamycin (50 µg/ml) and chloramphenicol (30 µg/ml) at 37°C. The cells were diluted 100 times in fresh medium and grown till OD_{600} = 0.6. 1 ml of cells were pelleted, washed with sterile PBS and dissolved in 1 ml of PBS. The GFP fluorescence was determined at excitation 480 nm and emission 519 nm. Relative fluorescence was calculated by taking a ratio of fluorescence and OD_{600}. Iron deficient conditions were induced by addition of 200 µM 2,2-Dipyridyl. The cells were again incubated for 30 minutes at 37°C and the relative

fluorescence was determined after incubation. Since, pRPT22 is a multi-copy plasmid and there is a *lac* promoter present, a leaky background expression of GFP was observed in the background making it difficult to detect repression of *sodB* expression. Therefore, instead of determining repression of fluorescence, a variable degree of change in fluorescence under iron deficiency was seen among the strains. The measure of ribo-regulation was determined by calculating the relative change in the fluorescence of *gfp* before and after 2,2-DIP treatment.

4.11.6 Biofilm formation

Overnight cultures *A. baumannii* were diluted 100 times in fresh LB supplemented with chloramphenicol. 500 µl of each was added to a borosilicate tube and incubated at 30°C for 48 hours. After incubation, the cell suspension was collected and its OD_{600} was determined. The tubes were washed with copious amounts of sterile water and allowed to dry. 500 µl of 1% freshly prepared crystal violet solution was added to each tube and incubated at room temperature for 30 minutes. The tubes were washed again with copious amounts of sterile water. The stain was dissolved in 500 µl of methanol and OD_{575} was recorded. The ratio of OD_{575} and OD_{600} was determined for each tube.

4.11.7 Desiccation resistance

The overnight cultures of *A. baumannii* cells were diluted 100 times in fresh LB broth. 10 µl of the suspension was taken in a well of polystyrene 96-well plate and allowed to dry at 25°C with 40% relative humidity for 48 hours. Following desiccation, the cells were resuspended in LB broth and log dilutions were spotted on LB agar plates. Survival was determined by relative loss of CFU as compared to the pre-desiccated condition.

4.11.8 Adhesion to mammalian cells

The *A. baumannii* cells were grown overnight at 37°C in LB broth and diluted 100 times in fresh LB broth. The cells were grown till $OD_{600} = 0.6$ and were harvested by centrifugation. The cell pellet was washed with PBS and resuspended in cell growth medium (DMEM supplemented with 10% fetal bovine serum). The embryonic kidney cells, HEK 293, were grown in the cell growth medium, in 24-well polystyrene plates, at 37°C and 5% CO_2. At the time of infection, the medium was drained out from the wells and replaced with the medium containing bacterial cells to ensure MoI of 100. The cells were incubated for one hour after which the medium was drained out again and the wells were carefully washed with PBS. After three washings, PBS supplemented with 0.1% Triton X-100 was added and the cells were scrapped off from the wells. Dilutions of the scrapped cells were made in sterile PBS and spread on LB agar plates. The plates were incubated overnight at 37°C and the CFUs were enumerated.

4.11.9 *In vitro* antimicrobial susceptibility assay

Minimum inhibitory concentration (MIC) of various drugs was determined by broth microdilution method, using 96-well plates, in Mueller Hinton (MH) (Merck, Germany) medium, according to the CLSI guidelines. Growth was monitored by optical density readings at 600 nm (OD_{600}) after 12 hours of incubation using Spectramax plus plate reader (Molecular Devices, USA).

4.11.10 Virulence in mice

6-8 weeks old female BALB/c mice were obtained from Central Animal Facility, NIPER Mohali. The mice were housed in the animal facility at Department of Biotechnology, IIT Roorkee. The protocol for animal experiments was approved by the Institute Animal Ethics Committee (IAEC) under the reference number BT/IAEC/2014/07/REV.

Upto 6 mice were kept in one filter-top cage and the cages were washed and changed every fourth day. The mice were regularly fed with mice specific diet pellets and pure water. Two days prior to infection, the mice were injected intraperitoneally with 200 mg/kg dose of cyclophosphamide (Figure 4.4). *A. baumannii* cells were grown till OD_{600} = 0.6. Cells were collected from 1 ml of suspension, washed twice in equal amount of sterile PBS and resuspended in same volume of PBS. 200 µl of cell suspension (corresponding to 10^8 CFU/ml) was injected intravenously through the tail vein into each mouse (n=5). The mice were sacrificed after 24 hours of infection by cervical dislocation. Kidney, liver and spleen were excised and homogenized in 1ml of sterile PBS. Dilutions of the organ homogenate were spread on LB agar plates and the colonies were counted after 16 hours of incubation at 37°C.

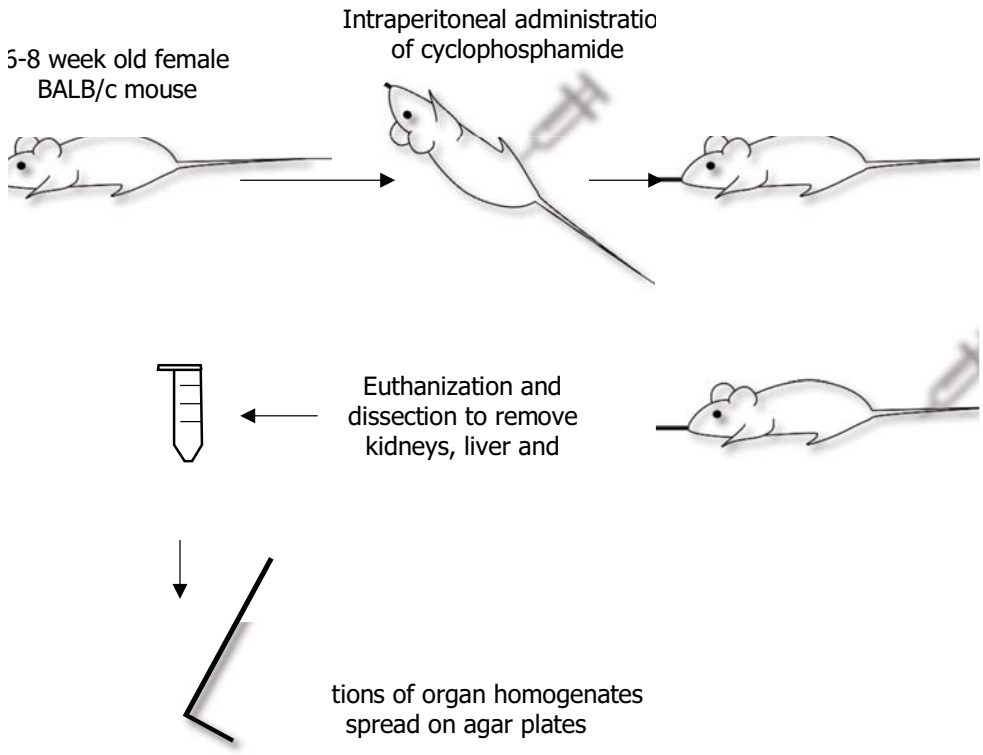

Figure 4.4. Schematic of the overall animal experiment.

4.12 Sequence-structure analysis of *abaF* using bioinformatic tools

The AbaF protein sequence was obtained from the NCBI Protein database using the identifier, A1S_1331. The FASTA sequence was used as query to BLAST (blast.ncbi.nlm.nih.gov/Blast.cgi) against the non-redundant protein database and Conserved Domain Database (CDD) to identify homologs of AbaF, in an attempt to determine its biological significance. The trans-membrane helices (secondary structure) in AbaF were determined by HMMTOP (http://www.enzim.hu/hmmtop/) and visualized using the TMRPres2D application (http://bioinformatics.biol.uoa.gr/TMRPres2D/). The 3D model of AbaF was generated using SWISS-MODEL online tool (https://swissmodel.expasy.org).

4.13 Cloning and expression of *abaF* in *E. coli* KAM32

Primers oligoRPT14 and oligoRPT15 were used to amplify *abaF* with its native promoter and terminator. The 1.5 kb PCR product and the plasmid pUC18 were digested using EcoRI and HindIII restriction enzymes, in the following reaction (Table 4.23):

Table 4.23 Restriction digestion of *abaF* PCR product and pUC18 plasmid.

Component	Amount
10X Buffer R	1.0 µl
PCR product/plasmid	500 ng
EcoRI enzyme	0.5 µl
HindIII enzyme	0.5 µl
Nuclease free water	To make up10 µl

The digestion was carried out for 2 hours at 37°C. 0.5 µl of FastAP® alkaline phosphatase was added to the plasmid digestion mixture and incubated at 37°C for 10 more minutes. The enzymes were inactivated by incubation at 75°C for 5 minutes. The digested products were gel purified using MinElute kit (Qiagen). A typical ligation mixture was prepared as follows (Table 4.24):

Table 4.24 Ligation of *abaF* PCR product and pUC18 plasmid.

Components	Amount
10X Ligation buffer	1.0 µl
10mM ATP	1.0 µl
Digested PCR product (insert)	A 1:3 molar ratio (plasmid: insert) with at
Digested plasmid (vector)	least 50 ng DNA
Ligase enzyme	1.0 µl
Nuclease free water	To make up10 µl

Ligation reaction was carried out in a water bath at 22°C for at least two hours. The ligation mixture was transformed into *E. coli* DH5α electrocompetent cells. The resulting plasmid was designated as pRPT7. The plasmid pRPT7 was sub-cloned in the efflux deficient strain, *E. coli* KAM32, resulting in the strain *E. coli* KAM32/pUC_*abaF* or RPT 145. The plasmid pUC18 was also transformed into *E. coli* KAM32, resulting in the control strain *E. coli* KAM32/pUC18 or RPT 144.

4.14 *In vitro* drug susceptibility assay

Drug susceptibility assays were carried out using broth micro-dilution method in 96-well plates according to the CLSI guidelines. Two-fold dilutions of multitude of antibiotics, dyes and drug-like compounds were sequentially made in duplicates and the bacterial cells were added to the plates. The plates were incubated overnight in a humidity controlled Kuhner shaker. Growth was determined by examining wells for turbidity visible to the naked eye.

4.15 Ethidium bromide accumulation and efflux assay

EtBr is a small molecule that fluoresces when it enters the bacterial cells and binds to the cellular components. Therefore, the movement of EtBr across the bacterial membrane can be tracked by fluorescence measurements. The RPT 144 and RPT 145 were inoculated in LB broth supplemented with 100 µg/ml ampicillin and grown till OD_{600} = 0.5. The cells were collected by centrifugation at 2500 g for 5 minutes and washed twice in sterile PBS in a similar way. The cells were finally resuspended in PBS to OD_{600} = 0.3.

For EtBr accumulation, to the cell suspension, glucose and EtBr were added to make up the final concentration 0.4% (w/v) and 10 µg/ml, respectively. The fluorescence measurements were taken at excitation and emission wavelengths of 480 nm and 610 nm, respectively, as soon as EtBr was added, using a Spectramax M2e plate reader (Molecular Devices, USA). The fluorescence was recorded over a period of time. After 6 minutes, CCCP, the efflux inhibitor and energy de-coupler, was added at a final concentration of 25 µg/ml. However, measurements without CCCP were also taken in other wells.

In case of EtBr efflux, cells were preloaded with EtBr. The cell suspension was incubated with 10 µg/ml EtBr at 37°C for 15 minutes. After incubation, efflux was initiated by addition of glucose at a final concentration of 0.4% (w/v). The fluorescence measurements were taken, as soon as glucose was added, at excitation and emission wavelength of 480 nm and 610 nm, respectively. After 9 minutes, CCCP was added at a final concentration of 25 µg/ml. The fluorescence was read without the addition of CCCP as well.

4.16 Disruption of *abaF* and genetic complementation in *A. baumannii*

The *abaF* gene was disrupted by insertional inactivation using a suicide plasmid pMo130. The homologous recombination-based approach was used to induce a single cross over resulting in insertion of the plasmid in the host chromosome (Figure 4.5). A functional copy of the gene was expressed from a plasmid to complement for the inactivation.

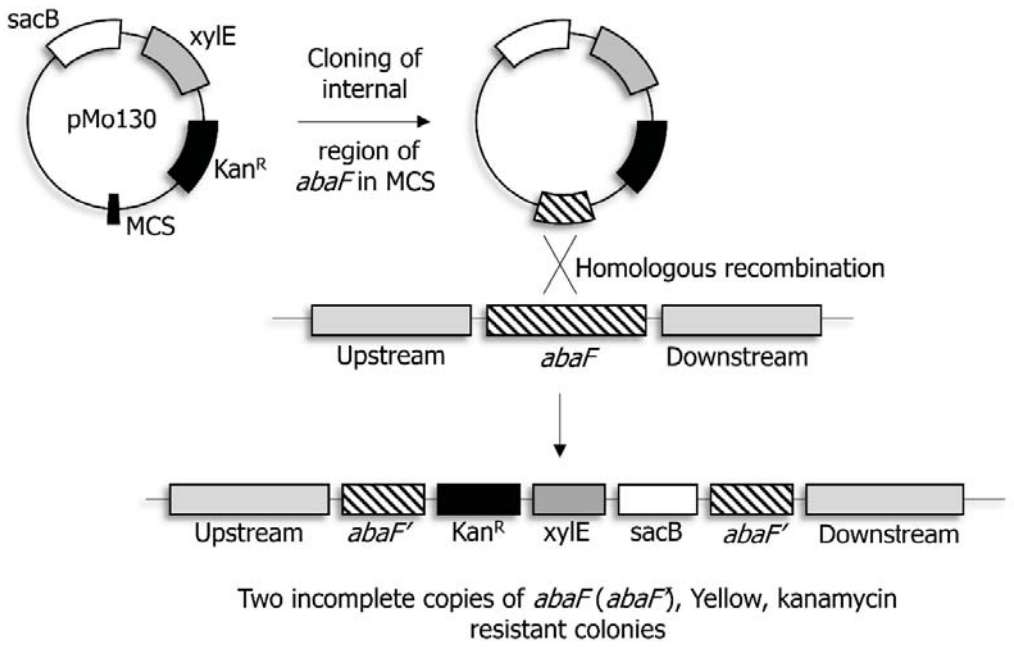

Figure 4.5 The general scheme for preparation of a construct and insertional inactivation (disruption) of *abaF*.

4.16.1 Cloning *abaF* region in allele exchange vector, pMo130

An internal region of *abaF* was amplified by PCR using the primers oligoRPT16 and oligoRPT17. The amplified product was cloned in a T-vector, pTZ57R/T, resulting in plasmid pRPT8. This internal region was then sub-cloned in an allele exchange vector, pMo130. The plasmids pRPT8 and pMo130 were double digested with BamHI and XbaI, according to the following conditions (Table 4.25):

Table 4.25 Restriction digestion of pMo130 plasmid and pRPT8 plasmid.

Components	Amount
10X Tango buffer	1.0 µl
Plasmid pMo130/pRPT8	500 ng
BamHI enzyme	0.5 µl
XbaI enzyme	0.5 µl
Nuclease free water	To make up10 µl

The digestion was carried out for an hour at 37°C and for the last 15 minutes 0.5 µl of FastAP was added to pMo130 digestion mixture. The enzymes were inactivated by incubation at 75°C for 5 minutes. The digested products were run on 1.5% agarose gel and a 200 bp fragment digested out from pRPT8 was excised and purified. The digested plasmid pMo130 and the 200 bp fragment were ligated as following (Table 4.26):

Table 4.26 Ligation of digested fragment from pMo130 plasmid and pRPT8 plasmid.

Components	Amount
10X Ligation buffer	1.0 µl
10mM ATP	1.0 µl
Digested fragment (insert)	A 1:3 molar ratio (plasmid: insert) with at
Digested plasmid pMo130 (vector)	least 50 ng DNA
Ligase enzyme	1.0 µl
Nuclease free water	To make up10 µl

The ligation was carried out overnight at 16°C and the ligation mixture was subsequently transformed into *E. coli* DH5α electrocompetent cells. The resulting recombinant plasmid was named pRPT9 and the strain was designated as RPT 116.

The plasmid pRPT9 was transformed into a conjugation competent strain *E. coli* S17-1 λpir. And the plasmid pRPT9 was thereafter conjugally transferred to *A. baumannii* ATCC 17978.

4.16.2 Conjugal transfer of plasmid from *E. coli* S17-1 λpir to *A. baumannii*

The *E. coli* S17-1 λpir cells carrying the plasmid pRPT9 were grown overnight from a fresh plate in LB broth supplemented with 50 mg/l kanamycin. The cells were grown to exponential phase, $OD_{600} \approx 0.5$. Similarly, *A. baumannii* cells were also grown to exponential phase in LB broth without any antibiotics. 1 ml of *E. coli* and 2 ml of *A. baumannii* cell suspension was centrifuged at 2500 g for 5 minutes. The cell pellets were washed in fresh LB broth and both the pellets were together resuspended in 100 µl of LB broth. The cell suspension was spotted on a 0.4 µm nylon filter laid over an LB agar plate. The suspension was allowed to dry and incubated for 16 hours at 30°C. After incubation, the bacterial biomass was collected from the nylon filter by scrapping and resuspended in 400 µl PBS by repeated tapping. 100 µl of this suspension was spread on LB agar plated supplemented with 25 µg/ml ampicillin and 15 µg/ml kanamycin. The plates were incubated overnight at 37°C. The colonies that appeared after incubation were patched on a fresh LB agar plate containing 25 µg/ml ampicillin and 15 µg/ml kanamycin. The colonies were checked for yellow coloration by spraying 0.4 M pyrocatechol and the resulting yellow colonies were streaked to isolate pure colonies.

4.16.3 Genetic complementation of *abaF* disruption

The *abaF* region was amplified using the primers OligoRPT18 and OligoRPT19 and purified. The purified product and plasmid pWHN678 were digested with BamHI according to the following reaction (Table 4.27):

Table 4.27 Restriction digestion of *abaF* PCR product and pWHN678 plasmid.

Component	Amount
10X BamHI buffer	1.0 µl
PCR product/plasmid	500 ng
BamHI enzyme	0.5 µl
Nuclease free water	To make up10 µl

The digestion was carried out for 2 hours at 37°C. 0.5 µl of FastAP® alkaline phosphatase was added to the plasmid digestion mixture and incubated at 37°C for 10 more minutes. The enzymes were inactivated by incubation at 75°C for 5 minutes. The digested products were gel purified using MinElute kit (Qiagen). A typical ligation mixture was prepared as follows (Table 4.28):

Table 4.28 Ligation of *abaF* PCR product and pWHN678 plasmid.

Components	Amount
10X Ligation buffer	1.0 µl
10 mM ATP	1.0 µl
Digested fragment (insert)	A 1:3 molar ratio (plasmid: insert) with at
Digested plasmid pWHN678 (vector)	least 50 ng DNA
Ligase enzyme	1.0 µl
Nuclease free water	To make up10 µl

Ligation was carried out at 16°C overnight and the mixture was subsequently transformed into electrocompetent *E. coli* DH5α, resulting in the plasmid, pRPT10. The plasmid was isolated and transformed into electrocompetent cells of RPT 103 and the resulting strain was named as RPT 152.

4.17 Fosfomycin treatment and isolation of total RNA

A single colony of *A. baumannii* ATCC 17978 was picked from a freshly streaked LB agar plate and inoculated in 5 ml LB broth. The cells were grown overnight at 37°C with 250 rpm orbital shaking. The overnight culture was diluted 100 times in LB broth and incubated at 37°C with shaking, till the $OD_{600} \approx 0.6$. The cells were divided into four different aliquots. Each aliquot was treated with a different concentration, namely, 256 µg/ml (1X MIC), 512 µg/ml (2X MIC) and 1024 µg/ml (4X MIC), of fosfomycin for 2 hours at 37°C. One aliquot was kept as control with no fosfomycin treatment. Total RNA was isolated from all the samples according to the protocol

described earlier. The total RNA was DNase treated (as described earlier) and quantified. cDNA was synthesized from the total RNA using SuperScript III reverse transcriptase (Table 4.29).

Table 4.29 Reaction mixture for reverse transcription using SuperScript III reverse transcriptase (Stage I).

Component	Amount
RNA sample	Up to 1 µg
10 µM Random hexamer primer	4.0 µl
10 mM dNTPs	5.0 µl
RNase free water	Up to 13 µl

The mixture was heated to 65°C for 5 minutes and allowed to cool down to room temperature. Following were added to the reaction mixture (Table 4.30):

Table 4.30 Reaction mixture for reverse transcription using SuperScript III reverse transcriptase (Stage II).

Component	Amount
5X First strand synthesis buffer	4.0 µl
0.1 mM DTT	1.0 µl
RNase out RNase inhibitor	1.0 µl
SuperScript III Reverse transcriptase	1.0 µl

The mixture was incubated for 5 minutes at 25°C before incubating at 50°C for 60 minutes. The reverse transcriptase was inactivated by incubation at 70°C for 15 minutes. The cDNA was stored at -20°C till further use.

4.18 *In vitro* selection of fosfomycin resistant mutants

A. baumannii cells were streaked on an LB agar plate and incubated overnight at 37°C. The colonies were subsequently streaked on to LB agar supplemented with 256 µg/ml (1X MIC) fosfomycin. The plates were incubated at 37°C overnight. The colonies after overnight incubation were further streaked on to LB agar plates containing 256 µg/ml fosfomycin. This was repeated for three generations to achieve fosfomycin resistant mutants. The *A. baumannii* cells resistant to 1X MIC were similarly made resistant to 2X and 4X MIC of fosfomycin (Figure 4.6). Total RNA was isolated from log phase cultured of all the three resistant strains, as described earlier, and reverse transcribed to cDNA.

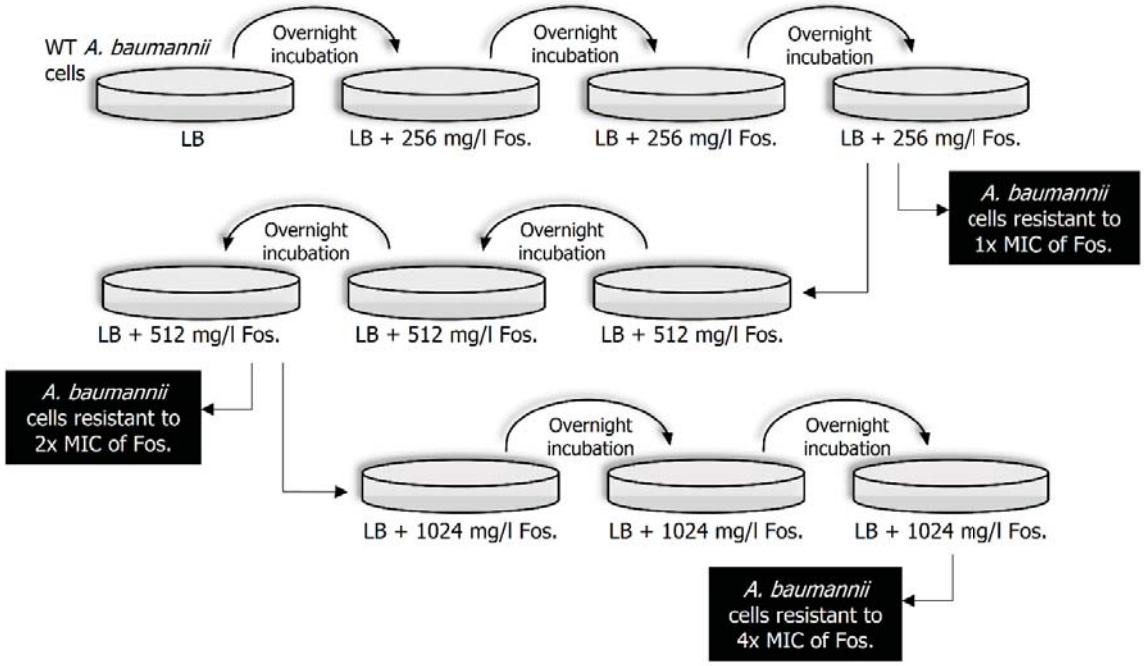

Figure 4.6 The general scheme for generation of fosfomycin resistant mutants of *A. baumannii*.

4.19 Quantitative real-time PCR (qPCR)

Quantitative real-time PCR was performed using Cephid Smart Cycler and Maxima SYBR Green/ROX qPCR Master Mix. A typical reaction was assembled as follows (Table 4.31):

Table 4.31 Reaction mixture for qPCR

Component	Amount
2X master mix	12.5 µl
10 µM forward primer	0.5 µl
10 µM reverse primer	0.5 µl
cDNA	Up to 200 ng
Nuclease free water	Up to 25 µl

For amplification of an internal region of *abaF*, primers used were oligoRPT16 and oligoRPT17. Primer pairs oligoRPT20-oligoRPT21 and oligoRPT57-oligoRPT58 were used for amplification of an internal region of AbsR25 and *groEL* (internal control), respectively.

A typical program for amplification was as follows (Table 4.32):

Table 4.32 Cycling conditions for qPCR of AbsR25, *groEL* and *abaF* genes.

Step	Conditions	Cycles
Initial denaturation	95°C for 10 minutes	1
Cycle denaturation	95°C for 15 seconds	
Cycle annealing	50°C for 30 seconds	40
Cycle extension	72°C for 30 seconds (with optics)	

4.20 Biofilm formation assay

A single colony of wild type *A. baumannii*, RPT 103 and RPT 152 was inoculated into LB broth and incubated overnight at 37°C. The overnight culture was diluted 100 times in fresh LB and 200 µl of this fresh culture was added to multiple wells of a 96-well microtiter plate. The plate was incubated at 37°C in a humidity controlled Kuhner shaker for 24 hours. After incubation, the plate was read at 600 nm using Spectramax M2e plate reader. The wells were drained and washed with sterile PBS. The washed wells were stained with 200 µl of freshly prepared 1% crystal violet solution, for 20 minutes. The wells were drained and washed again in PBS. The stain from the biofilms was dissolved by adding 200 µl of 95% methanol and the plate was read at 595 nm. The OD_{595} of each well was divided by its respective OD_{600} for relative quantification of biofilm.

4.21 *Caenorhabditis elegans* survival assay

Overnight cultures of wild type *A. baumannii*, RPT 103 and RPT 152 were spotted on the middle of LB agar plates and incubated at 37°C to form a lawn of bacteria in the center of the plate. 10 adult N2 wild type *C. elegans* worms were picked up and placed on the center of the plate. The experiment was done in triplicates, making 30 worms for each strain. The plates were incubated at 25°C and every day the worms were transferred to fresh plates to avoid problems of spawning. The worms that showed neither response to touch by sterile needle nor any movement under the microscope, were considered to be dead. The number of surviving worms was recorded every day.

4.22 Prediction of small RNAs in *A. baumannii*

A comprehensive effort undertaken in the laboratory previously resulted in identification of 31 small RNAs in *A. baumannii*. The bioinformatics search was based on three important features of small RNA:

a) Inter-genomic location
b) Secondary structure
c) Rho-independent transcription termination

A range of online programs and bioinformatics tools were utilized to assess the *A. baumannii* genome for these aforementioned properties and 31 candidate small RNA were identified and named as AbsR1 (*Acinetobacter baumannii* small RNA) to AbsR31 (Figure 4.7). From this list, AbsR1 was picked up for further validation.

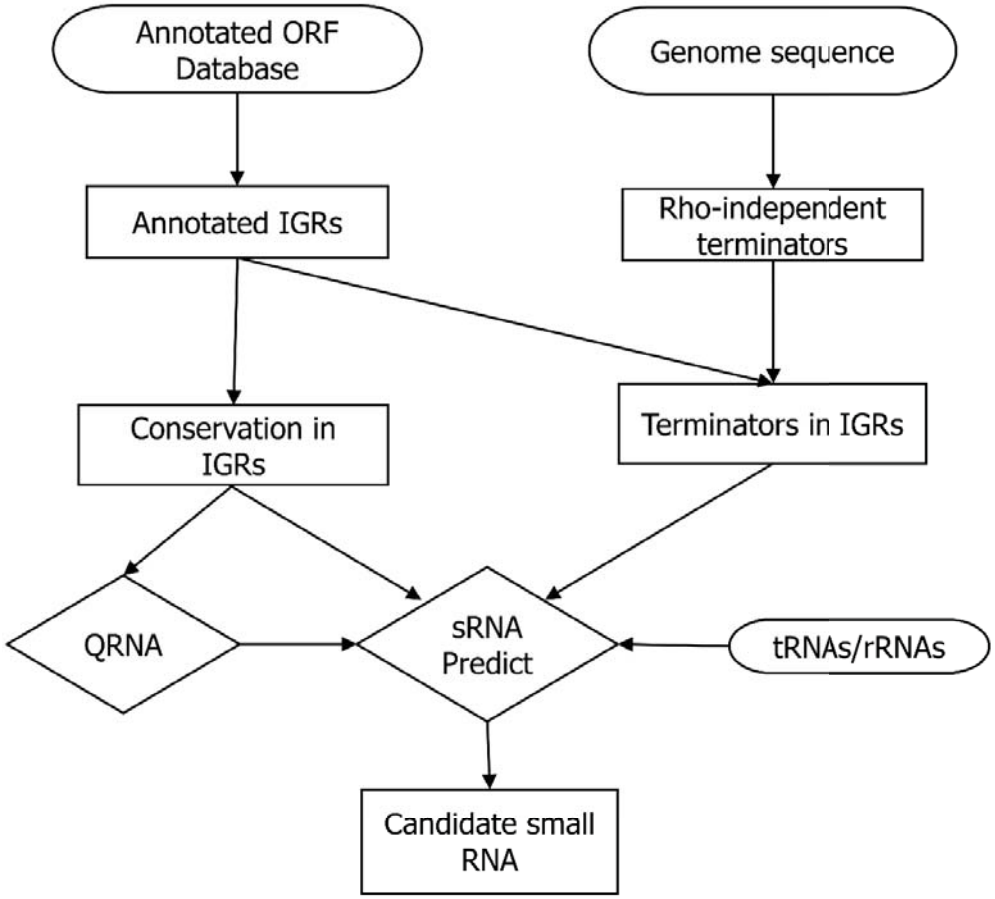

Figure 4.7 Computational pipeline for identification of small RNA in *A. baumannii* (Taken from [11]).

4.23 Validation of AbsR1 small RNA by Northern Blotting

Northern Blotting was employed to determine the expression of predicted small RNA, AbsR1. The total RNA was extracted from *A. baumannii* cells at different stages of growth and resolved on a denaturing gel. The RNA was transferred on to a nylon membrane where hybridization with a labelled probe was performed. After hybridization the blot is developed by incubating the membrane with the substrate of the enzyme tagged on the probe (Figure 4.8). The developed blot is visualized either on a typhoon scanner or by exposure to a photosensitive film.

4.23.1 Total RNA extraction

A single colony of *A. baumannii* ATCC 17978 was picked up from a freshly streaked LB plate, inoculated into fresh LB broth and incubated at 37°C and 250 rpm shaking overnight. The overnight grown cells were diluted 100 times into fresh LB broth and were incubated again at 37°C. Samples were withdrawn at different growth stages, namely, lag phase (OD_{600} = 0.4), log phase (OD_{600} = 1.6) and stationary phase (OD_{600} = 3.2). The cells were harvested by centrifugation and suspended in 1ml of TRI reagent. The suspension was incubated at room temperature for 5 minutes before 200 µl chloroform was added. The samples were vigorously mixed and incubated at room temperature for another 10-15 minutes. The samples were then centrifuged at 12000g for 15 minutes at 4°C. The RNA containing aqueous layer was carefully collected, avoiding any contact with the lower layers, in a fresh microcentrifuge tube. 500 µl of isopropanol was added and the mixture was kept at room temperature for about 20 minutes to precipitate the RNA from the aqueous solution. The precipitated RNA was collected as a pellet by centrifugation at 12000g for 10 minutes at 4°C. The pellet was washed in 1 ml of 75% ethanol by centrifugation at 7500g for 5 minutes at 4°C. The pellet was air dried by inverting the tubes on a paper towel. Finally, the pellet was dissolved in 30 µl of RNase free water supplemented with 1 mM EDTA and incubated at 55°C for 10 minutes. The RNA samples were run on 2% agarose gel to check the integrity.

The samples were treated with DNase I to remove any contaminating DNA. A typical reaction was made up as described below (Table 4.33).

Table 4.33 DNase treatment of total RNA using DNase I enzyme.

Component	Volume
RNA sample	28 µl
DNase I buffer	4 µl
DNase I enzyme	4 µl
RNase free water	Upto 40 µl

After incubation at 37°C for 30 minutes, the DNase I enzyme was inactivated by addition of 5mM EDTA and heat inactivation at 70°C for 10 minutes.

4.23.2 Denaturing PAGE

Denaturing PAGE is preferred to resolve RNA as it avoids the formation secondary structures like hairpins and duplexes. 10% Urea gel containing 8 M urea was prepared (Appendix I) and was cast in vertical electrophoresis assembly from CBS Scientific. As soon as TEMED was

added, the mixture was quickly poured in pre-cleaned glass plates and the assembly was kept on a flat surface and a 12-well comb was inserted. Extra care was taken to ensure there were no air bubbles. The gel was allowed to set.

Once set, the gel was clamped onto the running apparatus which was filled with 1X TBE. The gel was pre-run for about 20 minutes. Empty wells were loaded with 50% glycerol. The gel was run for about 4-5 hours till the xylene cyanol dye traversed about 4/5th of the gel. After running, the gel was carefully taken out of the plates and immersed in a 0.5µg/ml solution of ethidium bromide. The gel was stained on a gel rocker for 20 minutes and then wrapped in a cling film. The gel was viewed under UV illumination and the target area, where the small RNA is expected to be, was excised out.

4.23.3 Electro-transfer to positively charged nylon membrane

The RNA was transferred to a positively charged nylon membrane, for blotting, from the excised piece of urea gel. The electric current assisted electro-transfer was carried out using Bio-Rad mini PROTEAN tetra system. The nylon membrane was cut into a piece measuring the gel slice. The membrane was kept next to the gel and both were sandwiched between a stack of Whatman filter papers already soaked in electro-transfer buffer. Avoiding any bubbles in the system, the Whatman paper-gel-membrane-Whatman paper sandwich was locked in an electro-transfer cassette and put in the electro-transfer tank apparatus filled with electro-transfer buffer. The electrodes were connected making sure that the gel was towards the negative electrode and the membrane was towards the positive electrode. The electro-transfer was carried out at 4°C, 20V for 3-4 hours. Once the electro-transfer was complete, the membrane was dried and baked at 80°C for 30 minutes. The membrane was then covered by cling film and stored at 4°C till further use.

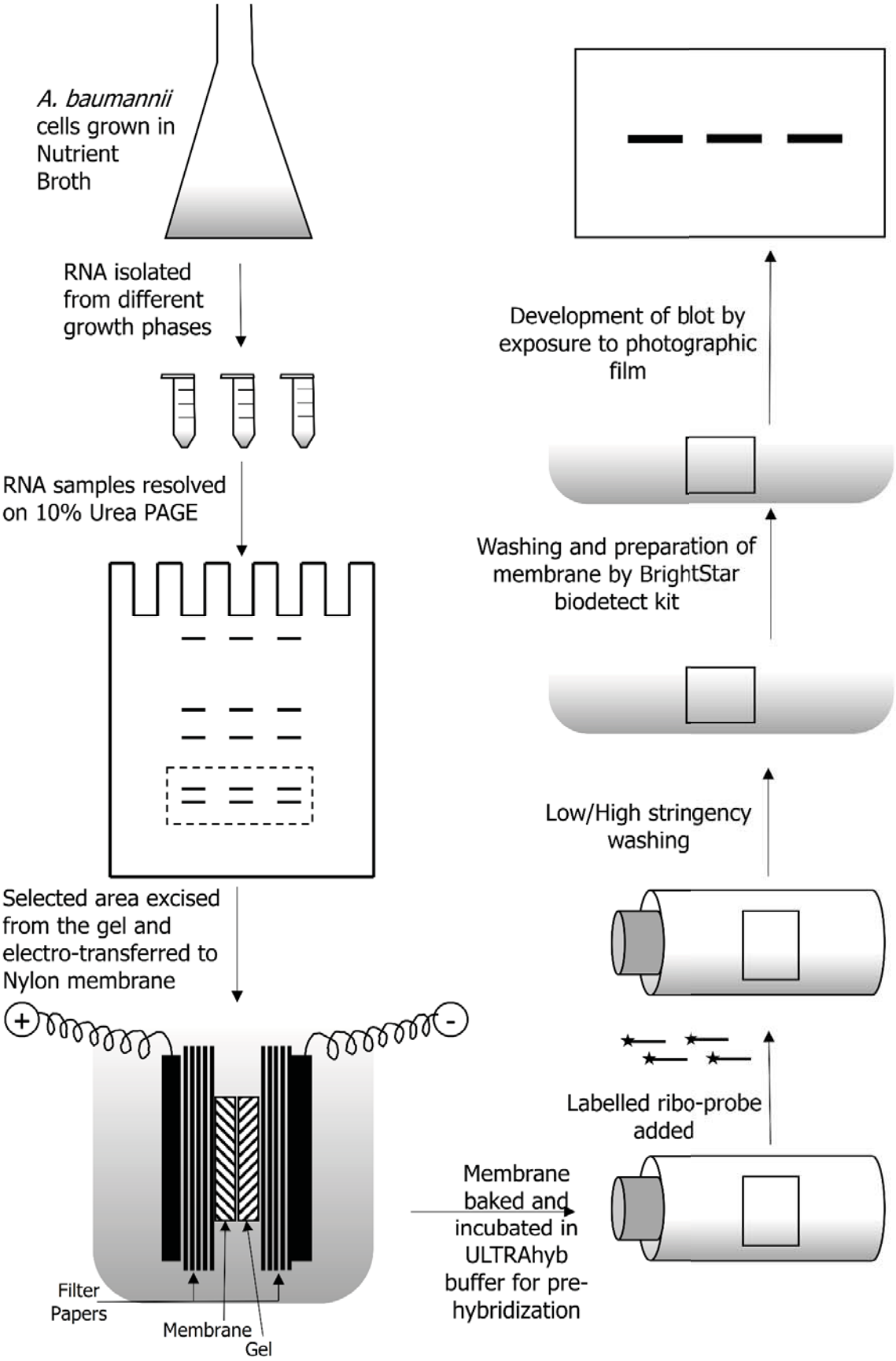

Figure 4.8 The general procedure of Northern Blotting.

4.23.4 Construction of a riboprobe

Riboprobe was prepared by *in vitro* transcription of a DNA template using a mirVana miRNA probe construction kit. This DNA template, OligoRPT1, was designed to carry a specific sequence (CCTGTCTC) at its 3' end to allow for hybridization with the T7 promoter primer (Figure 4.9). Single stranded DNA template was obtained in lyophilized form from Imperial Life Sciences. The oligonucleotide was reconstituted in nuclease-free water to make the concentration 100 µM. The following reaction was set up for hybridization of T7 promoter primer to the single stranded DNA oligonucleotide (Table 4.34).

Table 4.34 Reaction mixture for hybridization of T7 promoter primer to template single stranded DNA.

Component	Amount
T7 promoter primer	5 µl
DNA hybridization buffer	5 µl
100 µM template	30 µl

The mixture was incubated for 5 minutes at 70°C and then left at room temperature for annealing/hybridization in the next 10 minutes. After hybridization, fill-in reaction using Klenow DNA polymerase was performed. To the previous reaction mixture, following components were added (Table 4.35):

Table 4.35 End filling reaction to generate double stranded DNA carrying T7 promoter.

Component	Amount
10X Klenow reaction buffer	2 µl
10X dNTP mix	2 µl
Nuclease free water	4 µl
Exo-Klenow	2 µl

All the components were mixed with gentle pipetting and the mixture was incubated at 37°C for 30 minutes. The double stranded DNA template thus prepared was stored at -20°C till use for transcription.

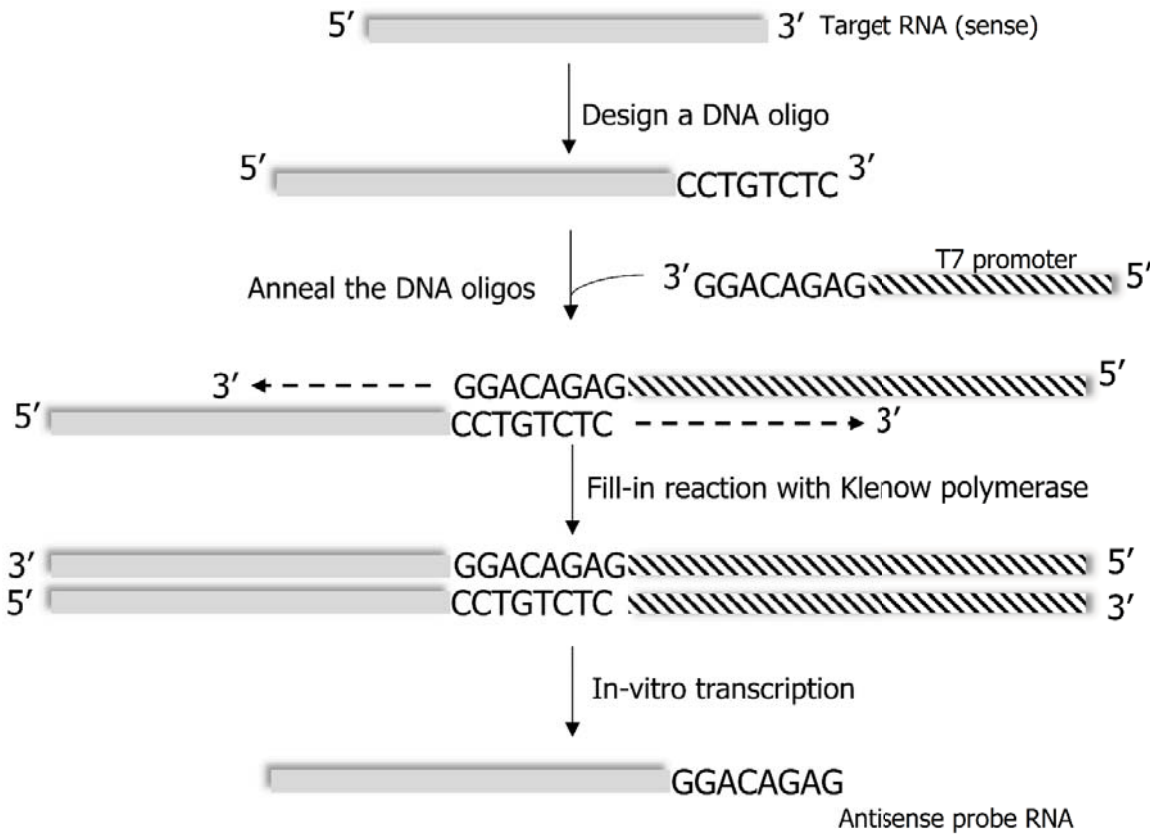

Figure 4.9 Preparation of a template for riboprobe using the mirVana probe construction kit.

A typical transcription reaction was set up as follows to obtain functional riboprobe from DNA template (Table 4.36):

Table 4.36 *In vitro* transcription reaction for generation of riboprobe.

Component	Amount
5X Transcription buffer	4 µl
dsDNA template	2 µl
10 mM ATP	1 µl
10 mM CTP	1 µl
10 mM GTP	1 µl
10 mM UTP	1 µl
T7 RNA polymerase	30 units
Nuclease free water	To make up 20 µl

The mixture was mixed by gentle pipetting and was incubated at 37°C for 2 hours. After the incubation, 1µl of DNase I (1 U/µl) was added and the mixture was further incubated at 37°C for15 minutes to remove any DNA template.

The riboprobe transcribed from the DNA template was checked on 2% agarose gel and subsequently purified using Qiagen Nucleotide removal kit, following the manufacturer's instructions (Appendix II).

4.23.5 Biotin labelling of riboprobe

Biotin labelling was performed using BrightStar psoralen-biotin kit (ThermoScientific, USA). The kit contains biotin conjugated to planar psoralen molecules. These molecules intercalate between the nucleic acid bases similar to ethidium bromide. Upon exposure to long wavelength UV light, these psoralen molecules form covalent bonds with the nucleic acids like tyhmidines, uridines and cytidines with preference for the former (Figure 4.10). The hybridization ability of riboprobes is not affected by the psoralen intercalation.

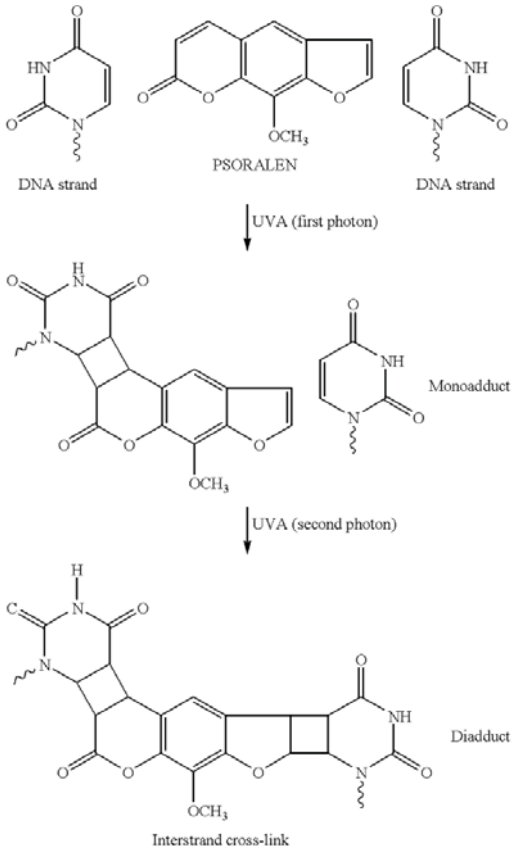

Figure 4.10 Psoralen biotin and its intercalation in DNA.

A clean untreated 96-well plate was kept on ice. 10 µl of RNA sample was added to one of the wells, 1µl of the psoralen-biotin mix was also added to the same well and both the components were mixed properly by pipetting. A long-range UV lamp (365 nm) was placed exactly over the 96-well plate and was covered from all the sides to avoid any unnecessary illumination. The setup was kept like this for 45 minutes for labelling. The labelled riboprobes were taken in a fresh

microcentrifuge tube and 89 µl of TE buffer was added to the tube. 200 µl of water saturated butanol (provided with the kit) was added to this tube and mixed vigorously. The mixture was centrifuged at 7000 g for a minute and the top layer of butanol containing extra psoralen as removed. This washing step was repeated once again and the washed and labelled riboprobe was stored in -80°C in dark until further use.

4.23.6 Northern hybridization

Northern hybridization was performed using the Ambion NorthernMax kit. The membrane, onto which the total RNA was electro-transferred, was taken in a clean hybridization bottle. The bottle containing ULTRAhyb buffer, supplied with the kit, was put in a water bath and heated up to 65°C to dissolve any precipitates. The bottle was swirled to make the contents homogenous. 10 ml of ULTRAhyb buffer was added to the bottle containing the membrane and the bottle was attached to the hybridization oven. The oven temperature was set to 50°C and rotation to 15 rpm. The pre-hybridization, with the buffer alone, was allowed to run for about 2 hours.

After two hours of pre-hybridization, the biotin-labelled riboprobe was added to the ULTRAhyb buffer. 100 µl of the labelled riboprobe prepared earlier was thawed and added to 1 ml of pre-warmed ULTRAhyb buffer. The mixture was pipetted well to mix the riboprobe and was then added to the bottle containing the ULTRAhyb buffer and the membrane, for hybridization. The hybridization was carried out for up to 12 hours.

4.23.7 Development of the blot

After hybridization was completed, the membrane was taken out of the hybridization bottle and washed according to the manufacturer's instructions. The nylon membrane was retrieved from the hybridization bottles in a flat container. The membrane was washed with a series of different buffers and developed using the CDP-star chemiluminescent substrate provided in the NorthernMax kit (ThermoScientific, USA).

The blot was washed with low stringency wash buffer twice at room temperature for 5 minutes on a rocker shaker. Second washing of blot was performed with high stringency wash buffer twice for 10 min at 42°C in an incubator shaker at 100 rpm (ThermoScientific, USA). The blot was subsequently washed in buffers provided with the Bright Star Biodetection kit (ThermoScientific, USA) for the detection of signal.

The blot was washed twice with 25 ml of 1X wash buffer for 5 minutes each. The wash buffer is provided at 5X concentration, so it must be diluted prior to use in MilliQ water. After washing membrane was incubated twice in 25 ml blocking buffer for 5 minutes each. The blot was once

again incubated in 50 ml of blocking buffer for 30 min. Strep-Alkaline Phosphatase (Strep-AP) solution was prepared mixing together of 10 ml Blocking Buffer and 0.5 µl Strep-AP provided in the kit. The blot was incubated with Strep-AP for another 30 minutes. After enzyme treatment, the blot was incubated in 25 mL of blocking buffer for 10 minutes. The blot was then washed twice with 50 ml of 1X wash buffer (5 minutes each) and then in 25 ml of 1X assay buffer (10 minutes) provided with the kit. The assay buffer is provided at 10X concentration and is diluted similar to the wash buffer. After incubation in assay buffer, the blot was dipped in 3 mL CDP-Star substrate. Regular but gentle swirling was done to ensure complete coverage of the blot by the substrate. After 5 minutes, the blot was quickly blotted on a piece of Whatman filter paper to remove excess CDP-Star, without letting the membrane dry and was wrapped in a single layer of plastic, and exposed to X-ray film at room temperature.

CDP-Star reaches peak light emission in 2 hours, then emission falls to a plateau which persists for several days.

4.23.8 Visualization of the blot

After 2 hours of incubation in CDP-Star, the membrane was taken to the dark room for exposure. A photographic film was cut to the size of the membrane and was kept with the membrane for exposure. The exposed film was developed using silver bromide-based developer and fixer solutions commonly used for photography. The developed film was dried in a hot air oven and scanned using a common scanner.

4.24 Expression of AbsR1 under various simulated environmental conditions

To determine whether AbsR1 was involved in fitness of *A. baumannii*, its expression was determined under various stress conditions that the microbe is likely to face in the environment. These stress conditions were induced by different additives and incubation conditions. The relative expression of AbsR1 was assayed by carrying out a Northern Blot.

4.24.1 Induction of various stress

Actively growing *A. baumannii* cells were exposed briefly to different physical as well as chemical agents to simulate stress conditions (Figure 4.11). A singe colony of *A. baumannii* ATCC 17978 was inoculated in nutrient broth and incubated overnight at 37°C. The overnight culture was diluted 100 times in fresh NB and the cells were allowed to grow at 37°C till OD_{600} = 1.2. The cells were divided into aliquots of 20 ml in sterile 50 ml centrifuge tubes and the stress conditions were induced as follows:

4.24.1.1 Oxidative stress

To a 20 ml aliquot, Hydrogen peroxide (H_2O_2) was added to a final concentration of 1 mM. The cells were incubated at 37°C for a period of 30 minutes.

4.24.1.2 Thermal stress

To induce thermal stress, a 20 ml aliquot was incubated at 45°C for 30 minutes in a water bath.

4.24.1.3 Cold stress

Another 20 ml aliquot was incubated for 30 minutes in an ice bucket.

4.24.1.4 Osmotic stress

The cells were exposed to osmotic stress by addition of NaCl to a final concentration of 500 mM. The cells were incubated at 37°C for 30 minutes.

4.24.1.5 Acidic stress

A 20 ml aliquot was centrifuged at 2000g for 10 minutes. The supernatant was discarded and the pellet was resuspended in sterile NB maintained at pH 5. The cells were subsequently incubated at 37°C for 30 minutes.

4.24.1.6 Alkaline stress

Similar to the acidic stress, the cells in a 20 ml aliquot were centrifuged and the pellet was resuspended in NB maintained at pH 9. The suspension was incubated for 30 minutes at 37°C.

The cells were exposed to the stress condition for 30 minutes and the cell growth was arrested by addition of a stop solution (5% phenol solution in ethanol). Total RNA was subsequently isolated from these cells and Northern hybridization was carried out as explained earlier.

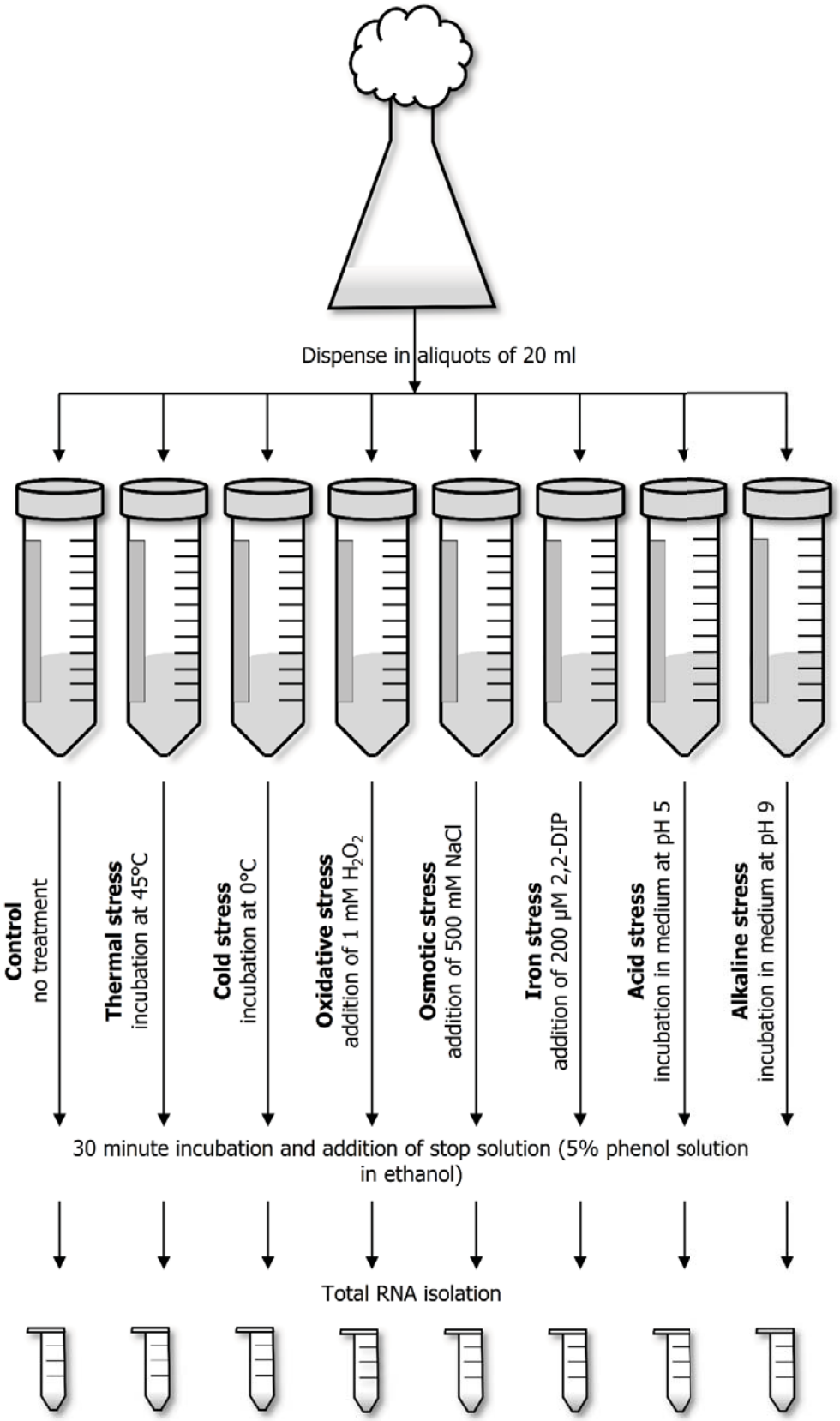

Figure 4.11 Overall scheme of exposure of *A. baumannii* cells to various stress for analysis of AbsR1 expression.

4.25 Determination of sequence of small RNA by 3' and 5' rapid amplification of cDNA ends (RACE)

RACE is a commonly applied technique to determine the 3' and 5' ends of a transcript through sequencing of cDNA generated using the RNA as template. RNA ligase mediated RACE is a variation of conventional RACE where an RNA adaptor is ligated to the primary RNA transcript and using PCR a single band is generated and sequenced (Figure 4.12).

FirstChoice RLM-RACE kit was used for RACE mapping of small RNA Absr1. The protocol supplied along with the kit was followed omitting the early steps where RNA is treated with alkaline phosphatase as prokaryotic RNA is not capped with methylguanosine on the 5' end (Appendix II). Internal primers OligoRPT2 and OligoRPT3 were designed for 5'and 3' RACE PCR respectively. The amplicons generated from the PCR were cloned in a T-vector, pTZ57R/T (Fermentas) and sent for sequence analysis.

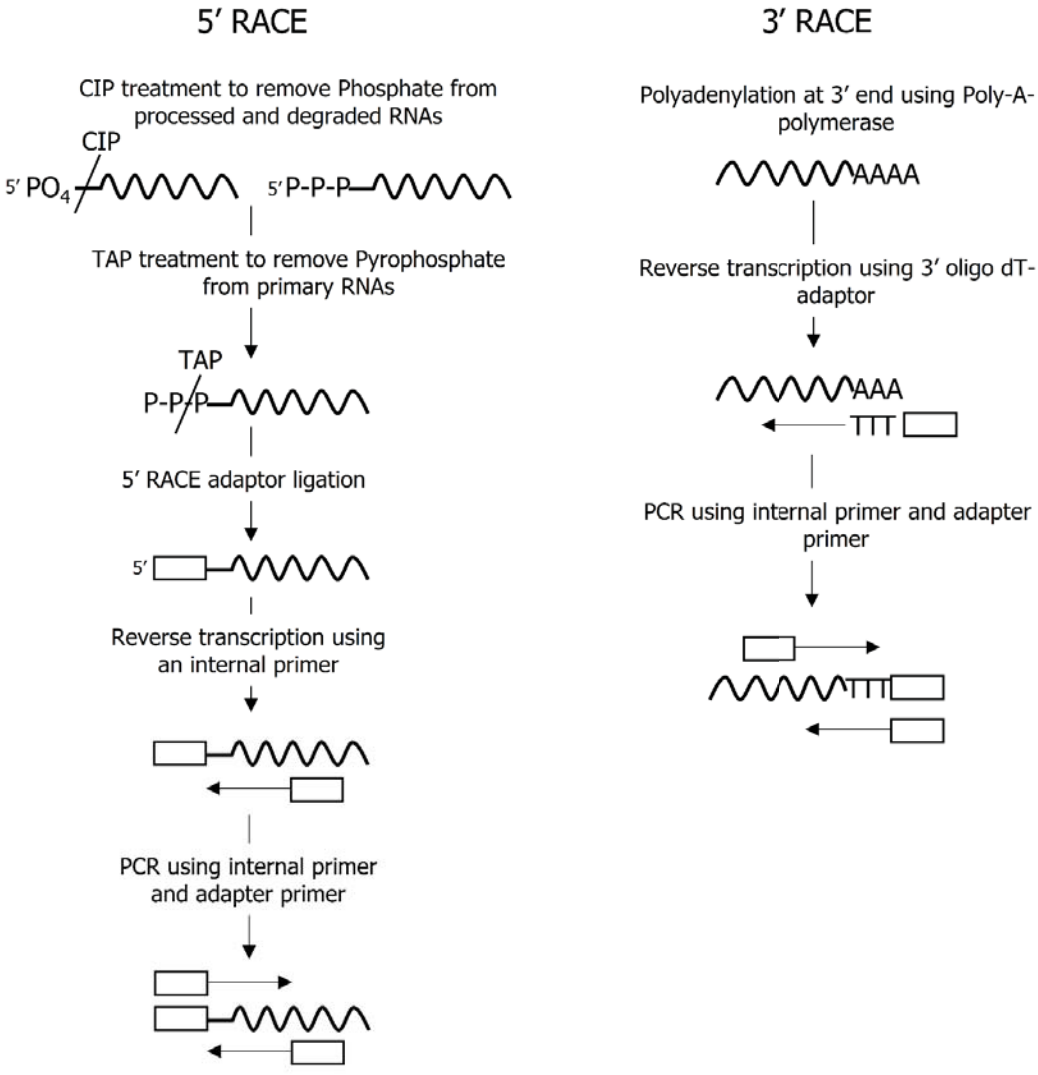

Figure 4.12 The general procedure for RLM-RACE to determine transcription start and stop sites.

4.26 Generation of AbsR1 knock-out *A. baumannii* cells

AbsR1 deletion strain of *A. baumannii* was generated following a PCR based homologous recombination. *A. baumannii* cells were made recombination-competent by expressing an *A. baumannii recT* homolog from a plasmid, pAT02. A recombineering construct carrying a 500 bp region upstream and 500 bp region downstream of AbsR1 coding region and carrying a kanamycin cassette flanked by FRT sites was generated by cloning different parts together (Figure 4.13). Finally, a recombineering PCR product was amplified from this construct carrying the kanamycin cassette flanked by 125 bp of upstream and downstream regions. This recombineering PCR product was transformed into *A. baumannii* cells expressing RecT. Recombinant cells were selected on kanamycin containing medium and were confirmed for allele replacement by PCR.

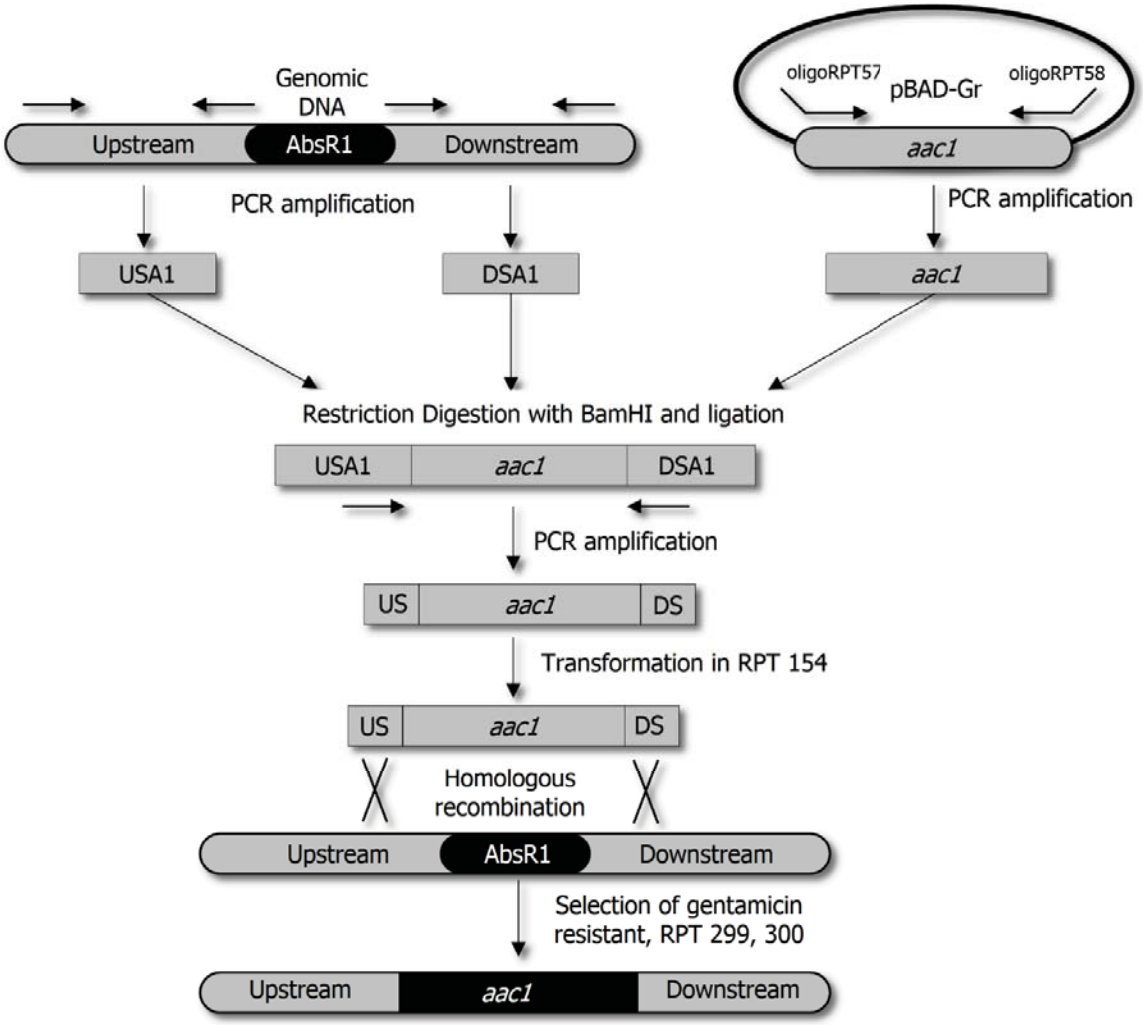

Figure 4.13 Generation of an AbsR1 deletion mutant by allele replacement.

Another plasmid pAT03, expressing FLP recombinase enzyme was transformed in recombinant cells carrying kanamycin at the genomic locus of AbsR1. FLP recombinase enzyme identifies the FRT sites and excises the region between them leaving just a small scar sequence, resulting in a markerless AbsR1 deletion mutant.

4.26.1 Generation of *A. baumannii* strain expressing *A. baumannii* RecT

The *A. baumannii* ATCC 17978 cells were made electrocompetent by repeatedly washing an early log phase culture (OD_{600} = 0.6) with ice-cold 10% glycerol. A 50 µl aliquot of electrocompetent cells was taken in a 2 mm electroporation cuvette and the plasmid pAT02 was added. Electroporation was carried out at 2300 kV and the cells were immediately resuspended in pre-warmed SOC medium. The cells were incubated at 37°C for an hour before spreading on LB plates supplemented with 100 µg/ml ampicillin. The plates were incubated for 12 hours and the resulting colonies were selected which were designated as RPT 154.

A single colony of RPT 154 was picked, inoculated into LB broth supplemented with 100 µg/ml ampicillin and incubated overnight at 37°C overnight with agitation. The overnight culture was diluted 100 times in fresh LB-ampicillin broth supplemented with 2 mM IPTG (for expression of recombinase) and grown till early log phase (OD_{600} = 0.6). The cells were subsequently harvested by centrifugation and made electrocompetent by washing with ice-cold 10% glycerol. The electrocompetent cells of RPT 154 were stored at -80°C till further use.

4.26.2 Generation of recombineering construct and recombineering PCR product

Primers OligoRPT4 and OligoRPT5 were designed for amplification of a 500 bp upstream region of AbsR1 (USA1) carrying a NotI and a BamHI restriction site on the ends. Similarly, primers OligoRPT6 and OligoRPT7 were designed to amplify a 500 bp region downstream of AbsR1 (DSA1) and carrying the restriction sites for BamHI and XbaI. Another set of primers OligoRPT57 and OligoRPT58, carrying BamHI restriction site on either end was designed for amplification of gentamycin cassette (*aac1*). The genomic DNA of *A. baumannii* served as a template for amplification of USA1 and DSA1 while *aac1* was amplified using a plasmid pBAD-Gr as template. Typical PCR reaction for amplification of these products is given below (Table 4.37).

Table 4.37 A typical PCR reaction mixture for amplification of *aac1*, USA1 and DSA1.

Component	Amount
10X Ex Taq buffer	5.0 µl
2 mM dNTPs	5.0 µl

10 µM forward primer	1.0 µl
10 µM reverse primer	1.0 µl
Template DNA (gDNA/plasmid)	Upto 10 ng
Ex Taq DNA polymerase	1.0 unit
Nuclease free water	To make up 50.0 µl

Upon amplification, all the three PCR products were gel purified and quantitated. Digestion reactions, for cloning the PCR products into a recombineering product, were set up as follows (Table 4.38):

Table 4.38 Restriction digestion of USA1, DSA1 and *aac1* PCR products.

Component	Amount
10X BamHI buffer	2.0 µl
USA1/DSA1/*aac1* PCR product	500 ng
BamHI	0.5 µl
Nuclease free water	To make up 20 µl

The digestion was carried out for 2 hours at 37°C. 0.5 µl of FastAP® alkaline phosphatase was added to the digestion mixture containing USA1 and DSA1 and incubated at 37°C for 10 more minutes. The enzymes were inactivated by incubation at 75°C for 5 minutes. After digestion all the products were gel purified using MinElute kit (Qiagen) and ligated as follows (Table 4.39):

Table 4.39 Ligation of USA1, DSA1 and *aac1* PCR products.

Component	Amount
10X T4 ligase buffer	1.5 µl
Digested PCR products	An equimolar mixture of all the three PCR products (USA1/DSA1/*aac1*) with at least 50 ng DNA
10 mM rATP	1.5 µl
T4 DNA ligase	1.0 µl
Nuclease free water	To make up 15 µl

The ligation product was used as a template in a PCR reaction using primers OligoRPT4 and OligoRPT7 for amplification of a PCR product carrying NotI restriction site at one end and XbaI at the other end (Table 4.40).

Table 4.40 PCR reaction mixture for amplification of US-aac1-DS amplicon.

Component	Amount
10X Ex Taq buffer	5.0 µl
2 mM dNTPs	5.0 µl
10 µM OligoRPT4	1.0 µl
10 µM OligoRPT7	1.0 µl
Template DNA (ligation mix)	2.0 µl
Ex Taq DNA polymerase	1.0 unit
Nuclease free water	To make up 50.0 µl

This PCR product was gel purified and digested using NotI and XbaI. The plasmid pMo130 was also similarly digested (Table 4.41).

Table 4.41 Restriction digestion of pMo130 and US-aac1-DS PCR product.

Component	Amount
10X Buffer O	2.0 µl
pMo130/PCR product	500 ng
NotI	0.5 µl
XbaI	1.0 µl
Nuclease free water	To make up 20 µl

The digestion was carried out for 4 hours at 37°C. 0.5 µl of FastAP® alkaline phosphatase was added to the plasmid digestion mixture and incubated at 37°C for 10 more minutes. The enzymes were inactivated by incubation at 75°C for 5 minutes. The digested products were gel purified using MinElute kit (Qiagen). A typical ligation mixture was prepared as follows (Table 4.42):

Table 4.42 Ligation of pMo130 and US-*aac1*-DS PCR product.

Component	Amount
10X T4 ligase buffer	1.5 µl
Digested PCR product	A 1:3 molar ratio (plasmid: insert) with at
Digested pMo130	least 50 ng DNA
10 mM rATP	1.5 µl
T4 DNA ligase	1.0 µl
Nuclease free water	To make up 15 µl

Ligation was carried out at 22°C for 2 hours. The ligation mixture was transformed into electrocompetent *E. coli* DH5α and the transformants were selected on LB agar plate supplemented with 10 µg/ml gentamicin. The recombinant plasmid thus generated was designated as RPT 230.

A new set of primers, OligoRPT10 and OligoRPT11, was designed for amplification of 125 bp region upstream and downstream of AbsR1 coding region. A PCR reaction was set up using these primers and the ligation mixture as template. The PCR product was run on 0.8% agarose gel and the band corresponding to 1.75 (0.125 + 0.125 + 1.5) kb was excised form the gel.

4.26.3 Screening of recombinant *A. baumannii* with replaced AbsR1 allele

The recombineering PCR product was concentrated and 5 µg of this PCR product was used to transform electrocompetent cells of RPT 154, using an electroporator. The PCR product was added to a 100 µl aliquot of competent cells, with ~10^{10} cells, and electroporated at 1.8 kV in a 2 mm electroporation cuvette. The cells were incubated in 1 ml SOC medium, supplemented with 2 mM IPTG, for two hours and then spread on LB agar plates supplemented with gentamicin (5 µg/ml). After overnight incubation the colonies that appeared were picked up for a colony PCR using the primers OligoRPT4 and OligoRPT7 that would yield an amplicon of 2.4 kb in case of successful allele exchange by homologous recombination.

4.26.4 Validation of AbsR1 allele replacement

To ensure that the allele replacement had indeed occurred in one of the colonies, the colony was purified by repeated streaking on increasing amounts of gentamicin (up to 50 µg/ml) for three days. Two purified colonies (obtained independently) were inoculated in 5 mL of LB and genomic DNA was isolated from the overnight culture. The genomic DNA was used as a template in a series of PCR reactions.

Using the primers OlogoRPT63 (forward primer for *aac1*) and OligoRPT62 (reverse primer for DSA1) a PCR reaction was carried out with gDNA of suspected AbsR1 deletion mutant and wild type *A. baumannii* ATCC 17978. In case of allele replacement there would be an amplification (1.5 kb) but there won't be any amplification in the wild type (due to the absence of *aac1*). Another PCR was carried out using a different set of primers OligoRPT65 (forward primer for AbsR1) and OligoRPT62 (reverse primer for DSA1). In case of allele replacement there would be no amplification (due to absence of AbsR1) and there would be amplification only when wild type genomic DNA is used as template. The *A. baumannii* cells with AbsR1 allele replaced with *aac1* were designated as RPT 299 and RPT 300.

4.27 Computational assessment of AbsR10 for detection of *A. baumannii*

The sequence of AbsR10 was obtained by computational analysis as described earlier [11]. The sequence was used as a query in nucleotide BLAST against all the sequenced *A. baumannii* genomes. A common region was determined from the sequence alignment, resulting in selection of a 151 bp fragment for detection purpose. To assess the specificity, the 151 bp sequence was used as a query in another nucleotide BLAST search with the *Acinetobacteraceae* excluded from the target database. Primers were designed using this sequence and were individually searched using nucleotide BLAST to avoid any similarity with other sequences (Table 4.43).

Table 4.43 Pathogenic bacteria used as controls to assess the specificity of AbsR10 based *A. baumannii* detection system.

Organism	Characteristics
Salmonella typhi	Gram negative, rod shaped bacterium
Klebsiella pneumonia	Gram negative, rod shaped bacterium
Enterobacter sakazakii	Gram negative, rod shaped bacterium
Vibrio cholerae	Gram negative, comma shaped bacterium
Staphylococcus aureus	Gram positive, spherical shaped bacterium
Shigella flexneri	Gram negative, rod shaped bacterium
Streptococcus mutans	Gram positive, spherical shaped bacterium
Pseudomonas aeruginosa	Gram negative, rod shaped bacterium

4.28 PCR amplification of unique AbsR10 region

Genomic DNA of all the strains of *A. baumannii* was isolated using GeneJET genomic DNA isolation kit (ThermoScientific), according to the manufacturer's instructions. A PCR reaction was set up as follows (Table 4.44):

Table 4.44 Reaction mixture for amplification of AbsR10 unique region.

Component	Amount
10X Dynazyme II buffer	2.5 µl
2 mM dNTPs	2.5 µl
10 µM forward primer	0.5 µl
10 µM reverse primer	0.5 µl
Template DNA	Upto 200 ng
Dynazyme II polymerase	0.5 Units

Water	To make up 25 µl

The cycling conditions were set as follows (Table 4.45):

Table 4.45 Cycling conditions for amplification of AbsR10 unique region.

Event	Temperature	Time
Initial denaturation	94°C	60 seconds
Cycle denaturation	94°C	15 seconds
Cycle annealing	48°C	25 seconds
Cycle extension	72°C	15 seconds
Final extension	72°C	5 minutes

The PCR was run for 30 cycles and the products were resolved on 2% agarose gel.

4.29 Simulation of clinical surfaces

A single colony of *A. baumannii* was inoculated into 5 ml of LB broth and incubated at 37°C overnight with agitation. The overnight culture was diluted 100 times in fresh LB and 200 µl was dispensed into wells of a sterile polystyrene 96-well plate. 2 ml of culture was poured into sterile borosilicate glass tubes. The tubes and the 96-well plate were incubated at 30°C with no agitation for 48 hours. After the incubation, the culture was drained and the tubes as well as the wells of the 96-well plate were washed thrice in sterile PBS. A few of the wells and tubes were stained with crystal violet (as described in section 3.20) to visualize the biofilm formed. From the rest of the tubes and wells, the biofilm was scrapped off and resuspended in NFW.

The suspension was heated to 95°C for 5 minutes. The suspension was cooled to room temperature and centrifuged at maximum speed in a table top centrifuge for 2 minutes. The clear supernatant was collected and used as template in PCR reaction.

4.30 Quantitative PCR

4.30.1 General reaction conditions

Quantitative PCR was performed using Cephid SmartCycler II and Roche LightCycler 480 SYBR Green I master mix. A typical reaction for qPCR was assembled as follows (Table 4.46):

Table 4.46 qPCR reaction mixture for amplification of AbsR10 unique region.

Component	Amount
2X master mix	12.5 µl
10 µM forward primer	0.5 µl
10 µM reverse primer	0.5 µl
Template DNA	variable
Water	To make up 25 µl

4.30.2 DNA for standard curve

For generation of a standard curve, DNA isolation was carried out using GeneJET genomic DNA isolation kit (ThermoScientific, USA) from overnight grown cells of *A. baumannii*. Prior to DNA isolation, the number of cells in the culture was determined. 100 µl of overnight culture was withdrawn and the cells were harvested by centrifugation at 2500 g for 5 minutes. The cell pellet was washed and resuspended in PBS. The cells were counted using a Neubauer chamber. 1.5 ml of the cell suspension was used to isolate DNA (Appendix II).

The amount of genomic DNA used in the qPCR reaction was 124.6 ng, 1.246 ng, and 12.46 pg.

5 Characterization of the Sm-like protein, Hfq, in *A. baumannii*

Previous studies carried out by our group identified some novel small RNA in *A. baumannii* [11]. Most of these sRNA were predicted to be *trans*-acting sRNA (as they were predicted in intergenic regions with their own rho-independent terminators), including the well characterized sRNA, AbsR25. Gram negative bacteria often express sRNA chaperones that assist these trans-acting sRNA to interact efficiently with their cognate mRNA targets. These RNA chaperones belong to multiple families, however, the most dominant among them is the Sm-like bacterial protein, Hfq. The functional homolog of Hfq in *A. baumannii* was not reported, but the presence of trans-acting sRNA warranted the presence of an RNA chaperone. So, the RNA chaperone Hfq in *A. baumannii* was identified and characterized.

5.1 *A. baumannii* codes for an unusually long Hfq protein with a glycine rich C-terminus

A sequence similarity search, performed by BLAST, using *E. coli* Hfq as query against the *A. baumannii* ATCC 17978 proteome returned a 168 amino acid long protein annotated as A1S_3785. Multiple sequence alignment (MSA) of this sequence with already characterized and well-studied counterparts from other bacterial species revealed a significant level of similarity at the N-terminal region (Figure 5.1) with conserved Gln8, Phe39, Lys56 and His57, known to be involved in RNA binding [2]. However, a striking feature was the length of the *A. baumannii* Hfq protein. While the Hfq homologs in most of the Gram-negative bacteria are about 100 amino acids long, the *A. baumannii* Hfq is 168 amino acids long with extra residues at the C-terminus (Figure 5.2). In fact, presence of an elongated Hfq protein is a phenomenon shared by all the sequenced members of Moraxellaceae family which comprises of the genus *Moraxella, Acinetobacter, Psychrobacter and Alkanindeges*. The C-terminal region (CTR) in *A. baumannii* Hfq carries a distinctive repetitive GGFGGQ amino acid pattern (Figure 5.1) suggesting a duplication event in the evolutionary history of *A. baumannii*.

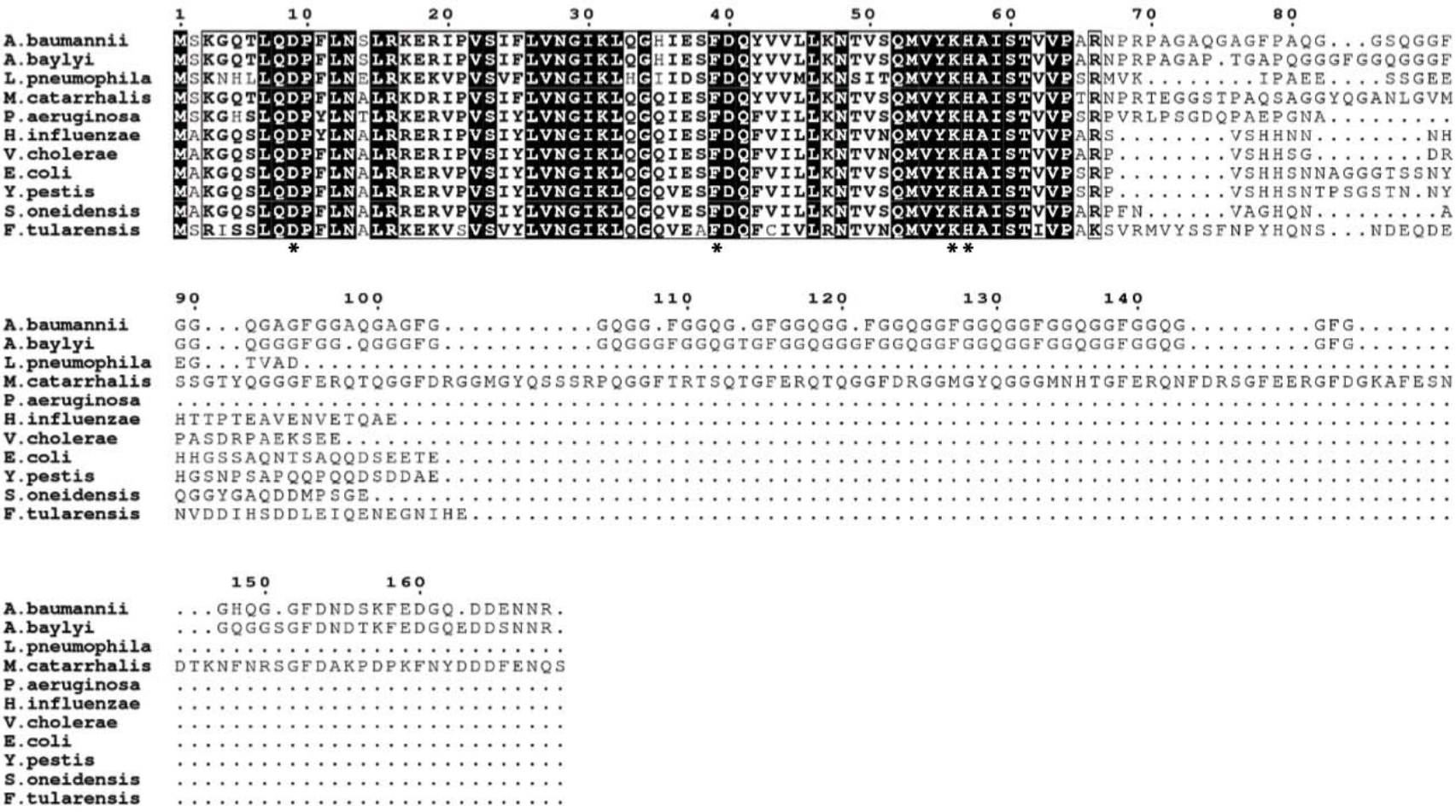

Figure 5.1 Multiple Sequence Alignment (MSA) with Hfq from other Gram-negative bacteria. The sequences of Hfq protein were derived from the NCBI protein database and aligned using Clustal Omega and visualized using ESPript3. The conserved residues necessary for RNA binding have been marked with an asterisk (*). The Hfq proteins of *A. baumannii*, *A. baylyi* and *M. catarrhalis* carry a glycine-rich extension at their C-terminus.

>gi|193077694|gb|ABS90210.2| hypothetical protein A1S_3785
[Acinetobacter baumannii ATCC 17978]
MSKGQTLQDPFLNSLRKERIPVSIFLVNGIKLQGHIESFDQYVVLLKNTVSQMVYKHAISTVVPARNPRP
AGAQGAGFPAQGGSQGGFGGQGAGFGGAQGAGFGGQGGFGGQGGFGGQGGFGGCGGFGGQGGFGGQGGFG
GQGGFGGHQGGFDNDSKFEDGQDDENNR

>gb|CP000521.1|:2465843-2466349 Acinetobacter baumannii ATCC 17978,
complete genome
TTAACGATTGTTTTCGTCGTCTTGACCATCTTCAAATTTAGAATCGTTATCAAAACCGCCTTGATGTCCG
CCGAAGCCGCCTTGACCACCGAAGCCGCCTTGACCACCGAAGCCACCTTGACCACCGAAGCCGCCTTGAC
CACCGAAGCCGCCTTGACCACCGAAGCCACCTTGACCACCGAAGCCGCCTTGGCCACCGAAGCCAGCACC
TTGAGCACCACCAAAGCCAGCGCCTTGACCACCGAAGCCACCTTGACTACCACCCTGAGCTGGGAAACCT
GCACCTTGTGCACCTGCTGGACGTGGGTTACGAGCTGGAACAACTGTAGAAATTGCGTGTTTGTAAACCA
TTTGACTTACAGTATTTTTTAGTAAAACAACATATTGGTCAAAAGATTCAATATGACCTTGTAATTTAAT
ACCGTTAACAAGGAAAATAGAAACTGGGATGCGTTCTTTACGGAGAGAATTTAAGAACGGATCTTGTAAA
GTTTGACCTTTAGACAT

ATGTCTAAAGGTCAAACTTTACAAGATCCGTTCTTAAATTCTCTCCGTAAAGAACGCATCCCAGTTTCTA
TTTTCCTTGTTAACGGTATTAAATTACAAGGTCATATTGAATCTTTTGACCAATATGTTGTTTTACTAAA
AAATACTGTAAGTCAAATGGTTTACAAACACGCAATTTCTACAGTTGTTCCAGCTCGTAACCCACGTCCA
GCAGGTGCACAAGGTGCAGGTTTCCCAGCTCAGGGTGGTAGTCAAGGTGGCTTCGGTGGTCAAGGCGCTG
GCTTTGGTGGTGCTCAAGGTGCTGGCTTCGGTGGCCAAGGCGGCTTCGGTGGTCAAGGTGGCTTCGGTGG
TCAAGGCGGCTTCGGTGGTCAAGGCGGCTTCGGTGGTCAAGGTGGCTTCGGTGGTCAAGGCGGCTTCGGT
GGTCAAGGCGGCTTCGGCGGACATCAAGGCGGTTTTGATAACGATTCTAAATTTGAAGATGGTCAAGACG
ACGAAAACAATCGTTAA

Figure 5.2 The amino acid and nucleic acid sequence of *A. baumannii* Hfq. Since the Hfq protein is coded on the complementary strand in *A. baumannii*, the mRNA sequence is also provided.

Since *A. baumannii* Hfq is encoded on the complementary strand, the mRNA sequence was derived by taking the reverse complement of the sequence available at the NCBI Nucleotide database (Figure 5.2). The codon usage frequency for Glycine in the CTR is quite similar to that of rest of the *A. baumannii* proteins which suggests that the C-terminus of Hfq evolved in *A. baumannii* rather than the bacterium obtaining this sequence via horizontal gene transfer (Table 5.1).

Table 5.1 Frequency of glycine codon usage in *Acinetobacter baumannii* ATCC 17978 and frequency of glycine codons in C-terminus of Hfq.

Codon triplet for Glycine	Frequency in *A. baumannii* ATCC 17978 (determined from codons per 1000)	Frequency in Hfq C-terminus
GGU	52% (34.8/67)	58% (28/48)
GGC	23% (15.4/67)	39% (19/48)
GGA	15% (10.3/67)	2% (1/48)
GGG	10% (6.5/67)	-

A closer look at the protein sequence alignment reveals that this glycine rich CTR is a signature of Moraxellaceae family (Figure 5.3) with the well-studied Hfq from *A. baylyi* bearing a similar extension despite significant difference in the genetic organization (Figure 5.4) [314].

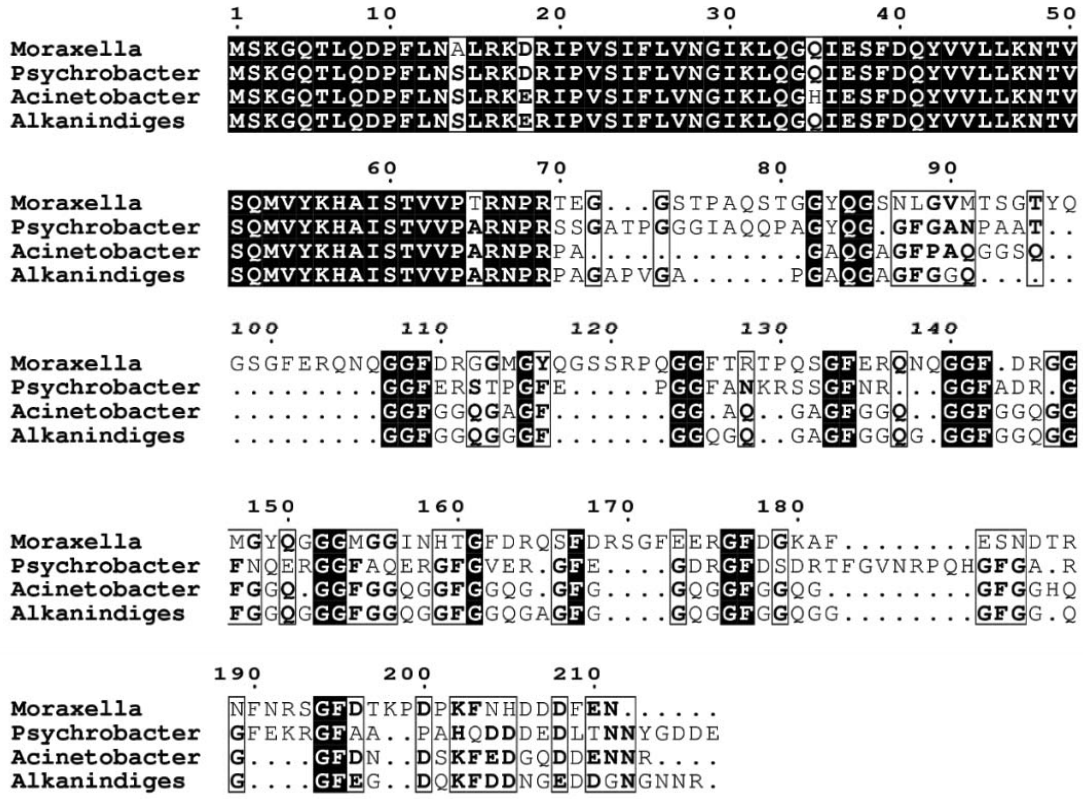

Figure 5.3 Multiple sequence alignment of Hfq proteins from the Moraxellaceae family members. The protein sequences were derived from the NCBI protein database after BLAST search using *A. baumannii* Hfq as a query and Moraxellaceae as subject database. The candidate proteins were aligned using Clustal Omega and the alignment was visualized using ESPript3.

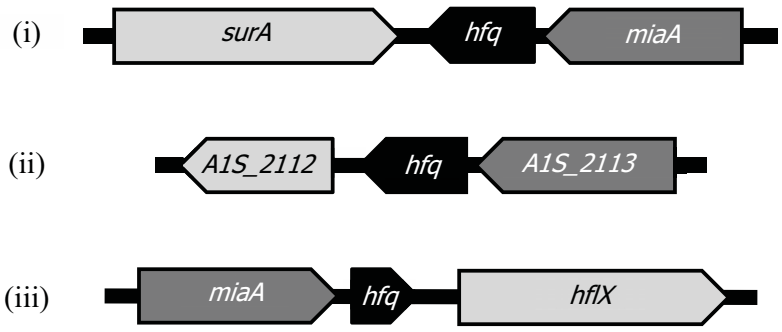

Figure 5.4 Genetic organization of *hfq* in (I) *A. baylyi*, the closest known organism to *A. baumannii* to have an experimentally verified Hfq protein; (ii) in *A. baumannii*; and (iii) in *E. coli*.

It was predicted that the CTR of *A. baumannii* Hfq falls into random coils (Figure 5.5) and the Hfq 3D model (Figure 5.6) prepared using homology modelling, takes into consideration only the first 72 amino acids due to the fact that this CTR has no homology to the structures submitted to Protein Data Bank (PDB). This makes the CTR of *A. baumannii* Hfq unique and different from the previously studied CTR of case of *E. coli* and *V. cholerae* Hfq [315–317].

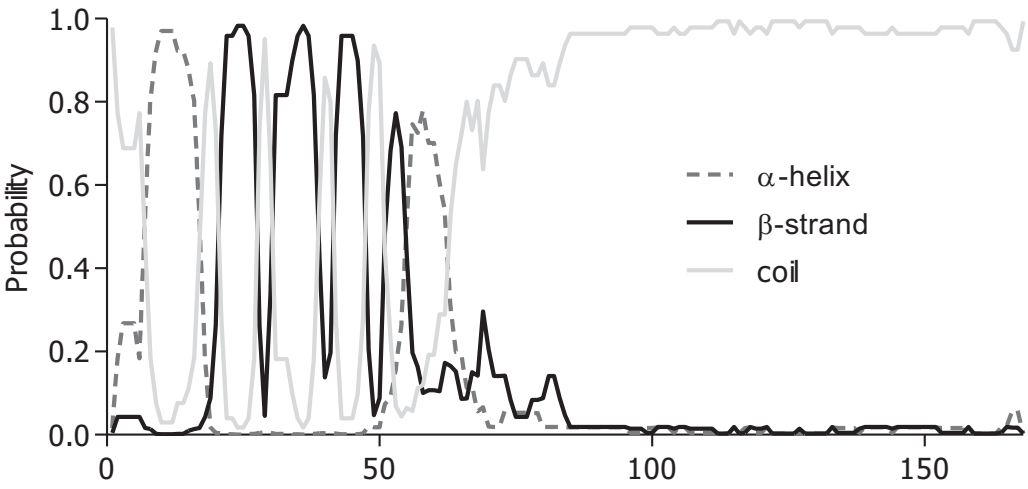

Figure 5.5 Secondary structure of Hfq predicted using the online program NetSurfP.

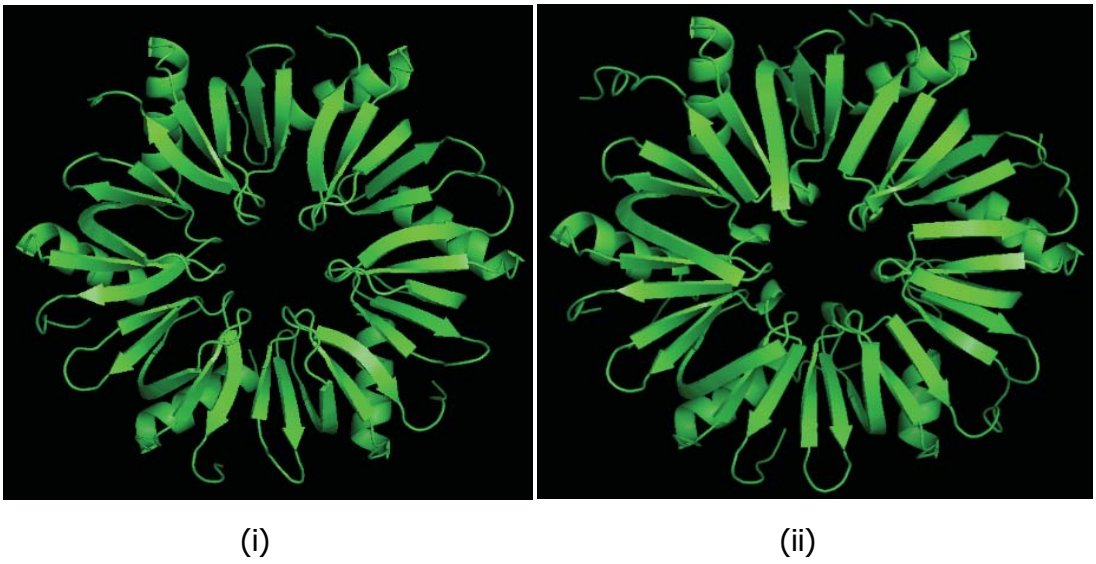

Figure 5.6 Homology modelling of *A. baumannii* Hfq. Hfq protein of *A. baumannii* was modelled by SWISS-MODEL using *Pseudomonas aeruginosa* Hfq (PDB id: 1u1s.1.E) as the closest template (sequence identity 73.08%; GMQE = 0.35 and QMEAN = 0.8). (i) The *P. aeruginosa* Hfq, (ii) *A. baumannii* Hfq.

In order to ensure that *A. baumannii* indeed expressed the characteristic long Hfq protein, Matrix-assisted laser desorption/ionization time-of-flight mass spectrometry (MALDI-TOF MS) based analysis was carried out. Total proteins from *A. baumannii* ATCC 17978 were TCA precipitated and resolved on 15% Tricine-SDS-PAGE. The band pertaining to *A. baumannii* Hfq (the one that was not prominent in case of *A. baumannii Δhfq* proteins) was excised from the gel and the protein was eluted. The tryptic digests of this protein were used for MS analysis. The Hfq protein was confidently identified from a mixture of total proteins with two different peptides, Mowse score: Peptide1 = 39, Peptide2 = 52 (Figure 5.7).

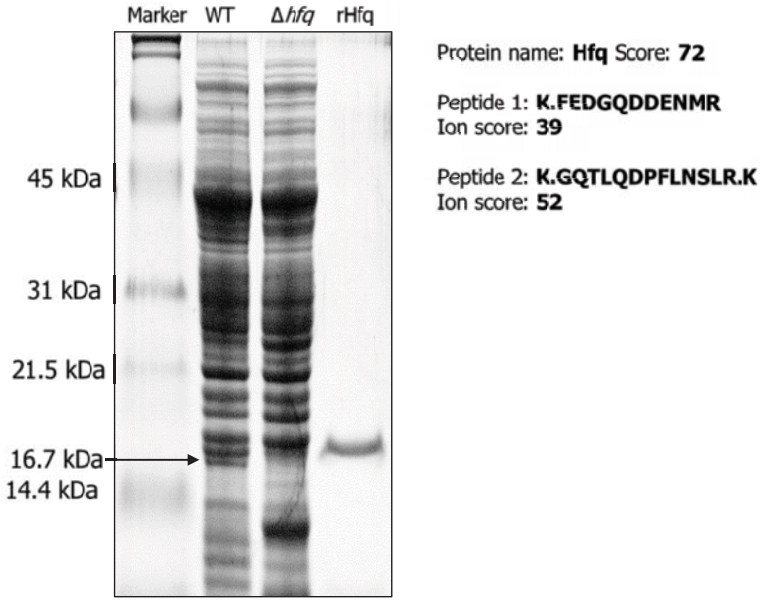

Figure 5.7 Detection of Hfq expression in *Acinetobacter baumannii* ATCC 17978. TCA precipitated total proteins of *A. baumannii* WT (WT) and *A. baumannii* Δ*hfq* (Δ*hfq*) were resolved on 15% Tricine-SDS-PAGE along with the purified recombinant Hfq protein (rHfq) and Bio-Rad pre-stained Broad range marker (marker). The band absent in protein fraction of *A. baumannii* Δ*hfq* but present in those of *A. baumannii* WT (marked with arrowhead) was eluted out of the gel and subjected to MS-MS analysis to confirm that Hfq was indeed expressed as a 16.7 kDa protein. Tabulated results of MS analysis detailing the two peptides detected and their scores are depicted.

5.2 *A. baumannii* Hfq is an RNA chaperone as it interacts with sRNA

Electrophoretic Mobility Shift Assay (EMSA) was carried out to assess the *in vitro* RNA binding activity of *A. baumannii* Hfq. The recombinant Hfq at various concentrations was incubated with a fixed concentration of three different small RNA, the *E. coli* small RNA - DsrA, MicA and the *A. baumannii* sRNA - AbsR25. The Hfq protein formed complexes with all the three sRNA, as shown by retardation profiles of the sRNA obtained after staining the gel with SYBR Green II dye (Figure 5.8). Bovine serum albumin (BSA) was used as a negative control and no binding

was observed between sRNA and BSA. Similarly, no binding was observed between Hfq and randomly selected DNA molecules (Figure 5.9).

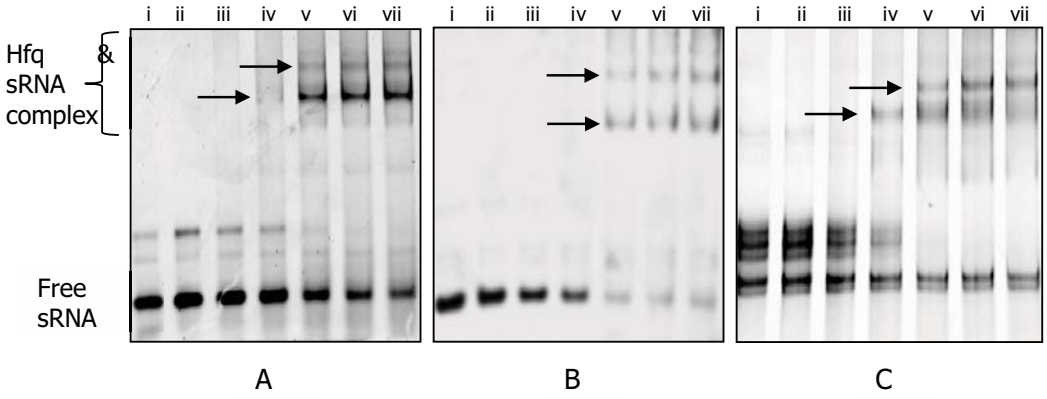

Figure 5.8 Electrophoretic Mobility Shift Assay to assess Hfq and sRNA interaction. *In vitro* synthesized transcripts of *E. coli* sRNAs MicA (A) and DsrA (B) and *A. baumannii* sRNA, AbsR25 (C) at a fixed concentration of 2 pmol were incubated with increasing concentrations of Hfq ranging from 0 to 25 pmol, for complex formation (marked by arrowheads). Lane (i), sRNA alone; Lane (ii), sRNA + BSA; Lane (iii) to (vii), sRNA + 5, 10, 15, 20 and 25 pmol Hfq protein, respectively.

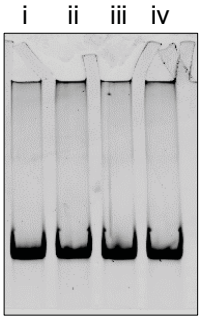

Figure 5.9 Assessment of Hfq binding with random DNA sequences. 200bp random PCR products, 2pmol in amount, were incubated with 25 pmol Hfq and run on 6% native gel. Lane (i), PCR product 1; Lane (ii), PCR product 1 with Hfq; Lane (iii), PCR product 2; Lane (iv), PCR product 2 with Hfq. The gel was stained with SYBR green I to visualize the nucleotides.

5.3 The C-terminus of Hfq is required for better sRNA interaction

To investigate the functional importance of the C-terminus in RNA chaperoning, truncated versions of recombinant Hfq protein were expressed and purified for RNA interaction studies. Hfq_{66} (66 amino acids) contained only the core Sm domain; Hfq_{72} (72 amino acids) consisted of the residues that align with the PDB template, *P. aeruginosa* Hfq; Hfq_{92} (92 amino acids) was a truncation that had mean length of *E. coli* (102 amino acids) and *P. aeruginosa* Hfq (82 amino acids) with a very short stretch of glycine rich repeats (Figure 5.10). Hfq_{168} refers to the full-length wild type version of *A. baumannii* Hfq. The recombinant truncated versions of A.

baumannii were expressed in *E. coli* BL21 (DE3) and purified by Ni-NTA affinity chromatography (Figure 5.11).

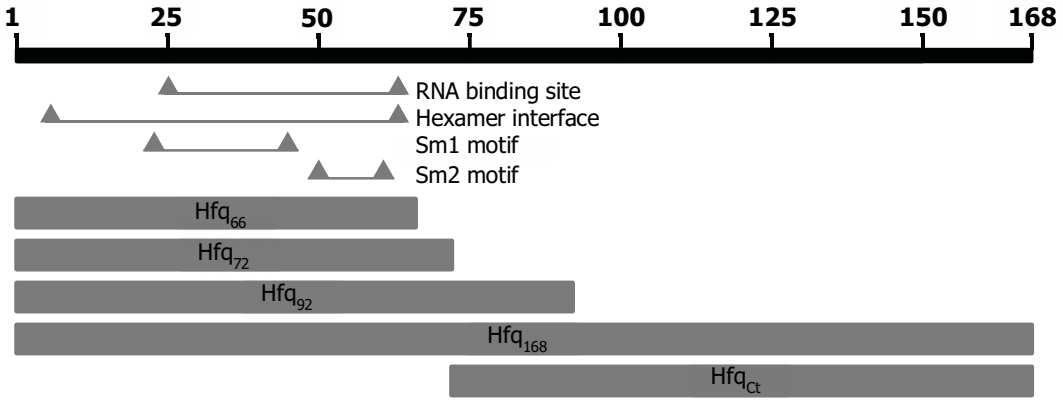

Figure 5.10 The various truncations of Hfq. Hfq_{66} (66 amino acids), Hfq_{72} (72 amino acids), Hfq_{92} (92 amino acids) and Hfq_{Ct} (72-168 amino acids).

Since the truncated versions of Hfq protein had high pKa values, they retained positive charge at pH 8.0. Therefore, EMSA could not be used to study sRNA-protein interactions in case of the truncated versions of Hfq protein. To alleviate this problem, quantitative *in vitro* RNA-protein interactions were studied by isothermal calorimetry (ITC). The AbsR25 small RNA was titrated into purified Hfq variants and the dissociation constant (K_d) values were determined (Figure 5.12). Although all the variants could bind to AbsR25, the binding affinity of Hfq_{168} was highest, followed by Hfq_{72} and Hfq_{92}. Hfq_{66} had the least binding affinity towards AbsR25 small RNA (Figure 5.12). This significance of CTR and its dynamics with sRNA were missed in the report on *A. baylyi* Hfq and a very recent report on *A. baumannii* Hfq [314,318].

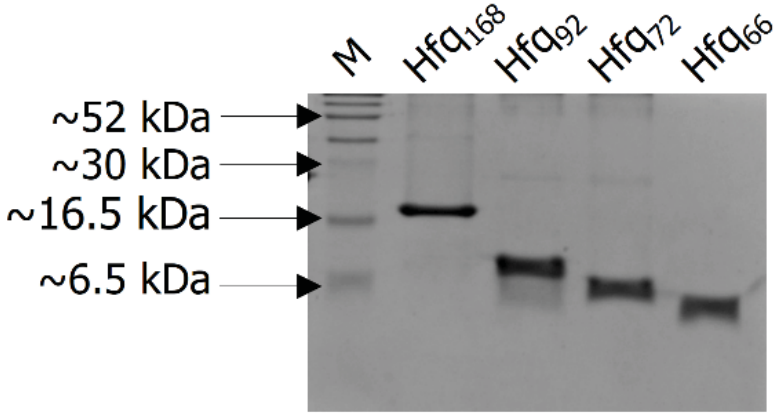

Figure 5.11 Recombinant truncated versions of *A. baumannii* Hfq were expressed in E. coli and purified by Ni-NTA affinity chromatography. The purified proteins were resolved on 12% Tricine-SDS-PAGE. The lane M contains BLUltra prestained protein ladder (GeneDireX).

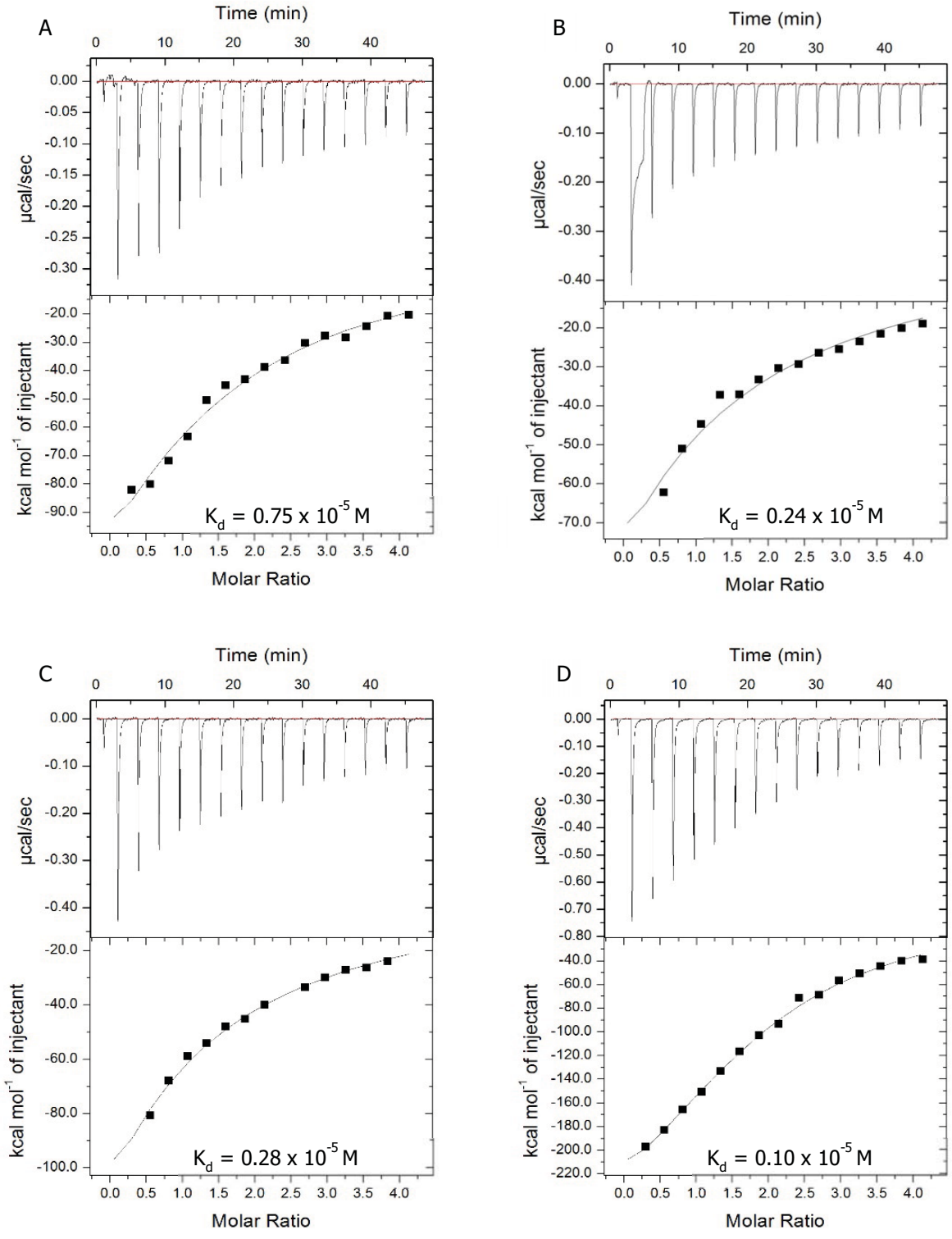

Figure 5.12 ITC based interaction between sRNA, AbsR25 and Hfq truncations. 1 µM protein samples were titrated with 25 µM AbsR25 over series of injections and binding affinities (dissociation constant, Kd) was determined for A) Hfq_{66}, B) Hfq_{72}, C) Hfq_{92} and D) Hfq_{168}.

5.4 Truncated Hfq protein variants maintain their secondary structure over a range of temperature

The Hfq protein is thermostable and retains its secondary structure even at high temperatures [275]. To assess whether the C-terminus is an important factor in determining this thermostability, we compared the CD spectra of the truncated Hfq protein variants over a range of temperatures. Despite previous reports on C-terminus dependent stability [275], results of this study showed that all the truncations of Hfq maintained their secondary structure as there was a little change in the spectra at increasing temperatures and the mean molar ellipticity at 208 nm remained fairly constant for all the truncated versions (Figure 5.13).

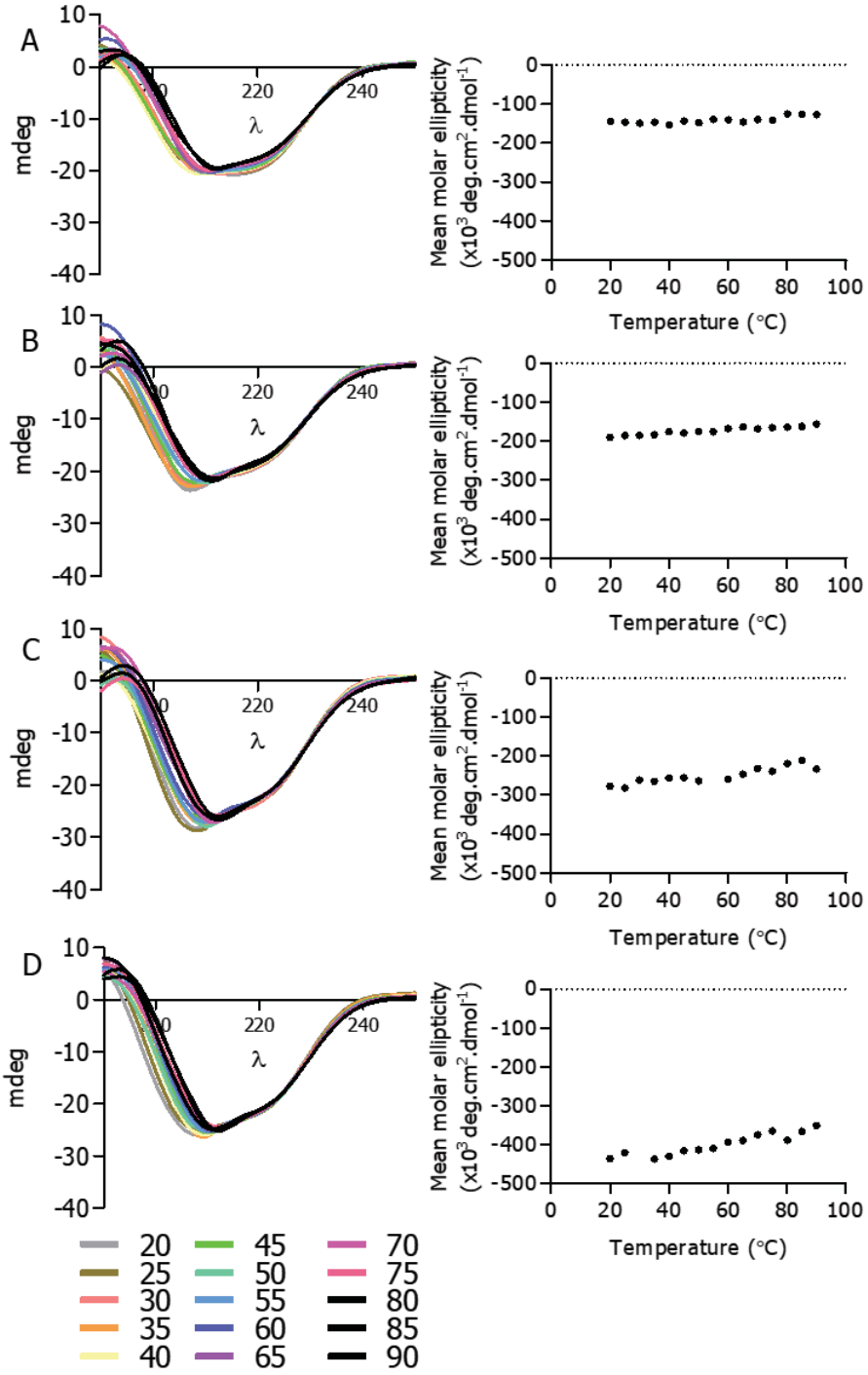

Figure 5.13 The secondary structure of Hfq truncations was studied by assessing the CD spectra of the purified proteins at various temperatures. The CD spectra of Hfq_{66} (A), Hfq_{72} (B), Hfq_{92} (C) and Hfq_{168} (D) and corresponding molar ellipticity at 208 nm (over a range of temperatures) indicates that the truncations of Hfq are thermostable similar to the full-length protein.

5.5 Hfq is required for growth and stress tolerance with C-terminus being indispensable

Considering the importance of CTR in RNA binding and already reported role of Hfq-sRNA based regulation in physiology of other Gram negative bacteria, we hypothesized that the CTR would also be important for normal physiological processes of *A. baumannii* [319]. An *hfq* deletion mutant of *A. baumannii* was constructed using a homologous recombination-based approach. The *hfq* allele was replaced with KanFRT (kanamycin resistance cassette flanked by FRT sites), which was confirmed by PCR. The amplicon in case of wild type cells was ~1500 bp long which was ~2500 bp in case of allele exchange (Figure 5.14 B). The KanFRT cassette was removed by expression of FLP recombinase and the excision was confirmed by PCR (Figure 5.14 C).

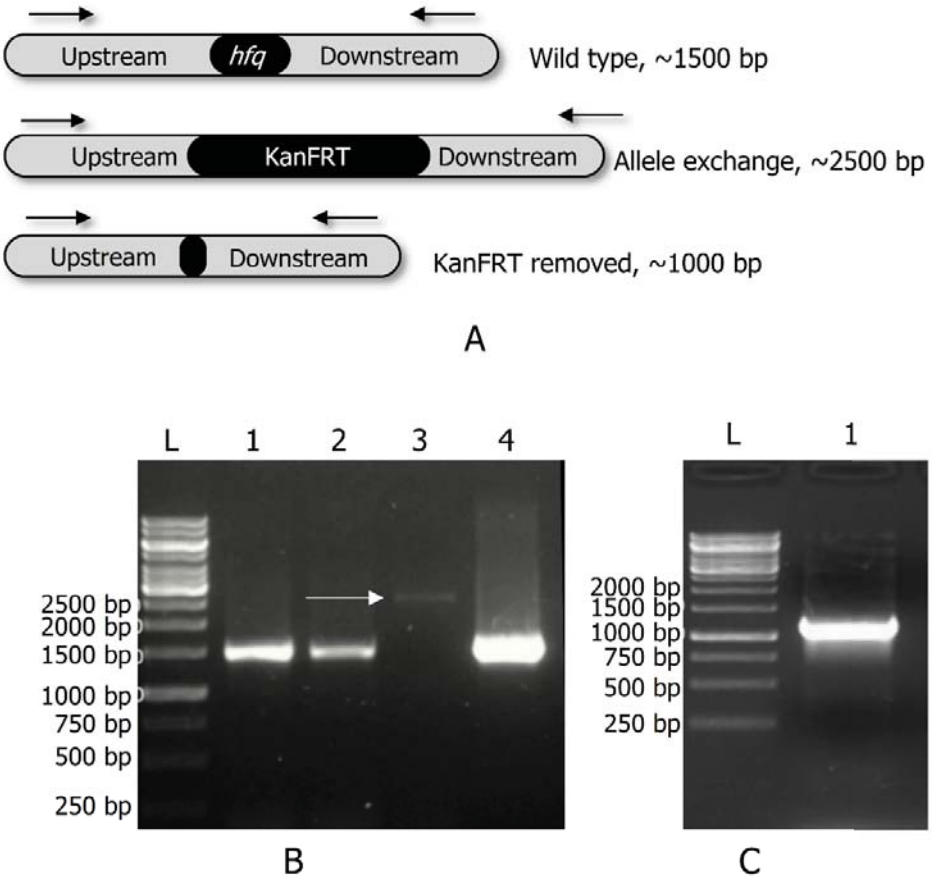

Figure 5.14 Verification of *hfq* deletion. (A) The presence of different alleles results in amplification of PCR products with varying lengths. (B) The transformants obtained after transforming the recombineering PCR product were screened for allele exchange. The required band was achieved in lane 3 which is marked by an arrowhead. The lane L contains Generuler 1 kb ladder. (C) The KanFRT allele was removed by expression of FLP recombinase and PCR amplification of ~1100 bp confirmed the excision.

The deletion of *hfq* in *A. baumannii Δhfq* was complemented by plasmid borne expression of different variants of *hfq* from the native promoter (Figure 5.15).

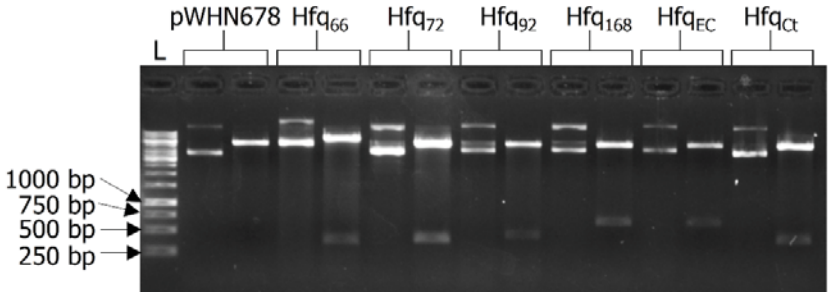

Figure 5.15 Variants of Hfq were cloned in the BamHI site of pWHN678 plasmid. The plasmids were digested with BamHI and resolved in 1% agarose gel. The adjacent lanes contain undigested and digested plasmids. The lane L contains Generuler 1kb ladder.

The expression of the truncated versions of Hfq was determined to be similar by Western blotting (Figure 5.16).

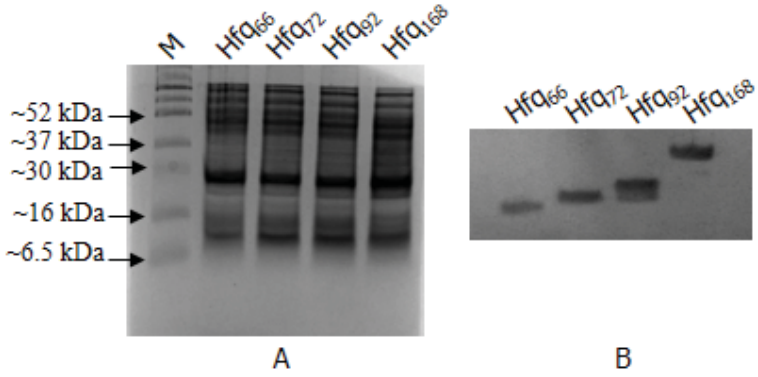

Figure 5.16 Western blot to assess the expression of truncated versions of Hfq. *A. baumannii* cells (expressing different truncated version of Hfq from plasmid) were grown till late log phase and were lysed to obtain total proteins. 25 µg total protein was resolved in each lane on 15% Tricine-SDS-PAGE (A). The expression of variants of Hfq was probed using a rabbit anti-Hfq antibody (raised using *E. coli* Hfq) and HRP-conjugated anti-rabbit antibody (B).

The loss of *hfq* in *A. baumannii* resulted in stunted growth as compared to the wild type cells (Figure 5.17). Plasmid borne expression of full length Hfq (Hfq_{168}) could complement the growth defect very well but Hfq_{66} and Hfq_{Ct} could not. There was a marked difference in the length of the lag phase and the final optical density. Other constructs, Hfq_{72}, Hfq_{92} and Hfq_{EC} had an almost similar growth profile which was close, at best, to the wild type or the Hfq_{168} complemented phenotype. This apparently similar growth profiles of wild type *A. baumannii* and *A. baumannii* expressing truncated versions of Hfq might explain why the importance of C-terminus of Hfq was not pursued in previous studies [314,318].

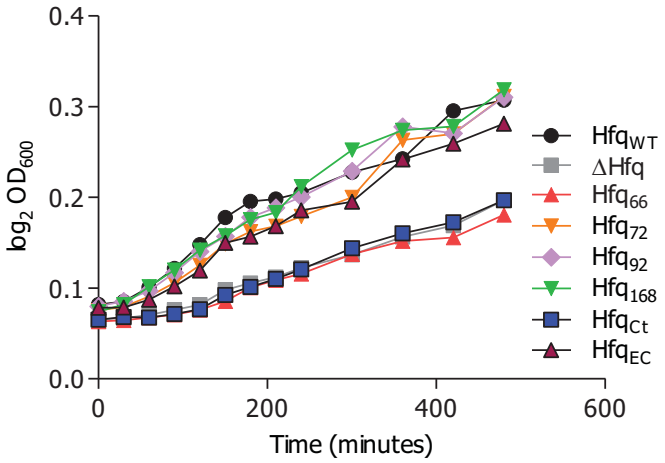

Figure 5.17 The growth profile of all the strains. The bacterial strains were grown at 37°C, 200 rpm shaking and the growth was monitored by measuring the absorbance at 600 nm. Each point represents mean of triplicates with standard deviation as error bars. Statistical significance was determined by one-way analysis of variance (ANOVA) and the P-value was 0.0014.

Since small RNA are involved in cellular adaptation to environmental stress, Hfq is intricately involved as well [319]. To validate this claim, the *A. baumannii* cells were subjected to oxidative, thermal, acidic and osmotic stress by using various physical and chemical agents. The wild type cells had a better survival rate after a brief exposure to methyl viologen, an oxidizing agent, than the cells lacking *hfq* (Figure 5.18 i). The importance of CTR was highlighted from the fact that only the full length Hfq expressed in *trans* could complement the deficit in oxidative stress adaptation. Although the *E. coli* Hfq could also complement for the loss of *hfq* in this case, but only up to a limited extent. Similar observations were made in case of thermal stress tolerance (Figure 5.18 ii) as the percentage survival of wild type cells was about 5 times higher than the *hfq* debilitated cells after a brief heat shock.

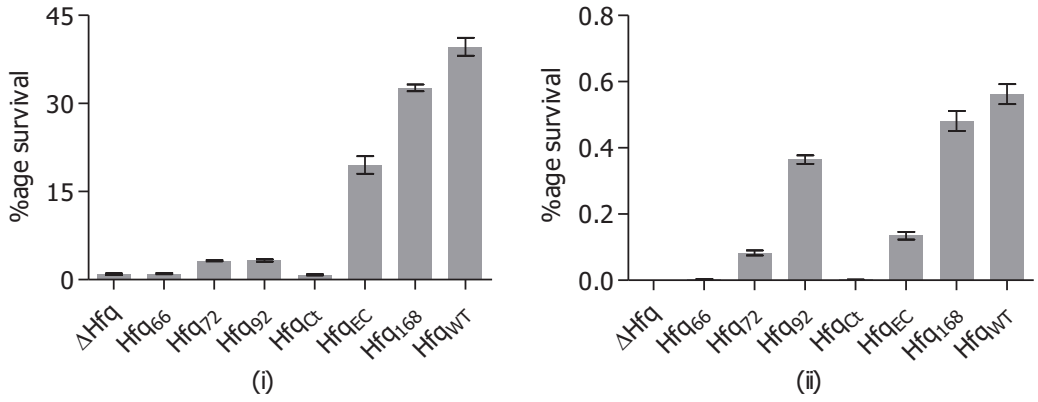

Figure 5.18 (i) Effect of Hfq deletion and presence of C-terminus on oxidative stress tolerance. The actively growing cells were briefly exposed to methyl viologen and surviving cells were determined. The percentage survival was determined with respect to the untreated control. (ii) Effect of Hfq deletion and presence of C-terminus on thermal stress tolerance. The actively growing cells were briefly exposed to 55°C and surviving cells were determined. The percentage survival was determined with respect to the untreated control. Each bar represents the mean of triplicates with the error bar representing the standard deviation. Statistical significance was determined by one-way analysis of variance (ANOVA) and the P-value was <0.0001.

The impact of Hfq on acidic and osmotic stress tolerance was assessed by spotting serial dilutions of overnight cultures of *A. baumannii* cells onto LB agar plates at pH 5 and plates supplemented with 2% NaCl. The growth of *A. baumannii* cells at pH 5 (Figure 5.19) was reminiscent of the pattern seen in oxidative and thermal stress tolerance. The wild type cells and the cells complemented with full length Hfq could adapt to the stress and grew well in contrast to the cells expressing Hfq without the CTR. However, the same could not be concluded from the growth on NaCl (Figure 5.19) as no clear results were obtained.

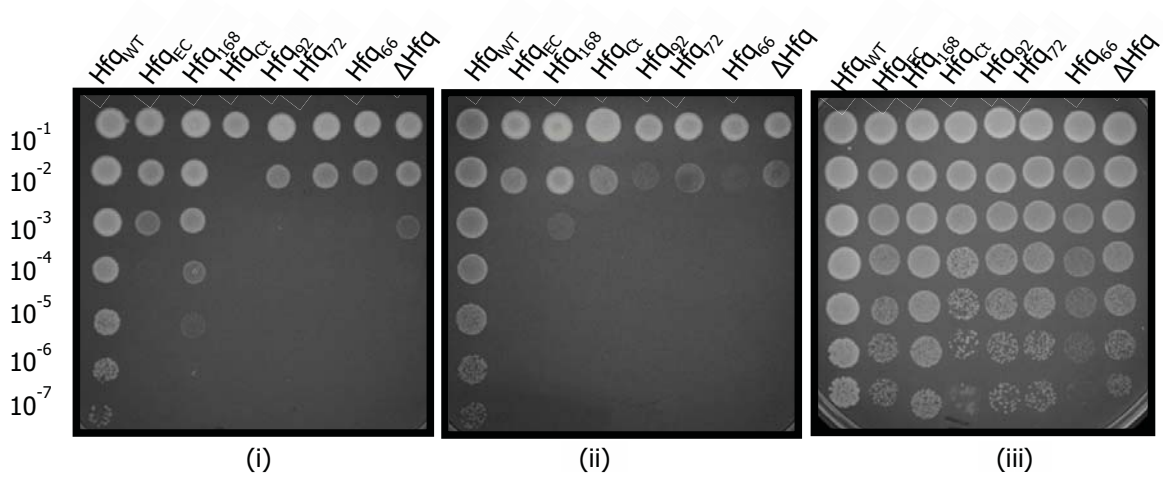

Figure 5.19. (i) Effect of Hfq deletion and presence of C-terminus on acid stress tolerance. Overnight grown cells were diluted in fresh LB and spotted on plate containing LB agar at pH 5. The plate was incubated

overnight at 37°C and the growth was compared to the control plate (iii, containing LB at pH 7). (ii) Effect of Hfq deletion and presence of C-terminus on osmotic stress tolerance. Overnight grown cells were diluted in fresh LB and spotted on plate containing LB agar supplemented with 2% NaCl. The plate was incubated overnight at 37°C and the growth was compared to the control plate (iii, containing LB agar). (iii) Overnight grown cells were diluted in fresh LB and spotted on plate containing LB agar.

5.6 The presence of C-terminus is important for functional Hfq in carbon metabolism

The impact of Hfq and the requirement of CTR for a normal growth profile of *A. baumannii* led us to suspect its role in adaptation to carbon sources. A panel of various carbon sources including sugars, sugar acids, organic acids, amino acids, nucleosides and a few stress causing agents is available in a 96-well format in the BIOLOG GEN III microplates™ (Biolog Inc., USA) (Table 5.2). These plates were used to assess the growth of *A. baumannii* cells in presence of different carbon sources. Metabolic activity is detected in these plates by change in the color of a tetrazolium dye, which can be measured spectrophotometrically

Table 5.2. List of carbon sources and stress inducing agents in the 96-well Gen III MicroPlate™

Carbon source	Carbon source	Carbon source	Stress agent
Dextrin	L-rhamnose	D-glucuronic acid	pH6
D-maltose	Inosine	Glucuronamide	pH5
D-trehalose	D-sorbitol	Mucic acid	1% NaCl
D-cellobiose	D-mannitol	Quinic acid	4% NaCl
Gentiobiose	D-arabitol	D-saccharic acid	8% NaCl
Sucrose	Myo-inositol	p-hydroxy-phenylacetic acid	1% Sodium lactate
D-turancose	Glycerol	Methyl pyruvate	Fusidic acid
Stacyose	D-glucose-6-phosphate	D-lactic acid methyl ester	D-serine
D-raffinose	D-fructose-6-phosphate	L-lactic acid	Troleandomycin
α-D-lactose	D-aspartic acid	Citric acid	Rifamycin
D-mellobiose	D-serine	α-keto-glutaric acid	Minocycline
β-methyl-D-Glucoside	Gelatin	D-malic acid	Lincomycin
D-salicin	Glycyl-L-proline	L-malic acid	Guanidine HCl
N-acetyl-D-glucosamine	L-alanine	Bromo-succinic acid	Niaproof 4
N-acetyl-β-D-Mannosamine	L-arginine	Tween 40	Vancomycin
N-acetyl-D-Galactosamine	L-aspartic acid	γ-amino butyric acid	Tetrazolium Violet
N-acetyl neuraminic acid	L-glutamic acid	α-hydroxy-butyric acid	Tetrazolium blue
α-D-glucose	L-histidine	β-hydroxy-D,L-butyric acid	Nalidixic acid

D-mannose	L-pyroglutamic acid	α-keto-butyric acid	Lithium chloride
D-fructose	L-serine	Acetoacetic acid	Potassium tellurite
D-galactose	Pectin	Propionic acid	Aztreonam
3-Methyl glucose	D-galacturonic acid	Acetic acid	Sodium butyrate
D-fucose	L-galactonic acid lactone	Formic acid	Sodium bromate
L-fucose	D-gluconic acid		

It was observed that the cells lacking *hfq* were deficient in metabolism of various carbon sources, despite similar growth of all the cells in the control wells (Figure 5.20). The inability of *hfq* deletion mutant to metabolize certain substrates hints at the involvement of an Hfq dependent sRNA based switch over mechanism that helps the bacterium to utilize alternate sources of carbon [320]. Importantly, a few of these substrates including glucose, galactose, and mannose were not metabolized by cells expressing truncated Hfq variants suggesting that *A. baumannii*, under stress, employs sRNA to regulate metabolism of these substrates. It was also interesting to note that the cells expressing Hfq_{92} could utilize certain substrates like fucose, rhamnose, stachyose (Figure 5.20), but the cells expressing a similarly sized *E. coli* Hfq (but lacking the CTR repeats) could not, highlighting the importance of glycine rich repeats. Since *Acinetobacter* spp. have been historically known to be involved in bioremediation and biotransformation, this unique structure of C-terminus in Hfq might be assisting sRNA-mRNA interactions involved in metabolism of these substrates [321–323].

Substrate/Stress agent	ΔHfq	Hfq_{66}	Hfq_{72}	Hfq_{92}	Hfq_{EC}	Hfq_{168}	Hfq_{WT}
D-Cellobiose	-0.03	-0.03	0.00	0.04	0.00	0.05	0.06
Gentiobiose	0.02	0.03	-0.01	0.07	-0.01	0.05	0.31
D-Turanose	-0.01	0.02	-0.04	0.04	-0.02	0.06	0.17
Stachyose	0.00	-0.02	-0.04	0.09	0.00	0.08	0.09
D-Melibiose	-0.02	0.01	-0.04	0.10	-0.04	0.07	0.38
8% NaCl	0.00	0.00	0.00	0.00	0.00	0.06	0.19
α-D-Glucose	-0.02	-0.03	-0.04	0.02	0.00	0.40	0.72
D-Mannose	-0.04	0.00	0.00	0.01	0.00	0.41	0.45
D-Fructose	0.10	0.13	0.06	0.14	0.06	0.15	0.30
D-Galactose	-0.03	-0.03	0.00	0.06	0.00	0.32	0.52
3-Methyl Glucose	-0.03	-0.01	-0.03	0.07	-0.02	0.40	0.40
D-Fucose	0.07	0.07	0.05	0.17	0.07	0.41	0.62
L-Fucose	0.04	0.05	-0.01	0.13	0.02	0.07	0.19
L-Rhamnose	0.00	0.01	-0.04	0.09	-0.02	0.08	0.13
Inosine	0.00	0.00	0.00	0.00	0.00	0.00	0.10
D-Sorbitol	0.00	0.00	-0.04	-0.02	0.00	0.06	0.05
D-Aspartic Acid	-0.03	-0.03	0.00	0.07	0.00	0.05	0.06
Glycyl-L-Proline	0.04	0.21	0.23	0.27	0.04	0.10	0.56
L-Arginine	0.11	0.32	0.37	0.51	0.08	0.53	1.19
D-Gluconic Acid	0.08	0.41	0.17	0.27	0.03	0.26	0.70
Quinic Acid	-0.02	-0.03	-0.04	0.05	0.00	0.85	1.45

D-Lactic Acid Methyl Ester	0.00	0.02	0.06	0.18	-0.01	0.07	0.15
α-Keto-Glutaric Acid	1.05	0.65	0.65	0.69	0.55	0.57	0.55
D-Malic Acid	-0.04	0.28	0.20	0.37	0.00	0.43	0.77
Nalidixic Acid	0.00	0.00	0.00	-0.04	0.28	0.16	0.39
Potassium Tellurite	0.01	0.00	0.01	-0.03	0.01	0.79	1.71
Formic Acid	-0.04	0.00	0.00	-0.03	0.00	0.08	0.06
Sodium Butyrate	1.34	1.12	0.81	0.77	0.95	0.59	0.08
Positive Control	1.66	1.65	1.61	1.73	1.60	1.51	1.70

Low High

Growth

Figure 5.20 The effect of Hfq deletion and truncation on carbon metabolism in *A. baumannii*. The growth of *hfq* mutant and complemented strains was assayed on Gen III microplates and is depicted in varying colors ranging from low growth (yellow) to increased growth (red).

5.7 The C-terminus is required for Hfq auto-regulation and sRNA-based regulation

It has been previously reported that the core Sm domain of *E. coli* Hfq could bind to sRNA *in vitro* but was deficient in regulatory roles [324]. We questioned if the C-terminus in *A. baumannii* was important for Hfq to fulfil its regulatory roles. Hfq auto-regulates its expression by binding to its mRNA, resulting in a feedback inhibition loop (Figure 5.21).

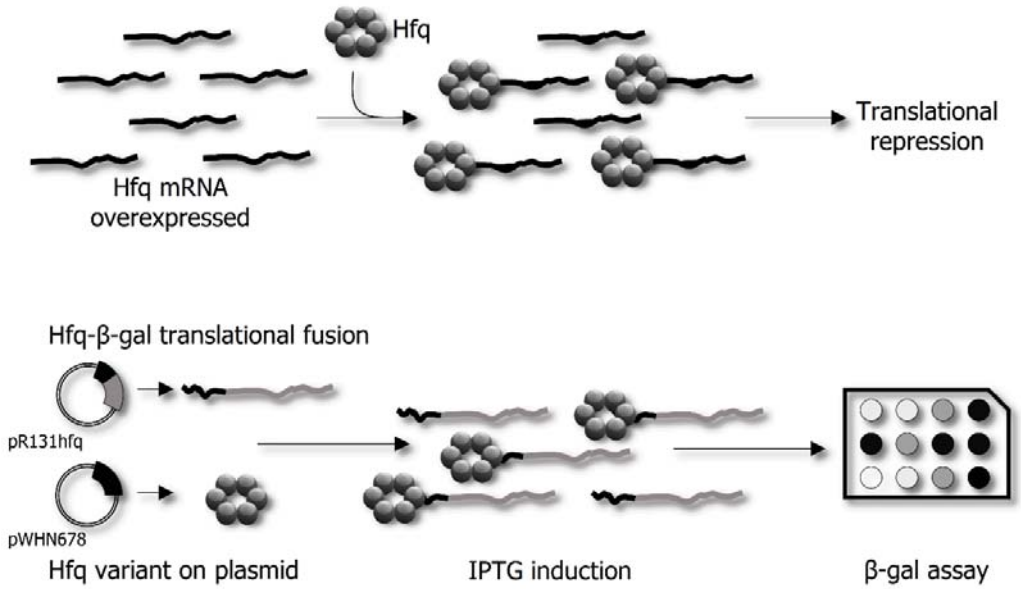

Figure 5.21 Auto-regulation of Hfq. To control the expression of *hfq*, the Hfq binds to its mRNA and represses the translation. The various Hfq constructs were co-expressed in *E. coli Δhfq* along with an Hfq-lacZ

translational fusion. The expression of Hfq-lacZ fusion was induced by addition of IPTG and the expression levels were determined by ONPG based β-galactosidase assay.

The truncated versions of Hfq and translational fusion of *hfq-lacZ* were co-expressed in *E. coli* Δ*hfq*. The cells were induced with IPTG to express *hfq-lacZ* fusion and simulate conditions where Hfq is overexpressed (Figure 5.21). The ability of different variants of Hfq to auto-regulate the expression of Hfq was measured as the ability to repress the activity of β-galactosidase. It was observed that the Hfq variants deficient in C-terminus were deficient in auto-regulation (Figure 5.22) implying that CTR is involved in autoregulatory role of Hfq in *A. baumannii*. Although some degree of auto-regulation was observed in case of Hfq_{72} and Hfq_{92} but it was not as high as compared to the wild type *A. baumannii* Hfq (Hfq_{168}).

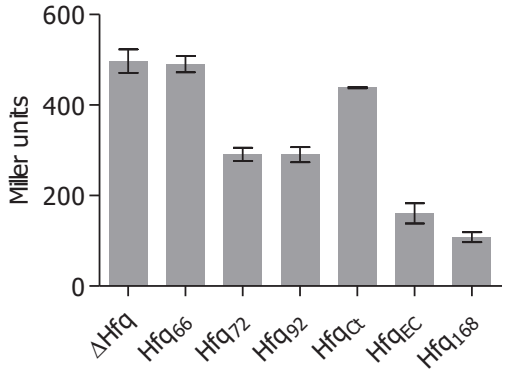

Figure 5.22 Auto-regulation was determined as the activity of β-galactosidase expressed as Miller units. Each bar represents mean of three experiments and the error bars represent standard deviation. Statistical significance was determined by one-way analysis of variance (ANOVA) and the P-value was <0.0001.

Since the C-terminus was deemed important for auto-regulation of *hfq* expression, we proceeded to assess whether it was important for small RNA based regulation as well. RyhB, an *E. coli* small RNA, negatively regulates the expression of *sodB*, when it is overexpressed, by binding to its 5' UTR (Figure 5.23) [325]. This interaction is facilitated by Hfq and the absence of Hfq abolishes this regulatory control leading to uncontrolled expression of *sodB*. A translational fusion between 5' UTR of *A. baumannii sodB* and Green Fluorescent Protein (GFP) was co-expressed along with Hfq variants in *E. coli* Δ*hfq*.

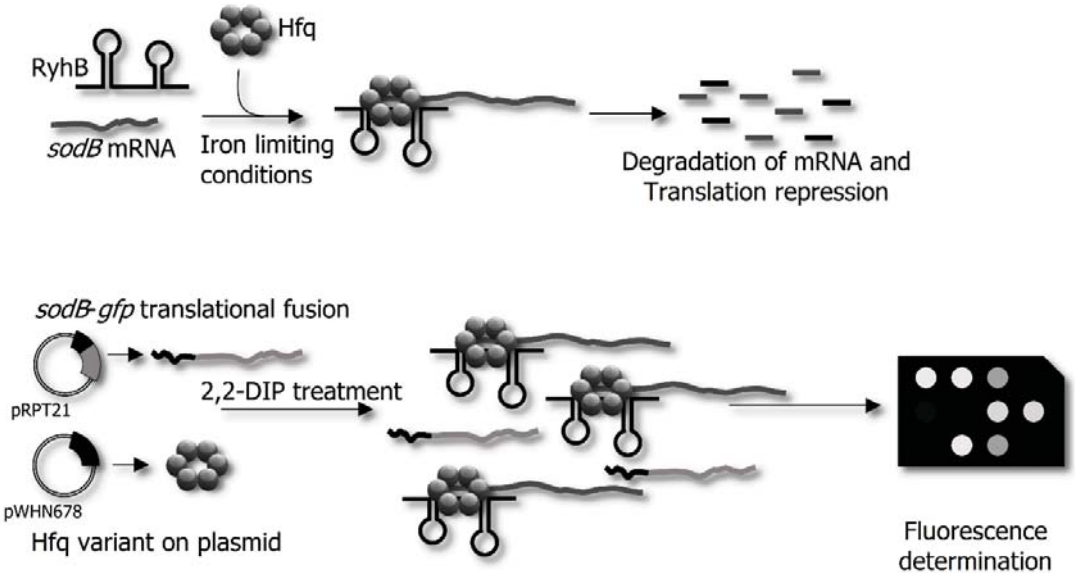

Figure 5.23 Ribo-regulation of *sodB* mRNA. Under iron limiting conditions, RyhB binds to *sodB* mRNA, assisted by Hfq, and causes translational repression of *sodB*. The various Hfq constructs were co-expressed in *E. coli Δhfq* along with an *sodB-gfq* translational fusion carrying the 5'-UTR of *A. baumannii sodB* gene. Iron deficient conditions were created by addition of 2,2-Dipyridyl and the expression of *sodB-gfp* fusion was determined by measuring fluorescence of the cells.

We observed a lower relative change in GFP fluorescence in cells expressing full length Hfq than the Hfq deficient cells (Figure 5.24) indicating the participation of *A. baumannii* Hfq in the RyhB-sodB regulatory circuit. The increase in GFP fluorescence in case of Hfq_{168} was 5 times lower than that of Hfq_{72} and Hfq_{92}, indicating that the CTR is required for efficient ribo-regulation. Since auto-regulation and ribo-regulation are dependent on successful RNA-Hfq interaction, these processes were affected, similar to the in vitro sRNA binding, when CTR was removed from Hfq. However, the inability of Hfq_{72} and Hfq_{92} to participate in auto- and ribo-regulation, despite very similar sRNA binding, could be explained due unavailability of critical acidic residues at the C-terminal tip of the Hfq [326]. The C-terminal tip of Hfq_{168} has similar acidic residues, (Asp153, Asp155, Glu159, Asp160, Asp163, Asp164, Glu165; Figure 5.1) which accounts for successful auto- and ribo-regulation by this variant in an *E. coli* genetic background.

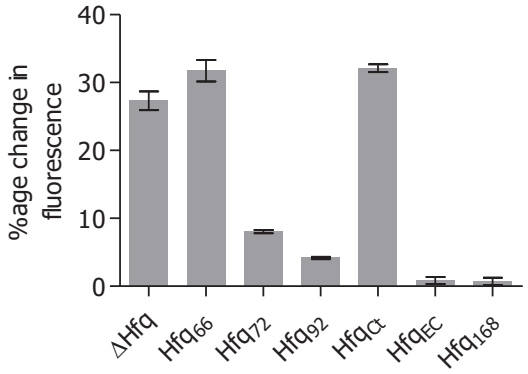

Figure 5.24 Ribo-regulation was determined as percentage change in cellular fluorescence on addition of 2,2-Dipyridyl as compared to untreated conditions. Each bar represents mean of three experiments and the error bars represent standard deviation. Statistical significance was verified by one-way ANOVA followed by Tukey's multiple comparisons test.

5.8 The C-terminus is important for virulence

Being a clinically relevant bacterium, virulence mechanisms of *A. baumannii* are of great interest. We studied the role of Hfq in virulence of *A. baumannii* in terms of resistance to desiccation, biofilm formation, adherence to eukaryotic cell membranes, organ load in infected mice models and antibiotic resistance, all of which have led to its success as a pathogen.

In an *in vitro* simulation of the hospital conditions, the *A. baumannii* cultures were allowed to dry in a polystyrene microtiter plate. The cells were revived by adding fresh medium and the surviving population was determined by spotting the dilutions on an LB agar plate. It was clear that Hfq is a vital factor for survival under desiccation (Figure 5.25) as the deletion mutant as well as the cells expressing Hfq devoid of CTR had a limited revival. The revival of cells expressing the full length Hfq (Hfq_{168}) proves that full length Hfq with the CTR is necessary for rescue of *hfq* debilitated cells from desiccation.

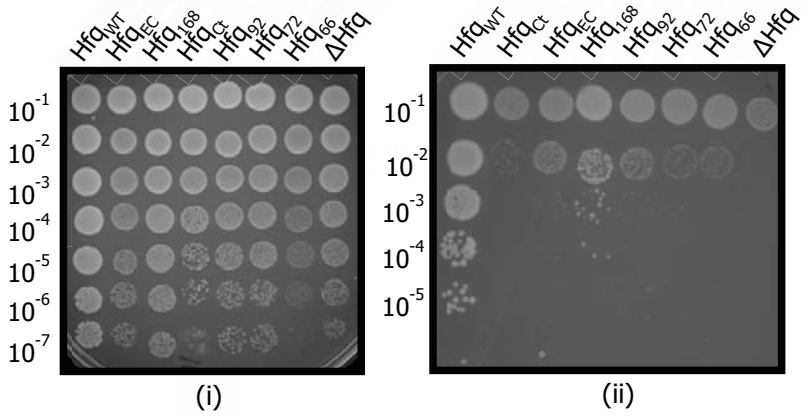

Figure 5.25 Desiccation assay. Actively growing *A. baumannii* cells were desiccated in a polystyrene 96-well plate at 25°C and 40% relative humidity. After 60 hours, the desiccated cells were resuspended in LB broth and dilutions were spotted on LB agar plates (ii). Serial dilutions of cells prior to the desiccation were also spotted (i).

In vitro biofilm formation was assessed by microtiter plate biofilm assay. The *A. baumannii* cells were allowed to form biofilms on polystyrene plates which were stained with crystal violet and quantified. The cells devoid of Hfq were deficient in biofilm formation, an effect that could be complemented by the expression of full length Hfq, Hfq_{168} (Figure 5.26). The expression of Hfq lacking the C-terminus (Hfq_{66}, Hfq_{72}, Hfq_{92} and Hfq_{EC}) could not restore the biofilm at par with the biofilm formed in case of wild type *A. baumannii*.

To assess bacterial adhesion, the initiation of infection, *A. baumannii* cells were allowed to infect HEK 293 cells and the number of CFU adhered to the membranes of the eukaryotic cells was determined. The deletion of *hfq* led to about 1 log reduction in adherence of *A. baumannii* cells (Figure 5.26). The importance of CTR in adhesion is obvious as complementation by full length Hfq restores the ability of *A. baumannii* to adhere to the eukaryotic cells. However, the cells expressing Hfq variants lacking the C-terminus only partially restore it.

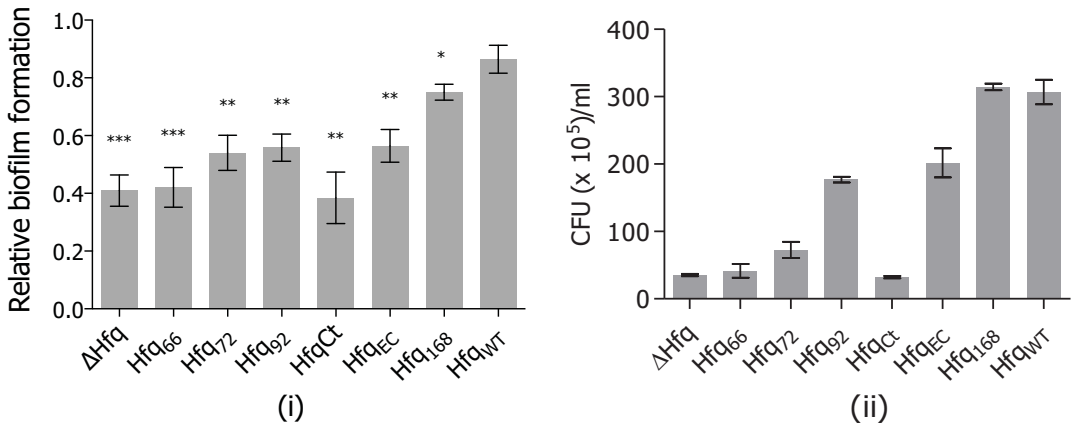

Figure 5.26 (i) Microtiter plate biofilm assay. Actively growing cells of *A. baumannii* were added to wells of a microtiter plate and incubated for 48 hours at 30°C. The biomass was stained with 1% CV, dissolved in methanol and quantified by measuring optical density at 575 nm (OD_{575}). Relative biofilm formation was determined by calculating the ratio of OD_{575} and OD_{600}. (ii) Adhesion of *A. baumannii* cells to the human embryonic kidney cells (HEK 293). The *A. baumannii* cells were incubated with the HEK 293 cells, at an MoI of 100 for an hour. The cells were subsequently washed and their dilutions were spread on LB agar plates to determine the number of cells adhering to the eukaryotic cell membrane. Each bar represents mean of three experiments and the error bars represent standard deviation. Statistical significance was verified by one-way ANOVA followed by Tukey's multiple comparisons test.

The virulence of *A. baumannii* was also studied in mice models of infection. The mice were immunocompromised by administration of cyclophosphamide and injected intravenously with various *A. baumannii* strains, separately. The mice were sacrificed after 24 hours of infection. Organ homogenates were made for kidney, liver and spleen excised from the mice in PBS and their dilutions were spread on LB agar plates to determine the bacterial load in these organs. Spleen appeared to be the most affected organ followed by kidneys and liver. There was an average 3 log decreased bacterial load in case of *hfq* debilitated cells as compared to the wild type cells (Figure 5.27). The bacterial load in case of cells expressing Hfq lacking the CTR was higher than the deletion mutant but significantly less than the cells expressing full length Hfq. This again reflects the importance of full length Hfq with an intact CTR.

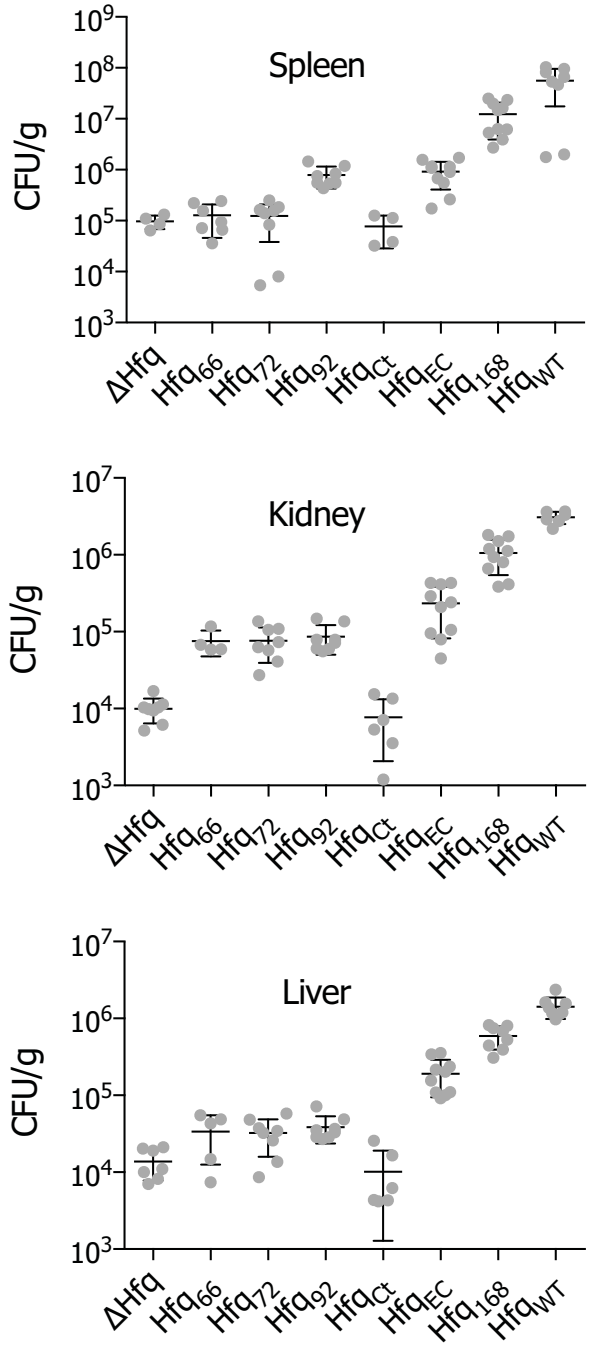

Figure 5.27 Organ load of bacterial cells in mice infected with *A. baumannii*. The mice were rendered neutropenic by administration of cyclophosphamide and were subsequently infected by *A. baumannii* via intra-venous injection. The mice were sacrificed after 24 hours of infection and the organ homogenates were prepared in PBS. Dilutions of the organ homogenates were spread on LB agar plates to determine the number of CFU. Each point represents mean of five different mice (n=5) and the error bars represent standard deviation. Statistical significance was determined by one-way analysis of variance (ANOVA) and the P-value was <0.0001.

The *A. baumannii* strains were examined for their antibiotic resistance. Being a rather sensitive strain, deletion of *hfq* in *A. baumannii* ATCC 17978 did not display a major change in resistance towards most of the drugs [327]. However, a two-fold reduction in MIC of nalidixic acid and gentamycin was observed in *A. baumannii Δhfq*, a phenomenon that could be reversed only by the expression of full length Hfq (Table 5.3).

Table 5.3 Minimum inhibitory concentrations (MIC) of antibacterials that showed variation in antibacterial potential against *A. baumannii* strains expressing variant of Hfq.

Antibacterial agent	MIC (in µg/ml)							
	ΔHfq	**Hfq_{66}**	**Hfq_{72}**	**Hfq_{92}**	**Hfq_{168}**	**Hfq_{EC}**	**Hfq_{Ct}**	**Hfq_{WT}**
Nalidixic acid	3	3	3	3	6	3	3	6
Gentamycin	2.4	2.4	2.4	2.4	4.8	2.4	1.2	4.8
Meropenem	8	4	4	4	2	4	8	2

An interesting finding was the increase in resistance towards meropenem in *A. baumannii Δhfq*, which was not found in the wild type cells as well as cells expressing the full length Hfq. These observations hint at involvement of sRNA in drug resistance in *A. baumannii* and the subsequent importance of Hfq. It is also evident that the CTR region is important to maintain this activity of Hfq. Taken together, these results reflect the importance of Hfq in governing virulence of *A. baumannii* and validate the importance of CTR in these effects.

5.9 *A. baumannii* Hfq can complement deletion in *E. coli* with C-terminus playing no role

The *A. baumannii* Hfq protein is larger than other bacterial Hfq owing to the extra baggage added on by residues on the CTR that are not homologous to the Hfq of other Gram-negative species (Figure 5.1). With the aim to investigate the possibility if the *A. baumannii* Hfq has the capability to function in the same manner as the *E. coli* Hfq protein, the wild type *A. baumannii hfq* gene and the other complementing constructs were expressed in the *E. coli* Δ*hfq*. As reported earlier, *E. coli* Δ*hfq* was deficient in growth in LB medium and plasmid borne expression of *E. coli* Hfq restored the growth (Figure 5.28 A). Similar restoration was also observed when the loss of *hfq* in *E. coli* was complemented with *A. baumannii* Hfq. However, it was worthwhile to note that the expression of *A. baumannii* Hfq, even without the CTR, could complement and restore the growth. Since it could complement the growth defect in *E. coli*, we tried to assess if the *A. baumannii* Hfq sans the CTR could restore the growth defect in *E. coli* under various stress conditions as well. Growth of *E. coli* Δ*hfq* and respective complemented strains under stress was evaluated by spotting the dilutions of overnight cultures on LB agar plates that were

supplemented with 2% NaCl (Figure 5.28 B), 200 µM 2,2-Dipyridyl (Figure 5.28 C), 100µM H2O2 (Figure 5.28 D), pH 5 (Figure 5.28 E) and on an LB agar plate that was incubated at 42°C (Figure 5.28 F). These plates mimicked the osmotic, nutritive (specifically iron), oxidative, acidic and thermal stress, respectively. It was observed that *A. baumannii* could complement for the loss of *hfq* in *E. coli* under various stress conditions as well. It was worthwhile to note that in all the cases the Hfq_{72} and Hfq_{92} were as competent as Hfq_{168} suggesting no involvement of CTR in stress cope-up in *E. coli*. However, Hfq_{66} could not complement for the loss of *hfq*, which is in line with previous observations. Therefore, data from this work concludes that *A. baumannii* Hfq can functionally replace the *E. coli* Hfq for growth under normal as well as stressed conditions, with the CTR apparently playing no specific role.

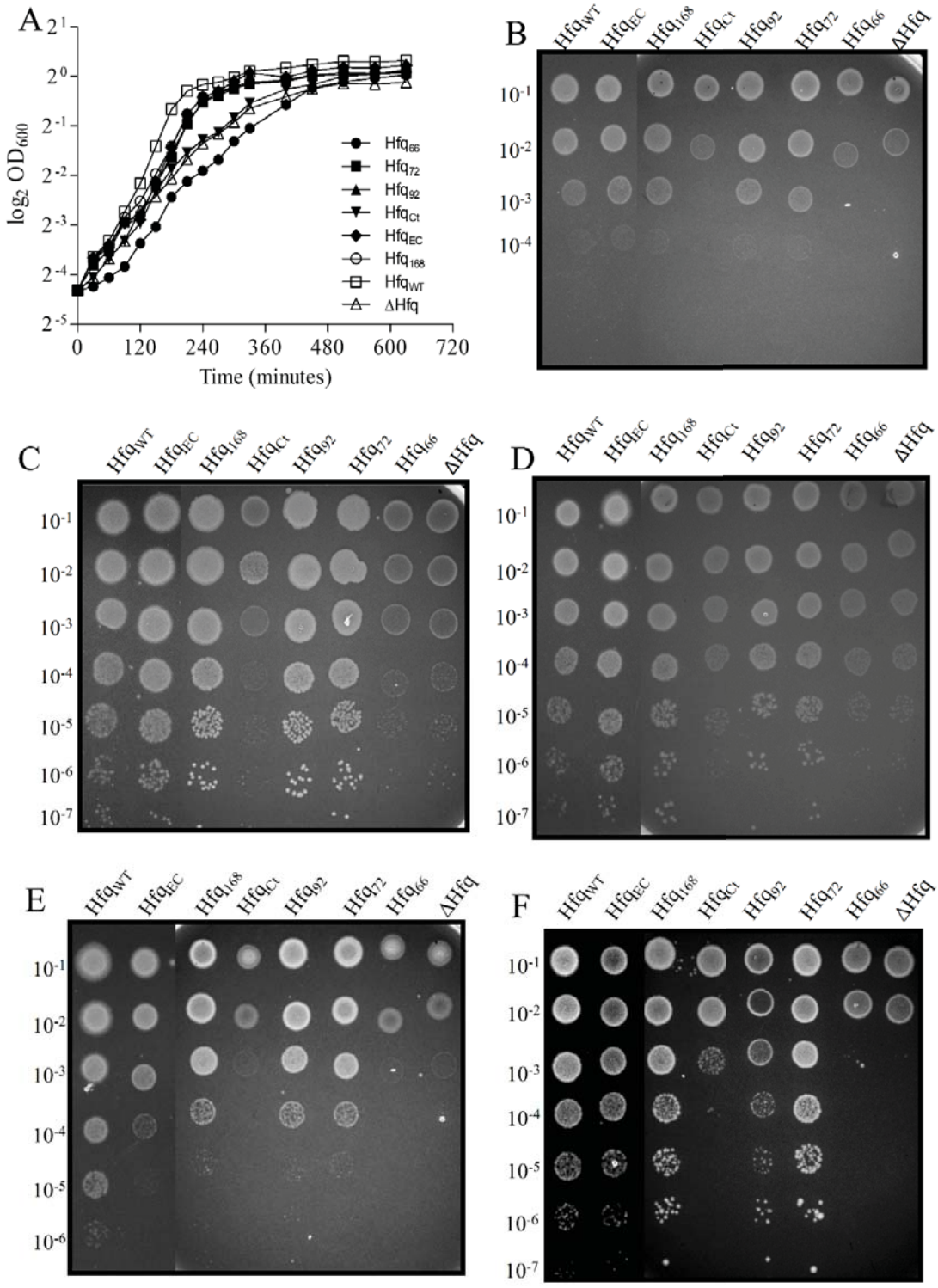

Figure 5.28 Complementation of *E. coli Δhfq* with *A. baumannii* Hfq. A) The growth profile of all the strains. The bacterial strains were grown at 37°C, 200 rpm shaking and the growth was monitored by measuring the absorbance at 600 nm B-F) Impact of C-terminus of Hfq on stress tolerance in *E. coli*. The *E. coli* cells were subjected to various stress by spotting dilutions of overnight culture on agar plates containing B) 2% NaCl, C) 200 µM 2,2-Dipyridyl, D) 100µM H_2O_2, E) pH 5, and F) incubated at 42°C. The ΔHfq in each case carried the empty plasmid pWHN678.

5.10 Discussion

Overall, the findings of this work suggest that Hfq governs physiological properties like growth, stress tolerance as well as virulence insinuating that *A. baumannii* recruits small RNA for regulation of these processes. This also establishes the importance of Hfq as a central regulator of physiological processes in *A. baumannii*, as deletion of *hfq* disturbs a myriad of processes. This falls in line with the previous observations made in the lab regarding the expression of *trans*-acting small RNAs in *A. baumannii*. The RNA chaperoning activity of Hfq and its *in vitro* interaction with AbsR25 better explains the *in vivo* activities of AbsR25 and also paves the way for identification of more *trans*-acting small RNA. In addition, this work tried to demystify the presence and establish the importance of glycine rich repeats at the C-terminus. These repeats are characteristic of the Moraxellaceae family and not present in Hfq proteins of other genera. Therefore, most of the studies on C-terminus of Hfq have focused the attention on residues that follow the Sm domain (from 66 amino acid onwards) simply due to the fact that other bacterial Hfq proteins don't have this glycine rich CTR [317,324,328]. Although it is known that Hfq_{66} is deficient in many physiological capabilities, there are conflicting reports about the importance of amino acids from 66-72. Therefore, we used both the truncations in complementation experiments to rule out any problems due to experimental setup [324,328,329]. Our observations indicate a marked difference in physiology of cells expressing Hfq_{66}, Hfq_{72} and Hfq_{92} and confirm the importance of residues that lie beyond the Sm domain.

Sequence analysis also suggests that Hfq might belong to a category of proteins bundled under an umbrella term, intrinsically unstructured proteins [330]. Such proteins, despite varied origins, share certain characteristic features like a) compositional bias, b) presence of small residues, c) presence of amino acids that provide flexibility and d) lower frequency of hydrophobic residues; all of which *A. baumannii* Hfq conforms to [330,331]. The fact that intrinsically unstructured proteins are highly regulated and placed under auto-regulatory control furthers the notion that Hfq belongs to this category of proteins [321]. Intrinsically unstructured proteins are also found in the eukaryotic glycine rich protein (GRP) family. The members GRP family have an RNA recognition domain (RRN) at the N-terminus and a glycine rich domain at the C-terminus [332].

This glycine rich tail imparts flexibility and assists these proteins in RNA binding and interaction with other protein partners. Coincidently, a search for domains in the Hfq sequence reveals a distant relation of the CTR to the GRP family (Figure 5.29). Considering the structure and function of Hfq, a C-terminal assist in homo- as well as heteromeric interactions seems to be an obvious advantage. Interestingly, GRPs have been reported to be central in RNA chaperoning

```
hmmpfam - search one or more sequences against HMM database
HMMER 2.3.2 (Oct 2003)
Copyright (C) 1992-2003 HHMI/Washington University School of Medicine
Freely distributed under the GNU General Public License (GPL)
- - - - - - - - - - - - - - - - - - - - - - - - - - - - - - - - - - - - - -
HMM file:                 ALL_LIB_bin.HMM
Sequence file:            hmmpfam-search-4932-1505200123.in
- - - - - - - - - - - - - - - - - - - - - - - - - - - - - - - - - - - - - -

Query sequence: ABHFQ
Accession:      [none]
Description:    [none]

Scores for sequence family classification (score includes all domains):
Model     Description                                        Score    E-value  N
--------  -----------                                        -----    ------- ---
TIGR02383 Hfq: RNA chaperone Hfq                             134.7    3.8e-37   1
PF01423   LSM: LSM domain                                    50.9    6.2e-12   1
PF07172   GRP: glycine-rich protein family                  -24.7      0.038   1

Parsed for domains:
Model     Domain  seq-f seq-t    hmm-f hmm-t      score  E-value
--------  ------- ----- -----    ----- -----      -----  -------
TIGR02383   1/1       5    64 ..     1    61 []   134.7  3.8e-37
PF01423     1/1       5    64 ..     1    71 []    50.9  6.2e-12
PF07172     1/1      53   152 ..     1   134 []   -24.7    0.038

Alignments of top-scoring domains:
TIGR02383: domain 1 of 1, from 5 to 64: score 134.7, E = 3.8e-37
                   *->qnlQDqFLNtlRkeripVtvfLvNGvqLkGvIksFDnFtVLLesqgk
                      q lQD+FLN lRkeripV++fLvNG++L+G I+sFD+++VLL++  +
       ABHFQ     5    QTLQDPFLNSLRKERIPVSIFLVNGIKLQGHIESFDQYVVLLKNTVS 51

                      QqLiYKHAISTisP<-*
                      Q ++YKHAIST++P
       ABHFQ    52 Q-MVYKHAISTVVP    64

PF01423: domain 1 of 1, from 5 to 64: score 50.9, E = 6.2e-12
                   *->kfLkklFLN.lR.lgkrVtVeLknGrelrGtLkgfDqfmNlvLddve
                      + L++ FLN+lR+ + +V+++L nG +l+G++++fDq+++l+   v+
       ABHFQ     5    QTLQDPFLNsLRkERIPVSIFLVNGIKLQGHIESFDQYVVLLKNTVS 51

                      EtidgkknrklGlvliRGnnIvlisp<-*
                      +             ++++++I++++p
       ABHFQ    52 Q-------------MVYKHAISTVVP    64

PF07172: domain 1 of 1, from 53 to 152: score -24.7, E = 0.038
                   *->MASKallLLGLlLAavLLisSEVaaadltEeaeksnteKseseeeVq
                      M  K          a   is+ V a+             ++++ +
       ABHFQ    53    MVYKH---------A---ISTVVPARNP----------RPAGAQGAG 77

                      ddkyGGgGyhgGGynGGGGgGfgggGgGGYgGgGGggygGG.GyygGGGG
                       + +GG    +GG+ G G  Gfgg  g G+gG GG g++GG G++gG GG
       ABHFQ    78 FPAQGG---SQGGFGGQG-AGFGGAQGAGFGGQGGFGGQGGfGGQGGFGG 123

                      YgGGGghvayGG.gGGgygGGGGypGGyGngGGGYgGGG<-*
                       gG      +GG+gG g++GG G+ GG+    GG++GG
       ABHFQ   124 QGG------FGGqGGFGGQGGFGGQGGF----GGHQGGF    152
```

Figure 5.29 Analysis of protein motifs in the Hfq sequence using tigr-pfam.

and stress adaptation, much like Hfq [333]. All these observations may be an inkling of an evolutionary relation between the prokaryotic and eukaryotic LSM proteins.

Unfortunately, at this time the exact mechanistic details of the involvement of glycine rich repeats are not known. It has recently been revealed that the length of the flexible tail between the core Sm domain and the acidic C-terminal residues is critical in determining the stringency in substrate specificity [326]. The necessity of the interaction between the acidic residues on this tip and the basic residues in the core of Hfq is probably the reason why the CTR does not assume a fixed secondary structure but is rich in flexible residues like glycine. This elongated tail may have caused a relaxed specificity of substrate selection in Hfq, allowing better interaction with low affinity sRNA. Theoretically, this immensely expands the substrate range of *A. baumannii* Hfq and might even allow yet to be discovered interactions. Future studies aimed at structural characterization of *A. baumannii* Hfq may assist in elucidation of the role of C-terminus at the molecular level. Another avenue opened up by this study is the identification of sRNA involved in regulation of physiological processes in *A. baumannii*. The defects brought about by *hfq* deletion point towards the involvement of small RNA in those respective processes and a careful experimentation and analysis could reveal these small RNA in future.

The perturbation of virulence in absence of Hfq means that Hfq could in itself be considered as a significant virulence factor. This generates a considerable interest in further studies aimed at targeting Hfq as a plausible drug target. With the advent of drug resistance, it has become pertinent to identify novel targets and adapt alternative strategies to target bacterial pathogens. In such a scenario, inhibiting virulence could be a viable and effective way of tackling infections and avoiding the advent of resistance. Hfq could be used as a target in such an anti-virulence therapy, where the drugs targeting this protein would result in diminished virulence of the bacterium and allow the immune system to mount an effective response. Future experiments in this direction are already underway.

6 Characterization of A1S_1331, the primary target of AbsR25

Our group's previous studies had characterized a novel small RNA, AbsR25, which regulates the expression of a few transporter proteins in *A. baumannii* [334]. Such transporters are generally involved in solute transfer across the bacterial membranes, including antibiotics and other drugs. By qPCR-based assays to evaluate expression profiles, A1S_1331 was identified as the primary target of AbsR25. The expression of A1S_1331 was inversely related to that of AbsR25. The protein A1S_1331 was annotated as a putative Major Facilitator Superfamily (MFS) transporter but it was not characterized for its activity. Therefore, experiments were designed and carried out to validate A1S_1331 as a transporter and determine its importance in antibiotic resistance and other physiological processes in *A. baumannii*.

>A1S_1331
ATGACGACAACACTAAAAAAGGTAGTCGCGGCCTCTATGGTCGGCTCCGTAGCAGAATGG
TATGAATTTTTCCTTTATGGCACCGCTTCTGCCCTCGTCTTTGGCGAACTTTTCTTTCAA
CAAACTGGCAATGCTATAGATGGAATTTTGGCGGCCTTTGCTCTGTATGCCGTTGGCTTT
TTAGCAAGACCTCTCGGTGGCCTCGTGTTTGGTCACTACGGCGATAAAATTGGGCGCAAG
AAATTATTGCAAATTAGCCTGATCATTGTCGGTATCACTACTTTTTTAATGGGCTGTATT
CCGACCTTTCATCAAATTGGCTATTGGGCTCCTACACTCCTAGTGATATTACGTTTAATT
CAAGGTTTTGCTTTTGGTGGTGAATGGGGCGGCGCAGTTATTTTAGTTTCAGAGCACAGT
CCAGATGATCGCAGAGGTTATTGGGCAAGCTGGCCACAAACTGGTGTACCGCTCGGAAAT
TTAGTAGCCACACTGGTTTTATTATTACTTTCAAAAAACCTCTCACCCGAACAATTTCTA
GATTGGGGGTGGCGCTGTGCATTCTGGTTCTCAGCAGTCGTGGTACTGATTGGTTTATGG
ATTCGAAAAAATGTAGACGATGCCGAAGTGTTTAAAGAAGCACAGGCCAAACAACAGCTT
CTTGAAAAGCAACAACTCGGGATTATTGAGGTTTTAAAATATCATAAGAAATCTGTTATT
GCGGGTATCGGTGCCAGATTTGCAGAAAATATTTTGTACTATATGGTGGTTACTTTTTCG
ATCAGTTATTTAAAGTTAGTCGTCCATAAAGATACTTCGCAGATCTTACTGCTCATGTTC
GGCGCTCATCTGATCCATTTCTTTATTATTCCTTTTATGGGGCATTTAAGCGATATATTT
GGCCGTAAACCTATTTACCTTATTGGGGCTGTACTTACTGCTTTTTGGGGTTTTGTCGGC
TTTCCTTTAATGGATACAGGCAATGACTGGCTCATTATGTTAGCAATTGTGCTTGGTTTA
TTTATTGAGTCCATGACCTACTCGCCTTACTCTGCGTTAATGACTGAGTTATTTCCAACT
CACATCCGCTATACGGCGCTTTCATTTTGTTATCAAGTCGCACCCATTATGGCAGGTTCG
CTTGCTCCATTAATTGCCCTAACATTACTCAAAGAATTTAATAGTTCGATTCCGATTTCT
TTATATTTGGTTGCCGCAAGTCTGATTTCTATTGTCTCGATTTTGCTGGTGAAAGAAACC
AAAGGCCGATCTCTAGCTTTTAAAGATTAA

>A1S_1331
MTTTLKKVVAASMVGSVAEWYEFFLYGTASALVFGELFFQQTGNAIDGILAAFALYAVGF
LARPLGGLVFGHYGDKIGRKKLLQISLIIVGITTFLMGCIPTFHQIGYWAPTLLVILRLI
QGFAFGGEWGGAVILVSEHSPDDRRGYWASWPQTGVPLGNLVATLVLLLLSKNLSPEQFL
DWGWRCAFWFSAVVVLIGLWIRKNVDDAEVFKEAQAKQQLLEKQQLGIIEVLKYHKKSVI
AGIGARFAENILYYMVVTFSISYLKLVVHKDTSQILLLMFGAHLIHFFIIPFMGHLSDIF
GRKPIYLIGAVLTAFWGFVGFPLMDTGNDWLIMLAIVLGLFIESMTYSPYSALMTELFPT
HIRYTALSFCYQVAPIMAGSLAPLIALTLLKEFNSSIPISLYLVAASLISIVSILLVKET
KGRSLAFKD

Figure 6.1 Nucleotide and amino acid sequence of A1S_1331, the primary target of small RNA AbsR25. The sequences were obtained from NCBI's Nucleotide and Protein database, respectively.

6.1 A1S_1331 is an MFS transporter

Bioinformatic analysis of the A1S_1331 protein sequence (Figure 6.1) revealed that it belongs to Major Facilitator Superfamily (MFS) of transporters. The predicted secondary structure of

A1S_1331 has characteristic 12 transmembrane helices with two homologous 6-helix domains formed at N- and C-terminus (Figure 6.2). Like the other proteins of this class, the two 6-helix bundles are connected via a cytoplasmic loop with the C- and the N-terminus of the protein buried in the cytoplasm [335].

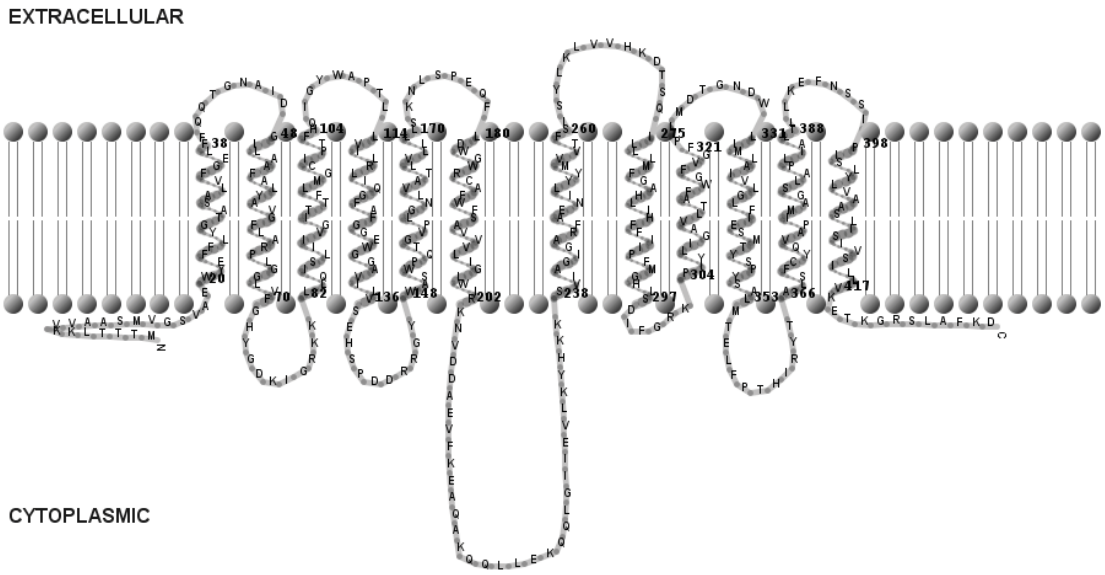

Figure 6.2 Prediction of secondary structure of A1S_1331 using HMMTOP. The secondary structure of A1S_1331 was predicted from the sequence information using the online tool HMMTOP. The protein contains 12 trans-membrane helices that are typical to a sub-class of MFS transporters. Both the N-terminus and the C-terminus are buried in the cytoplasm.

The transmembrane helices together form a cavity which allows for the substrate movement after binding to the lining amino acid residues (Figure 6.3).

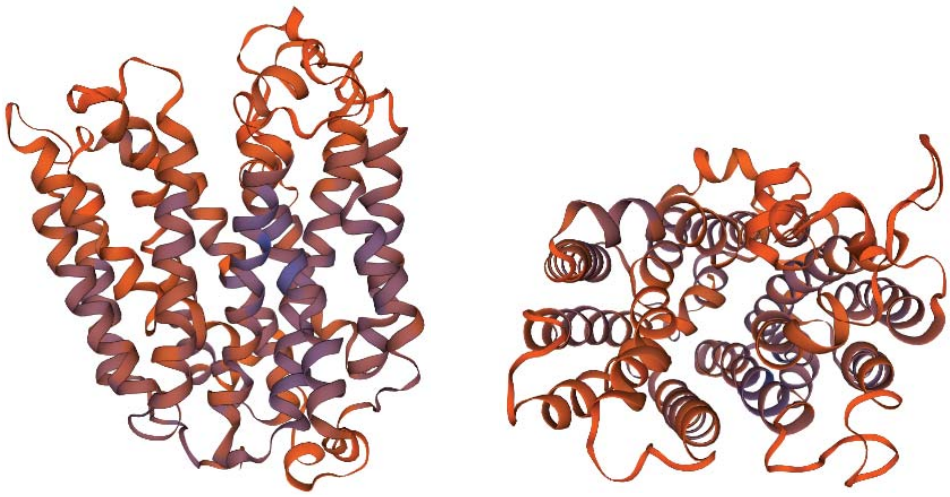

(a) (b)

Figure 6.3 3D model of A1S_1331 prepared using SWISS-MODEL. The six-helix groups form a barrel like structure, as seen from the side view (a), with a central cavity for solute movement, as seen in the top view (b). (QMEAN = -6.44; GMQE = 0.60)

6.2 A1S_1331 decreases fosfomycin susceptibility of *E. coli* KAM32, hence AbaF

E. coli KAM32 is a double knockout of efflux genes *ydhE* and *acrB*, making it deficient in efflux of antibiotics [336]. It is used as a model strain for expression and assessment of efflux pumps. Any changes in drug susceptibilities of *E. coli* KAM32 on expression of an efflux pump is therefore, attributable to the particular efflux pump and the drug in question is its substrate. The A1S_1331 ORF, along with its promoter and terminator, was cloned in pUC18 resulting in the plasmid pRPT7. The plasmid was transformed into *E. coli* KAM32, resulting in the strain RPT 145. The plasmid pUC18 itself was also transformed into *E. coli* KAM32 to form the control strain RPT 144. Of the antibacterial compounds tested, a 16-fold decrease in susceptibility for fosfomycin was observed in RPT 145 (*E. coli* KAM32/pUC_*abaF*) as compared to RPT 144 (*E. coli* KAM32/pUC18) (Table 6.1). The MIC values of kanamycin were 8-folds higher and those of chloramphenicol, minocycline, clindamycin, tetracycline, nalidixic acid and ethidium bromide (EtBr) were 2-folds higher in RPT 145. No significant change in MIC values of other antibacterials was observed. Since fosfomycin appeared to be the primary substrate of A1S_1331, the protein was designated as AbaF (*A. baumannii* fosfomycin resistance).

Table 6.1 Minimum inhibitory concentrations of various compounds for *E. coli* KAM32/pUC18 and *E. coli* KAM32/pUC18_*abaF*

S. No.	Compound	MIC (mg/L)	
		***E. coli* KAM32/pUC18**	***E. coli* KAM32/pUC18_*abaF***
1.	Fosfomycin	2	32
2.	Chloramphenicol	0.25	0.50
3.	Ethidium bromide	4	8
4.	Minocycline	0.5	1
5.	Tetracycline	0.06	0.12
6.	Nalidixic acid	2	4
7.	Kanamycin	4	32
8.	Clindamycin	2	4
9.	Gentamycin	1	1
10.	Tobramycin	1	1
11.	Streptomycin	4	4
12.	Amikacin	0.5	0.5
13.	Ofloxacin	0.01	0.01
14.	Chlorhexidine	0.25	0.25
16.	Ciprofloxacin	0.0015	0.0015
17.	Trimethoprim	0.01	0.01
18.	Erythromycin	0.5	0.5

6.3 EtBr fluorometric assays establish AbaF as an efflux pump

Since EtBr is a common substrate for most of the efflux pumps, fluorometric assays using EtBr were performed to determine if AbaF was involved in active efflux [337]. EtBr enters the cells via passive diffusion and fluoresces upon binding to the cellular components. The efflux pumps actively pump out EtBr from the cytoplasm leading to decrease in fluorescence. Therefore, the movement of EtBr, determined by fluorometric measurements, can serve as a measure for efflux activity of transporter proteins (Figure 6.4).

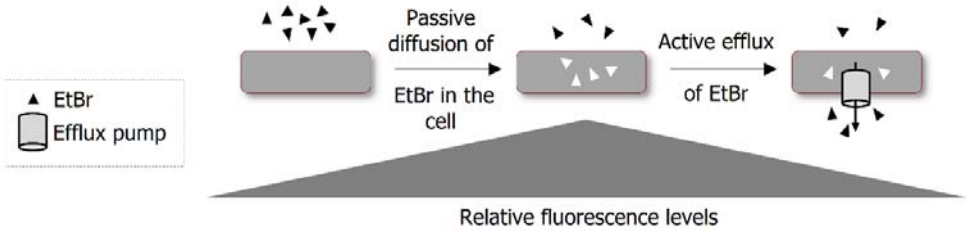

Figure 6.4 General scheme of EtBr based fluorometric assay for efflux determination. The cytoplasmic fluorescence of EtBr upon binding to cellular components is determined as a measure of EtBr accumulation. In presence of glucose, the transporter proteins efflux out EtBr, leading to a decrease in fluorescence, a measure of EtBr efflux.

The accumulation of EtBr was lower in *E. coli* KAM32 cells expressing AbaF (Figure 6.5 (a)) than *E. coli* KAM32/pUC18. Addition of the energy decoupler and efflux inhibitor CCCP caused an increase in accumulation of EtBr in both the types of cells and the accumulation finally plateaued over time. Similarly, when *E. coli* KAM32/pUC18_abaF and *E. coli* KAM32/pUC18 cells loaded with EtBr were energized by glucose, the efflux of EtBr (as measured by decrease in the fluorescence) was higher in case of *E. coli* KAM32/pUC18_abaF (Figure 6.5 (b)). The addition of CCCP blocked the efflux and the EtBr fluorescence started to build up in both cells. These observations suggest that AbaF actually works as an energy dependent efflux pump. The EtBr accumulation was low in cells expressing AbaF owing to expulsion of EtBr by AbaF. The efflux of EtBr from cells expressing AbaF again corroborates the finding that AbaF is an efflux pump.

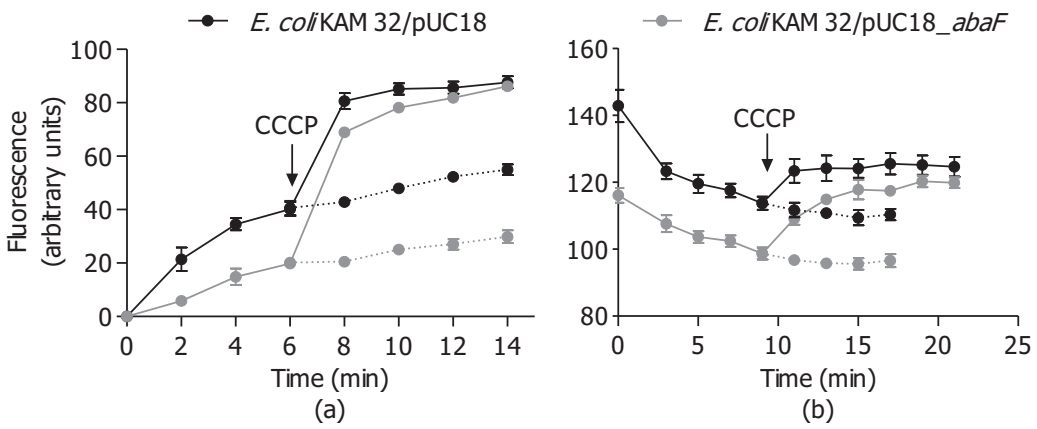

Figure 6.5 (a) Accumulation of EtBr. EtBr accumulation in *E. coli* KAM32/pUC18 (black circles) and *E. coli* KAM32/pUC18_abaF (grey circles), in presence of glucose, was determined using a fluorescence plate reader. (b) Efflux of EtBr. *E. coli* KAM32/pUC18 and *E. coli* KAM32/pUC18_abaF cells were pre-incubated with EtBr and 0.4% glucose was added to initiate efflux. The efflux inhibitor CCCP was added to the reaction mixture at the time point marked by an arrowhead. The dotted lines represent relative fluorescence in cases where CCCP was not added at the specified time point.

6.4 Disruption of *abaF* increases susceptibility of *A. baumannii* to fosfomycin

Over expression of *abaF* in *E. coli* KAM32 suggested the involvement of this transporter in efflux of fosfomycin and subsequently a role in resistance against the drug. To assess the importance of AbaF in *A. baumannii*, the *abaF* ORF was disrupted (*A. baumannii ΔabaF*, RPT 103) and was genetically complemented by expression of *abaF* from a plasmid (pRPT10) resulting in the strain *A. baumannii pabaF* (RPT 152). This inactivation of *abaF* resulted in resulted in an 8-fold increase in sensitivity to fosfomycin (Table 6.2). The fosfomycin resistance was restored by plasmid borne expression of AbaF (in *A. baumannii pabaF*). The sensitivity profile against kanamycin could not be determined as insertion of pMo130 (the suicide plasmid used for insertional inactivation of *abaF*) resulted in chromosomally encoded kanamycin resistance. However, there was no change in MIC of other aminoglycosides tested. Additionally, despite increased sensitivity of *A. baumannii ΔabaF* towards chloramphenicol, the effect of plasmid borne complementation could not be studied due to the presence of a chloramphenicol resistance marker in the complementing plasmid.

Table 6.2 MICs of various compounds for *A. baumannii* WT, *A. baumannii ΔabaF* and *A. baumannii pabaF*

Compound	MIC (µg/ml)		
	***A. baumannii* WT**	***A. baumannii ΔabaF***	***A. baumannii pabaF***
Fosfomycin	256	32	256
Chloramphenicol	8	2	-
EtBr	1	4	2
Minocycline	0.125	0.125	0.125
Gentamycin	1	1	1
Tobramycin	1	1	1
Streptomycin	16	16	16
Amikacin	0.5	0.5	0.5
Tetracycline	2	2	2
Nalidixic acid	0.5	0.5	0.5

6.5 Fosfomycin treatment induces the expression of *abaF*

In order to determine the direct role of AbaF in fosfomycin resistance by efflux, actively growing *A. baumannii* cells were treated with increasing concentrations of fosfomycin. The cells were exposed to fosfomycin for two hours and the total RNA from the treated cells was extracted. From the total RNA, cDNA was synthesized and *abaF* expression was quantified using *groEL* as an internal control in a quantitative Polymerase Chain Reaction (qPCR). *abaF* expression in fosfomycin treated cells was determined relative to the untreated cells. There was a 2.5-fold and 2.9-fold increase in the expression of *abaF* in *A. baumannii* cells treated with 1x MIC (256 µg/ml) and 2x MIC (512 µg/ml) of fosfomycin, respectively, as compared to the expression of *abaF* in cells that were not treated with fosfomycin (Figure 6.6). A further 7-fold increase was observed in case of cells treated with 4x MIC (1024 µg/ml) of fosfomycin. This indicates that fosfomycin induces the expression of *abaF* and AbaF is directly involved in mediating fosfomycin resistance.

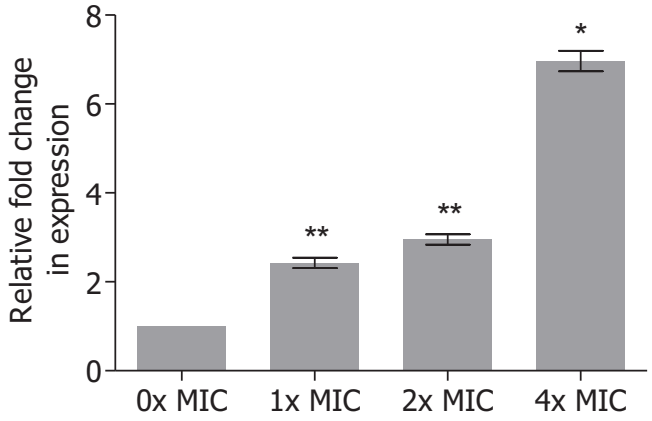

Figure 6.6 Induction of *abaF* expression by fosfomycin treatment. Actively growing cells of *A. baumannii* ATCC 17978 were treated with increasing concentrations (corresponding to 1x, 2x and 4x MIC) of fosfomycin for two hours. Change in expression of *abaF* relative to expression in control condition (0x MIC) was determined by qPCR with *groEL* as the internal control (P values have been summarized for all the pairs in the paired student's t-test).

6.6 Exposure to fosfomycin results in selection of drug resistant mutants with increased expression of *abaF*

Since AbaF is directly involved in fosfomycin resistance, it was hypothesized that the expression of *abaF* must be important for survival of *A. baumannii* in presence of fosfomycin. To validate this hypothesis, expression of *abaF* was assessed in fosfomycin resistant mutants of *A. baumannii*. Growth of wild type *A. baumannii* cells in presence of increasing amounts of fosfomycin led to isolation of drug resistant mutants fairly easily. The expression *abaF* in cells resistant to 1x MIC, 2x MIC and 4x MIC concentrations was determined by qPCR. The quantitation was achieved by comparing the expression with that of an internal control (*groEL*). It was observed that the expression of *abaF* was about 2.5 times higher (P value <0.02) in cells resistant to 1x MIC of fosfomycin than the cells growing in absence of fosfomycin (Figure 6.7) which increased to about 6 times in cells resistant to 2x MIC of fosfomycin (P value <0.01) and about 14 times in cells resistant to 4x MIC of fosfomycin (P value <0.02). This gradual increase in expression of *abaF* in fosfomycin resistant mutants validated our hypothesis that AbaF is important for survival in presence of fosfomycin.

Since the expression of *abaF* is regulated by AbsR25, the expression of AbsR25 was simultaneously determined by qPCR. The expression of AbsR25 was low in these fosfomycin resistant mutants, 0.05-fold (1x MIC, P value <0.001); 0.15-fold (2x MIC, P value <0.001) and

0.2-fold (4x MIC, P value <0.001) as compared to wild type *A. baumannii*; in line with our previous observations.

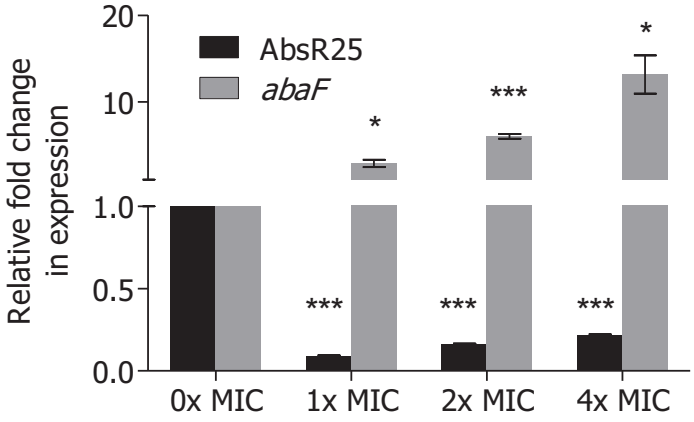

Figure 6.7. Expression of AbsR25 and *abaF* in fosfomycin resistant mutants. Fosfomycin resistant mutants of *A. baumannii* were selected by serially passaging the wild type cells in presence of increasing concentrations of fosfomycin (corresponding to 1x, 2x and 4x MIC). Change in expression of AbsR25 (black bars) and *abaF* (grey bars) relative to wild type (0x MIC) cells was determined by qRT-PCR (P values have been summarized for all the pairs in the paired student's t-test).

6.7 Biofilm formation is affected by disruption of *abaF*

Biofilms are an important characteristic of *A. baumannii* which help the bacterium to survive on inanimate objects and resist the action of various antibiotics. There are reports on involvement of efflux pumps in expulsion of biofilm material from the cellular inside to the exterior. Therefore, to assess the involvement of AbaF in biofilm material extrusion, biofilms of wild type *A. baumannii*, *A. baumannii ΔabaF* and *A. baumannii pabaF* were allowed to form on the wells of 96-well microtiter plate. The cellular biomass (the biofilm) was stained with 1% crystal violet after 24 hours of static incubation at 37°C. The stain picked up by the biomass was dissolved in 95% ethanol and the OD_{595} was determined spectrophotometrically. The relative biofilm was determined as ratio of OD_{600} of the cell suspension in the wells (prior to staining) and OD_{595} of the dissolved stain. Disruption of *abaF* resulted in reduced biofilm formation (Figure 6.8). The defect in biofilm formation was complemented when *abaF* was expressed in a plasmid (in *A. baumannii pabaF*). Thus, AbaF might be involved in efflux of cementing materials that helps the *A. baumannii* cells to form biofilms.

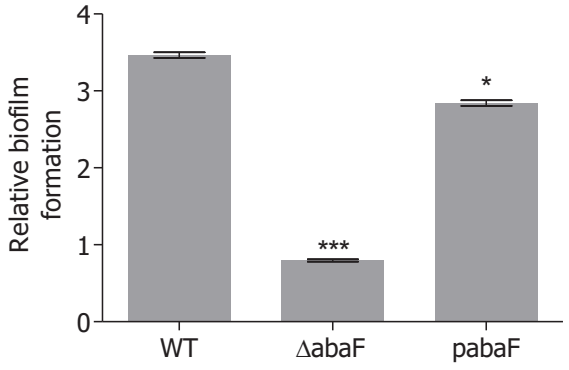

Figure 6.8 Biofilm formation by wild type *A. baumannii*, *A. baumannii ΔabaF* and *A. baumannii pabaF*. The bars represent mean of triplicate values with error bar representing standard deviation (P values have been summarized for each pair in paired student's t-test).

6.8 AbaF is required for virulence of *A. baumannii* in *C. elegans*

With experimental evidence that AbaF is involved in resistance and biofilm formation in *A. baumannii*, we wished to assess its importance in virulence. Efflux pumps, in addition to antibiotics and biofilm material, can efflux virulence factors or host-derived antimicrobial chemicals. *C. elegans* worms have been used as a model organism to study virulence of *A. baumannii* in previous studies [338]. We used *C. elegans* worms to determine the effect of *abaF* deletion on virulence of *A. baumannii*. The worms were reared on agar plates with a centrally placed lawn of bacterial cells for feeding. It was observed that no worm survived till the 7th day feeding on wild type *A. baumannii* cells. However, the last surviving worm feeding on *A. baumannii ΔabaF* cells survived for 11 days (Figure 6.9). This prolonged survival of *C. elegans* worms feeding on *A. baumannii ΔabaF* cells proves that the virulence potential of *A. baumannii* is affected on deletion of AbaF. Thus, AbaF plays a significant role in virulence of *A. baumannii* as well.

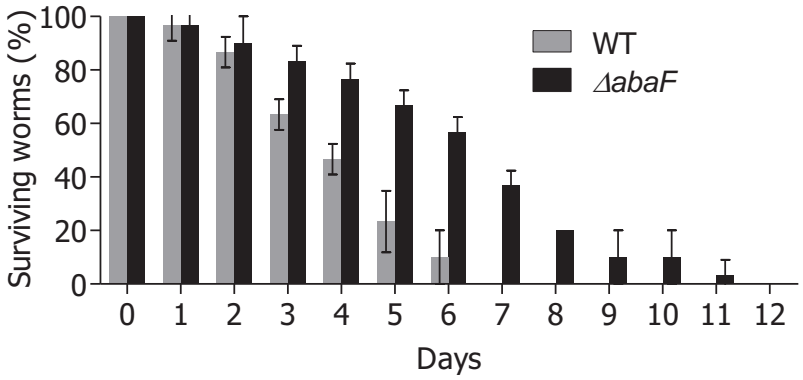

Figure 6.9 Survival of *C. elegans* worms feeding on wild type *A. baumannii* and *A. baumannii ΔabaF*. The percentage survival of worms feeding on wild type *A. baumannii* (grey bars) and *A. baumannii ΔabaF* (black bars) was determined by counting the number of live worms in each plate over the course of time (P value <0.05 in student's paired t-test).

6.9 *abaF* is expressed in majority of clinical strains in our collection

The importance of AbaF had so far been studied using the lab adapted strain of *A. baumannii* (ATCC 17978). However, to determine the relevance of fosfomycin efflux mediated by AbaF, clinical strains were analyzed for the expression of this efflux pump and the susceptibility of fosfomycin in presence of an efflux pump inhibitor. 24 clinical strains of *A. baumannii*, resistant to fosfomycin, were available in the lab and were screened for *abaF* expression by Reverse Transcriptase Polymerase Chain Reaction (RT-PCR). 92% of the clinical strains of *A. baumannii* tested positive for the expression of *abaF* during exponential growth phase (Figure 6.10). The MIC of fosfomycin for clinical strains decreased by a factor of 2-fold (37.5%), 4-fold (20.8%), 8-fold (33.3%) and 16-fold (4.1%) in presence of efflux inhibitor CCCP (Table 6.3), suggesting the role of efflux in fosfomycin resistance. Therefore, the efflux mediated resistance to fosfomycin is a relevant problem in clinical settings.

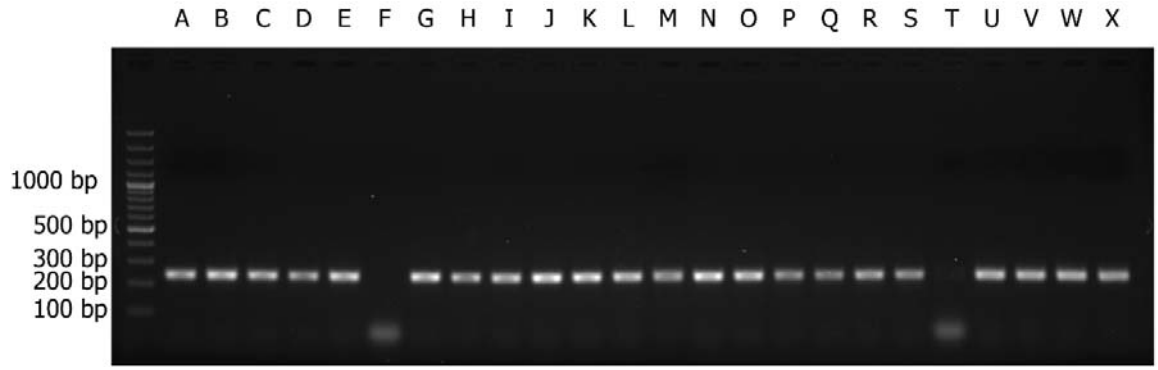

Figure 6.10 Expression of *abaF* in clinical strains of *A. baumannii*. A 230 bp internal region of *abaF* was amplified by PCR (30 cycles) using cDNA synthesized from total RNA of 24 clinical strains of *A. baumannii*. The lane designations (A-X) denote the clinical strain (*A. baumannii* RPTC1 – RPTC24). The first lane contains Fermentas 100bp plus DNA ladder. *groEL* was used as an internal control to verify cDNA amplification (not shown in this figure).

Table 6.3 Minimum Inhibitory Concentration (MIC) of fosfomycin against clinical strains in presence and absence of the efflux pump inhibitor CCCP.

Strain	MIC of fosfomycin (mg/L)		
	In absence of CCCP	In presence of CCCP (4 mg/L)	Fold change
A. baumannii RPTC 1	256	128	2
A. baumannii RPTC 2	256	128	2
A. baumannii RPTC 3	256	128	2
A. baumannii RPTC 4	512	128	4
A. baumannii RPTC 5	256	64	4
A. baumannii RPTC 7	256	128	2
A. baumannii RPTC 8	256	32	8
A. baumannii RPTC 9	128	16	8
A. baumannii RPTC 10	128	16	8
A. baumannii RPTC 11	256	128	2

A. baumannii RPTC 12	128	32	4
A. baumannii RPTC 13	128	16	8
A. baumannii RPTC 14	256	128	2
A. baumannii RPTC 15	256	32	8
A. baumannii RPTC 16	256	16	16
A. baumannii RPTC 17	256	32	8
A. baumannii RPTC 18	256	64	4
A. baumannii RPTC 19	256	32	8
A. baumannii RPTC 20	256	64	4
A. baumannii RPTC 21	128	64	2
A. baumannii RPTC 22	256	128	2
A. baumannii RPTC 23	128	64	2
A. baumannii RPTC 24	256	32	8

6.10 Discussion

Acinetobacter baumannii is a threat in clinical settings due to multitude of infections, recalcitrance, natural competence and multiple drug resistance [339]. In our previous report, we identified a novel regulatory small RNA, AbsR25, in *A. baumannii*. It was observed that AbsR25 was involved in negative regulation of a putative efflux pump gene, *abaF*; based on the observations in qPCR experiments [334]. This prompted us to study the properties of AbaF and we conducted a series of basic experiments to study the importance of AbaF in *A. baumannii*.

AbaF was annotated as MFS family transporter due to the presence of characteristic 12 trans-membrane helical domains that are associated with MFS family [340]. Experimental evidence indicates that AbaF is a transporter that is responsible for efflux of fosfomycin in *E. coli* KAM32. Although a variety of mechanisms of resistance against fosfomycin have been explained, there is no report of efflux mediated resistance against this antibiotic which is quite an interesting aspect of this transporter.

The *A. baumannii* cells with disrupted *abaF* were 8-fold more sensitive to fosfomycin (corroborating the results obtained using over expression model of *E. coli*) and the MIC value was 32 μg/ml which falls below the European Committee on Antimicrobial Susceptibility Testing (EUCAST) breakpoint for fosfomycin resistance. Interestingly, the *abaF* debilitated cells were also 4 times more susceptible to chloramphenicol, an observation that wasn't evident in *E. coli* KAM32. Chloramphenicol might as well be another secondary substrate of AbaF which can be a subject for later studies. A further direct involvement of AbaF in active efflux of fosfomycin was suggested by increase in expression of *abaF* on brief exposure (two hours) to fosfomycin. The increased expression of *abaF* in *A. baumannii* might be assisting the cells in effluxing out the excess of antibiotic and hence cell survival. In case of a prolonged exposure to fosfomycin, *A. baumannii* cells that were resistant to the antibacterial action of fosfomycin were obtained. These resistant mutants selected in presence of high amounts of fosfomycin also showed increased expression of *abaF*. The *A. baumannii* cells overexpressing the fosfomycin resistance determinant, *abaF*, had a clear advantage and therefore were selected over the others. In line with our previous observations, the expression of AbsR25 in the cells overexpressing *abaF* was low. However, the expression of AbsR25 was not inversely related to the change in expression of *abaF*, which indicates that AbsR25 has targets other than *abaF*.

The importance of AbaF is highlighted by the fact that it is constitutively expressed in most, if not all, of the clinical strains of *A. baumannii* during active growth. However, it is quite interesting to note that despite expressing *abaF*, not all the clinical strains were sensitized to fosfomycin on inhibition of efflux by CCCP. This observation hints that efflux, though an important reason, might not be the only mechanism responsible for fosfomycin resistance. There must be other fosfomycin resistance mechanisms active in these clinical strains that did not show any significant change in MIC of fosfomycin in presence of CCCP. However, this should not lead to undermining the role of efflux mediated resistance to fosfomycin. It might be a case similar to fluoroquinolone resistance which is mediated by efflux as well as gyrase mutations [341].

It is surprising that despite a general consensus that fosfomycin is not active against *A. baumannii*, there is no concrete evidence in the literature explaining the reasons for the same. Recently, synergistic activity of fosfomycin with colistin, minocycline and polymyxin B against multi-drug resistant *A. baumannii* has revived the interest in fosfomycin as a drug of choice [342,343]. However, the high frequency of mutant selection and adaptations leading to increased expression of *abaF* (and increased efflux of fosfomycin thereof), as per our observations, could

compromise the success of these combinatorial therapeutics. However, compromising the activity of AbaF could be a potential therapeutic option to revive the activity of fosfomycin. Fosfomycin is a drug of choice for treatment of UTIs as it maintains its activity at acidic pH that is prevalent in urinary tract [344]. A combination of inhibitor of AbaF with fosfomycin (similar to fosfomycin and CCCP combination) could therefore be used in clinics to tackle *A. baumannii* in UTIs

Some more interesting findings from disruption of *abaF* in *A. baumannii* were impaired biofilm formation and decreased virulence. Since its disruption resulted in reduced biofilm formation, AbaF might also be one of the efflux pumps that are involved in extrusion of biofilm material. Such efflux pumps have been reported to be involved in biofilm formation in *E. coli*, *Pseudomonas aeruginosa*, *Salmonella enterica*, *S. aureus* and *Klebsiella* strains [345–348]. Efflux pump inhibition and disruption has been implicated in decreased virulence owing to proposed capacity of efflux pumps to expel host derived antibacterial factors [349]. AbaF also seems to play a similar role in *A. baumannii* which is evident by the markedly high survival of *C. elegans* on *A. baumannii* cells with disrupted *abaF*.

7 Characterization of a novel small RNA AbsR1 in *A. baumannii*

Our group's previous studies identified 31 putative small RNA in *A. baumannii* [11]. However, only three of them were validated by Northern blotting. No further experimentation had been carried out to validate the remaining 28 candidate small RNA, so there was no information on their expression and role in the physiology of *A. baumannii*. Therefore, the expression of other small RNA was assessed by Northern blotting and one novel small RNA, AbsR1 was identified.

7.1 AbsR1 expression was validated by Northern blotting

AbsR1 was picked up from the list of putative sRNA and a probe to detect this sRNA by Northern blot was designed. The single stranded DNA probe was ligated to a T7 promoter adaptor converted to double standard DNA by end filling using Klenow fragment. This double stranded DNA was used as a template to drive RNA synthesis by T7 RNA polymerase in an *in vitro* transcription reaction. The RNA probe was labelled with psoralen-biotin and stored till further use.

A. baumannii ATCC 17978 cells were grown in nutrient broth and the total cellular RNA was isolated at different growth stages, namely, lag phase, log phase and stationary phase. The total RNA was DNase treated and resolved on 10% denaturing PAGE containing 8M urea. Since the predicted length of AbsR1 small RNA was just over 100 nts, the gel was run for long till the xylene cyanol in the dye, which migrates at about 50 bp in 10% denaturing gel, traverses 4/5th of the gel. The gel was run for a longer duration to ensure enough separation from the 5S rRNA, which often interferes with the probe hybridization.

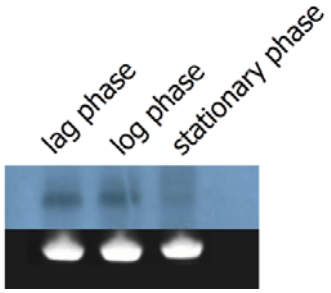

Figure 7.1 Expression of AbsR1 during different phases of growth in *A. baumannii*. The 5S rRNA (stained in the lower section of the figure) was used as the loading control.

It was observed that AbsR1 is expressed and is a bona fide small RNA (Figure 7.1). Its expression was maximal in the lag and the log phase which decreased in the stationary phase. Therefore, the candidate sRNA AbsR1 was validated to be a bona fide sRNA with a growth dependent expression profile.

7.2 AbsR1 is over expressed under acid stress

Since small RNA are transiently over expressed when cells are exposed to stress, the expression of AbsR1 was determined by exposing *A. baumannii* cells to various stress conditions. The environmental stress was simulated by addition of NaCl (osmotic stress), H_2O_2 (oxidative), 2, 2-DIP (iron limiting conditions); by incubation at 45°C (thermal stress) and 0°C (cold stress) (Figure 7.2); and by exchanging the growth medium for modified growth medium maintained at pH 5 (acidic stress) and pH 9 (alkaline stress) (Figure 7.3). Importantly, the cells were exposed transiently to the stress to capture the rapid changes in sRNA expression and make the experiment more physiologically relevant. Total RNA was isolated and Northern blotting was carried out to study the expression of AbsR1. The expression of AbsR1 was higher in case of pH 5 treated cells (Figure 7.3). This hints that AbsR1 might be involved in regulation of response to acidic stress.

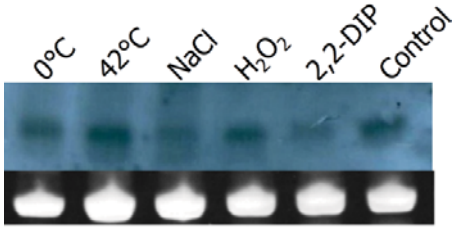

Figure 7.2 Expression analysis of AbsR1 under different stress conditions. The cells were treated with various physical and chemical agents, as mentioned above the lanes, to induce stress. The control cells were not treated with anything. The 5S rRNA (stained in the lower section of the figure) was used as the loading control.

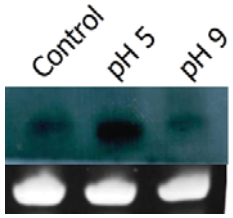

Figure 7.3 Expression analysis of AbsR1 under different pH conditions. The cells were grown and the growth medium was exchanged with media at pH 5 and pH 9 for 30 minutes. The 5S rRNA (stained in the lower section of the figure) was used as the loading control.

7.3 Transcription start and stop sites of AbsR1 were identified

To determine the exact sequence of AbsR1, the transcription start and stop sites were determined by RACE mapping. RACE mapping involves PCR mediated amplification of the 3' and 5' ends of an RNA (converted to cDNA by specific adaptors) and subsequent DNA sequencing. The 3' and 5' RACE mapping was carried out using RLM-RACE kit (ThermoScientific, USA)

following the manufacturer's instructions. Using RACE mapping, AbsR1 was determined to be an 89 nt long small RNA (Figure 7.4).

```
>Acinetobacter baumannii ATCC 17978 AbsR1
TTTAAAGTCCTGATGAGGATTAAGCATAAAACAGAAAAGTTATTTCTGCTT
TTGCTTCGGTAGAGTAAAGCTTTATCTATTACTTATCA

>Acinetobacter baumannii ATCC 17978 AbsR1
UUUAAAGUCCUGAUGAGGAUUAAGCAUAAAACAGAAAAGUUAUUUCUGCUU
UUGCUUCGGUAGAGUAAAGCUUUAUCUAUUACUUAUCA
```

Figure 7.4 Nucleotide sequence of AbsR1 as determined by DNA sequencing and the RNA sequence.

The AbsR1 sequence was conserved among the *A. baumannii* strains with no apparent sequence similarity with other member of *Acinetobacteraceae* (except *A. calcoaceticus*) and other bacterial genera.

Figure 7.5 Genomic locus of AbsR1. In all the sequenced Acinetobacter genomes, AbsR1 is present between the 50S ribosomal protein coding genes.

The AbsR1 sRNA is located between the genes coding for ribosomal proteins and this context is also conserved among the *A. baumannii* strains (Figure 7.5). The folding of AbsR1 was determined by the mfold server. The folding points out two regions (37-43 and 65-71) which can act as seed regions for interaction with mRNA targets (Figure 7.6).

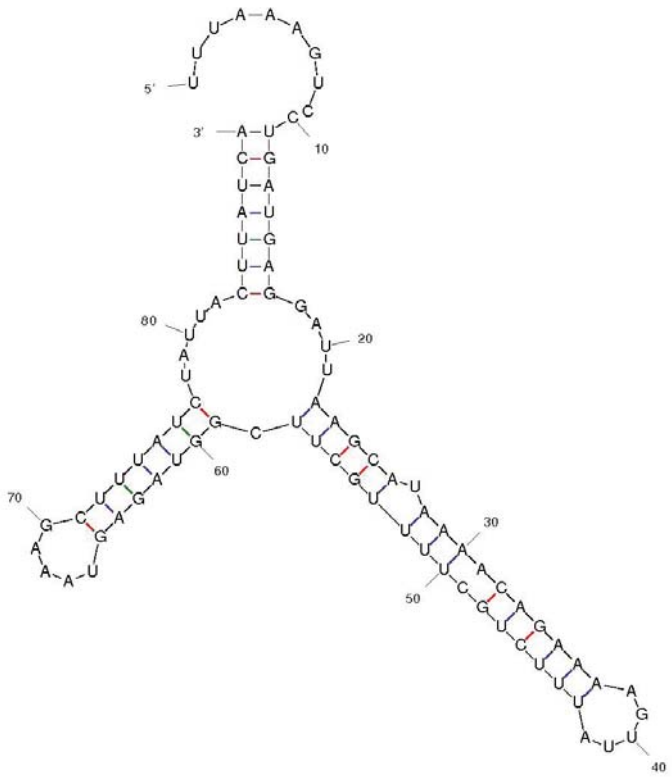

Figure 7.6 Native folding state of AbsR1 small RNA as determined by the mfold server. Folding of RNA provides clues about the residues which might be involved in interaction with partner mRNAs from their availability in single stranded loops.

7.4 AbsR1 deletion mutant is sensitive to acidic stress

The homologous recombination-based approach used to delete the *hfq* gene was utilized to generate an AbsR1 deletion mutant *A. baumannii*. A recombineering PCR product carrying gentamicin resistance gene *aac1* flanked by 125 bp upstream and downstream region of AbsR1 coding locus was generated by cloning various parts in a vector pMo130. The recombineering PCR product was transformed into *A. baumannii* cells expressing homolog of RecT recombinase. The transformants were screened for allele replacement (AbsR1 with *aac1*) on LB agar plates containing 5 µg/ml gentamicin. PCR was carried out using primers that anneal to a region upstream and a region downstream of AbsR1 coding region to determine allele exchange (Figure 7.7).

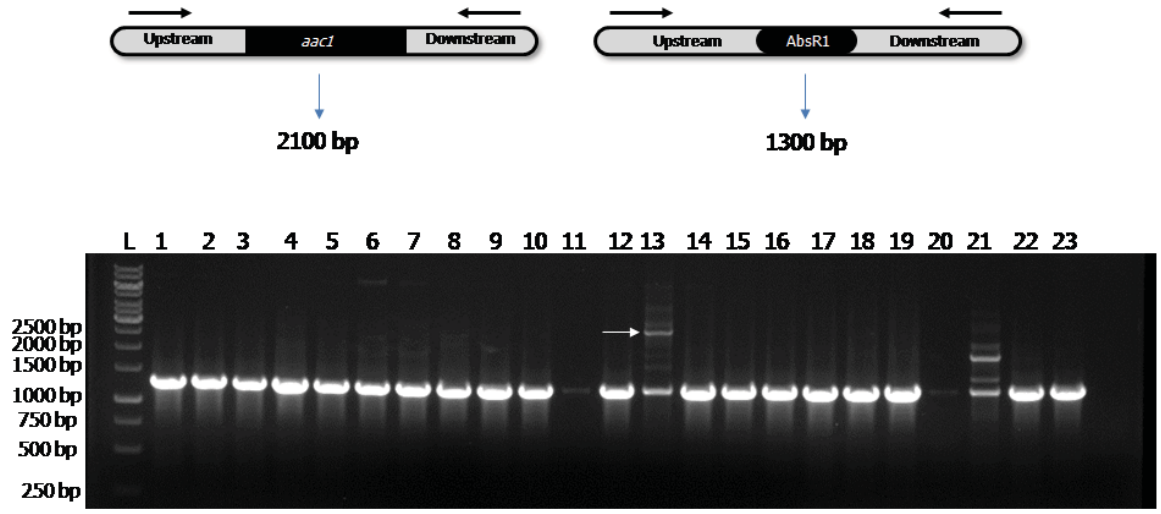

Figure 7.7 PCR screening of AbsR1 allele replacement by *aac1*. The amplicon of required size was found in case of colony number 13 which is marked by an arrowhead.

The colony which yielded the required amplicon was purified by streaking on LB agar plate containing 10 µg/ml gentamicin. Two colonies (13a and 13b) were picked up from that plate and were screened again using different set of primers. Two PCR reactions were carried out one using forward primer for AbsR1 and one for *aac1* with a common reverse primer (Figure 7.8). In both the colonies, amplification was achieved only in case when the forward primer for *aac1* was used validating the allele replacement and subsequent deletion of AbsR1.

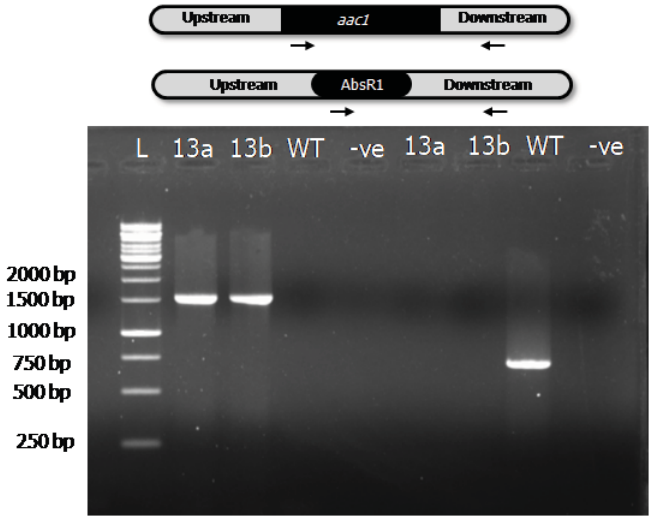

Figure 7.8 Secondary screening of AbsR1 deletion mutant using different forward primers (as mentioned in the schematic above). The lane L contains Fermentas 1 kb ladder. Positive amplification is achieved in case of 13a and 13b colonies when forward primer of *aac1* was used. Amplification in wild type (WT) was achieved only in case forward primer for AbsR1 was used.

The wild type *A. baumannii* (WT) and AbsR1 deletion mutant (ΔAb1) were grown in LB and the overnight cultures were spotted on LB agar plates supplemented with different stress creating agents. There was no difference in growth of WT and ΔAb1 in presence of 2,2-DIP (iron depletion), pH 9 (alkaline stress), H_2O_2 (oxidative stress). There was a minor difference in the growth in presence of 2% NaCl (osmotic stress). The wild type bacterium grew better in presence of salt than ΔAb1 (Figure 7.9).

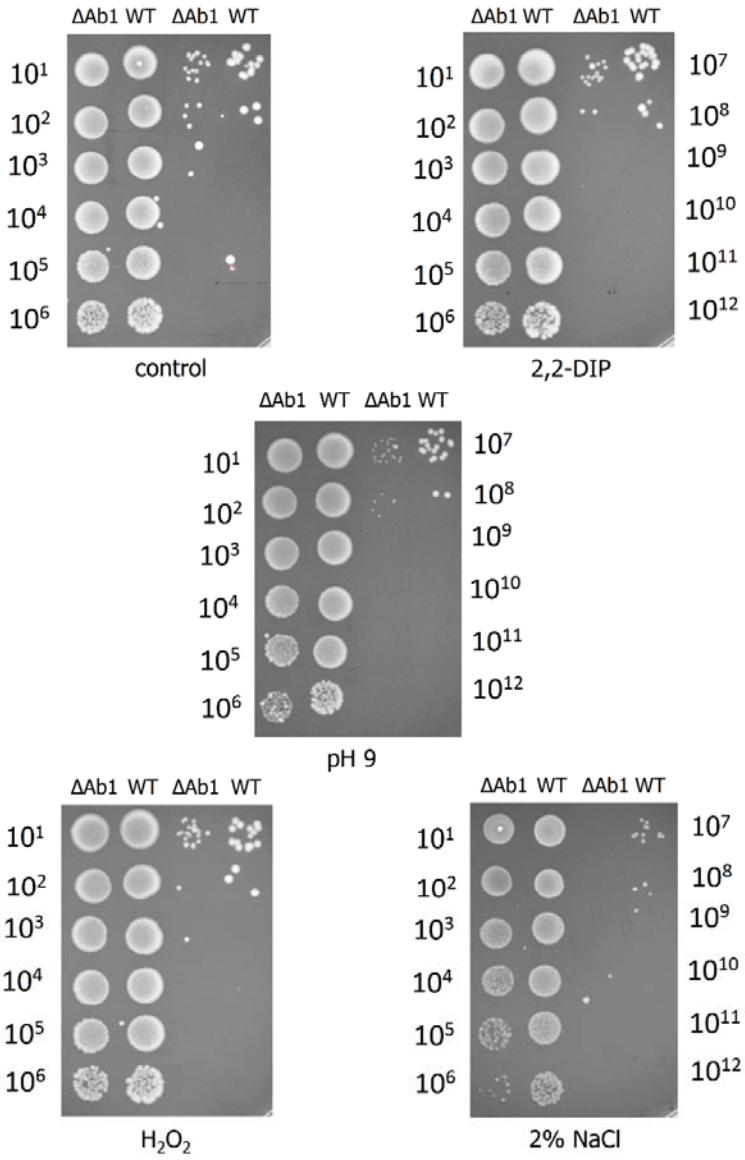

Figure 7.9 Growth of *A. baumannii* wild type (WT) and AbsR1 deletion mutant (ΔAb1) in presence of different stress creating agents.

However, there was a marked difference between the growth of wild type cells and ΔAb1 cells in pH 5 (acidic stress) (Figure 7.10). This difference indicates that AbsR1 is important for survival in acidic conditions. These results seem to corroborate the previously speculated role of

AbsR1 in acidic stress. Both these observations indicate that AbsR1 sRNA might be an important regulator of acidic stress response.

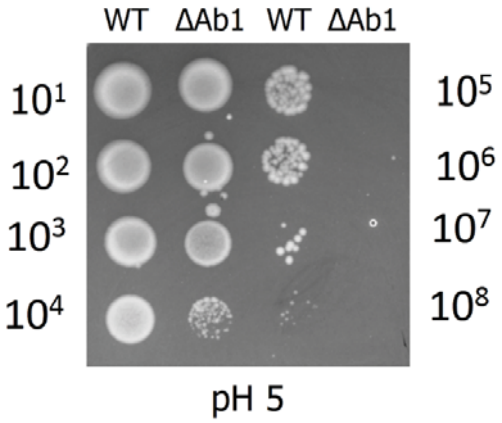

Figure 7.10 Growth of *A. baumannii* WT and ΔAb1 at pH 5.

7.5 Discussion

Small RNA are now seen as important regulators of stress response in bacteria [229]. They base pair with their target mRNA and regulate translation, thereby effectively regulating the bacterial responses to various stress. Our lab had previously identified 31 candidate small RNA in *A. baumannii* by a computational approach and expression of three novel sRNA was validated [11].

Since no information was available on the expression profile of other candidate sRNA, expression of a novel candidate, AbsR1 was assessed by Northern blotting. AbsR1 is maximally expressed during early growth stages and its expression increases when the *A. baumannii* cells are exposed to acidic stress. Further characterization to determine the transcriptional start and stop sites of AbsR1 revealed that it is an 89 nt long small RNA, about 20 nt shorter than its predicted length. It was interesting to note that the AbsR1 sequence is conserved throughout the *A. baumannii* species. The gene coding for AbsR1 lies between the genes that code for the 50S ribosomal proteins. This genomic context is also conserved throughout the *A. baumannii* species, which itself hints at the functional importance of this small RNA.

Since *A. baumannii* is not an enteric pathogen, it was difficult to ascribe the role of this small RNA in management of acidic stress. However, *A. baumannii* is in fact known to colonize human skin, which has an acidic pH and it thrives in the urinary tract which again has an acidic environment. Thus, this small RNA may be an assisting factor in adaptation to the skin and

urinary tract area, where the bacterium faces an acidic challenge. To ascertain the role of AbsR1 in physiology of *A. baumannii*, a deletion mutant of AbsR1 was generated. The growth of the deletion mutant was compared with that of the wild type bacterium in presence of different stress creating agents. A prominent defect in growth of the deletion mutant at pH 5 furthers the notion that AbsR1 might be involved in management of acidic stress in *A. baumannii*. The observation that AbsR1 is overexpressed when the bacteria face acidic challenge and the defect in growth of AbsR1 deletion mutant on acidic medium fall in line to indicate that AbsR1 is an important factor for *A. baumannii* to cope up with acidic stress. Further experiments using the transcriptomic and proteomic information of the AbsR1 deletion mutant as well as similar information from *A. baumannii* cells exposed to acidic stress could reveal more information on the physiological role of AbsR1 in *A. baumannii.*

Another very peculiar observation about the AbsR1 deletion mutant was regarding the colony morphology. The colonies of *A. baumannii* ΔAb1growing on LB agar were significantly smaller than the wild type *A. baumannii* colonies. This size variation was observed even on plates that were supplemented with reagents that induced various stress. This variation in colony size could be due to certain metabolic defects that might have arisen due to deletion of AbsR1 and subsequent disruption of a metabolic pathway. However, without experimental evidence this hypothesis can not be validated. It forms another interesting lead that could be followed in the future to reveal information linking AbsR1 to the metabolism of *A. baumannii*.

8 PCR based detection of *A. baumannii* on clinical surfaces using its non-coding signature

Detection of pathogens in a rapid and high-throughput manner is a significant challenge in the clinical settings. *A. baumannii* colonizes the hospital environment and survives there for long durations of time [22]. Conventional techniques are dependent on culture-based methods and often take a long time. Nucleic acid based techniques are time saving and are amenable to quantitative high throughput [21]. From the sequences of our previously identified candidate sRNA, a specific region in the *A. baumannii* genome was identified that could serve the purpose of a detection marker in a PCR based detection scheme.

8.1 AbsR10 region is unique to *A. baumannii*

The computational analysis of *A. baumannii* genome for putative sRNA yielded 31 candidates [11]. Of all the candidates, AbsR10, a 175 nt long candidate sRNA, was of special interest (Figure 8.1).

```
AbsR10>gi|126640115|ref|NC_009085.1|    Acinetobacter
baumannii  ATCC  17978,  complete  genome\-2543367\-
2543541
AAGAGAACCATATGGTTCTCTTTAGATTTTGAATTGTAATTTTCTTAATTTT
ATATTGGCATTTATACTTTTATTTATTTTCAGATCAATATGTTTTCCCCCAC
CAAAACTGATCTGCTTCTTCTTTTGCGCTATGTTGAACATGAGCATTGGCAT
GCCATTTCATATCCATTGT
```

Figure 8.1 Nucleotide sequence of AbsR10 candidate small RNA. Taken from [3].

BLAST analysis revealed that some parts of AbsR10 sequence are unique to *A. baumannii* with no similarity with other bacteria. Such unique signature sequences in pathogenic bacteria can be used for specific detection purposes [350]. Of the 175 bp genomic sequence, a 151 bp sequence was identified, that could be used as a marker for *A. baumannii* (Figure 8.2). Primers OligoRPT59 and OligoRPT60 were designed to amplify this sequence by polymerase chain reaction.

>NC_009085 Acinetobacter baumannii ATCC 17978 -
nucleotides 2543371-2543521 (151)
ACCATATGGTTCTCTTTAGATTTTGAATTGTAATTTTCTTAATTTTATATTG
GCATTTATACTTTTATTTATTTTCAGATCAATATGTTTTCCCCCACCAAAAC
TGATCTGCTTCTTCTTTTGCGCTATGTTGAACATGAGCATTGGCATG

Figure 8.2 Nucleotide sequence of the 151 bp target sequence in AbsR10 that is specific to *A. baumannii*.

8.2 Primers designed to amplify a specific region in AbsR10 can identify *A. baumannii*

The primers (OligoRPT59 and OligoRPT60) were used in a PCR reaction using genomic DNA from *A. baumannii* ATCC 17978. A band corresponding to 151 bp was amplified. To assess whether the primers could indeed be used to identify other strains of *A. baumannii*, genomic DNA from clinical strains was isolated and PCR was performed using AbsR10 specific primers. It was interesting to note that there was amplification in all the strains (Figure 8.3). This implies that the AbsR10 based detection system could detect 100% of the clinical strains and this system could be used in the clinical setting.

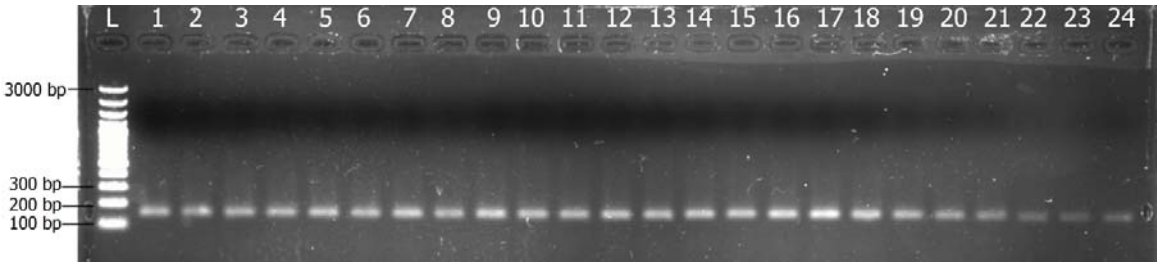

Figure 8.3 PCR amplification of AbsR10 region from various clinical strains of *A. baumannii*. The PCR products obtained using genomic DNA of RPTC 1–24 (Lane 1-24) were resolved on a 2% agarose gel. The lane L contains Generuler 100 bp plus ladder.

8.3 The identification primers are specific to *A. baumannii*

It was proved that the PCR based detection system could detect *A. baumannii* with 100% accuracy. However, to validate the utility of a detection system it is important that the system not only detects the target organism but is specific and does not yield any false positives. To negate the possibility of false positives, i.e. amplification if genomic DNA from other pathogenic bacteria is present, PCR was carried out using genomic DNA of various Gram positive and Gram-negative pathogens (*Salmonella typhi, Klebsiella pneumoniae*, *Enterobacter sakazakii*, *Vibrio cholerae*, *Staphylococcus aureus*, *Shigella flexneri*, *Streptococcus mutans*, and *Pseudomonas*

aeruginosa). A universal 16S control reaction was included to check the validity of the PCR reaction (Figure 8.4). No amplification was found in case of other pathogenic bacteria which confirms the specificity of the primers (Figure 8.5).

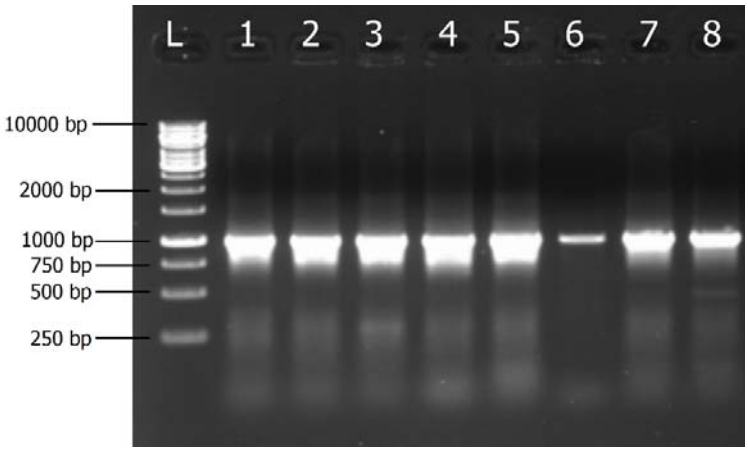

Figure 8.4 PCR amplification of 16S rDNA region using genomic DNA from various bacterial pathogens. The PCR reactions using genomic DNA of *S. typhi* (1), *K. pneumoniae* (2), *E. sakazakii* (3), *V. cholerae* (4), *S. aureus* (5), *S. flexneri* (6), *S. mutans* (7), and *P. aeruginosa* (8) were run on a 1% agarose gel. Lane (L) contains Generuler 1kb ladder.

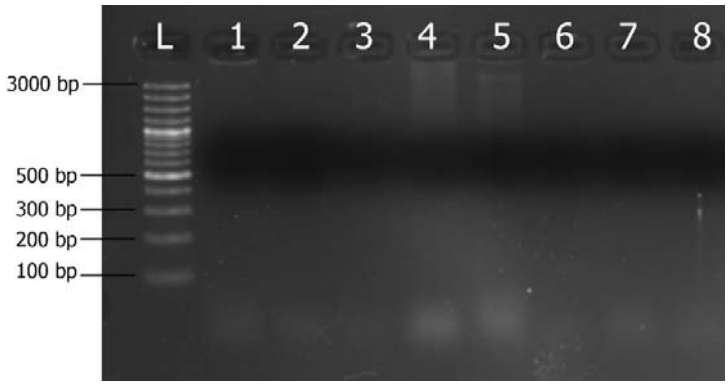

Figure 8.5 PCR amplification of AbsR10 unique region using genomic DNA from various bacterial pathogens. The PCR reactions using genomic DNA of *S. typhi* (1), *K. pneumoniae* (2), *E. sakazakii* (3), *V. cholerae* (4), *S. aureus* (5), *S. flexneri* (6), *S. mutans* (7), and *P. aeruginosa* (8) were run on a 2% agarose gel. Lane (L) contains Generuler 100 bp plus ladder.

8.4 The PCR based detection can be carried out on hospital derived samples

The validation of PCR based detection system had been performed using purified genomic DNA from the bacterial cells. However, to achieve purified DNA, culture-based approach had been used which is rather time consuming and cumbersome if the number of samples is very high. Since *A. baumannii* is a highly recalcitrant bacterium, it forms resistant biofilms on clinical surfaces. It remains viable for extremely long durations of time in a dry and desiccated state [22]. This assists in dissemination of bacterial infection in clinics and aids in persistence. Therefore, it

is important to have a rapid detection method that can identify *A. baumannii* from the clinical surfaces.

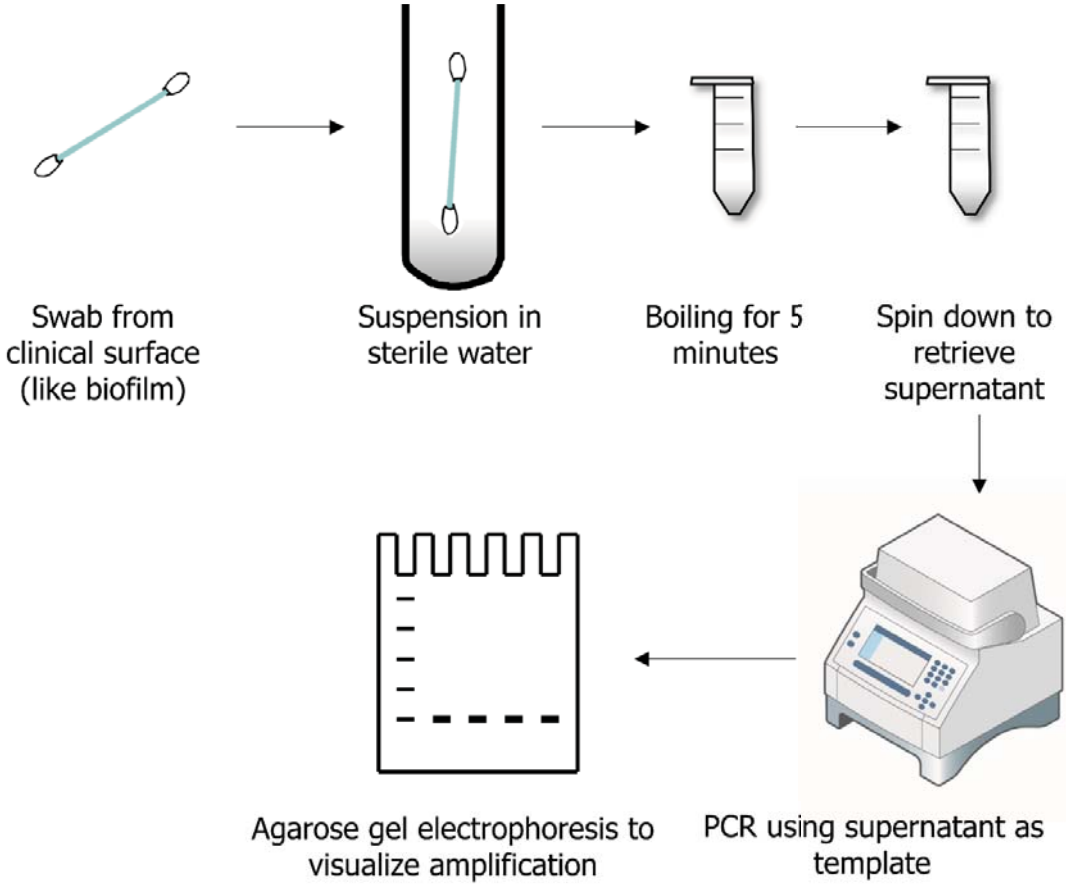

Figure 8.6 Detection of *A. baumannii* using PCR and AbsR10 specific primers.

To simulate clinical conditions in the lab, *A. baumannii* cells were allowed to form biofilms on the polystyrene and glass surfaces. The biofilm formed was retrieved by scrapping and the resulting biomass was resuspended in nuclease free water (Figure 8.6). The suspension was boiled and centrifuged to yield a clear supernatant. PCR reaction was carried out using this supernatant as template. The desired amplification was achieved which proves that this PCR based system could be used to detect *A. baumannii* cells in clinical samples as well, without any culture-based enrichment (Figure 8.7).

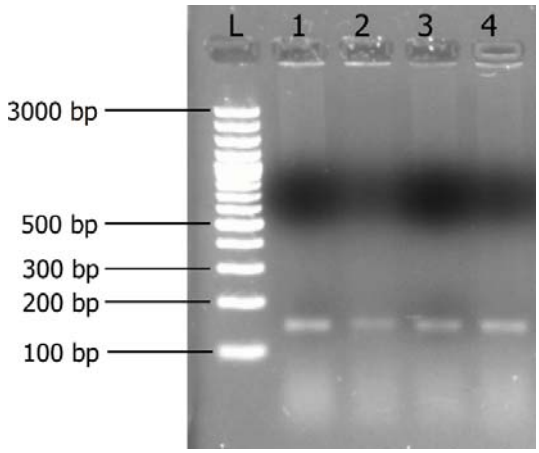

Figure 8.7 PCR amplification of AbsR10 unique region using biofilm material as template DNA. The biofilm was formed using four randomly chosen clinical strains of *A. baumannii*, RPTC 16 (1), RPTC 17 (2), RPTC 18 (3) and RPTC 19 (4). The lane (L) contains Generuler 100 bp plus ladder.

8.5 Quantitative detection of *A. baumannii* can be achieved by qPCR

To quantitatively determine *A. baumannii* cells, a standard curve of qPCR amplification with known amounts of template DNA was prepared. Overnight culture of *A. baumannii* was taken for DNA isolation. The number of cells was determined using a Neubauer chamber and the genomic DNA was isolated. The genomic DNA obtained was quantified spectrophotometrically by using Nanodrop. The number of cells and quantity of DNA obtained in three independent experiments was averaged to derive a relation between the two parameters:

$$1 \text{ ng of DNA} = 3.8 * 10^5 \text{ cells}$$

However, according to the theoretical calculations to determine the DNA yield,

$$1 \text{ ng of DNA} = 3.1 * 10^5 \text{ cells}$$

It is clear that the amount of DNA isolated from the given number of cells is much lower than the theoretical limit, which reflects on the experimental constraints imposed by the DNA isolation method.

For standard curve, fixed concentrations of genomic DNA were used and the C_T values for each were recorded. A curve was plotted between the C_T values and the amount of DNA which yielded a straight line indicating a linear relationship between the amount of DNA and the C_T value (Figure 8.8).

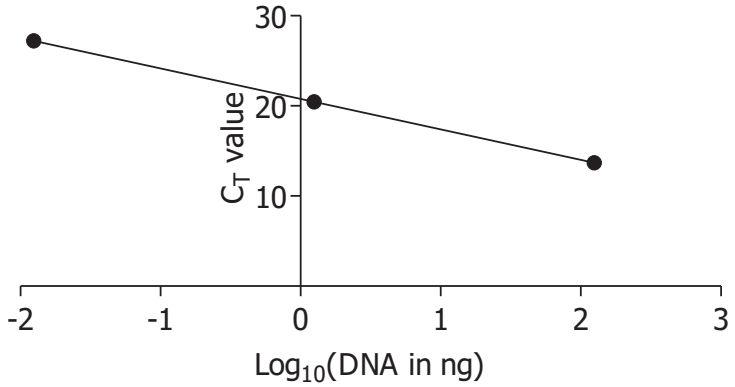

Figure 8.8 Linear relation between the amount of DNA and the corresponding CT values

From Figure 8.8, the linear equation is:

$$y = -3.3825x + 20.771$$

Where y is the C_T value and x is the amount of DNA [$\log_{10}$ (amount of DNA in ng)]. Rearranging this equation:

$$x = \frac{20.771 - y}{3.3825}$$

Or,

$$\log10(\text{DNA amount in ng}) = \frac{(20.771 - \text{CT Value})}{3.3825}$$

Or,

$$\text{DNA (ng)} = \text{antilog10}\left[\frac{(20.771 - \text{CT value})}{3.3825}\right]$$

Since the number of cells was determined prior to the isolation of DNA, the amount of DNA can be replaced with the number of cells.

$$1 \text{ ng of DNA} = 3.8 * 10^5 \text{ cells}$$

Which implies that,

$$124.6 \text{ ng of DNA} = 4.73 * 10^7 \text{ cells}$$

$$1.246 \text{ ng of DNA} = 4.73 * 10^5 \text{ cells}$$

$$12.46 \text{ pg of DNA} = 4.73 * 10^3 \text{ cells}$$

Using the relation between amount of DNA and the number of cells, plot can be drawn between C_T values and number of cells (Figure 8.9).

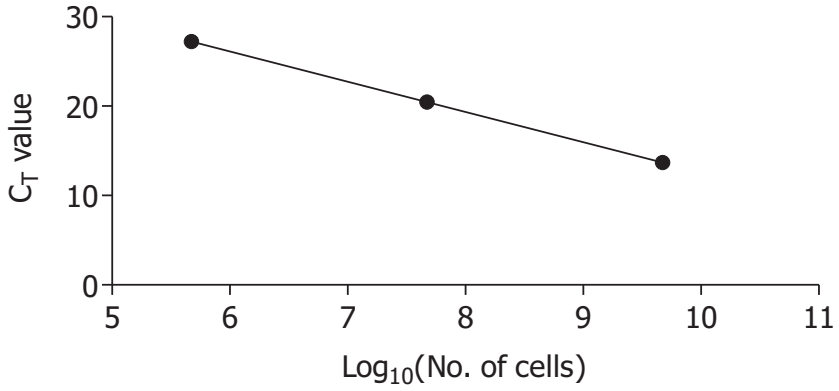

Figure 8.9 Linear relation between the number of cells and corresponding CT values

From Figure 8.9, the linear equation is:

$$y = -3.3825x + 46.408$$

Where y is the C_T value and x is the number of cells [$\log_{10}$ (number of cells)]. Rearranging this equation:

$$x = \frac{46.408 - y}{3.3825}$$

Or,

$$\log10(\text{No. of cells}) = \frac{(46.408 - \text{CT Value})}{3.3825}$$

Or,

$$\text{No. of cells} = \text{antilog10}\left[\frac{(46.408 - \text{CT value})}{3.3825}\right]$$

Thus, an equation was derived to determine the number of cells from the C_T value. Using this equation one can calculate the number of cells from the C_T values determined by the qPCR, resulting in quantitative detection of *A. baumannii*.

8.6 Discussion

Acinetobacter baumannii is a major problem in clinical settings and has become one of the leading causes of hospital acquired infections throughout the world [351]. The problem is

aggravated by the ability of *A. baumannii* to form biofilms and survive for long periods on dry and desiccated surfaces. The detection of *A. baumannii* on clinical surfaces by the conventional culture-based methods is highly time consuming and not that efficient. According to a study on detection of *A. baumannii* from hospital surfaces, conventional methods identified *A. baumannii* on 39% of the test samples whereas the PCR based method identified *A. baumannii* on 77% of them [352]. This highlights the importance of PCR based methods for achieving higher sensitivity and rapidness. We developed an assay on similar lines using a non-coding region of *A. baumannii* which is specific to the bacterium. The previously reported methods use the bacterial virulence factor OmpA for the purpose of detection [352]. However, sequence alterations in virulence factors to augment pathogenicity and redundancy in the genetic code could easily abrogate the utility of a detection system based on their nucleotide sequence. In contrast, sRNA activity is highly dependent on the nucleotide sequence making it a less likely hotspot for mutations. The AbsR10 region is not only specific to *A. baumannii* but is also prevalent in clinical strains as 100% (n=24) of the strains used in this study carried a copy on the genome. It can potentially form the basis of a more robust detection system.

Although the method could be exploited to determine *A. baumannii* quantitatively, it suffers from a limitation brought about by the nature of method used for DNA isolation. We performed our experiments using purified genomic DNA that was isolated using a commercially available kit (resulting in about 82% efficiency). However, we cannot estimate the number of cells and the efficiency of genomic DNA isolation in case of real-world samples where the detection has to be carried out from clinical surfaces with minimal use of DNA isolation kits. Another limitation is the inability of the PCR to distinguish between live and the dead cells. The positive amplification could, in addition to presence of pathogen, indicate the presence of DNA alone. This might be a reason why culture based methods were not able to identify *A. baumannii* where the PCR based method could [352]. However, the clinical implications of presence of genomic DNA are not yet known. This DNA could serve as a medium for horizontal gene transfer which can potentially lead to isolation of viable, drug-resistant pathogens from the same surfaces.

In future, this DNA sequence based method could be conjugated to metal nanoparticle based systems to further simplify the detection, obviating the need of complex machinery and sophisticated enzymes [353,354]. Thus, this identification of a specific region in *A. baumannii* holds potential to be used in future detection systems.

9 Conclusions and future perspectives

The results of the work carried out in this thesis led to some important conclusions and at the same time opened up avenues for more research and experimentation.

9.1 The C-terminus of *A. baumannii* Hfq is a physiologically important part.

The major conclusion drawn from this work is the importance of the glycine rich C-terminus in Hfq of *A. baumannii*. The *A. baumannii* Hfq is extra-long owing to the residues at C-terminus. This extension seems to be a common feature of the Moraxellaceae family and could have been a result of a duplication event in the evolutionary history of this family as the sequence analysis suggests that this part is not likely to have been obtained via horizontal gene transfer. Earlier studies on Hfq proteins in Moraxellaceae family had ignored the importance of this compositionally biased region as the deletion of this specific region did not have much impact on the growth of the bacterial cells. However, this extension is a physiologically important part as the *A. baumannii* cells expressing Hfq protein lacking this C-terminal domain revealed defects in various physiological processes like stress cope-up, carbon metabolism, drug resistance and virulence. Moreover, the Hfq protein variants lacking the C-terminus were deficient in RNA binding, autoregulation of Hfq expression and sRNA mediated riboregulation. Earlier studies on Hfq protein in the Moraxellaceae family had not focused on the importance of the C-terminus in physiological context. Recent findings that correlate the length of the C-terminal extension with substrate specificity of Hfq warrant biophysical studies of truncated variants of Hfq with multiple sRNA to determine variation in substrate specificity. Future experimentation could also be carried out to reveal how this flexible C-terminal tail is actually involved in assisting sRNA or sRNA-mRNA interaction with the RNA-interacting surfaces on Hfq.

9.2 AbaF is an MFS efflux pump responsible for fosfomycin resistance in *A. baumannii.*

AbaF, a novel fosfomycin resistance efflux pump, was identified in this work. The efflux pump is one of the primary targets of AbsR25, a small RNA in *A. baumannii*. This efflux pump is responsible for intrinsic fosfomycin resistance in *A. baumannii* as its inactivation leads to increased susceptibility towards the antibiotic. Moreover, the increased expression of *abaF* on fosfomycin challenge and in fosfomycin resistant mutants, points out its direct involvement in mediating fosfomycin resistance. The resistance due to AbaF is clinically relevant as about 92% of the clinical strains used in this study expressed AbaF and their susceptibility towards

fosfomycin increased in presence of an efflux pump inhibitor, CCCP. Apart from this, AbaF also plays a role in extrusion of biofilm material and is an important factor in *A. baumannii* virulence. Future experiments can be designed to identify inhibitors of AbaF which could potentiate the activity of fosfomycin against clinical strains of *A. baumannii*. Since fosfomycin is an important drug in case of urinary tract infections, a combination therapy making use of fosfomycin and AbaF inhibitor could be a valid therapeutic option against *A. baumannii* in UTIs.

9.3 AbsR1 is a novel *A. baumannii* sRNA that is involved in regulation of response to acid stress.

A novel small RNA, AbsR1 was validated in this thesis. This small RNA was one of the 31 candidate sRNA that were predicted in a previous study carried out in the lab. The candidate sRNA sequence was used to design a probe and which was used to detect AbsR1 sRNA in Northern blotting. The AbsR1 sRNA was maximally expressed during the early stages of growth. Using the RACE mapping technique, the transcriptional start and stop sites of AbsR1 were determined, whereby it was also determined that AbsR1 is an 89 nt long sRNA. Since most of the sRNA are regulators of stress response, their expression increases when cells are subjected to environmental stress. The expression of AbsR1 was determined under various stress conditions and it was observed that the expression of AbsR1 increased when A. baumannii cells were subjected to acidic stress. A deletion mutant of AbsR1 was generated and its survival under different stress conditions was determined. Unsurprisingly, the AbsR1 deletion mutant was susceptible to acidic challenge and a prominent growth defect in pH 5 medium was observed. These observations are an inkling that AbsR1 might be playing a role in regulation of cellular response to acidic challenge. Further experiments would be required to directly implicate AbsR1 in acidic stress cope-up. These experiments could include analysis of transcriptome/proteome under acidic stress or identification of targets of AbsR1 and analysis of their role in acid stress tolerance. Over expression of AbsR1 and co-expression of AbsR1 with its target mRNA fused to reporter genes could also yield important information. It is important to characterize the targets of sRNA as they are the effectors that are regulated by sRNA and finally mediate cellular response to environmental stress.

9.4 A PCR based method based on AbsR10, a unique intergenic region in *A. baumannii* genome, could be used to rapidly detect *A. baumannii* in clinical settings.

A specific sequence in the candidate AbsR10 coding region was identified as unique to *A. baumannii*. This sequence was explored to design a PCR based detection system *for A. baumannii*. The primers designed for amplification of this region could identify the type strains of *A. baumannii* as well as all the clinical strains of *A. baumannii* in the lab. The AbsR10 based detection system is specific for *A. baumannii* as there was no amplification when genomic DNA from various other pathogenic bacteria was used as a template. Thus, the AbsR10 PCR based detection system in highly specific for *A. baumannii*. Using this system, A. baumannii can be directly detected from the clinical surfaces in a rapid and high throughput fashion as it was seen in a simulation of hospital surfaces. Therefore, the detection is not only specific but also obviates the need of culture-based enrichment, which is a conventional practice for detection of bacterial pathogens. This assay could be further improved upon to circumvent the PCR step. Conjugation of specific oligos on gold nanoparticles could lead to development of an assay where colorimetric response could be produced without the need of any special equipment. This update would make the detection system even faster without compromising on the specificity.

10 Appendices

10.1 Appendix I: Chemical reagents and compositions

10.1.1 Chemical reagents and kits used

Reagent	Supplier
10X Dulbecco's PBS	ThermoScientific, USA
2,2-Dipyridyl	Sigma Aldrich, USA
30% Acrylamide mix (29:1)	Himedia India
Accuscript cDNA synthesis kit	Agilent, USA
Acetonitrile	Sigma Aldrich, USA
Acrylamide	ThermoScientific, USA
Agar agar	Himedia, India; Merck, Germany
Agarose	Lonza, Switzerland
All antibiotics	Sigma Aldrich, USA
All restriction enzymes	ThermoScientific, USA
Ammonium chloride	Himedia India
Ammonium persulphate	SRL, India
BCA protein estimation kit	ThermoScientific, USA
Bisacrylamide	ThermoScientific, USA
Boric acid	ThermoScientific, USA
Bovine Serum Albumin	ThermoScientific, USA
Bradford's reagent	Himedia, India
Bright Star Biodetection kit	ThermoScientific, USA
BrightStar psoralen-biotin kit	ThermoScientific, USA
Bromophenol blue	Himedia India
Calcium chloride	Himedia India
Carbonyl cyanide 3-chlorophenylhydrazone	Sigma Aldrich, USA
Chloroform	AMRESCO, USA
Cholesterol	Merck, Germany
Clarity ECL Substrate	BioRad, USA
CloneJET PCR cloning kit	ThermoScientific, USA
Cyclophosphamide	BioBasic, Canada; TCI India
Diethyl pyrocarbonate	ThermoScientific, USA

DNA oligomers	Sigma Aldrich, USA
DNase I	ThermoScientific, USA
DNase I (for cell lysis solution)	ThermoScientific, USA
dNTPs	ThermoScientific, USA
DTT	ThermoScientific, USA
Dulbecco′s Modified Eagle′s Medium	Himedia, India
Dynazyme II DNA polymerase	ThermoScientific, USA
EMSA kit	ThermoScientific, USA
Ethanol	Himedia India
Ethidium bromide	Sigma Aldrich, USA
Ethylenediaminetetraacetic acid	Himedia India
Ex Taq DNA polymerase	Takara, Japan
FastAP® alkaline phosphatase	ThermoScientific, USA
Fetal bovine serum	ThermoScientific, USA
FirstChoice RLM-RACE kit	ThermoScientific, USA
FITC labelled anti-rabbit antibody	Jackson Immunoresearch, USA
GeneJET genomic DNA purification kit	ThermoScientific, USA
GeneJET PCR purification kit	ThermoScientific, USA
GeneJET Plasmid miniprep kit	ThermoScientific, USA
Glucose	Himedia India
Glycerol	Himedia India
HRP labelled anti-rabbit antibody	Jackson Immunoresearch, USA
Imidazole	Himedia India
Isopropanol	AMRESCO, USA
Isopropyl β-D-1-thiogalactopyranoside	Sigma Aldrich, USA
LB broth	Himedia India; SRL, India
Lysozyme (hen egg)	ThermoScientific, USA
Magnesium sulphate	AMRESCO, USA
Maxima SYBR Green/ROX qPCR Master Mix	ThermoScientific, USA
Methanol	Himedia, India
Methyl viologen	Sigma Aldrich, USA
MH broth	Himedia India; SRL, India; Merck, Germany
MinElute gel extraction kit	Qiagen, USA

mirVana miRNA probe construction kit	ThermoScientific, USA
NaCl	Himedia India
Ni-NTA matrix	Qiagen, USA
NorthernMax kit	ThermoScientific, USA
Nutrient broth	Merck, Germany
Ortho-Nitrophenyl-β-galactoside	Sigma Aldrich, USA
Peptone	Merck, Germany
Phenylmethylsulphonyl fluoride	Sigma Aldrich, USA
Poly-L-lysine	Sigma Aldrich, USA
Potassium chloride	Himedia, India
Potassium phosphate	Himedia, India
Pyrocatechol	Sigma Aldrich, USA
QIAquick Nucleotide removal kit	Qiagen, USA
rNTPs	ThermoScientific, USA
Roche LightCycler 480 SYBR Green I master mix	Roche, Germany
SDS	Himedia India
Sequencing grade trypsin	Sigma Aldrich, USA
SOC medium	Himedia India
Sodium phosphate dibasic	BioBasic, Canada
Sodium phosphate monobasic	BioBasic, Canada
SuperScript III reverse transcriptase	ThermoScientific, USA
T4 DNA ligase	ThermoScientific, USA
TEMED	Himedia, India
TRI reagent	ThermoScientific, USA; Himedia, India; BioBasic, Canada
Tricine	Himedia, India
Trifluoroacetic acid	Himedia, India
Tris base	AMRESCO, USA
Triton X-100	BioBasic, Canada
Tween 20	BioBasic, Canada
Urea	ThermoScientific, USA
Xylene cyanol	Himedia, India
α-cyano-4-hydroxy cinnamic acid	Bruker Daltonics, Germany

β-mercaptoethanol	BioBasic, Canada

10.1.2 Antibiotics and Antibacterials

Antibiotic	Stock concentration	Solvent
Amikacin	5 mg/ml	Water
Ampicillin	100 mg/ml	Water
Chloramphenicol	30 mg/ml	Ethanol
Chlorhexidine	5 mg/ml	Water
Ciprofloxacin	5 mg/ml	Dilute HCl
Clindamycin	5 mg/ml	DMSO
Erythromycin	5 mg/ml	Ethanol
Ethidium bromide	5 mg/ml	Water
Fosfomycin	5 mg/ml	Water
Gentamicin	15 mg/ml	Water
Kanamycin	50 mg/ml	Water
Meropenem	5 mg/ml	DMSO
Minocycline	5 mg/ml	Water
Nalidixic acid	5 mg/ml	1 M NaOH
Ofloxacin	5 mg/ml	1 M NaOH
Streptomycin	5 mg/ml	Water
Tetracycline	15 mg/ml	Ethanol
Tobramycin	5 mg/ml	Water
Trimethoprim	5 mg/ml	DMSO

10.1.3 Tris-tricine-SDS composition

Prepare the following stock solutions:

3 M Tris-Cl pH 8.45: Dissolve 36.33 g of Tris base in 70 ml of water. Bring the pH to 8.45 using concentrated HCl. Make up the volume to 100 ml using water.

10% Ammonium persulfate (APS): Dissolve 1 g of APS in 10 ml of RNase free water.

10.1.3.1 1X Cathode buffer (to be put on top of wells)

Component	Amount	Final concentration
Tris base	12.11 g	100 mM

Tricine	17.92 g	100 mM
SDS	1 g	0.1%
Autoclaved distilled water	To make 1000 ml	

10.1.3.2 5X Anode buffer (to be put in the tank)

Component	Amount	Final concentration
Tris base	121.1 g	1 M
Autoclaved distilled water	To make 1000 ml	

The pH of the buffer was adjusted to 8.9. The buffer was diluted five times before use.

10.1.3.3 2X Gel loading buffer:

Component	Amount	Final concentration
1 M Tris-Cl pH 6.8	1 ml	100 mM
Glycerol	2 ml	20%
Bromophenol blue	20 mg	2 mg/ml
DTT	0.31 g	200 mM
SDS	0.4 g	4%
Autoclaved distilled water	To make 10 ml	

10.1.3.4 Separating gel

Component	Amount (for 10% gel)	Amount (for 12% gel)
3 M Tris-Cl pH 8.45	3.3 ml	3.3 ml
30% Acrylamide mix (29:1)	3.3 ml	3.9 ml
Autoclaved distilled water	3.3 ml	2.7 ml
10% APS	100 µl	100 µl
TEMED	4 µl	4 µl

10.1.3.5 3% Stacking gel

Component	Amount
3 M Tris-Cl pH 8.45	1.2 ml
30% Acrylamide mix (29:1)	1.3 ml
Autoclaved distilled water	2.1 ml
10% APS	40 µl
TEMED	4 µl

10.1.4 Buffers for protein purification

Prepare the following stock solutions:

1 M Tris-Cl pH 8.0: Dissolve 121.1 g of Tris base in 700 ml of water. Bring the pH to 8.0 using concentrated HCl. Make up the volume to 1000 ml using water.

3 M Imidazole pH 8.0: Dissolve 20.42 g of imidazole in 40 ml of water. Adjust the pH of the solution to 8.0 using concentrated HCl and make up the volume to 100 ml using water.

3 M NaCl: Dissolve 175.32 g NaCl in 800 ml of water. Make up the volume to 1000 ml using water.

100 PMSF: Dissolve 17.42 g PMSF in isopropanol/ethanol.

10 mg/ml DNase I: Dissolve 10 mg of DNase I in 1 ml of water.

1 M NH_4Cl: Dissolve 53.491 g ammonium chloride in 700 ml water. Make up the volume to 1000 ml in water.

10.1.4.1 Lysis buffer

Component	Amount	Final concentration
1 M Tris-Cl pH 8.0	1 ml	20 mM
3 M Imidazole pH 8.0	334 µl	20 mM
3 M NaCl	8.3 ml	500 mM
50% Glycerol	5 ml	5%
DNase I	50 µl	10 µg/ml
100 mM PMSF	500 µl	1 mM
Autoclaved distilled water	To make 50 ml	

10.1.4.2 Equilibration buffer

Component	Amount	Final concentration
1 M Tris-Cl pH 8.0	1 ml	20 mM
3 M Imidazole pH 8.0	334 µl	20 mM
3 M NaCl	8.3 ml	500 mM
50% Glycerol	5 ml	5%
Autoclaved distilled water	To make 50 ml	

10.1.4.3 Wash buffer I

Component	Amount	Final concentration
1 M Tris-Cl pH 8.0	1 ml	20 mM

3 M Imidazole pH 8.0	835 µl	50 mM
3 M NaCl	8.3 ml	500 mM
50% Glycerol	5 ml	5%
Autoclaved distilled water	To make 50 ml	

10.1.4.4 Wash buffer II

Component	Amount	Final concentration
1 M Tris-Cl pH 8.0	1 ml	20 mM
3 M Imidazole pH 8.0	1.6 ml	100 mM
3 M NaCl	8.3 ml	500 mM
50% Glycerol	5 ml	5%
Autoclaved distilled water	To make 50 ml	

10.1.4.5 Elution buffer

Component	Amount	Final concentration
1 M Tris-Cl pH 8.0	1 ml	20 mM
3 M Imidazole pH 8.0	8.3 ml	500 mM
3 M NaCl	8.3 ml	500 mM
50% Glycerol	5 ml	5%
Autoclaved distilled water	To make 50 ml	

10.1.4.6 Dialysis buffer

Component	Amount	Final concentration
1 M Tris-Cl pH 8.0	20 ml	20 mM
1 M Ammonium chloride	200 ml	200 mM
3 M NaCl	166.7 ml	500 mM
50% Glycerol	100 ml	5%
Autoclaved distilled water	To make 1000 ml	

10.1.5 10X TBE buffer

Component	Amount	Concentration
Tris base	121.1 g	1 M
Boric acid	61.8 g	1 M
EDTA (disodium salt)	7.4 g	0.02 M
RNase free water	To make 1000 ml	

The pH of TBE doesn't need to be adjusted. However, if precipitates appear in the final solution, adjust the pH to 8.0.

10.1.6 50X TAE buffer

Component	Amount	Concentration
Tris base	242 g	40 mM
Acetic acid	57.1 ml	-
0.5 M EDTA pH 8.0	100 ml	1 mM
DNase free water	To make 1000 ml	

10.1.7 Urea PAGE mix

Prepare the following stock reagents:

40% Acrylamide mix: Dissolve 47.5g of acrylamide and 2.5 g of Bisacrylamide in 125 ml of RNase free water. Store in an amber colored bottle.

Urea PAGE mix was prepared as follows:

Component	Amount	Concentration
Urea	210 g	8 M
10X TBE	50 ml	1X
40% Acrylamide/ Bisacrylamide mix (29:1)	125 ml	10%
RNase free water	To make 500 ml	

10% Urea PAGE was prepared as follows:

Component	Amount
Urea PAGE mix	50 ml
10% APS	500 µl
TEMED	10 µl

10.1.8 Electrotransfer buffer

Component	Amount	Concentration
Tris base	3.0 g	25 mM
Glycine	11.22 g	192 mM
Methanol	200 ml	20%

RNase free water	To make 1000 ml

10.1.9 TE buffer

Component	Amount	Concentration
Tris base	121.1 mg	10 mM
EDTA	37.22 mg	1 mM
Water	To make 100 ml	

10.1.1010X PBS

Component	Amount	Concentration
$Na_2HPO_4.7H_2O$	25.6 g	95.5 mM
NaCl	80 g	1.3 M
KCl	2 g	26.8 mM
KH_2PO_4	2 g	14.7 mM
Water	To make 1000 ml	

Mix all components and autoclave. Dilute in sterile water before using.

10.1.11NorthernMax kit components

ULTRAhyb buffer: 50% deionized formamide, 5% Denhardt solution, 1% SDS, 5X SSC (standard sodium citrate), 5% dextran sulphate, 250 µg/ml herring sperm DNA.

Low stringency wash buffer composition: 2X SSC, 0.1% SDS.

High Stringency Wash buffer composition: 0.1X SSC, 0.1% SDS.

10.1.12 Reagents for EMSA

Most of the reagents were provided with the kit.

10,000X SYBR® Green EMSA nucleic acid gel

6X EMSA gel-loading solution

5X binding buffer

8% Native gel was prepared as follows:

Component	Amount	Concentration
40% Acrylamide mix (29:1)	4 ml	8%
10X TBE	1 ml	0.5X

10% APS	200 µl	1%
TEMED	5 µl	-
RNase free water	To make up 20 ml	

10.1.13 Z buffer for β-galactosidase assay

Component	Amount	Concentration
Na_2HPO_4	427.3 mg	60.2 mM
$NaH_2PO_4.H_2O$	316 mg	45.8 mM
KCl	37.3 mg	10 mM
$MgSO_4.7H_2O$	12.3 mg	1 mM
Water	To make up 50 ml	
β-mercaptoethanol	140 µl just prior to use	

10.1.14 Substrates and stress creating agents in BIOLOG GenIII plates

Carbon source	Carbon source	Carbon source	Stress agent
Dextrin	L-rhamnose	D-glucuronic acid	pH6
D-maltose	Inosine	Glucuronamide	pH5
D-trehalose	D-sorbitol	Mucic acid	1% NaCl
D-cellobiose	D-mannitol	Quinic acid	4% NaCl
Gentiobiose	D-arabitol	D-saccharic acid	8% NaCl
Sucrose	Myo-inositol	p-hydroxy-phenylacetic acid	1% Sodium lactate
D-turancose	Glycerol	Methyl pyruvate	Fusidic acid
Stacyose	D-glucose-6-phosphate	D-lactic acid methyl ester	D-serine
D-raffinose	D-fructose-6-phosphate	L-lactic acid	Troleandomycin
α-D-lactose	D-aspartic acid	Citric acid	Rifamycin
D-mellobiose	D-serine	α-keto-glutaric acid	Minocycline
β-methyl-D-Glucoside	Gelatin	D-malic acid	Lincomycin
D-salicin	Glycyl-L-proline	L-malic acid	Guanidine HCl
N-acetyl-D-glucosamine	L-alanine	Bromo-succinic acid	Niaproof 4

N-acetyl-β-D-Mannosamine	L-arginine	Tween 40	Vancomycin
N-acetyl-D-Galactosamine	L-aspartic acid	γ-amino butyric acid	Tetrazolium Violet
N-acetyl neuraminic acid	L-glutamic acid	α-hydroxy-butyric acid	Tetrazolium blue
α-D-glucose	L-histidine	β-hydroxy-D,L-butyric acid	Nalidixic acid
D-mannose	L-pyroglutamic acid	α-keto-butyric acid	Lithium chloride
D-fructose	L-serine	Acetoacetic acid	Potassium tellurite
D-galactose	Pectin	Propionic acid	Aztreonam
3-Methyl glucose	D-galacturonic acid	Acetic acid	Sodium butyrate
D-fucose	L-galactonic acid lactone	Formic acid	Sodium bromate
L-fucose	D-gluconic acid		

10.1.15 Nematode Growth Medium (NGM)

Prepare the following stock solutions:

1 M $CaCl_2.2H_2O$: Dissolve 14.7 g of $CaCl_2.2H_2O$ in 70 ml of water. Make up the volume to 100 ml with water. Autoclave it to sterilize.

1 M KH_2PO_4: Dissolve 13.6 g of KH_2PO_4 in 70 ml of water. Make up the volume to 100 ml with water. Autoclave it to sterilize.

1 M $MgSO_4.7H_2O$: Dissolve 24.6 g of $MgSO_4.7H_2O$ in 70 ml of water. Make up the volume to 100 ml with water. Autoclave it to sterilize.

5 mg/ml Cholesterol: Dissolve 50 mg of cholesterol in ethanol. Do not autoclave.

Component	Amount	Concentration
Agar	17.0 g	1.7% (w/v)
NaCl	2.9 g	50 mM
Peptone	2.5 g	0.25% (w/v)
Water	To make up 1000 ml	
1 M $CaCl_2$	1 ml	1 mM
1 M KH_2PO_4	25 ml	25 mM
1 M $MgSO_4.7H_2O$	1 ml	1 mM

5 mg/ml Cholesterol	1 ml	5 μg/ml

Mix the first four components and autoclave. Let the mixture cool down before adding the last four reagents.

10.1.16 Reagents for Western blotting

10.1.16.1 Tris-buffered saline (TBS)

Component	Amount	Concentration
Tris base	2.4 g	20 mM
NaCl	8.0 g	137 mM
Water	To make up 1000 ml	

Adjust the pH to 7.6 using concentrated HCl.

10.1.16.2 Tris-buffered saline with Tween (TBST)

Component	Amount	Concentration
Tris base	2.4 g	20 mM
NaCl	8.0 g	137 mM
Tween 20	1.0 ml	0.1% (v/v)
Water	To make up 1000 ml	

Adjust the pH to 7.6 before adding Tween 20.

10.1.16.3 Blocking buffer

Component	Amount	Concentration
Non-fat dried milk	5.0 g	5% (w/v)
TBST	To make up 100 ml	

10.1.16.4 Tris-glycine transfer buffer

Component	Amount	Concentration
Tris base	6.0 g	25 mM
Glycine	28.8 g	192 mM
Tween 20	400 ml	20% (v/v)
Water	To make up 2000 ml	

10.2 Appendix II: Standard procedures

10.2.1 Genomic DNA isolation

Bacterial genomic DNA was isolated using GeneJET Genomic DNA Purification kit (ThermoScientific, USA).

1. Inoculate a single bacterial colony in 5 ml LB broth supplemented with appropriate antibiotics. Incubate overnight at 37°C with agitation.
2. Harvest up to 10^9 bacterial cells in a 1.5- or 2-ml microcentrifuge tube by centrifugation for 10 min at 5000 g. Discard the supernatant.
3. Resuspend the pellet in 180 µl of Digestion Solution. Add 20 µl of Proteinase K Solution and mix thoroughly by vortexing or pipetting to obtain a uniform suspension.
4. Incubate the sample at 56 °C while vortexing occasionally or use a shaking water bath, rocking platform or thermomixer until the cells are completely lysed (~30 min).
5. Add 20 µl of RNase A Solution, mix by vortexing and incubate the mixture for 10 min at room temperature.
6. Add 200 µl of Lysis Solution to the sample. Mix thoroughly by vortexing for about 15 s until a homogeneous mixture is obtained.
7. Add 400 µl of 50% ethanol and mix by pipetting or vortexing.
8. Transfer the prepared lysate to a GeneJET Genomic DNA Purification Column inserted in a collection tube. Centrifuge the column for 1 min at 6000 g. Discard the collection tube containing the flow-through solution. Place the GeneJET Genomic DNA Purification Column into a new 2 ml collection tube.
9. Add 500 µl of Wash Buffer I (with ethanol added). Centrifuge for 1 min at 8000 g.
10. Discard the flow-through and place the purification column back into the collection tube.
11. Add 500 µl of Wash Buffer II (with ethanol added) to the GeneJET Genomic DNA Purification Column. Centrifuge for 3 min at maximum speed (≥12000 g).
12. Discard the collection tube containing the flow-through solution and transfer the GeneJET Genomic DNA Purification Column to a sterile 1.5 ml microcentrifuge tube.
13. Add 200 µl of Elution Buffer to the center of the GeneJET Genomic DNA Purification Column membrane to elute genomic DNA. Incubate for 2 min at room temperature and centrifuge for 1 min at 8000 g.

10.2.2 Purification of riboprobes

The riboprobes and in vitro transcribed small RNA were purified using QIAquick Nucleotide Removal kit (Qiagen, USA).

1. Add 10 volumes of Buffer PNI to 1 volume of sample and mix. Place a QIAquick spin column in a provided 2 ml collection tube.
2. Apply the sample to the QIAquick spin column and centrifuge for 1 min at 6000 rpm.
3. Discard the flow-through and place the QIAquick spin column back into the same collection tube.
4. Add 750 µl Buffer PE and centrifuge for 1 min at 3800 x g (6000 rpm).
5. Discard the flow-through and place the QIAquick spin column back in the same collection tube. Centrifuge for an additional 1 min at 17,900 x g (13,000 rpm).
6. Place the QIAquick spin column in a clean 1.5 ml microcentrifuge tube.
7. To elute RNA, add 30–50 µl RNase free water to the center of the QIAquick membrane, let the column stand for 1 min, and then centrifuge.

10.2.3 Purification of DNA from agarose gels.

For purification of DNA from agarose gels QIAMinelute kit was used as it allows to elute DNA in small quantities resulting in higher concentrations.

1. Add 5 volumes of Buffer PB to 1 volume of the PCR reaction and mix. Check that the color of the mixture is yellow (similar to Buffer PB without the PCR sample). If the color of the mixture is orange or violet, add 10 µl 3 M sodium acetate, pH 5.0, and mix. The color of the mixture will turn to yellow.
2. Place a MinElute column in a provided 2 ml collection tube. Apply the sample to the MinElute column and z centrifuge for 1 min.
3. Discard flow-through and place the MinElute column back into the same collection tube.
4. Add 750 µl Buffer PE to the MinElute column and z centrifuge for 1 min.
5. Discard flow-through and place the MinElute column back in the same collection tube.
6. Centrifuge the column in a 2 ml collection tube (provided) for 1 min. Residual ethanol from Buffer PE will not be completely removed unless the flow-through is discarded before this additional centrifugation.
7. Place each MinElute column in a clean 1.5 ml microcentrifuge tube.
8. To elute DNA, add 10 µl nuclease free water to the center of the MinElute membrane. (Ensure that the elution buffer is dispensed directly onto the center of the membrane for

complete elution of bound DNA.) Let the column stand for 1 min, and then centrifuge the column for 1 min.

10.2.4 Plasmid DNA isolation

Plasmid DNA was isolated using GeneJET miniprep kit (ThermoScientific, USA).

1. Resuspend the pelleted cells in 250 µl of the Resuspension Solution. Transfer the cell suspension to a microcentrifuge tube. The bacteria should be resuspended completely by vortexing or pipetting up and down until no cell clumps remain.
2. Add 250 µl of the Lysis Solution and mix thoroughly by inverting the tube 4-6 times until the solution becomes viscous and slightly clear. Do not vortex to avoid shearing of chromosomal DNA. Do not incubate for more than 5 min to avoid denaturation of supercoiled plasmid DNA.
3. Add 350 µl of the Neutralization Solution and mix immediately and thoroughly by inverting the tube 4-6 times. It is important to mix thoroughly and gently after the addition of the Neutralization Solution to avoid localized precipitation of bacterial cell debris. The neutralized bacterial lysate should become cloudy.
4. Centrifuge for 5 min to pellet cell debris and chromosomal DNA.
5. Transfer the supernatant to the supplied GeneJET spin column by pipetting. Avoid disturbing or transferring the white precipitate. Centrifuge for 1 min. Discard the flow-through and place the column back into the same collection tube.
6. Add 500 µl of the Wash Solution to the GeneJET spin column. Centrifuge for 30-60 seconds and discard the flow-through. Place the column back into the same collection tube.
7. Discard the flow-through and centrifuge for an additional 1 min to remove residual Wash Solution. This step is essential to avoid residual ethanol in plasmid preps.
8. Transfer the GeneJET spin column into a fresh 1.5 ml microcentrifuge tube (not included). Add 50 µl of the nuclease free water to the center of GeneJET spin column membrane to elute the plasmid DNA. Take care not to contact the membrane with the pipette tip. Incubate for 2 min at room temperature and centrifuge for 2 min.

10.2.5 RLM RACE procedure

10.2.5.1 5' RACE

10.2.5.1.1 TAP treatment

Assemble the following reaction in an RNase free tube.

Component	Amount
Total RNA	5 µl
10X TAP buffer	1 µl
Tobacco acid pyrophosphatase	2 µl
Nuclease free water	2 µl

Mix the components and incubate at 37°C for one hour.

10.2.5.1.2 Adapter ligation

Assemble the following reaction in an RNase free tube.

Component	Amount
TAP treated Total RNA	2 µl
5' RACE adapter	1 µl
10X RNA ligase buffer	1 µl
T4 RNA ligase (2.5 U/µl)	2 µl
Nuclease free water	4 µl

Mix the components and incubate at 37°C for one hour.

10.2.5.1.3 Reverse transcription

Assemble the following reaction in an RNase free tube.

Component	Amount
Ligated RNA	2 µl
dNTP mix	4 µl
Random decamers	2 µl
10X RT buffer	2 µl
RNase inhibitor	1 µl
M-MLV reverse transcriptase	1 µl

Nuclease free water	8 µl

Mix the components and incubate at 42°C for one hour.

10.2.5.1.4 PCR for RACE

Using a gene specific primer (to be used as a reverse primer) a PCR is carried out. Assemble the following reaction in a PCR tube.

Component	**Amount**
RT reaction from previous step	1 µl
10X Ex Taq buffer	5 µl
dNTP mix	4 µl
5' RACE gene specific primer (10 µM)	2 µl
5' RACE primer	2 µl
Ex Taq polymerase	1 U
Nuclease free water	To make up 50 µl

Sequence the PCR product obtained to determine the 5' sequence of the transcription start site.

10.2.5.2 3' RACE

10.2.5.2.1 Poly-A-polymerase treatment

Assemble the following reaction in an RNase free tube.

Component	**Amount**
Total RNA	1 µg
10 X Poly-A-polymerase buffer	2 µl
10 mM ATP	2 µl
Poly-A-polymerase	1 µl
RNase free water	To make up 20 µl

Mix the components and incubate at 37°C for 30 minutes. Clean up the RNA using the QIAquick Nucleotide Removal kit (Qiagen, USA).

10.2.5.2.2 Reverse transcription

Component	**Amount**
Poly-A tailed RNA	2 µl

dNTP mix	4 µl
3’ RACE adapter	2 µl
10X RT buffer	2 µl
RNase inhibitor	1 µl
M-MLV reverse transcriptase	1 µl
Nuclease free water	8 µl

Mix the components and incubate at 42°C for one hour.

10.2.5.2.3 PCR for RACE

Using a gene specific primer (to be used as a forward primer) a PCR is carried out. Assemble the following reaction in a PCR tube.

Component	**Amount**
RT reaction from previous step	1 µl
10X Ex Taq buffer	5 µl
dNTP mix	4 µl
3’ RACE gene specific primer (10 µM)	2 µl
3’ RACE primer	2 µl
Ex Taq polymerase	1 U
Nuclease free water	To make up 50 µl

Sequence the PCR product obtained to determine the 5’ sequence of the transcription start site.

10.2.6 Protein estimation using Bradford’s reagent

For protein estimation Bradford’s reagent was used. The protocol for protein estimation was optimized for low amount of sample volumes in microtiter plates. To a well of the plate, 200 µl of Bradford’s reagent was added. 2.5 µl of sample (either crude or dilution of sample in appropriate buffer) was added to the wells containing Bradford’s reagent and was mixed thoroughly. The plate was incubated at room temperature for 10 minutes and the well were read at 595 nm in a 96-well plate reader. Using dilutions of BSA, a standard curve was drawn and the concentrations of unknown protein samples were determined using this standard curve.

10.3 Appendix III: List of strains used

Strain	Relevant characteristics	Source/ Reference
Acinetobacter baumannii ATCC 17978 (RPT 71)	Wild type strain	Purchased from ATCC
E. coli BL21 DE3 (RPT 2)	*hsdS gal* (*cIts*857 *ind*1 *Sam*7 *nin*5 *lacUV5*-T7 gene *1*)	Invitrogen, USA
E. coli DH5α	*supE44 hsdR17 recA1 endA1 gyrA96 thi-1 relA1*	Invitrogen, USA
E. coli KAM32 (RPT 100)	Efflux deficient strain of *E. coli*, Δ*ydhE;* Δ*acrB*	Dr. Ashima Bhardwaj, IIAR, Gandhinagar, India
E. coli S17-1 λpir (RPT 99)	*TpR SmR recA, thi, pro, hsdR-M+RP4: 2-Tc:Mu: Km Tn7 λpir*	Dr. Soumya Roy Choudhary, IMTECH, Chandigarh, India
E. coli Δhfq	Deletion mutant of *hfq* in *E. coli* BW25113	Keio collection
RPT 96	*E. coli* DH5α carrying pRPT1	This study
RPT 98	*A. baumannii* ATCC 17978 carrying pWHN678	This study
RPT 102	*Acinetobacter baumannii Δhfq (with* KanFRT cassette)	This study
RPT 103	*A. baumannii ΔabaF*	This study
RPT 106	*E. coli* DH5α pRPT14	This study
RPT 115	*E. coli* DH5α carrying pRPT4	This study
RPT 144	*E. coli* KAM32 carrying pUC18	This study
RPT 145	*E. coli* KAM32 carrying pRPT7	This study
RPT 147	*E. coli* DH5α carrying pRPT10	This study
RPT 152	*A. baumannii pabaF*	This study
RPT 154	*A. baumannii* ATCC 17978 carrying pAT02 plasmid	This study
RPT 155	*E. coli* DH5α carrying pMo130	This study
RPT 175	*E. coli* DH5α carrying pAT02	This study
RPT 176	*E. coli* DH5α carrying pAT03	This study

RPT 180	*E. coli* DH5α carrying pRPT3	This study
RPT 181	*E. coli* DH5α carrying pRPT5	This study
RPT 186	*E. coli* DH5α carrying pRPT25	This study
RPT 187	*E. coli* DH5α carrying pRPT24	This study
RPT 197	*E. coli* DH5α carrying pRPT15	This study
RPT 204	*E. coli* DH5α carrying pRPT16	This study
RPT 205	*E. coli* DH5α carrying pRPT17	This study
RPT 206	*E. coli* DH5α carrying pRPT18	This study
RPT 207	*E. coli* DH5α carrying pRPT14	This study
RPT 208	*E. coli* DH5α carrying pRPT19	This study
RPT 214	*E. coli Δhfq* carrying pR131hfq	This study
RPT 230	*E. coli* DH5α carrying pRPT11	This study
RPT 233	*Acinetobacter baumannii Δhfq*	This study
RPT 234	RPT 233 carrying pRPT15	This study
RPT 235	RPT 233 carrying pRPT16	This study
RPT 236	RPT 233 carrying pRPT17	This study
RPT 237	RPT 233 carrying pRPT14	This study
RPT 238	RPT 233 carrying pRPT18	This study
RPT 239	RPT 233 carrying pRPT19	This study
RPT 240	RPT 233 carrying pWHN678	This study
RPT 244	*E. coli Δhfq* carrying pR131Hfq and pWHN678	This study
RPT 245	*E. coli Δhfq* carrying pR131Hfq and pRPT15	This study
RPT 246	*E. coli Δhfq* carrying pR131Hfq and pRPT16	This study
RPT 247	*E. coli Δhfq* carrying pR131Hfq and pRPT17	This study
RPT 248	*E. coli Δhfq* carrying pR131Hfq and pRPT18	This study
RPT 249	*E. coli Δhfq* carrying pR131Hfq and pRPT14	This study
RPT 250	*E. coli Δhfq* carrying pR131Hfq and pRPT19	This study

RPT 258	*E. coli Δhfq* carrying pWHN678	This study
RPT 259	*E. coli Δhfq* carrying pRPT15	This study
RPT 260	*E. coli Δhfq* carrying pRPT16	This study
RPT 261	*E. coli Δhfq* carrying pRPT17	This study
RPT 262	*E. coli Δhfq* carrying pRPT18	This study
RPT 263	*E. coli Δhfq* carrying pRPT14	This study
RPT 266	*E. coli* DH5α carrying pCP20	This study
RPT 269	*E. coli Δhfq* with the KanFRT cassette removed	This study
RPT 270	RPT 269 carrying pRPT22	This study
RPT 271	RPT 258 carrying pRPT22	This study
RPT 272	RPT 259 carrying pRPT22	This study
RPT 273	RPT 260 carrying pRPT22	This study
RPT 274	RPT 261 carrying pRPT22	This study
RPT 275	RPT 263 carrying pRPT22	This study
RPT 276	RPT 262 carrying pRPT22	This study
RPT 277	RPT 291 carrying pRPT22	This study
RPT 278	*E. coli* BW25113 carrying pRPT1 and pRPT22	This study
RPT 296	*E. coli* DH5α carrying pRPT7	This study
RPT 299	*A. baumannii ΔabsR1*; Gen^r	This study
RPT 300	*A. baumannii ΔabsR1*; Gen^r	This study
RPT291	*E. coli Δhfq* carrying pRPT19	This study

10.4 Appendix IV: List of plasmids used

Plasmid	Characteristic	Source
pRPT1	pWHN678	[123]
pRPT2	Full length *A. baumannii* Hfq cloned in pET-28; Kan^r	This study
pRPT3	Hfq66 cloned in pET-28; Kan^r	This study
pRPT4	Hfq72 cloned in pET-28; Kan^r	This study
pRPT5	Hfq92 cloned in pET-28; Kan^r	This study
pRPT6	pMo130; Kan^r	Addgene, Inc.
pRPT7	*abaF* cloned with native regulatory elements in pUC18; Amp^r	This study
pRPT8	Internal fragment of *abaF* cloned in pTZ57R/T; Amp^r	This study
pRPT9	Internal fragment of *abaF* cloned in pMo130; Kan^r	This study
pRPT10	*abaF* cloned with native regulatory elements in pWHN678; Chl^r	This study
pRPT11	*aac1* cloned with 500 bases upstream and downstream of AbsR1 in pMo130	
pRPT14	hfq_{168} cloned in pWHN678; Chl^r	This study
pRPT15	hfq_{66} cloned in pWHN678; Chl^r	This study
pRPT16	hfq_{72} cloned in pWHN678; Chl^r	This study
pRPT17	hfq_{92} cloned in pWHN678; Chl^r	This study
pRPT18	hfq_{Ct} cloned in pWHN678; Chl^r	This study
pRPT19	hfq_{EC} cloned in pWHN678; Chl^r	This study
pRPT20	pNYL, a modified form of pZE-21-MCS containing no RBS upstream the MCS; Kan^r	Dr. Naveen Kumar Navani, IIT Roorkee
pRPT21	*gfp* (lacking the RBS) cloned in pRPT20; Kan^r	This study
pRPT22	*sodB-gfp* translational fusion cloned in pRPT20; Kan^r	This study
pRPT23	500 bp Upstream region of *hfq* cloned in puc18; Amp^r	This study
pRPT24	500 bp Upstream and downstream region of *hfq* cloned in puc18; Amp^r	This study
pRPT25	500 bp Upstream and downstream region of *hfq* cloned with KanFRT cassette in puc18; Kan^r, Amp^r	This study
pAT02	Plasmid expressing *A. baumannii* RecT homolog; Amp^r	

pAT03	Plasmid expressing FLP recombinase for expression in *A. baumannii*; Amp^r	Dr. Bryan Davies, University of Texas, San Antonio, USA
pCP20	Plasmid expressing FLP recombinase for expression in *E. coli*; Amp^r	Prof. Raghavan Varadarajan, IISc Bangalore, India
pR131hfq	Plasmid with 131 nts of *hfq* ORF fused in frame with *lacZ* under *lac* promoter; Amp^r	Prof. Udo Bläsi, University of Vienna, Austria
pKD4	Plasmid carrying KanFRT cassette; Kan^r	

10.5 Appendix V: List of oligonucleotides used

Name of the Oligo	Sequence	Characteristic
OligoRPT1	AGAATTTTAAAGTCCTGATGAGGATTAAGCATAAAACAGAAAAGTTATTTCTGCTTTTGCTTCGGTAGAGTA	AbsR1 probe DNA template
OligoRPT2	GCTTTACTCTACCGAAGCAAAAGCAG	internal 5' RACE primer
OligoRPT3	GTCCTGATGAGGATTAAGC	internal 3' RACE primer
OligoRPT4	ATTAGAATTCACTGTACGTGTAGCTGTATTTGC	For amplification of region 500 bp upstream of AbsR1
OligoRPT5	GGGCGGATCCACTTAACCAAGTTAAAAC	
OligoRPT6	GTTAGGATCCGGACTTTGAATTGATAAATG	For amplification of region 500 bp downstream of AbsR1
OligoRPT7	ATTATCTAGATACCTTGAAATGCACA	
OligoRPT8	CTTTGATGCTGCTGCAATCCG	For amplification of AbsR1 region
OligoRPT9	GGAGGAACAAATCACACCACCG	with 125 bp overhangs
OligoRPT10	ATTAGGATCCGTTGGTACTGTAACTCCTGACG	For amplification of AbsR1 coding region with native promoter and
OligoRPT11	ATTAGGATCCGAAGCAACTTCACTTACTTCTGC	terminator
OligoRPT14	ATCGACATGTCTAAAGGTCAAACTTTACAAG	For cloning abaF with its native promoter in pUC18
OligoRPT15	ATCGCTCGAGACGATTGTTTTCGTCGTCTTG	
OligoRPT16	ATCGGGATCCAGCAAAATTTGCACACTGTC	For amplification of an internal region of *abaF*
OligoRPT17	ATCGGGATCCTTGCAAAGAACCTATTAATCTAAAT	

OligoRPT18	ATCGGGATCCCTAAAGGTCAAACTTTACAAG	For cloning abaF, with its native regulatory elements, in pWHN678
OligoRPT19	ATCGGGATCCACGATTGTTTTCGTCGTCTTG	
OligoRPT20	CCTTTTAAATCATGTGTAGG	For amplification of an internal region of Absr25
OligoRPT21	GAAGCAGGCTTTTTAATCAT	
OligoRPT22	ATCGACATGTCTAAAGGTCAAACTTTACAAG	Forward primer for cloning Hfq in pet-28
OligoRPT23	ATCGCTCGAGACGATTGTTTTCGTCGTCTTG	Reverse primer for cloning full length Hfq in pet-28
OligoRPT24	GTTACTCGAGACGAGCTGGAACAACTGTAG	Reverse primer for cloning Hfq66 in pet-28
OligoRPT25	AATACTCGAGTGCTGGACGTGGGTTACG	Reverse primer for cloning Hfq72 in pet-28
OligoRPT26	ATTACTCGAGGCCTTGACCACCGAAGCCAC	Reverse primer for cloning Hfq92 in pet-28
OligoRPT27	GCGTAATACGACTCACTATAGGGAAAGACGGCGATTTGTTATC	For amplification of MicA template
OligoRPT28	AAAAAGGCCACTCGTGAGTGG	
OligoRPT29	GCGTAATACGACTCACTATAGGAACACATCAGATTTCCTGGTGTAAC	For amplification of DsrA template
OligoRPT30	AAATCCCGACCCTGAGGGGG	
OligoRPT31	GCGTAATACGACTCACTATAGGTTTAAGTTCCTTTTAAATCATGTG	For amplification of AbsR25 template
OligoRPT32	ATTCTATTCAATAGTTTGGAATAATAC	
OligoRPT33	ATTAGAATTCACCTATCCCTAATAATTTAAGAG	For amplification of 500 bp region upstream of *hfq*
OligoRPT34	TTATGGATCCAATTGATTAGCTTGAAAAAAACC	

OligoRPT35	ATTAGGATCCACATTTTTAACTCCAAAAAAAAATTT	For amplification of 500 bp region downstream of hfq
OligoRPT36	TATTAAGCTTGCAGGCAGAACAAACCAAAAAATG	
OligoRPT37	ATTAGGATCCGTGTAGGCTGGAGCTGCTTC	For amplification of KanFRT cassette
OligoRPT38	ATTAGGATCCATGGGAATTAGCCATGGTCC	
OligoRPT39	CAGAACACTGCACAATGCTGC	For amplification of *hfq* with 125 bp overhang
OligoRPT40	GCAGGAAATGGAGGATAAAGCC	
OligoRPT41	TAGCGGATCCAAGCAAAATTTGCACACTGTC	For amplification of *hfq* with its promoter and terminator
OligoRPT42	GCGCGGATCCTTAATATGCTTTTTTATATTTTTAAAGCC	
OligoRPT43	TAGTGGATCCATGAGTAAAGGAGAAGAACTTTTC	For cloning *gfp* in pRPT20
OligoRPT44	TATAACGCGTCTATTTGTATAGTTCATCCATGCC	
OligoRPT45	ATTAGAATTCAATCTGTGTTATGCGTATTAATTAGATC	For cloning *sodB* to get an *sodB-gfq* fusion in pRPT20
OligoRPT46	ATATGGATCCATCATCATAGCCATATGGAAGTG	
OligoRPT47	AACACGCAATTTCTACAGTTGTTCCAGCTCGTTAATTGATTAGCTTGAAAAAAACCAGTCAGTGATGAC	Forward primer for amplification of 3'UTR for overlap with *hfq66*
OligoRPT48	TTGTTCCAGCTCGTAACCCACGTCCAGCAGGTTAATTGATTAGCTTGAAAAAAACCAGTCAGTGATGAC	Forward primer for amplification of 3'UTR for overlap with *hfq72*
OligoRPT49	GTGGTAGTCAAGGTGGCTTCGGTGGTCAAGGCTAATTGATTA	Forward primer for amplification of 3'UTR for overlap with *hfq92*

	GCTTGAAAAAAACCAGTCAG TGATGAC	
OligoRPT50	CCCTGAGCTGGGAAACCTGC ACCTTGTGCACCCATTTTTAA CTCCAAAAAAAAATTTTTAAA TCAGCGC	Reverse primer for amplification of 5'UTR for overlap with *hfqCt*
OligoRPT51	ATGGGTGCACAAGGTGCAGG	Forward primer for amplification of 3' region of *hfqCt*
OligoRPT52	TTAACGAGCTGGAACAACTGT AGAAATTGC	Reverse primer for amplification of 5' region of *hfq66*
OligoRPT53	TTAACCTGCTGGACGTGGGTT AC	Reverse primer for amplification of 5' region of *hfq72*
OligoRPT54	TTAGCCTTGACCACCGAAGCC AC	Reverse primer for amplification of 5' region of *hfq92*
OligoRPT55	ATTTGGATCCGTTATCGCCAG ATGTGG	For amplification of *E. coli hfq* with its promoter and terminator
OligoRPT56	AAATGGATCCGGGGAACACA GGATCG	
OligoRPT57	TCGTCTACGCGGTCTTTCTT	For amplification of an internal
OligoRPT58	CAGCGCACAAAATCACTGTT	region of *groEL*
OligoRPT59	CCATATGGTTCTCTTTAGATT TTGAA	For amplification of a specific unique region in AbsR10
OligoRPT60	GCATGCCAATGCTCATGTT	
OligoRPT61	GGTGCGACTACATTACCTGC	For amplification of 540 bp
OligoRPT62	TGAGTGCTGTAATGAGGCGA	upstream and 770 bp downstream region of AbsR1
OligoRPT63	TTTTGGATCCGACATAAGCCT GTTCGGTTC	For amplification of *aac1*
OligoRPT64	ATTAGGATCCGACGACTTGAC CCTGCCA	
OligoRPT65	GCGTAATACGACTCACTATAG GTTTAAAGTCCTGATGAGGAT TAAGC	For amplification of AbsR1 coding region

OligoRPT66	TGATAAGTAATAGATAAAGC TTTACTCTACCG

Bibliography

1. Peleg AY, Seifert H, Paterson DL. Acinetobacter baumannii: emergence of a successful pathogen. Clin Microbiol Rev 2008; 21:538–582.
2. Doi Y, Murray GL, Peleg AY. Acinetobacter baumannii: evolution of antimicrobial resistance-treatment options. Semin Respir Crit Care Med 2015; 36:85–98.
3. Gonzalez-Villoria AM, Valverde-Garduno V. Antibiotic-Resistant Acinetobacter baumannii Increasing Success Remains a Challenge as a Nosocomial Pathogen. J Pathog 2016; 2016:.
4. Rice LB. Federal Funding for the Study of Antimicrobial Resistance in Nosocomial Pathogens: No ESKAPE. J Infect Dis 2008; 197:1079–1081.
5. Roca I, Espinal P, Vila-Farrés X, Vila J. The Acinetobacter baumannii Oxymoron: Commensal Hospital Dweller Turned Pan-Drug-Resistant Menace. Front Microbiol 2012; 3:148.
6. Vincent J-L, Rello J, Marshall J, Silva E, Anzueto A, Martin CD, Moreno R, Lipman J, Gomersall C, Sakr Y, Reinhart K, EPIC II Group of Investigators. International study of the prevalence and outcomes of infection in intensive care units. JAMA 2009; 302:2323–2329.
7. Camp C, Tatum OL. A Review of Acinetobacter baumannii as a Highly Successful Pathogen in Times of War. Lab Med 2010; 41:649–657.
8. Howard A, O'Donoghue M, Feeney A, Sleator RD. Acinetobacter baumannii. Virulence 2012; 3:243–250.
9. Lee C-R, Lee JH, Park M, Park KS, Bae IK, Kim YB, Cha C-J, Jeong BC, Lee SH. Biology of Acinetobacter baumannii: Pathogenesis, Antibiotic Resistance Mechanisms, and Prospective Treatment Options. Front Cell Infect Microbiol 2017; 7:55.
10. Iyer VR, Sharma R, Pathania R, Navani NK. Small RNAs of Pathogenic Bacteria: Not Small Enough to be Overlooked for Therapeutics. Mol Cell Pharmacol 2012; 4:17–30.
11. Sharma R, Arya S, Patil SD, Sharma A, Jain PK, Navani NK, Pathania R. Identification of Novel Regulatory Small RNAs in Acinetobacter baumannii. PLOS ONE 2014; 9:e93833.
12. Chitsaz M, Brown MH. The role played by drug efflux pumps in bacterial multidrug resistance. Essays Biochem 2017; 61:127–139.
13. Pichon C, Felden B. Proteins that interact with bacterial small RNA regulators. FEMS Microbiol Rev 2007; 31:614–625.
14. Attaiech L, Glover JNM, Charpentier X. RNA Chaperones Step Out of Hfq's Shadow. Trends Microbiol 2017; 25:247–249.
15. Gottesman S, Storz G. RNA reflections: Converging on Hfq. RNA 2015; 21:511–512.

16. Panja S, Schu DJ, Woodson SA. Conserved arginines on the rim of Hfq catalyze base pair formation and exchange. Nucleic Acids Res 2013; 41:7536–7546.
17. Chao Y, Vogel J. The role of Hfq in bacterial pathogens. Curr Opin Microbiol 2010; 13:24–33.
18. Schilling D, Gerischer U. The Acinetobacter baylyi hfq Gene Encodes a Large Protein with an Unusual C Terminus. J Bacteriol 2009; 191:5553–5562.
19. Kuo H-Y, Chao H-H, Liao P-C, Hsu L, Chang K-C, Tung C-H, Chen C-H, Liou M-L. Functional Characterization of Acinetobacter baumannii Lacking the RNA Chaperone Hfq. Front Microbiol 2017; 8:2068.
20. Sheen TR, Jimenez A, Wang N-Y, Banerjee A, Sorge NM van, Doran KS. Serine-Rich Repeat Proteins and Pili Promote Streptococcus agalactiae Colonization of the Vaginal Tract. J Bacteriol 2011; 193:6834–6842.
21. Nadkarni MA, Martin FE, Jacques NA, Hunter N. Determination of bacterial load by real-time PCR using a broad-range (universal) probe and primers set. Microbiology 2002; 148:257–266.
22. Peleg AY, Seifert H, Paterson DL. Acinetobacter baumannii: emergence of a successful pathogen. Clin Microbiol Rev 2008; 21:538–582.
23. Glew RH, Moellering RC, Kunz LJ. Infections with Acinetobacter calcoaceticus (Herellea vaginicola): clinical and laboratory studies. Medicine (Baltimore) 1977; 56:79–97.
24. Daly A, Postic B, Kass E. Infections due to organisms of the genus Herellea. B5W and B. anitratum. Arch Intern Med 1962; 110:580–591.
25. A Study of the Moraxella Group II. Oxidative-negative Species (Genus Acinetobacter). no date; .
26. BRISOU J, PREVOT AR. Studies on bacterial taxonomy. X. The revision of species under Acromobacter group. Ann Inst Pasteur 1954; 86:722–728.
27. Al Atrouni A, Joly-Guillou M-L, Hamze M, Kempf M. Reservoirs of Non-baumannii Acinetobacter Species. Front Microbiol 2016; 7:49.
28. Bouvet PJM, Grimont PAD. Taxonomy of the Genus Acinetobacter with the Recognition of Acinetobacter baumannii sp. nov., Acinetobacter haemolyticus sp. nov., Acinetobacter johnsonii sp. nov., and Acinetobacter junii sp. nov. and Emended Descriptions of Acinetobacter calcoaceticus and Acinetobacter lwoffii. Int J Syst Evol Microbiol 1986; 36:228–240.
29. Dijkshoorn L, van der Toorn J. Acinetobacter species: which do we mean? Clin Infect Dis Off Publ Infect Dis Soc Am 1992; 15:748–749.

30. Chang WN, Lu CH, Huang CR, Chuang YC. Community-acquired Acinetobacter meningitis in adults. Infection 2000; 28:395–397.
31. Visca P, Seifert H, Towner KJ. Acinetobacter infection--an emerging threat to human health. IUBMB Life 2011; 63:1048–1054.
32. Dortet L, Legrand P, Soussy C-J, Cattoir V. Bacterial identification, clinical significance, and antimicrobial susceptibilities of Acinetobacter ursingii and Acinetobacter schindleri, two frequently misidentified opportunistic pathogens. J Clin Microbiol 2006; 44:4471–4478.
33. Loubinoux J, Mihaila-Amrouche L, Le Fleche A, Pigne E, Huchon G, Grimont PAD, Bouvet A. Bacteremia caused by Acinetobacter ursingii. J Clin Microbiol 2003; 41:1337–1338.
34. Endo S, Sasano M, Yano H, Inomata S, Ishibashi N, Aoyagi T, Hatta M, Gu Y, Yamada M, Tokuda K, Kitagawa M, Kunishima H, Hirakata Y, Kaku M. IMP-1-producing carbapenem-resistant Acinetobacter ursingii from Japan. J Antimicrob Chemother 2012; 67:2533–2534.
35. Chiu C-H, Lee Y-T, Wang Y-C, Yin T, Kuo S-C, Yang Y-S, Chen T-L, Lin J-C, Wang F-D, Fung C-P. A retrospective study of the incidence, clinical characteristics, identification, and antimicrobial susceptibility of bacteremic isolates of Acinetobacter ursingii. BMC Infect Dis 2015; 15:400.
36. Salzer HJF, Rolling T, Schmiedel S, Klupp E-M, Lange C, Seifert H. Severe Community-Acquired Bloodstream Infection with Acinetobacter ursingii in Person who Injects Drugs. Emerg Infect Dis 2016; 22:134–137.
37. Nemec A, Krizova L, Maixnerova M, Sedo O, Brisse S, Higgins PG. Acinetobacter seifertii sp. nov., a member of the Acinetobacter calcoaceticus-Acinetobacter baumannii complex isolated from human clinical specimens. Int J Syst Evol Microbiol 2015; 65:934–942.
38. Kishii K, Kikuchi K, Tomida J, Kawamura Y, Yoshida A, Okuzumi K, Moriya K. The first cases of human bacteremia caused by Acinetobacter seifertii in Japan. J Infect Chemother Off J Jpn Soc Chemother 2016; 22:342–345.
39. Yang Y, Wang J, Fu Y, Ruan Z, Yu Y. Acinetobacter seifertii Isolated from China: Genomic Sequence and Molecular Epidemiology Analyses. Medicine (Baltimore) 2016; 95:e2937.
40. Chusri S, Chongsuvivatwong V, Rivera JI, Silpapojakul K, Singkhamanan K, McNeil E, Doi Y. Clinical Outcomes of Hospital-Acquired Infection with Acinetobacter nosocomialis and Acinetobacter pittii. Antimicrob Agents Chemother 2014; 58:4172–4179.

41. Rafei R, Hamze M, Pailhoriès H, Eveillard M, Marsollier L, Joly-Guillou M-L, Dabboussi F, Kempf M. Extrahuman epidemiology of Acinetobacter baumannii in Lebanon. Appl Environ Microbiol 2015; 81:2359–2367.
42. Berlau J, Aucken HM, Houang E, Pitt TL. Isolation of Acinetobacter spp. including A. baumannii from vegetables: implications for hospital-acquired infections. J Hosp Infect 1999; 42:201–204.
43. Choi J-Y, Kim Y, Ko EA, Park YK, Jheong W-H, Ko G, Ko KS. Acinetobacter species isolates from a range of environments: species survey and observations of antimicrobial resistance. Diagn Microbiol Infect Dis 2012; 74:177–180.
44. Houang ETS, Chu YW, Leung CM, Chu KY, Berlau J, Ng KC, Cheng AFB. Epidemiology and Infection Control Implications of Acinetobacter spp. in Hong Kong. J Clin Microbiol 2001; 39:228–234.
45. Eveillard M, Kempf M, Belmonte O, Pailhoriès H, Joly-Guillou M-L. Reservoirs of Acinetobacter baumannii outside the hospital and potential involvement in emerging human community-acquired infections. Int J Infect Dis IJID Off Publ Int Soc Infect Dis 2013; 17:e802-805.
46. Centers for Disease Control and Prevention (CDC). Acinetobacter baumannii infections among patients at military medical facilities treating injured U.S. service members, 2002-2004. MMWR Morb Mortal Wkly Rep 2004; 53:1063–1066.
47. Karah N, Sundsfjord A, Towner K, Samuelsen Ø. Insights into the global molecular epidemiology of carbapenem non-susceptible clones of Acinetobacter baumannii. Drug Resist Updat 2012; 15:237–247.
48. Sievert DM, Ricks P, Edwards JR, Schneider A, Patel J, Srinivasan A, Kallen A, Limbago B, Fridkin S, National Healthcare Safety Network (NHSN) Team and Participating NHSN Facilities. Antimicrobial-resistant pathogens associated with healthcare-associated infections: summary of data reported to the National Healthcare Safety Network at the Centers for Disease Control and Prevention, 2009-2010. Infect Control Hosp Epidemiol 2013; 34:1–14.
49. Rodríguez-Baño J, Cisneros JM, Fernández-Cuenca F, Ribera A, Vila J, Pascual A, Martínez-Martínez L, Bou G, Pachón J, Grupo de Estudio de Infección Hospitalaria (GEIH). Clinical features and epidemiology of Acinetobacter baumannii colonization and infection in Spanish hospitals. Infect Control Hosp Epidemiol 2004; 25:819–824.
50. Agodi A, Auxilia F, Barchitta M, Brusaferro S, D'Alessandro D, Montagna MT, Orsi GB, Pasquarella C, Torregrossa V, Suetens C, Mura I, GISIO. Building a benchmark through

active surveillance of intensive care unit-acquired infections: the Italian network SPIN-UTI. J Hosp Infect 2010; 74:258–265.

51. Martins AF, Kuchenbecker RS, Pilger KO, Pagano M, Barth AL, CMCIES-PMPA/SMS Task Force. High endemic levels of multidrug-resistant Acinetobacter baumannii among hospitals in southern Brazil. Am J Infect Control 2012; 40:108–112.
52. Labarca JA, Salles MJC, Seas C, Guzmán-Blanco M. Carbapenem resistance in Pseudomonas aeruginosa and Acinetobacter baumannii in the nosocomial setting in Latin America. Crit Rev Microbiol 2016; 42:276–292.
53. Villar M, Cano ME, Gato E, Garnacho-Montero J, Miguel Cisneros J, Ruíz de Alegría C, Fernández-Cuenca F, Martínez-Martínez L, Vila J, Pascual A, Tomás M, Bou G, Rodríguez-Baño J, GEIH/GEMARA/REIPI-Ab20101 Group. Epidemiologic and clinical impact of Acinetobacter baumannii colonization and infection: a reappraisal. Medicine (Baltimore) 2014; 93:202–210.
54. Gupta V, Datta P, Chander J. Prevalence of metallo-beta lactamase (MBL) producing Pseudomonas spp. and Acinetobacter spp. in a tertiary care hospital in India. J Infect 2006; 52:311–314.
55. Mathai AS, Oberoi A, Madhavan S, Kaur P. Acinetobacter infections in a tertiary level intensive care unit in northern India: epidemiology, clinical profiles and outcomes. J Infect Public Health 2012; 5:145–152.
56. Bali NK, Fomda BA, Bashir H, Zahoor D, Lone S, Koul PA. Emergence of carbapenem-resistant Acinetobacter in a temperate north Indian State. Br J Biomed Sci 2013; 70:156–160.
57. Shah S, Singhal T, Naik R. A 4-year prospective study to determine the incidence and microbial etiology of surgical site infections at a private tertiary care hospital in Mumbai, India. Am J Infect Control 2015; 43:59–62.
58. Golia S, K T S, C L V. Microbial profile of early and late onset ventilator associated pneumonia in the intensive care unit of a tertiary care hospital in bangalore, India. J Clin Diagn Res JCDR 2013; 7:2462–2466.
59. Ginawi I, Saleem M, Sigh M, Vaish AK, Ahmad I, Srivastava VK, Abdullah AFM. Hospital acquired infections among patients admitted in the medical and surgical wards of a non-teaching secondary care hospital in northern India. J Clin Diagn Res JCDR 2014; 8:81–83.
60. Chung DR, Song J-H, Kim SH, Thamlikitkul V, Huang S-G, Wang H, So TM-K, Yasin RMD, Hsueh P-R, Carlos CC, Hsu LY, Buntaran L, Lalitha MK, Kim MJ, Choi JY, Kim SI, Ko KS, Kang C-I, Peck KR, Asian Network for Surveillance of Resistant Pathogens

Study Group. High prevalence of multidrug-resistant nonfermenters in hospital-acquired pneumonia in Asia. Am J Respir Crit Care Med 2011; 184:1409–1417.

61. Kuo S-C, Chang S-C, Wang H-Y, Lai J-F, Chen P-C, Shiau Y-R, Huang I-W, Lauderdale T-LY, TSAR Hospitals. Emergence of extensively drug-resistant Acinetobacter baumannii complex over 10 years: nationwide data from the Taiwan Surveillance of Antimicrobial Resistance (TSAR) program. BMC Infect Dis 2012; 12:200.
62. Dejsirilert S, Tiengrim S, Sawanpanyalert P, Aswapokee N, Malathum K. Antimicrobial resistance of Acinetobacter baumannii: six years of National Antimicrobial Resistance Surveillance Thailand (NARST) surveillance. J Med Assoc Thail Chotmaihet Thangphaet 2009; 92 Suppl 4:S34-45.
63. Madani N, Rosenthal VD, Dendane T, Abidi K, Zeggwagh AA, Abouqal R. Health-care associated infections rates, length of stay, and bacterial resistance in an intensive care unit of Morocco: findings of the International Nosocomial Infection Control Consortium (INICC). Int Arch Med 2009; 2:29.
64. Luna CM, Rodriguez-Noriega E, Bavestrello L, Guzmán-Blanco M. Gram-negative infections in adult intensive care units of latin america and the Caribbean. Crit Care Res Pract 2014; 2014:480463.
65. Spellberg B, Rex JH. The value of single-pathogen antibacterial agents. Nat Rev Drug Discov 2013; 12:963.
66. McConnell MJ, Actis L, Pachón J. Acinetobacter baumannii: human infections, factors contributing to pathogenesis and animal models. FEMS Microbiol Rev 2013; 37:130–155.
67. Bergogne-Bérézin E. The Increasing Role of Acinetobacter Species As Nosocomial Pathogens. Curr Infect Dis Rep 2001; 3:440–444.
68. Dijkshoorn L, Nemec A, Seifert H. An increasing threat in hospitals: multidrug-resistant Acinetobacter baumannii. Nat Rev Microbiol 2007; 5:939–951.
69. Gil-Perotin S, Ramirez P, Marti V, Sahuquillo JM, Gonzalez E, Calleja I, Menendez R, Bonastre J. Implications of endotracheal tube biofilm in ventilator-associated pneumonia response: a state of concept. Crit Care Lond Engl 2012; 16:R93.
70. Acinetobacter: Microbiology, Epidemiology, Infections, Management. CRC Press 1995; .
71. Villers D, Espaze E, Coste-Burel M, Giauffret F, Ninin E, Nicolas F, Richet H. Nosocomial Acinetobacter baumannii infections: microbiological and clinical epidemiology. Ann Intern Med 1998; 129:182–189.
72. Levin AS, Barone AA, Penço J, Santos MV, Marinho IS, Arruda EA, Manrique EI, Costa SF. Intravenous colistin as therapy for nosocomial infections caused by multidrug-resistant

Pseudomonas aeruginosa and Acinetobacter baumannii. Clin Infect Dis Off Publ Infect Dis Soc Am 1999; 28:1008–1011.

73. García-Garmendia JL, Ortiz-Leyba C, Garnacho-Montero J, Jiménez-Jiménez FJ, Monterrubio-Villar J, Gili-Miner M. Mortality and the increase in length of stay attributable to the acquisition of Acinetobacter in critically ill patients. Crit Care Med 1999; 27:1794–1799.
74. Falagas ME, Karveli EA, Kelesidis I, Kelesidis T. Community-acquired Acinetobacter infections. Eur J Clin Microbiol Infect Dis Off Publ Eur Soc Clin Microbiol 2007; 26:857–868.
75. Peng C, Zong Z, Fan H. Acinetobacter baumannii isolates associated with community-acquired pneumonia in West China. Clin Microbiol Infect Off Publ Eur Soc Clin Microbiol Infect Dis 2012; 18:E491-493.
76. Kumar S, Patil PP, Midha S, Ray P, Patil PB, Gautam V. Genome Sequence of Acinetobacter baumannii Strain 10441_14 Belonging to ST451, Isolated from India. Genome Announc 2015; 3:e01322-15.
77. Falagas ME, Rafailidis PI. Attributable mortality of Acinetobacter baumannii: no longer a controversial issue. Crit Care Lond Engl 2007; 11:134.
78. Wisplinghoff H, Perbix W, Seifert H. Risk factors for nosocomial bloodstream infections due to Acinetobacter baumannii: a case-control study of adult burn patients. Clin Infect Dis Off Publ Infect Dis Soc Am 1999; 28:59–66.
79. Hunt JP, Buechter KJ, Fakhry SM. *acinetobacter calcoaceticus* Pneumonia and the Formation of Pneumatoceles. J Trauma Inj Infect Crit Care 2000; 48:964–970.
80. Vallenet D, Nordmann P, Barbe V, Poirel L, Mangenot S, Bataille E, Dossat C, Gas S, Kreimeyer A, Lenoble P, Oztas S, Poulain J, Segurens B, Robert C, Abergel C, Claverie J-M, Raoult D, Médigue C, Weissenbach J, Cruveiller S. Comparative analysis of Acinetobacters: three genomes for three lifestyles. PloS One 2008; 3:e1805.
81. Livermore DM, Hope R, Brick G, Lillie M, Reynolds R, BSAC Working Parties on Resistance Surveillance. Non-susceptibility trends among Pseudomonas aeruginosa and other non-fermentative Gram-negative bacteria from bacteraemias in the UK and Ireland, 2001-06. J Antimicrob Chemother 2008; 62 Suppl 2:ii55-63.
82. Rossolini GM, Mantengoli E. Antimicrobial resistance in Europe and its potential impact on empirical therapy. Clin Microbiol Infect Off Publ Eur Soc Clin Microbiol Infect Dis 2008; 14 Suppl 6:2–8.
83. Morgan DJ, Weisenberg SA, Augenbraun MH, Calfee DP, Currie BP, Furuya EY, Holzman R, Montecalvo MC, Phillips M, Polsky B, Sepkowitz KA. Multidrug-resistant

Acinetobacter baumannii in New York City - 10 years into the epidemic. Infect Control Hosp Epidemiol 2009; 30:196–197.

84. Magiorakos A-P, Srinivasan A, Carey RB, Carmeli Y, Falagas ME, Giske CG, Harbarth S, Hindler JF, Kahlmeter G, Olsson-Liljequist B, Paterson DL, Rice LB, Stelling J, Struelens MJ, Vatopoulos A, Weber JT, Monnet DL. Multidrug-resistant, extensively drug-resistant and pandrug-resistant bacteria: an international expert proposal for interim standard definitions for acquired resistance. Clin Microbiol Infect 2012; 18:268–281.
85. Hujer KM, Hamza NS, Hujer AM, Perez F, Helfand MS, Bethel CR, Thomson JM, Anderson VE, Barlow M, Rice LB, Tenover FC, Bonomo RA. Identification of a new allelic variant of the Acinetobacter baumannii cephalosporinase, ADC-7 beta-lactamase: defining a unique family of class C enzymes. Antimicrob Agents Chemother 2005; 49:2941–2948.
86. Turton JF, Ward ME, Woodford N, Kaufmann ME, Pike R, Livermore DM, Pitt TL. The role of ISAba1 in expression of OXA carbapenemase genes in Acinetobacter baumannii. FEMS Microbiol Lett 2006; 258:72–77.
87. Corvec S, Poirel L, Naas T, Drugeon H, Nordmann P. Genetics and expression of the carbapenem-hydrolyzing oxacillinase gene blaOXA-23 in Acinetobacter baumannii. Antimicrob Agents Chemother 2007; 51:1530–1533.
88. Merino M, Acosta J, Poza M, Sanz F, Beceiro A, Chaves F, Bou G. OXA-24 carbapenemase gene flanked by XerC/XerD-like recombination sites in different plasmids from different Acinetobacter species isolated during a nosocomial outbreak. Antimicrob Agents Chemother 2010; 54:2724–2727.
89. Poirel L, Pitout JDD, Calvo L, Rodriguez-Martinez J-M, Church D, Nordmann P. In Vivo Selection of Fluoroquinolone-Resistant Escherichia coli Isolates Expressing Plasmid-Mediated Quinolone Resistance and Expanded-Spectrum β-Lactamase. Antimicrob Agents Chemother 2006; 50:1525–1527.
90. Higgins PG, Poirel L, Lehmann M, Nordmann P, Seifert H. OXA-143, a novel carbapenem-hydrolyzing class D beta-lactamase in Acinetobacter baumannii. Antimicrob Agents Chemother 2009; 53:5035–5038.
91. Cornaglia G, Giamarellou H, Rossolini GM. Metallo-β-lactamases: a last frontier for β-lactams? Lancet Infect Dis 2011; 11:381–393.
92. Pfeifer Y, Wilharm G, Zander E, Wichelhaus TA, Göttig S, Hunfeld K-P, Seifert H, Witte W, Higgins PG. Molecular characterization of blaNDM-1 in an Acinetobacter baumannii strain isolated in Germany in 2007. J Antimicrob Chemother 2011; 66:1998–2001.
93. Adams MD, Goglin K, Molyneaux N, Hujer KM, Lavender H, Jamison JJ, MacDonald IJ, Martin KM, Russo T, Campagnari AA, Hujer AM, Bonomo RA, Gill SR. Comparative

genome sequence analysis of multidrug-resistant Acinetobacter baumannii. J Bacteriol 2008; 190:8053–8064.

94. Naas T, Namdari F, Réglier-Poupet H, Poyart C, Nordmann P. Panresistant extended-spectrum beta-lactamase SHV-5-producing Acinetobacter baumannii from New York City. J Antimicrob Chemother 2007; 60:1174–1176.
95. Poirel L, Corvec S, Rapoport M, Mugnier P, Petroni A, Pasteran F, Faccone D, Galas M, Drugeon H, Cattoir V, Nordmann P. Identification of the novel narrow-spectrum beta-lactamase SCO-1 in Acinetobacter spp. from Argentina. Antimicrob Agents Chemother 2007; 51:2179–2184.
96. Potron A, Poirel L, Croizé J, Chanteperdrix V, Nordmann P. Genetic and biochemical characterization of the first extended-spectrum CARB-type beta-lactamase, RTG-4, from Acinetobacter baumannii. Antimicrob Agents Chemother 2009; 53:3010–3016.
97. Poirel L, Cabanne L, Vahaboglu H, Nordmann P. Genetic Environment and Expression of the Extended-Spectrum β-Lactamase blaPER-1 Gene in Gram-Negative Bacteria. Antimicrob Agents Chemother 2005; 49:1708–1713.
98. Poirel L, Mugnier PD, Toleman MA, Walsh TR, Rapoport MJ, Petroni A, Nordmann P. ISCR2, another vehicle for bla(VEB) gene acquisition. Antimicrob Agents Chemother 2009; 53:4940–4943.
99. Potron A, Munoz-Price LS, Nordmann P, Cleary T, Poirel L. Genetic features of CTX-M-15-producing Acinetobacter baumannii from Haiti. Antimicrob Agents Chemother 2011; 55:5946–5948.
100. Moubareck C, Brémont S, Conroy M-C, Courvalin P, Lambert T. GES-11, a novel integron-associated GES variant in Acinetobacter baumannii. Antimicrob Agents Chemother 2009; 53:3579–3581.
101. Robledo IE, Aquino EE, Santé MI, Santana JL, Otero DM, León CF, Vázquez GJ. Detection of KPC in Acinetobacter spp. in Puerto Rico. Antimicrob Agents Chemother 2010; 54:1354–1357.
102. Fournier P-E, Vallenet D, Barbe V, Audic S, Ogata H, Poirel L, Richet H, Robert C, Mangenot S, Abergel C, Nordmann P, Weissenbach J, Raoult D, Claverie J-M. Comparative genomics of multidrug resistance in Acinetobacter baumannii. PLoS Genet 2006; 2:e7.
103. Navia MM, Ruiz J, Vila J. Characterization of an integron carrying a new class D beta-lactamase (OXA-37) in Acinetobacter baumannii. Microb Drug Resist Larchmt N 2002; 8:261–265.

104. Ravasi P, Limansky AS, Rodriguez RE, Viale AM, Mussi MA. ISAba825, a functional insertion sequence modulating genomic plasticity and bla(OXA-58) expression in Acinetobacter baumannii. Antimicrob Agents Chemother 2011; 55:917–920.
105. Quale J, Bratu S, Landman D, Heddurshetti R. Molecular epidemiology and mechanisms of carbapenem resistance in Acinetobacter baumannii endemic in New York City. Clin Infect Dis Off Publ Infect Dis Soc Am 2003; 37:214–220.
106. del Mar Tomás M, Beceiro A, Pérez A, Velasco D, Moure R, Villanueva R, Martínez-Beltrán J, Bou G. Cloning and functional analysis of the gene encoding the 33- to 36-kilodalton outer membrane protein associated with carbapenem resistance in Acinetobacter baumannii. Antimicrob Agents Chemother 2005; 49:5172–5175.
107. Bou G, Cerveró G, Domínguez MA, Quereda C, Martínez-Beltrán J. Characterization of a nosocomial outbreak caused by a multiresistant Acinetobacter baumannii strain with a carbapenem-hydrolyzing enzyme: high-level carbapenem resistance in A. baumannii is not due solely to the presence of beta-lactamases. J Clin Microbiol 2000; 38:3299–3305.
108. Gribun A, Nitzan Y, Pechatnikov I, Hershkovits G, Katcoff DJ. Molecular and structural characterization of the HMP-AB gene encoding a pore-forming protein from a clinical isolate of Acinetobacter baumannii. Curr Microbiol 2003; 47:434–443.
109. Fernández-Cuenca F, Smani Y, Gómez-Sánchez MC, Docobo-Pérez F, Caballero-Moyano FJ, Domínguez-Herrera J, Pascual A, Pachón J. Attenuated virulence of a slow-growing pandrug-resistant Acinetobacter baumannii is associated with decreased expression of genes encoding the porins CarO and OprD-like. Int J Antimicrob Agents 2011; 38:548–549.
110. Magnet S, Courvalin P, Lambert T. Resistance-nodulation-cell division-type efflux pump involved in aminoglycoside resistance in Acinetobacter baumannii strain BM4454. Antimicrob Agents Chemother 2001; 45:3375–3380.
111. Damier-Piolle L, Magnet S, Brémont S, Lambert T, Courvalin P. AdeIJK, a resistance-nodulation-cell division pump effluxing multiple antibiotics in Acinetobacter baumannii. Antimicrob Agents Chemother 2008; 52:557–562.
112. Cayô R, Rodríguez M-C, Espinal P, Fernández-Cuenca F, Ocampo-Sosa AA, Pascual A, Ayala JA, Vila J, Martínez-Martínez L. Analysis of genes encoding penicillin-binding proteins in clinical isolates of Acinetobacter baumannii. Antimicrob Agents Chemother 2011; 55:5907–5913.
113. Cho YJ, Moon DC, Jin JS, Choi CH, Lee YC, Lee JC. Genetic basis of resistance to aminoglycosides in Acinetobacter spp. and spread of armA in Acinetobacter baumannii sequence group 1 in Korean hospitals. Diagn Microbiol Infect Dis 2009; 64:185–190.

114. Doi Y, Adams JM, Yamane K, Paterson DL. Identification of 16S rRNA methylase-producing Acinetobacter baumannii clinical strains in North America. Antimicrob Agents Chemother 2007; 51:4209–4210.
115. Su X-Z, Chen J, Mizushima T, Kuroda T, Tsuchiya T. AbeM, an H+-coupled Acinetobacter baumannii multidrug efflux pump belonging to the MATE family of transporters. Antimicrob Agents Chemother 2005; 49:4362–4364.
116. Hamouda A, Amyes SGB. Novel gyrA and parC point mutations in two strains of Acinetobacter baumannii resistant to ciprofloxacin. J Antimicrob Chemother 2004; 54:695–696.
117. Coyne S, Rosenfeld N, Lambert T, Courvalin P, Périchon B. Overexpression of resistance-nodulation-cell division pump AdeFGH confers multidrug resistance in Acinetobacter baumannii. Antimicrob Agents Chemother 2010; 54:4389–4393.
118. Srinivasan VB, Rajamohan G, Gebreyes WA. Role of AbeS, a Novel Efflux Pump of the SMR Family of Transporters, in Resistance to Antimicrobial Agents in Acinetobacter baumannii. Antimicrob Agents Chemother 2009; 53:5312–5316.
119. Vila J, Martí S, Sánchez-Céspedes J. Porins, efflux pumps and multidrug resistance in Acinetobacter baumannii. J Antimicrob Chemother 2007; 59:1210–1215.
120. Roca I, Marti S, Espinal P, Martínez P, Gibert I, Vila J. CraA, a major facilitator superfamily efflux pump associated with chloramphenicol resistance in Acinetobacter baumannii. Antimicrob Agents Chemother 2009; 53:4013–4014.
121. Ribera A, Roca I, Ruiz J, Gibert I, Vila J. Partial characterization of a transposon containing the tet(A) determinant in a clinical isolate of Acinetobacter baumannii. J Antimicrob Chemother 2003; 52:477–480.
122. Ribera A, Ruiz J, Vila J. Presence of the Tet M Determinant in a Clinical Isolate of Acinetobacter baumannii. Antimicrob Agents Chemother 2003; 47:2310–2312.
123. Sharma A, Sharma R, Bhattacharyya T, Bhando T, Pathania R. Fosfomycin resistance in Acinetobacter baumannii is mediated by efflux through a major facilitator superfamily (MFS) transporter-AbaF. J Antimicrob Chemother 2017; 72:68–74.
124. Arroyo LA, Herrera CM, Fernandez L, Hankins JV, Trent MS, Hancock REW. The pmrCAB operon mediates polymyxin resistance in Acinetobacter baumannii ATCC 17978 and clinical isolates through phosphoethanolamine modification of lipid A. Antimicrob Agents Chemother 2011; 55:3743–3751.
125. Moffatt JH, Harper M, Adler B, Nation RL, Li J, Boyce JD. Insertion sequence ISAba11 is involved in colistin resistance and loss of lipopolysaccharide in Acinetobacter baumannii. Antimicrob Agents Chemother 2011; 55:3022–3024.

126. Fernández-Reyes M, Rodríguez-Falcón M, Chiva C, Pachón J, Andreu D, Rivas L. The cost of resistance to colistin in Acinetobacter baumannii: a proteomic perspective. Proteomics 2009; 9:1632–1645.
127. Kim UJ, Kim HK, An JH, Cho SK, Park K-H, Jang H-C. Update on the Epidemiology, Treatment, and Outcomes of Carbapenem-resistant *Acinetobacter infections*. Chonnam Med J 2014; 50:37.
128. Chopra S, Ramkissoon K, Anderson DC. A systematic quantitative proteomic examination of multidrug resistance in Acinetobacter baumannii. J Proteomics 2013; 84:17–39.
129. Héritier C, Poirel L, Nordmann P. Cephalosporinase over-expression resulting from insertion of ISAba1 in Acinetobacter baumannii. Clin Microbiol Infect Off Publ Eur Soc Clin Microbiol Infect Dis 2006; 12:123–130.
130. Vahaboglu H, Oztürk R, Aygün G, Coşkunkan F, Yaman A, Kaygusuz A, Leblebicioglu H, Balik I, Aydin K, Otkun M. Widespread detection of PER-1-type extended-spectrum beta-lactamases among nosocomial Acinetobacter and Pseudomonas aeruginosa isolates in Turkey: a nationwide multicenter study. Antimicrob Agents Chemother 1997; 41:2265–2269.
131. Lee Y, Bae IK, Kim J, Jeong SH, Lee K. Dissemination of ceftazidime-resistant Acinetobacter baumannii clonal complex 92 in Korea. J Appl Microbiol 2012; 112:1207–1211.
132. Figueiredo S, Poirel L, Papa A, Koulourida V, Nordmann P. Overexpression of the naturally occurring blaOXA-51 gene in Acinetobacter baumannii mediated by novel insertion sequence ISAba9. Antimicrob Agents Chemother 2009; 53:4045–4047.
133. Higgins PG, Pérez-Llarena FJ, Zander E, Fernández A, Bou G, Seifert H. OXA-235, a novel class D β-lactamase involved in resistance to carbapenems in Acinetobacter baumannii. Antimicrob Agents Chemother 2013; 57:2121–2126.
134. Chen Y, Zhou Z, Jiang Y, Yu Y. Emergence of NDM-1-producing Acinetobacter baumannii in China. J Antimicrob Chemother 2011; 66:1255–1259.
135. Decousser JW, Jansen C, Nordmann P, Emirian A, Bonnin RA, Anais L, Merle JC, Poirel L. Outbreak of NDM-1-producing Acinetobacter baumannii in France, January to May 2013. Euro Surveill Bull Eur Sur Mal Transm Eur Commun Dis Bull 2013; 18:.
136. Akers KS, Chaney C, Barsoumian A, Beckius M, Zera W, Yu X, Guymon C, Keen EF, Robinson BJ, Mende K, Murray CK. Aminoglycoside resistance and susceptibility testing errors in Acinetobacter baumannii-calcoaceticus complex. J Clin Microbiol 2010; 48:1132–1138.

137. Liou GF, Yoshizawa S, Courvalin P, Galimand M. Aminoglycoside resistance by ArmA-mediated ribosomal 16S methylation in human bacterial pathogens. J Mol Biol 2006; 359:358–364.
138. Adams-Haduch JM, Paterson DL, Sidjabat HE, Pasculle AW, Potoski BA, Muto CA, Harrison LH, Doi Y. Genetic basis of multidrug resistance in Acinetobacter baumannii clinical isolates at a tertiary medical center in Pennsylvania. Antimicrob Agents Chemother 2008; 52:3837–3843.
139. Chopra S, Galande A. A fluoroquinolone-resistant Acinetobacter baumannii without the quinolone resistance-determining region mutations. J Antimicrob Chemother 2011; 66:2668–2670.
140. Beceiro A, Llobet E, Aranda J, Bengoechea JA, Doumith M, Hornsey M, Dhanji H, Chart H, Bou G, Livermore DM, Woodford N. Phosphoethanolamine modification of lipid A in colistin-resistant variants of Acinetobacter baumannii mediated by the pmrAB two-component regulatory system. Antimicrob Agents Chemother 2011; 55:3370–3379.
141. Moffatt JH, Harper M, Harrison P, Hale JDF, Vinogradov E, Seemann T, Henry R, Crane B, St Michael F, Cox AD, Adler B, Nation RL, Li J, Boyce JD. Colistin resistance in Acinetobacter baumannii is mediated by complete loss of lipopolysaccharide production. Antimicrob Agents Chemother 2010; 54:4971–4977.
142. Chopra I, Hawkey PM, Hinton M. Tetracyclines, molecular and clinical aspects. J Antimicrob Chemother 1992; 29:245–277.
143. Munita JM, Arias CA. Mechanisms of Antibiotic Resistance. Microbiol Spectr 2016; 4:.
144. Webber MA, Piddock LJV. The importance of efflux pumps in bacterial antibiotic resistance. J Antimicrob Chemother 2003; 51:9–11.
145. Mullié C, Bouharkat B, Guiheneuf R, Serra C, Touil-Meddah AT, Sonnet P. Efflux pumps in Acinetobacter baumannii: role in antibiotic resistance and interest of efflux pump inhibitors as additional therapeutic weapons. no date; 12.
146. Yoon E-J, Chabane YN, Goussard S, Snesrud E, Courvalin P, Dé E, Grillot-Courvalin C. Contribution of Resistance-Nodulation-Cell Division Efflux Systems to Antibiotic Resistance and Biofilm Formation in Acinetobacter baumannii. MBio 2015; 6:e00309-15.
147. Nowak-Zaleska A, Wieczór M, Czub J, Nierzwicki Ł, Kotłowski R, Mikucka A, Gospodarek E. Correlation between the number of Pro-Ala repeats in the EmrA homologue of Acinetobacter baumannii and resistance to netilmicin, tobramycin, imipenem and ceftazidime. J Glob Antimicrob Resist 2016; 7:145–149.
148. Huys G, Cnockaert M, Vaneechoutte M, Woodford N, Nemec A, Dijkshoorn L, Swings J. Distribution of tetracycline resistance genes in genotypically related and unrelated

multiresistant Acinetobacter baumannii strains from different European hospitals. Res Microbiol 2005; 156:348–355.

149. Rajamohan G, Srinivasan VB, Gebreyes WA. Molecular and functional characterization of a novel efflux pump, AmvA, mediating antimicrobial and disinfectant resistance in Acinetobacter baumannii. J Antimicrob Chemother 2010; 65:1919–1925.
150. Tayabali AF, Nguyen KC, Shwed PS, Crosthwait J, Coleman G, Seligy VL. Comparison of the virulence potential of Acinetobacter strains from clinical and environmental sources. PloS One 2012; 7:e37024.
151. Qiu H, KuoLee R, Harris G, Chen W. High susceptibility to respiratory Acinetobacter baumannii infection in A/J mice is associated with a delay in early pulmonary recruitment of neutrophils. Microbes Infect 2009; 11:946–955.
152. Jacobs AC, Hood I, Boyd KL, Olson PD, Morrison JM, Carson S, Sayood K, Iwen PC, Skaar EP, Dunman PM. Inactivation of phospholipase D diminishes Acinetobacter baumannii pathogenesis. Infect Immun 2010; 78:1952–1962.
153. Johnson TL, Waack U, Smith S, Mobley H, Sandkvist M. Acinetobacter baumannii Is Dependent on the Type II Secretion System and Its Substrate LipA for Lipid Utilization and In Vivo Fitness. J Bacteriol 2015; 198:711–719.
154. Russo TA, Beanan JM, Olson R, MacDonald U, Luke NR, Gill SR, Campagnari AA. Rat pneumonia and soft-tissue infection models for the study of Acinetobacter baumannii biology. Infect Immun 2008; 76:3577–3586.
155. Wand ME, Bock LJ, Turton JF, Nugent PG, Sutton JM. Acinetobacter baumannii virulence is enhanced in Galleria mellonella following biofilm adaptation. J Med Microbiol 2012; 61:470–477.
156. Vallejo JA, Beceiro A, Rumbo-Feal S, Rodríguez-Palero MJ, Russo TA, Bou G. Optimisation of the Caenorhabditis elegans model for studying the pathogenesis of opportunistic Acinetobacter baumannii. Int J Antimicrob Agents 2015; .
157. Bhuiyan MS, Ellett F, Murray GL, Kostoulias X, Cerqueira GM, Schulze KE, Mahamad Maifiah MH, Li J, Creek DJ, Lieschke GJ, Peleg AY. Acinetobacter baumannii phenylacetic acid metabolism influences infection outcome through a direct effect on neutrophil chemotaxis. Proc Natl Acad Sci U S A 2016; 113:9599–9604.
158. Giannouli M, Antunes LCS, Marchetti V, Triassi M, Visca P, Zarrilli R. Virulence-related traits of epidemic Acinetobacter baumannii strains belonging to the international clonal lineages I-III and to the emerging genotypes ST25 and ST78. BMC Infect Dis 2013; 13:282.
159. Verma S, Srikanth CV. Understanding the complexities of Salmonella–host crosstalk as revealed by in vivo model organisms. IUBMB Life no date; 67:482–497.

160. Fournier PE, Richet H. The epidemiology and control of Acinetobacter baumannii in health care facilities. Clin Infect Dis Off Publ Infect Dis Soc Am 2006; 42:692–699.
161. Nwugo CC, Arivett BA, Zimbler DL, Gaddy JA, Richards AM, Actis LA. Effect of ethanol on differential protein production and expression of potential virulence functions in the opportunistic pathogen Acinetobacter baumannii. PloS One 2012; 7:e51936.
162. Russo TA, Luke NR, Beanan JM, Olson R, Sauberan SL, MacDonald U, Schultz LW, Umland TC, Campagnari AA. The K1 capsular polysaccharide of Acinetobacter baumannii strain 307-0294 is a major virulence factor. Infect Immun 2010; 78:3993–4000.
163. Geisinger E, Isberg RR. Antibiotic modulation of capsular exopolysaccharide and virulence in Acinetobacter baumannii. PLoS Pathog 2015; 11:e1004691.
164. Beceiro A, Moreno A, Fernández N, Vallejo JA, Aranda J, Adler B, Harper M, Boyce JD, Bou G. Biological cost of different mechanisms of colistin resistance and their impact on virulence in Acinetobacter baumannii. Antimicrob Agents Chemother 2014; 58:518–526.
165. Wand ME, Bock LJ, Bonney LC, Sutton JM. Retention of virulence following adaptation to colistin in Acinetobacter baumannii reflects the mechanism of resistance. J Antimicrob Chemother 2015; 70:2209–2216.
166. Wong D, Nielsen TB, Bonomo RA, Pantapalangkoor P, Luna B, Spellberg B. Clinical and Pathophysiological Overview of Acinetobacter Infections: a Century of Challenges. Clin Microbiol Rev 2017; 30:409–447.
167. Choi CH, Hyun SH, Lee JY, Lee JS, Lee YS, Kim SA, Chae J-P, Yoo SM, Lee JC. Acinetobacter baumannii outer membrane protein A targets the nucleus and induces cytotoxicity. Cell Microbiol 2008; 10:309–319.
168. Kim SW, Choi CH, Moon DC, Jin JS, Lee JH, Shin J-H, Kim JM, Lee YC, Seol SY, Cho DT, Lee JC. Serum resistance of Acinetobacter baumannii through the binding of factor H to outer membrane proteins. FEMS Microbiol Lett 2009; 301:224–231.
169. Tilley D, Law R, Warren S, Samis JA, Kumar A. CpaA a novel protease from Acinetobacter baumannii clinical isolates deregulates blood coagulation. FEMS Microbiol Lett 2014; 356:53–61.
170. Liou M-L, Soo P-C, Ling S-R, Kuo H-Y, Tang CY, Chang K-C. The sensor kinase BfmS mediates virulence in Acinetobacter baumannii. J Microbiol Immunol Infect Wei Mian Yu Gan Ran Za Zhi 2014; 47:275–281.
171. Bahl CD, Hvorecny KL, Bridges AA, Ballok AE, Bomberger JM, Cady KC, O'Toole GA, Madden DR. Signature motifs identify an Acinetobacter Cif virulence factor with epoxide hydrolase activity. J Biol Chem 2014; 289:7460–7469.

172. Álvarez-Fraga L, Pérez A, Rumbo-Feal S, Merino M, Vallejo JA, Ohneck EJ, Edelmann RE, Beceiro A, Vázquez-Ucha JC, Valle J, Actis LA, Bou G, Poza M. Analysis of the role of the LH92_11085 gene of a biofilm hyper-producing Acinetobacter baumannii strain on biofilm formation and attachment to eukaryotic cells. Virulence 2016; 7:443–455.
173. Sun D, Crowell SA, Harding CM, De Silva PM, Harrison A, Fernando DM, Mason KM, Santana E, Loewen PC, Kumar A, Liu Y. KatG and KatE confer Acinetobacter resistance to hydrogen peroxide but sensitize bacteria to killing by phagocytic respiratory burst. Life Sci 2016; 148:31–40.
174. Lázaro-Díez M, Navascués-Lejarza T, Remuzgo-Martínez S, Navas J, Icardo JM, Acosta F, Martínez-Martínez L, Ramos-Vivas J. Acinetobacter baumannii and A. pittii clinical isolates lack adherence and cytotoxicity to lung epithelial cells in vitro. Microbes Infect 2016; 18:559–564.
175. Zimbler DL, Park TM, Arivett BA, Penwell WF, Greer SM, Woodruff TM, Tierney DL, Actis LA. Stress response and virulence functions of the Acinetobacter baumannii NfuA Fe-S scaffold protein. J Bacteriol 2012; 194:2884–2893.
176. Penwell WF, Arivett BA, Actis LA. The Acinetobacter baumannii entA gene located outside the acinetobactin cluster is critical for siderophore production, iron acquisition and virulence. PloS One 2012; 7:e36493.
177. Heindorf M, Kadari M, Heider C, Skiebe E, Wilharm G. Impact of Acinetobacter baumannii superoxide dismutase on motility, virulence, oxidative stress resistance and susceptibility to antibiotics. PloS One 2014; 9:e101033.
178. Zimbler DL, Arivett BA, Beckett AC, Menke SM, Actis LA. Functional features of TonB energy transduction systems of Acinetobacter baumannii. Infect Immun 2013; 81:3382–3394.
179. Esterly JS, McLaughlin MM, Malczynski M, Qi C, Zembower TR, Scheetz MH. Pathogenicity of clinical Acinetobacter baumannii isolates in a Galleria mellonella host model according to bla(OXA-40) gene and epidemiological outbreak status. Antimicrob Agents Chemother 2014; 58:1240–1242.
180. Srinivasan VB, Vaidyanathan V, Rajamohan G. AbuO, a TolC-like outer membrane protein of Acinetobacter baumannii, is involved in antimicrobial and oxidative stress resistance. Antimicrob Agents Chemother 2015; 59:1236–1245.
181. Fiester SE, Nwugo CC, Penwell WF, Neary JM, Beckett AC, Arivett BA, Schmidt RE, Geiger SC, Connerly PL, Menke SM, Tomaras AP, Actis LA. Role of the carboxy terminus of SecA in iron acquisition, protein translocation, and virulence of the bacterial pathogen Acinetobacter baumannii. Infect Immun 2015; 83:1354–1365.

182. Durante-Mangoni E, Del Franco M, Andini R, Bernardo M, Giannouli M, Zarrilli R. Emergence of colistin resistance without loss of fitness and virulence after prolonged colistin administration in a patient with extensively drug-resistant Acinetobacter baumannii. Diagn Microbiol Infect Dis 2015; 82:222–226.
183. Stahl J, Bergmann H, Göttig S, Ebersberger I, Averhoff B. Acinetobacter baumannii Virulence Is Mediated by the Concerted Action of Three Phospholipases D. PloS One 2015; 10:e0138360.
184. Repizo GD, Gagné S, Foucault-Grunenwald M-L, Borges V, Charpentier X, Limansky AS, Gomes JP, Viale AM, Salcedo SP. Differential Role of the T6SS in Acinetobacter baumannii Virulence. PloS One 2015; 10:e0138265.
185. Liu D, Liu Z-S, Hu P, Cai L, Fu B-Q, Li Y-S, Lu S-Y, Liu N-N, Ma X-L, Chi D, Chang J, Shui Y-M, Li Z-H, Ahmad W, Zhou Y, Ren H-L. Characterization of surface antigen protein 1 (SurA1) from Acinetobacter baumannii and its role in virulence and fitness. Vet Microbiol 2016; 186:126–138.
186. Richmond GE, Evans LP, Anderson MJ, Wand ME, Bonney LC, Ivens A, Chua KL, Webber MA, Sutton JM, Peterson ML, Piddock LJV. The Acinetobacter baumannii Two-Component System AdeRS Regulates Genes Required for Multidrug Efflux, Biofilm Formation, and Virulence in a Strain-Specific Manner. MBio 2016; 7:e00430-00416.
187. Gebhardt MJ, Gallagher LA, Jacobson RK, Usacheva EA, Peterson LR, Zurawski DV, Shuman HA. Joint Transcriptional Control of Virulence and Resistance to Antibiotic and Environmental Stress in Acinetobacter baumannii. MBio 2015; 6:e01660-01615.
188. de Léséleuc L, Harris G, KuoLee R, Xu HH, Chen W. Serum resistance, gallium nitrate tolerance and extrapulmonary dissemination are linked to heme consumption in a bacteremic strain of Acinetobacter baumannii. Int J Med Microbiol IJMM 2014; 304:360–369.
189. Wang N, Ozer EA, Mandel MJ, Hauser AR. Genome-wide identification of Acinetobacter baumannii genes necessary for persistence in the lung. MBio 2014; 5:e01163-01114.
190. Yoon E-J, Balloy V, Fiette L, Chignard M, Courvalin P, Grillot-Courvalin C. Contribution of the Ade Resistance-Nodulation-Cell Division-Type Efflux Pumps to Fitness and Pathogenesis of Acinetobacter baumannii. MBio 2016; 7:.
191. Mortensen BL, Rathi S, Chazin WJ, Skaar EP. Acinetobacter baumannii response to host-mediated zinc limitation requires the transcriptional regulator Zur. J Bacteriol 2014; 196:2616–2626.

192. Nairn BL, Lonergan ZR, Wang J, Braymer JJ, Zhang Y, Calcutt MW, Lisher JP, Gilston BA, Chazin WJ, de Crécy-Lagard V, Giedroc DP, Skaar EP. The Response of Acinetobacter baumannii to Zinc Starvation. Cell Host Microbe 2016; 19:826–836.
193. Subashchandrabose S, Smith S, DeOrnellas V, Crepin S, Kole M, Zahdeh C, Mobley HLT. Acinetobacter baumannii Genes Required for Bacterial Survival during Bloodstream Infection. MSphere 2016; 1:.
194. López-Rojas R, Domínguez-Herrera J, McConnell MJ, Docobo-Peréz F, Smani Y, Fernández-Reyes M, Rivas L, Pachón J. Impaired virulence and in vivo fitness of colistin-resistant Acinetobacter baumannii. J Infect Dis 2011; 203:545–548.
195. López-Rojas R, McConnell MJ, Jiménez-Mejías ME, Domínguez-Herrera J, Fernández-Cuenca F, Pachón J. Colistin resistance in a clinical Acinetobacter baumannii strain appearing after colistin treatment: effect on virulence and bacterial fitness. Antimicrob Agents Chemother 2013; 57:4587–4589.
196. Hraiech S, Roch A, Lepidi H, Atieh T, Audoly G, Rolain J-M, Raoult D, Brunel J-M, Papazian L, Brégeon F. Impaired virulence and fitness of a colistin-resistant clinical isolate of Acinetobacter baumannii in a rat model of pneumonia. Antimicrob Agents Chemother 2013; 57:5120–5121.
197. Smani Y, López-Rojas R, Domínguez-Herrera J, Docobo-Pérez F, Martí S, Vila J, Pachón J. In vitro and in vivo reduced fitness and virulence in ciprofloxacin-resistant Acinetobacter baumannii. Clin Microbiol Infect Off Publ Eur Soc Clin Microbiol Infect Dis 2012; 18:E1-4.
198. Gaddy JA, Arivett BA, McConnell MJ, López-Rojas R, Pachón J, Actis LA. Role of acinetobactin-mediated iron acquisition functions in the interaction of Acinetobacter baumannii strain ATCC 19606T with human lung epithelial cells, Galleria mellonella caterpillars, and mice. Infect Immun 2012; 80:1015–1024.
199. Lees-Miller RG, Iwashkiw JA, Scott NE, Seper A, Vinogradov E, Schild S, Feldman MF. A common pathway for O-linked protein-glycosylation and synthesis of capsule in Acinetobacter baumannii. Mol Microbiol 2013; 89:816–830.
200. Smani Y, Dominguez-Herrera J, Pachón J. Association of the outer membrane protein Omp33 with fitness and virulence of Acinetobacter baumannii. J Infect Dis 2013; 208:1561–1570.
201. Rumbo C, Tomás M, Fernández Moreira E, Soares NC, Carvajal M, Santillana E, Beceiro A, Romero A, Bou G. The Acinetobacter baumannii Omp33-36 porin is a virulence factor that induces apoptosis and modulates autophagy in human cells. Infect Immun 2014; 82:4666–4680.

202. Cerqueira GM, Kostoulias X, Khoo C, Aibinu I, Qu Y, Traven A, Peleg AY. A global virulence regulator in Acinetobacter baumannii and its control of the phenylacetic acid catabolic pathway. J Infect Dis 2014; 210:46–55.
203. Aranda J, Bardina C, Beceiro A, Rumbo S, Cabral MP, Barbé J, Bou G. Acinetobacter baumannii RecA protein in repair of DNA damage, antimicrobial resistance, general stress response, and virulence. J Bacteriol 2011; 193:3740–3747.
204. Schweppe DK, Harding C, Chavez JD, Wu X, Ramage E, Singh PK, Manoil C, Bruce JE. Host-Microbe Protein Interactions during Bacterial Infection. Chem Biol 2015; 22:1521–1530.
205. Elhosseiny NM, Amin MA, Yassin AS, Attia AS. Acinetobacter baumannii universal stress protein A plays a pivotal role in stress response and is essential for pneumonia and sepsis pathogenesis. Int J Med Microbiol IJMM 2015; 305:114–123.
206. Storz G, Vogel J, Wassarman KM. Regulation by Small RNAs in Bacteria: Expanding Frontiers. Mol Cell 2011; 43:880–891.
207. Gottesman S. The small RNA regulators of Escherichia coli: roles and mechanisms*. Annu Rev Microbiol 2004; 58:303–328.
208. Storz G. An Expanding Universe of Noncoding RNAs. Science 2002; 296:1260–1263.
209. Livny J, Waldor MK. Identification of small RNAs in diverse bacterial species. Curr Opin Microbiol 2007; 10:96–101.
210. Sittka A, Lucchini S, Papenfort K, Sharma CM, Rolle K, Binnewies TT, Hinton JCD, Vogel J. Deep Sequencing Analysis of Small Noncoding RNA and mRNA Targets of the Global Post-Transcriptional Regulator, Hfq. PLOS Genet 2008; 4:e1000163.
211. Sharma CM, Vogel J. Experimental approaches for the discovery and characterization of regulatory small RNA. Curr Opin Microbiol 2009; 12:536–546.
212. Massé E, Vanderpool CK, Gottesman S. Effect of RyhB Small RNA on Global Iron Use in Escherichia coli. J Bacteriol 2005; 187:6962–6971.
213. Andersen J, Forst SA, Zhao K, Inouye M, Delihas N. The function of micF RNA. micF RNA is a major factor in the thermal regulation of OmpF protein in Escherichia coli. J Biol Chem 1989; 264:17961–17970.
214. Papenfort K, Pfeiffer V, Mika F, Lucchini S, Hinton JCD, Vogel J. σE-dependent small RNAs of Salmonella respond to membrane stress by accelerating global omp mRNA decay. Mol Microbiol 2006; 62:1674–1688.
215. Boehm A, Vogel J. The csgD mRNA as a hub for signal integration via multiple small RNAs. Mol Microbiol 2012; 84:1–5.

216. The gcvB gene encodes a small untranslated RNA involved in expression of the dipeptide and oligopeptide transport systems in Escherichia coli - Urbanowski - 2000 - Molecular Microbiology - Wiley Online Library. no date; .
217. Beisel CL, Storz G. The Base-Pairing RNA Spot 42 Participates in a Multioutput Feedforward Loop to Help Enact Catabolite Repression in Escherichia coli. Mol Cell 2011; 41:286–297.
218. Bobrovskyy M, Vanderpool CK. The small RNA SgrS: roles in metabolism and pathogenesis of enteric bacteria. Front Cell Infect Microbiol 2014; 4:.
219. Gaida SM, Al-Hinai MA, Indurthi DC, Nicolaou SA, Papoutsakis ET. Synthetic tolerance: three noncoding small RNAs, DsrA, ArcZ and RprA, acting supra-additively against acid stress. Nucleic Acids Res 2013; 41:8726–8737.
220. Papenfort K, Förstner KU, Cong J-P, Sharma CM, Bassler BL. Differential RNA-seq of Vibrio cholerae identifies the VqmR small RNA as a regulator of biofilm formation. Proc Natl Acad Sci 2015; 112:E766–E775.
221. Davies BW, Bogard RW, Young TS, Mekalanos JJ. Coordinated Regulation of Accessory Genetic Elements Produces Cyclic Di-Nucleotides for V. cholerae Virulence. Cell 2012; 149:358–370.
222. Padalon-Brauch G, Hershberg R, Elgrably-Weiss M, Baruch K, Rosenshine I, Margalit H, Altuvia S. Small RNAs encoded within genetic islands of Salmonella typhimurium show host-induced expression and role in virulence. Nucleic Acids Res 2008; 36:1913–1927.
223. Gong H, Vu G-P, Bai Y, Chan E, Wu R, Yang E, Liu F, Lu S. A Salmonella Small Non-Coding RNA Facilitates Bacterial Invasion and Intracellular Replication by Modulating the Expression of Virulence Factors. PLOS Pathog 2011; 7:e1002120.
224. Pfeiffer V, Sittka A, Tomer R, Tedin K, Brinkmann V, Vogel J. A small non-coding RNA of the invasion gene island (SPI-1) represses outer membrane protein synthesis from the Salmonella core genome. Mol Microbiol 2007; 66:1174–1191.
225. Darfeuille F, Unoson C, Vogel J, Wagner EGH. An Antisense RNA Inhibits Translation by Competing with Standby Ribosomes. Mol Cell 2007; 26:381–392.
226. Beisel CL, Storz G. Base pairing small RNAs and their roles in global regulatory networks. FEMS Microbiol Rev 2010; 34:866–882.
227. Updegrove TB, Shabalina SA, Storz G. How do base-pairing small RNAs evolve? FEMS Microbiol Rev 2015; 39:379–391.
228. Otaka H, Ishikawa H, Morita T, Aiba H. PolyU tail of rho-independent terminator of bacterial small RNAs is essential for Hfq action. Proc Natl Acad Sci 2011; 108:13059–13064.

229. Dutta T, Srivastava S. Small RNA-mediated regulation in bacteria: A growing palette of diverse mechanisms. Gene 2018; 656:60–72.
230. Desnoyers G, Bouchard M-P, Massé E. New insights into small RNA-dependent translational regulation in prokaryotes. Trends Genet TIG 2013; 29:92–98.
231. Bouvier M, Sharma CM, Mika F, Nierhaus KH, Vogel J. Small RNA Binding to 5′ mRNA Coding Region Inhibits Translational Initiation. Mol Cell 2008; 32:827–837.
232. Massé E, Gottesman S. A small RNA regulates the expression of genes involved in iron metabolism in Escherichia coli. Proc Natl Acad Sci 2002; 99:4620–4625.
233. Bos J, Duverger Y, Thouvenot B, Chiaruttini C, Branlant C, Springer M, Charpentier B, Barras F. The sRNA RyhB Regulates the Synthesis of the Escherichia coli Methionine Sulfoxide Reductase MsrB but Not MsrA. PLOS ONE 2013; 8:e63647.
234. Chao Y, Li L, Girodat D, Förstner KU, Said N, Corcoran C, Śmiga M, Papenfort K, Reinhardt R, Wieden H-J, Luisi BF, Vogel J. In Vivo Cleavage Map Illuminates the Central Role of RNase E in Coding and Non-coding RNA Pathways. Mol Cell 2017; 65:39–51.
235. Bandyra KJ, Said N, Pfeiffer V, Górna MW, Vogel J, Luisi BF. The Seed Region of a Small RNA Drives the Controlled Destruction of the Target mRNA by the Endoribonuclease RNase E. Mol Cell 2012; 47:943–953.
236. Lalaouna D, Simoneau-Roy M, Lafontaine D, Massé E. Regulatory RNAs and target mRNA decay in prokaryotes. Biochim Biophys Acta 2013; 1829:742–747.
237. Chen H, Dutta T, Deutscher MP. Growth Phase-dependent Variation of RNase BN/Z Affects Small RNAs REGULATION OF 6S RNA. J Biol Chem 2016; 291:26435–26442.
238. Desnoyers G, Massé E. Noncanonical repression of translation initiation through small RNA recruitment of the RNA chaperone Hfq. Genes Dev 2012; 26:726–739.
239. Vanderpool CK, Gottesman S. The Novel Transcription Factor SgrR Coordinates the Response to Glucose-Phosphate Stress. J Bacteriol 2007; 189:2238–2248.
240. Papenfort K, Sun Y, Miyakoshi M, Vanderpool CK, Vogel J. Small RNA-Mediated Activation of Sugar Phosphatase mRNA Regulates Glucose Homeostasis. Cell 2013; 153:426–437.
241. Papenfort K, Vanderpool CK. Target activation by regulatory RNAs in bacteria. FEMS Microbiol Rev 2015; 39:362–378.
242. Battesti A, Majdalani N, Gottesman S. The RpoS-Mediated General Stress Response in Escherichia coli. Annu Rev Microbiol 2011; 65:189–213.
243. Sedlyarova N, Shamovsky I, Bharati BK, Epshtein V, Chen J, Gottesman S, Schroeder R, Nudler E. sRNA-Mediated Control of Transcription Termination in E. coli. Cell 2016; 167:111-121.e13.

244. Franze de Fernandez MT, Eoyang L, August JT. Factor fraction required for the synthesis of bacteriophage Qbeta-RNA. Nature 1968; 219:588–590.
245. Vogel J, Luisi BF. Hfq and its constellation of RNA. Nat Rev Microbiol 2011; 9:578–589.
246. Mura C, Randolph PS, Patterson J, Cozen AE. Archaeal and eukaryotic homologs of Hfq. RNA Biol 2013; 10:636–651.
247. Updegrove TB, Zhang A, Storz G. Hfq: the flexible RNA matchmaker. Curr Opin Microbiol 2016; 30:133–138.
248. Bilusic I, Popitsch N, Rescheneder P, Schroeder R, Lybecker M. Revisiting the coding potential of the E. coli genome through Hfq co-immunoprecipitation. RNA Biol 2014; 11:641–654.
249. Hussein R, Lim HN. Disruption of small RNA signaling caused by competition for Hfq. Proc Natl Acad Sci 2011; 108:1110–1115.
250. Sobrero P, Valverde C. The bacterial protein Hfq: much more than a mere RNA-binding factor. Crit Rev Microbiol 2012; 38:276–299.
251. Sukhodolets MV, Garges S. Interaction of Escherichia coli RNA polymerase with the ribosomal protein S1 and the Sm-like ATPase Hfq. Biochemistry (Mosc) 2003; 42:8022–8034.
252. Mohanty BK, Maples VF, Kushner SR. The Sm-like protein Hfq regulates polyadenylation dependent mRNA decay in Escherichia coli. Mol Microbiol 2004; 54:905–920.
253. Butland G, Peregrín-Alvarez JM, Li J, Yang W, Yang X, Canadien V, Starostine A, Richards D, Beattie B, Krogan N, Davey M, Parkinson J, Greenblatt J, Emili A. Interaction network containing conserved and essential protein complexes in Escherichia coli. Nature 2005; 433:531–537.
254. Morita T, Maki K, Aiba H. RNase E-based ribonucleoprotein complexes: mechanical basis of mRNA destabilization mediated by bacterial noncoding RNAs. Genes Dev 2005; 19:2176–2186.
255. Rabhi M, Espéli O, Schwartz A, Cayrol B, Rahmouni AR, Arluison V, Boudvillain M. The Sm-like RNA chaperone Hfq mediates transcription antitermination at Rho-dependent terminators. EMBO J 2011; 30:2805–2816.
256. Sauer E. Structure and RNA-binding properties of the bacterial LSm protein Hfq. RNA Biol 2013; 10:610–618.
257. Link TM, Valentin-Hansen P, Brennan RG. Structure of Escherichia coli Hfq bound to polyriboadenylate RNA. Proc Natl Acad Sci 2009; 106:19292–19297.
258. Sauer E, Weichenrieder O. Structural basis for RNA 3′-end recognition by Hfq. Proc Natl Acad Sci 2011; 108:13065–13070.

259. Sauter C, Basquin J, Suck D. Sm-like proteins in Eubacteria: the crystal structure of the Hfq protein from Escherichia coli. Nucleic Acids Res 2003; 31:4091–4098.
260. Ishikawa H, Otaka H, Maki K, Morita T, Aiba H. The functional Hfq-binding module of bacterial sRNAs consists of a double or single hairpin preceded by a U-rich sequence and followed by a 3′ poly(U) tail. RNA 2012; 18:1062–1074.
261. Večerek B, Rajkowitsch L, Sonnleitner E, Schroeder R, Bläsi U. The C-terminal domain of Escherichia coli Hfq is required for regulation. Nucleic Acids Res 2008; 36:133–143.
262. Olsen AS, Møller-Jensen J, Brennan RG, Valentin-Hansen P. C-terminally truncated derivatives of Escherichia coli Hfq are proficient in riboregulation. J Mol Biol 2010; 404:173–182.
263. Santiago-Frangos A, Jeliazkov JR, Gray JJ, Woodson SA. Acidic C-terminal domains autoregulate the RNA chaperone Hfq. ELife 2017; 6:e27049.
264. Santiago-Frangos A, Kavita K, Schu DJ, Gottesman S, Woodson SA. C-terminal domain of the RNA chaperone Hfq drives sRNA competition and release of target RNA. Proc Natl Acad Sci 2016; 113:E6089–E6096.
265. Fender A, Elf J, Hampel K, Zimmermann B, Wagner EGH. RNAs actively cycle on the Sm-like protein Hfq. Genes Dev 2010; 24:2621–2626.
266. Henderson CA, Vincent HA, Casamento A, Stone CM, Phillips JO, Cary PD, Sobott F, Gowers DM, Taylor JE, Callaghan AJ. Hfq binding changes the structure of Escherichia coli small noncoding RNAs OxyS and RprA, which are involved in the riboregulation of rpoS. RNA 2013; 19:1089–1104.
267. Dimastrogiovanni D, Fröhlich KS, Bandyra KJ, Bruce HA, Hohensee S, Vogel J, Luisi BF. Recognition of the small regulatory RNA RydC by the bacterial Hfq protein. ELife 2014; 3:.
268. Peng Y, Curtis JE, Fang X, Woodson SA. Structural model of an mRNA in complex with the bacterial chaperone Hfq. Proc Natl Acad Sci 2014; 111:17134–17139.
269. Holmqvist E, Reimegård J, Sterk M, Grantcharova N, Römling U, Wagner EGH. Two antisense RNAs target the transcriptional regulator CsgD to inhibit curli synthesis. EMBO J 2010; 29:1840–1850.
270. Hopkins JF, Panja S, McNeil SAN, Woodson SA. Effect of salt and RNA structure on annealing and strand displacement by Hfq. Nucleic Acids Res 2009; 37:6205–6213.
271. Soper T, Mandin P, Majdalani N, Gottesman S, Woodson SA. Positive regulation by small RNAs and the role of Hfq. Proc Natl Acad Sci 2010; 107:9602–9607.
272. Wagner EGH. Cycling of RNAs on Hfq. RNA Biol 2013; 10:619–626.

273. Moon K, Gottesman S. Competition among Hfq-binding small RNAs in Escherichia coli. Mol Microbiol 2011; 82:1545–1562.
274. Adamson DN, Lim HN. Essential Requirements for Robust Signaling in Hfq Dependent Small RNA Networks. PLOS Comput Biol 2011; 7:e1002138.
275. Arluison V, Folichon M, Marco S, Derreumaux P, Pellegrini O, Seguin J, Hajnsdorf E, Regnier P. The C-terminal domain of Escherichia coli Hfq increases the stability of the hexamer. Eur J Biochem 2004; 271:1258–1265.
276. Caillet J, Gracia C, Fontaine F, Hajnsdorf E. Clostridium difficile Hfq can replace Escherichia coli Hfq for most of its function. RNA 2014; 20:1567–1578.
277. Allam US, Krishna MG, Lahiri A, Joy O, Chakravortty D. Salmonella enterica Serovar Typhimurium Lacking hfq Gene Confers Protective Immunity against Murine Typhoid. PLOS ONE 2011; 6:e16667.
278. Robertson GT, Roop I. The Brucella abortus host factor I (HF-I) protein contributes to stress resistance during stationary phase and is a major determinant of virulence in mice. Mol Microbiol 1999; 34:690–700.
279. Sousa SA, Ramos CG, Moreira LM, Leitão JH. The hfq gene is required for stress resistance and full virulence of Burkholderia cepacia to the nematode Caenorhabditis elegans. Microbiol Read Engl 2010; 156:896–908.
280. Shakhnovich EA, Davis BM, Waldor MK. Hfq negatively regulates type III secretion in EHEC and several other pathogens. Mol Microbiol 2009; 74:347–363.
281. Hansen A-M, Kaper JB. Hfq affects the expression of the LEE pathogenicity island in enterohaemorrhagic Escherichia coli. Mol Microbiol 2009; 73:446–465.
282. Kulesus RR, Diaz-Perez K, Slechta ES, Eto DS, Mulvey MA. Impact of the RNA Chaperone Hfq on the Fitness and Virulence Potential of Uropathogenic Escherichia coli. Infect Immun 2008; 76:3019–3026.
283. Meibom KL, Forslund A-L, Kuoppa K, Alkhuder K, Dubail I, Dupuis M, Forsberg Å, Charbit A. Hfq, a Novel Pleiotropic Regulator of Virulence-Associated Genes in Francisella tularensis. Infect Immun 2009; 77:1866–1880.
284. Kadzhaev K, Zingmark C, Golovliov I, Bolanowski M, Shen H, Conlan W, Sjöstedt A. Identification of Genes Contributing to the Virulence of Francisella tularensis SCHU S4 in a Mouse Intradermal Infection Model. PLOS ONE 2009; 4:e5463.
285. McNealy TL, Forsbach-Birk V, Shi C, Marre R. The Hfq Homolog in Legionella pneumophila Demonstrates Regulation by LetA and RpoS and Interacts with the Global Regulator CsrA. J Bacteriol 2005; 187:1527–1532.

286. Attia AS, Sedillo JL, Wang W, Liu W, Brautigam CA, Winkler W, Hansen EJ. Moraxella catarrhalis Expresses an Unusual Hfq Protein. Infect Immun 2008; 76:2520–2530.
287. Fantappiè L, Metruccio MME, Seib KL, Oriente F, Cartocci E, Ferlicca F, Giuliani MM, Scarlato V, Delany I. The RNA Chaperone Hfq Is Involved in Stress Response and Virulence in Neisseria meningitidis and Is a Pleiotropic Regulator of Protein Expression. Infect Immun 2009; 77:1842–1853.
288. Pannekoek Y, Huis in 't Veld R, Hopman CTP, Langerak AAJ, Speijer D, Van Der Ende A. Molecular characterization and identification of proteins regulated by Hfq in Neisseria meningitidis. FEMS Microbiol Lett 2009; 294:216–224.
289. Dietrich Manuela, Munke Rebekka, Gottschald Marion, Ziska Elke, Boettcher Jan Peter, Mollenkopf Hans, Friedrich Alexandra. The effect of hfq on global gene expression and virulence in Neisseria gonorrhoeae. FEBS J 2009; 276:5507–5520.
290. Sonnleitner E, Hagens S, Rosenau F, Wilhelm S, Habel A, Jäger K-E, Bläsi U. Reduced virulence of a hfq mutant of Pseudomonas aeruginosa O1. Microb Pathog 2003; 35:217–228.
291. Sharma AK, Payne SM. Induction of expression of hfq by DksA is essential for Shigella flexneri virulence. Mol Microbiol 2006; 62:469–479.
292. Mitobe J, Morita-Ishihara T, Ishihama A, Watanabe H. Involvement of RNA-binding protein Hfq in the osmotic-response regulation of invE gene expression in Shigella sonnei. BMC Microbiol 2009; 9:110.
293. Bang I-S, Frye JG, McClelland M, Velayudhan J, Fang FC. Alternative sigma factor interactions in Salmonella: σE and σH promote antioxidant defences by enhancing σS levels. Mol Microbiol 2005; 56:811–823.
294. Sittka Alexandra, Pfeiffer Verena, Tedin Karsten, Vogel Jörg. The RNA chaperone Hfq is essential for the virulence of Salmonella typhimurium. Mol Microbiol 2006; 63:193–217.
295. Ansong C, Yoon H, Porwollik S, Mottaz-Brewer H, Petritis BO, Jaitly N, Adkins JN, McClelland M, Heffron F, Smith RD. Global Systems-Level Analysis of Hfq and SmpB Deletion Mutants in Salmonella: Implications for Virulence and Global Protein Translation. PLOS ONE 2009; 4:e4809.
296. Karasova D, Sebkova A, Vrbas V, Havlickova H, Sisak F, Rychlik I. Comparative analysis of Salmonella enterica serovar Enteritidis mutants with a vaccine potential. Vaccine 2009; 27:5265–5270.
297. Ding Y, Davis BM, Waldor MK. Hfq is essential for Vibrio cholerae virulence and downregulates σE expression. Mol Microbiol 2004; 53:345–354.

298. Nakano M, Takahashi A, Su Z, Harada N, Mawatari K, Nakaya Y. Hfq regulates the expression of the thermostable direct hemolysin gene in Vibrio parahaemolyticus. BMC Microbiol 2008; 8:155.
299. Geng J, Song Y, Yang L, Feng Y, Qiu Y, Li G, Guo J, Bi Y, Qu Y, Wang W, Wang X, Guo Z, Yang R, Han Y. Involvement of the Post-Transcriptional Regulator Hfq in Yersinia pestis Virulence. PLOS ONE 2009; 4:e6213.
300. Christiansen JK, Larsen MH, Ingmer H, Søgaard-Andersen L, Kallipolitis BH. The RNA-Binding Protein Hfq of Listeria monocytogenes: Role in Stress Tolerance and Virulence. J Bacteriol 2004; 186:3355–3362.
301. Bohn C, Rigoulay C, Bouloc P. No detectable effect of RNA-binding protein Hfq absence in Staphylococcus aureus. BMC Microbiol 2007; 7:10.
302. Schiano CA, Bellows LE, Lathem WW. The Small RNA Chaperone Hfq Is Required for the Virulence of Yersinia pseudotuberculosis. Infect Immun 2010; 78:2034–2044.
303. Bai G, Golubov A, Smith EA, McDonough KA. The Importance of the Small RNA Chaperone Hfq for Growth of Epidemic Yersinia pestis, but Not Yersinia pseudotuberculosis, with Implications for Plague Biology. J Bacteriol 2010; 192:4239–4245.
304. Roscetto E, Angrisano T, Costa V, Casalino M, Förstner KU, Sharma CM, Di Nocera PP, De Gregorio E. Functional characterization of the RNA chaperone Hfq in the opportunistic human pathogen Stenotrophomonas maltophilia. J Bacteriol 2012; 194:5864–5874.
305. Boudry P, Gracia C, Monot M, Caillet J, Saujet L, Hajnsdorf E, Dupuy B, Martin-Verstraete I, Soutourina O. Pleiotropic Role of the RNA Chaperone Protein Hfq in the Human Pathogen Clostridium difficile. J Bacteriol 2014; 196:3234–3248.
306. Gangaiah D, Labandeira-Rey M, Zhang X, Fortney KR, Ellinger S, Zwickl B, Baker B, Liu Y, Janowicz DM, Katz BP, Brautigam CA, Munson RS, Hansen EJ, Spinola SM. Haemophilus ducreyi Hfq Contributes to Virulence Gene Regulation as Cells Enter Stationary Phase. MBio 2014; 5:e01081-13.
307. Kim S, Hwang H, Kim K-P, Yoon H, Kang D-H, Ryu S. hfq Plays Important Roles in Virulence and Stress Adaptation in Cronobacter sakazakii ATCC 29544. Infect Immun 2015; 83:2089–2098.
308. Chiang M-K, Lu M-C, Liu L-C, Lin C-T, Lai Y-C. Impact of Hfq on Global Gene Expression and Virulence in Klebsiella pneumoniae. PLOS ONE 2011; 6:e22248.
309. Chambers JR, Bender KS. The RNA Chaperone Hfq Is Important for Growth and Stress Tolerance in Francisella novicida. PLOS ONE 2011; 6:e19797.

310. Bibova I, Skopova K, Masin J, Cerny O, Hot D, Sebo P, Vecerek B. The RNA Chaperone Hfq Is Required for Virulence of Bordetella pertussis. Infect Immun 2013; 81:4081–4090.
311. Hempel RJ, Morton DJ, Seale TW, Whitby PW, Stull TL. The role of the RNA chaperone Hfq in Haemophilus influenzae pathogenesis. BMC Microbiol 2013; 13:134.
312. Hämmerle H, Amman F, Večerek B, Stülke J, Hofacker I, Bläsi U. Impact of Hfq on the Bacillus subtilis Transcriptome. PLOS ONE 2014; 9:e98661.
313. Zhang A, Schu DJ, Tjaden BC, Storz G, Gottesman S. Mutations in interaction surfaces differentially impact E. coli Hfq association with small RNAs and their mRNA targets. J Mol Biol 2013; 425:3678–97.
314. Schilling D, Gerischer U. The Acinetobacter baylyi hfq gene encodes a large protein with an unusual C terminus. J Bacteriol 2009; 191:5553–5562.
315. Beich-Frandsen M, Večerek B, Konarev P V., Sjöblom B, Kloiber K, Hämmerle H, Rajkowitsch L, Miles AJ, Kontaxis G, Wallace B a., Svergun DI, Konrat R, Bläsi U, Djinović-Carugo K. Structural insights into the dynamics and function of the C-terminus of the E. coli RNA chaperone Hfq. Nucleic Acids Res 2011; 39:4900–4915.
316. Fortas E, Piccirilli F, Malabirade A, Militello V, Trépout S, Marco S, Taghbalout A, Arluison V. New insight into the structure and function of Hfq C-terminus. Biosci Rep 2015; 35:.
317. Vincent H a., Henderson C a., Ragan TJ, Garza-Garcia A, Cary PD, Gowers DM, Malfois M, Driscoll PC, Sobott F, Callaghan AJ. Characterization of Vibrio cholerae Hfq provides novel insights into the role of the Hfq C-terminal region. J Mol Biol 2012; 420:56–69.
318. Kuo H-Y, Chao H-H, Liao P-C, Hsu L, Chang K-C, Tung C-H, Chen C-H, Liou M-L. Functional Characterization of Acinetobacter baumannii Lacking the RNA Chaperone Hfq. Front Microbiol 2017; 8:2068.
319. Chao Y, Vogel J. The role of Hfq in bacterial pathogens. Curr Opin Microbiol 2010; 13:24–33.
320. Peleg AY, de Breij A, Adams MD, Cerqueira GM, Mocali S, Galardini M, Nibbering PH, Earl AM, Ward D V., Paterson DL, Seifert H, Dijkshoorn L. The Success of Acinetobacter Species; Genetic, Metabolic and Virulence Attributes. PLoS ONE 2012; 7:.
321. Paisio CE, Talano MA, González PS, Magallanes-Noguera C, Kurina-Sanz M, Agostini E. Biotechnological tools to improve bioremediation of phenol by *Acinetobacter* sp. RTE1.4. Environ Technol 2016; 37:2379–2390.
322. Hanson KG, Nigam A, Kapadia M, Desai AJ. Bioremediation of crude oil contamination with Acinetobacter sp. A3. Curr Microbiol 1997; 35:191–3.

323. Desouky A-E-H. Acinetobacter: environmental and biotechnological applications. Minireview Afr J Biotechnol 2003; 2:71–74.
324. Vecerek B, Rajkowitsch L, Sonnleitner E, Schroeder R, Bläsi U. The C-terminal domain of Escherichia coli Hfq is required for regulation. Nucleic Acids Res 2008; 36:133–43.
325. Massé E, Vanderpool CK, Gottesman S. Effect of RyhB small RNA on global iron use in Escherichia coli. J Bacteriol 2005; 187:6962–71.
326. Santiago-Frangos A, Jeliazkov JR, Gray JJ, Woodson SA. Acidic C-terminal domains autoregulate the RNA chaperone Hfq. ELife 2017; 6:.
327. Valentine SC, Contreras D, Tan S, Real LJ, Chu S, Xu HH. Phenotypic and molecular characterization of Acinetobacter baumannii clinical isolates from nosocomial outbreaks in Los Angeles County, California. J Clin Microbiol 2008; 46:2499–507.
328. Olsen AS, Møller-Jensen J, Brennan RG, Valentin-Hansen P. C-Terminally Truncated Derivatives of Escherichia coli Hfq Are Proficient in Riboregulation. J Mol Biol 2010; 404:173–182.
329. Updegrove TB, Zhang A, Storz G. Hfq: the flexible RNA matchmaker. Curr Opin Microbiol 2016; 30:133–138.
330. Dyson HJ, Wright PE. Intrinsically unstructured proteins and their functions. Nat Rev Mol Cell Biol 2005 63 2005; 6:197.
331. Rogelj Boris, Godin Katherine S., Shaw Christopher E., Ule Jernej. RNA Binding Proteins. Landes Bioscience and Springer Science; 2011.
332. Sachetto-Martins G, Franco LO, de Oliveira DE. Plant glycine-rich proteins: a family or just proteins with a common motif? Biochim Biophys Acta 2000; 1492:1–14.
333. Kim JS, Park SJ, Kwak KJ, Kim YO, Kim JY, Song J, Jang B, Jung CH, Kang H. Cold shock domain proteins and glycine-rich RNA-binding proteins from Arabidopsis thaliana can promote the cold adaptation process in Escherichia coli. Nucleic Acids Res 2007; 35:506–516.
334. Sharma R, Arya S, Patil SD, Sharma A, Jain PK, Navani NK, Pathania R. Identification of novel regulatory small RNAs in Acinetobacter baumannii. PLoS ONE 2014; 9:.
335. Hirai T, Heymann JAW, Maloney PC, Subramaniam S. Structural Model for 12-Helix Transporters Belonging to the Major Facilitator Superfamily. J Bacteriol 2003; 185:1712–1718.
336. Huda MN, Morita Y, Kuroda T, Mizushima T, Tsuchiya T. Na+-driven multidrug efflux pump VcmA from Vibrio cholerae non-O1, a non-halophilic bacterium. FEMS Microbiol Lett 2001; 203:235–239.

337. Blair JMA, Piddock LJV. How to Measure Export via Bacterial Multidrug Resistance Efflux Pumps. MBio 2016; 7:e00840-16.
338. Smith MG, Des Etages SG, Snyder M. Microbial Synergy via an Ethanol-Triggered Pathway. Mol Cell Biol 2004; 24:3874–3884.
339. Antunes LCS, Visca P, Towner KJ. Acinetobacter baumannii: evolution of a global pathogen. Pathog Dis 2014; 71:292–301.
340. Saier MH, Beatty JT, Goffeau a, Harley KT, Heijne WH, Huang SC, Jack DL, Jähn PS, Lew K, Liu J, Pao SS, Paulsen IT, Tseng TT, Virk PS. The major facilitator superfamily. J Mol Microbiol Biotechnol 1999; 1:257–279.
341. Baylay AJ, Piddock LJ V. Clinically relevant fluoroquinolone resistance due to constitutive overexpression of the PatAB ABC transporter in Streptococcus pneumoniae is conferred by disruption of a transcriptional attenuator. J Antimicrob Chemother 2015; 70:670–9.
342. Sirijatuphat R, Thamlikitkul V. Preliminary study of colistin versus colistin plus fosfomycin for treatment of carbapenem-resistant Acinetobacter baumannii infections. Antimicrob Agents Chemother 2014; 58:5598–5601.
343. Santimaleeworagun W, Wongpoowarak P, Chayakul P, Pattharachayakul S, Tansakul P, Garey KW. In vitro activity of colistin or sulbactam in combination with fosfomycin or imipenem against clinical isolates of carbapenem-resistant acinetobacter baumannii producing OXA-23 carbapenemases. Southeast Asian J Trop Med Public Health 2011; 42:890–900.
344. Fedrigo NH, Mazucheli J, Albiero J, Shinohara DR, Lodi FG, Machado AC dos S, Sy SKB, Tognim MCB. Pharmacodynamic Evaluation of Fosfomycin against Escherichia coli and Klebsiella spp. from Urinary Tract Infections and the Influence of pH on Fosfomycin Activities. Antimicrob Agents Chemother 2017; 61:e02498-16.
345. Baugh S, Ekanayaka AS, Piddock LJ V, Webber M a. Loss of or inhibition of all multidrug resistance efflux pumps of Salmonella enterica serovar Typhimurium results in impaired ability to form a biofilm. J Antimicrob Chemother 2012; 67:2409–2417.
346. Soto SM. Role of efflux pumps in the antibiotic resistance of bacteria embedded in a biofilm. Virulence 2013; 4:223–9.
347. He X, Lu F, Yuan F, Jiang D, Zhao P, Zhu J, Cheng H, Cao J, Lu G. Biofilm formation caused by clinical *Acinetobacter baumannii* isolates is associated with over-expression of the AdeFGH efflux pump. Antimicrob Agents Chemother 2015; 59:AAC.00877-15.
348. Kvist M, Hancock V, Klemm P. Inactivation of efflux pumps abolishes bacterial biofilm formation. Appl Environ Microbiol 2008; 74:7376–82.

349. Padilla E, Llobet E, Domenech-Sanchez A, Martinez-Martinez L, Bengoechea JA, Alberti S. Klebsiella pneumoniae AcrAB Efflux Pump Contributes to Antimicrobial Resistance and Virulence. Antimicrob Agents Chemother 2009; 54:177–183.
350. Váradi L, Lin Luo J, E. Hibbs D, D. Perry J, J. Anderson R, Orenga S, W. Groundwater P. Methods for the detection and identification of pathogenic bacteria: past, present, and future. Chem Soc Rev 2017; 46:4818–4832.
351. Fournier PE, Richet H, Weinstein RA. The Epidemiology and Control of Acinetobacter baumannii in Health Care Facilities. Clin Infect Dis 2006; 42:692–699.
352. McConnell MJ, Pérez-Ordóñez A, Pérez-Romero P, Valencia R, Lepe JA, Vázquez-Barba I, Pachón J. Quantitative Real-Time PCR for Detection of Acinetobacter baumannii Colonization in the Hospital Environment. J Clin Microbiol 2012; 50:1412–1414.
353. Buckingham WH, Domanus M, Hetzel S, Kunkel G, Storhoff J, Cork W. Direct detection of bacterial genomic DNA using gold nanoparticle probes. Conf Proc Annu Int Conf IEEE Eng Med Biol Soc IEEE Eng Med Biol Soc Annu Conf 2004; 3:1953–1955.
354. Verma MS, Rogowski JL, Jones L, Gu FX. Colorimetric biosensing of pathogens using gold nanoparticles. Biotechnol Adv 2015; 33:666–680.

Publications

Publications out of this thesis work:

Sharma R, Arya S, Patil SD, **Sharma A**, Jain PK, Navani NK, Pathania R. Identification of novel regulatory small RNAs in *Acinetobacter baumannii*. PLoS One. 2014 Apr 4;9(4):e93833.

Sharma A, Sharma R, Bhattacharyya T, Bhando T, Pathania R. Fosfomycin resistance in *Acinetobacter baumannii* is mediated by efflux through a major facilitator superfamily (MFS) transporter—AbaF. Journal of Antimicrobial Chemotherapy. 2016 Sep 20;72(1):68-74.

Sharma A, Dubey V, Sharma R, Devnath K, Gupta VK, Akhter J, Bhando T, Verma A, Ambatipudi K, Sarkar M, Pathania R. The unusual glycine-rich C terminus of the Acinetobacter baumannii RNA chaperone Hfq plays an important role in bacterial physiology. Journal of Biological Chemistry. 2018 Aug 31;293(35):13377-88.

Sharma A*, Gupta VK*, Pathania R. Efflux pump inhibitors for bacterial pathogens: from bench to bedside. Indian Journal of Medical Research. (Under review; invited review; *Equal contribution).

Other related publications:

Bhattacharyya T*, **Sharma A***, Akhter J, Pathania R. The small molecule IITR08027 restores the antibacterial activity of fluoroquinolones against multidrug-resistant Acinetobacter baumannii by efflux inhibition. International journal of antimicrobial agents. 2017 Aug 1;50(2):219-26. (*Equal contribution).

Gupta VK, Gaur R, **Sharma A**, Akther J, Saini M, Bhakuni RS, Pathania R. A novel bi-functional chalcone inhibits multi-drug resistant Staphylococcus aureus and potentiates the activity of fluoroquinolones. Bioorganic chemistry. 2019 Mar 1;83:214-25.

Posters and Presentations:

Sharma R., **Sharma A.**, Arya S., Das A.P., Narava M.K., Navani N.K., Pathania, R. Detection of *Acinetobacter baumannii* using its intergenic signature regions. International conference on Microbial World: Recent Innovations and Future Trends in Association of Microbiologist of India, KIIT Bhubaneshwar. November 22nd-25th, 2012.

Sharma A., Sharma R., Bhando T., Gaurav A. and Pathania R. Exploring the small RNA landscape of *Acinetobacter baumannii*: Another piece in the virulence jigsaw puzzle.

International Conference on Molecular signaling: Recent Trends in Biomedical and Translational Research, Indian Institute of Technology Roorkee. December 17-19th, 2013. (**Best Poster Award**)

Bhattacharya T., **Sharma A.**, Gaurav A., Bhando T., Akhter J., Dubey V. and Pathania R. Bad Bugs: Need drugs. Biotechnology Day, Indian Institute of Technology Roorkee. February 27th, 2016. (**Best Poster Award**)

Sharma A., Bhando T., Gaurav A., Akhter J., Dubey V., Pathnia R. Let's slay the superbug. Biotechnology Day, Indian Institute of Technology Roorkee. March 4th, 2017. (**Best Poster Award**)

Sharma A. Plasmizza: Your DNA pizza, the way you want. Industry Academia Meet-2017, Indian Institute of Technology Roorkee. March 25th, 2017. (**Second prize**)